ISSN 1520-295X

Seismic Performance Assessment of Seismically Isolated Buildings Designed by the Procedures of ASCE/SEI 7

by
Shoma Kitayama and Michael C. Constantinou

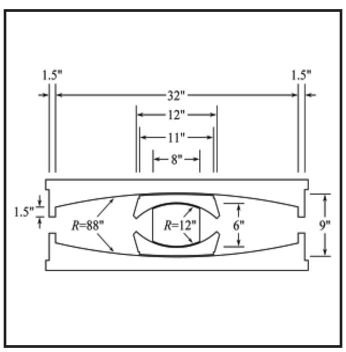

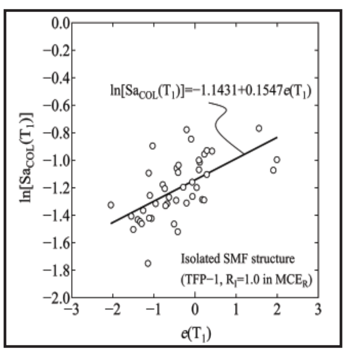

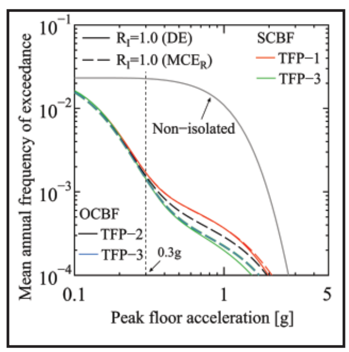

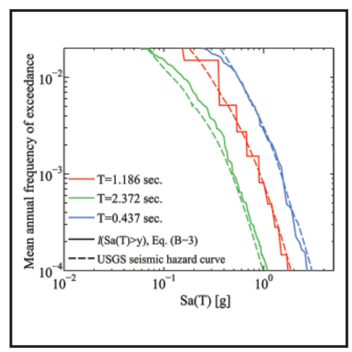

Technical Report MCEER-18-0004

April 14, 2018

This research was conducted at the University at Buffalo, State University of New York, and was supported primarily by MCEER.

Seismic Performance Assessment of Seismically Isolated Buildings Designed by the Procedures of ASCE/SEI 7

by

Shoma Kitayama[1] and Michael C. Constantinou[2]

Publication Date: April 14, 2018
Submittal Date: November 6, 2017

Technical Report MCEER-18-0004

1 Post-Doctoral Associate, Department of Civil, Structural and Environmental Engineering, University at Buffalo, State University of New York
2 Samuel P. Capen Professor, SUNY Distinguished Professor, Department of Civil, Structural and Environmental Engineering, University at Buffalo, State University of New York

MCEER
University at Buffalo, State University of New York
212 Ketter Hall, Buffalo, NY 14260
E-mail: *mceer@buffalo.edu*; Website: *http://buffalo.edu/mceer*

Preface

MCEER is a national center of excellence dedicated to the discovery and development of new knowledge, tools and technologies that equip communities to become more disaster resilient in the face of earthquakes and other extreme events. MCEER accomplishes this through a system of multidisciplinary, multi-hazard research, in tandem with complimentary education and outreach initiatives.

Headquartered at the University at Buffalo, The State University of New York, MCEER was originally established by the National Science Foundation in 1986, as the first National Center for Earthquake Engineering Research (NCEER). In 1998, it became known as the Multidisciplinary Center for Earthquake Engineering Research (MCEER), from which the current name, MCEER, evolved.

Comprising a consortium of researchers and industry partners from numerous disciplines and institutions throughout the United States, MCEER's mission has expanded from its original focus on earthquake engineering to one which addresses the technical and socio-economic impacts of a variety of hazards, both natural and man-made, on critical infrastructure, facilities, and society.

The Center derives support from several Federal agencies, including the National Science Foundation, Federal Highway Administration, Department of Energy, Nuclear Regulatory Commission, and the State of New York, foreign governments and private industry.

This report presents an analytical study of the seismic performance of seismically isolated buildings and comparable non-isolated buildings designed by the procedures of ASCE/SEI 7-10 and -16 at a particular location in California. The study concludes that seismically isolated buildings designed to the minimum criteria of either ASCE/SEI 7-10 or 7-16 at the considered location may have unacceptable probability of collapse in the maximum considered earthquake. The probability of collapse in the maximum considered earthquake becomes acceptable and the design may also meet criteria of improved performance in terms of story drift, residual drift and floor acceleration when they are designed with enhanced criteria of RI=1.0 and with isolators having a displacement capacity at initiation of stiffening equal to 1.5 times the average demand in the maximum considered earthquake. It is also observed that designs that meet the minimum criteria of ASCE/SEI 7-10 or 7-16 and without a displacement restrainer have unacceptably high probabilities of collapse. The study finds that seismically isolated structures designed by the enhanced criteria offer lower mean annual frequencies of exceeding important limits on story rift ratio, residual story drift ratio and peak floor acceleration than comparable non-isolated structures.

ABSTRACT

Seismically isolated buildings in the United States are currently designed and analyzed by the procedures of the ASCE/SEI 7-10 standard, Chapter 17 (ASCE, 2010). In the future, buildings will be designed and analyzed by the procedures of ASCE/SEI 7-16 (ASCE, 2017). Both ASCE standards require that the isolation system be detailed to accommodate the displacement demand calculated in the Risk-Targeted Maximum Considered Earthquake (MCE_R), where this displacement is the average of peak values calculated in seven nonlinear response history analyses. Both procedures permit the use of a response modification coefficient (R_I factor) between 1.0 and 2.0 depending on the seismic force-resisting system used. For the case of the ASCE/SEI 7-10 standard, the forces and drifts for the design are based on calculations using the design response (DE) spectrum, which is defined as being 2/3 of the MCE_R spectrum. For the case of the ASCE/SEI 7-16 standard, the forces and drifts for the design are based on calculations using the MCE_R spectrum.

This report investigates the reliability of the ASCE/SEI 7 provisions by studying an archetypical 6-story perimeter frame seismically isolated building designed with special concentrically braced frames (SCBF), ordinary concentrically braced frames (OCBF) and special moment resisting frames (SMF) for a location in California using the minimum criteria of ASCE/SEI 7-10 and ASCE/SEI 7-16 and also using enhanced design criteria. The isolation system consists of triple Friction Pendulum (FP) isolators with stiffening behavior at large displacement. Representative cases are also studied in which the stiffening behavior is replaced by the behavior of a moat wall. Additionally, double concave sliding isolators are considered and designed per minimum criteria and without a displacement restrainer, a practice permitted by the ASCE/SEI 7 standards. Non-isolated structures, also with braced and moment frame configurations, are designed and studied.

This study presents results on (1) the conditional probability of collapse on the occurrence of the MCE_R of the designed isolated structures and comparable non-isolated structures, and (2) information on the mean annual frequency of exceedance of the peak story drift ratio, the residual story drift ratio and the peak floor and roof acceleration. It is shown that (a) seismically isolated buildings designed to the minimum criteria of ASCE/SEI 7-10 or 7-16 may have

unacceptable probability of collapse in the MCE_R, (b) the probability of collapse in the MCE_R is acceptable and the design may also meet criteria of improved performance in terms of story drift, residual drift and floor acceleration when the structure is designed for R_I=1.0 (either for the DE or the MCE_R) and the isolators have a displacement capacity at initiation of stiffening equal to $1.5D_M$, (c) the behavior described in item (b) is also achieved by the use of moat walls instead of stiffening isolators, also placed at distance $1.5D_M$, (d) reducing the R_I factor may not provide any advantage unless the displacement capacity of the isolators is accordingly increased, (e) designs that meet the minimum criteria of ASCE/SEI 7-10 or 7-16 and without any displacement restrainer have unacceptably high probabilities of collapse, (f) OCBF designed by the minimum criteria of ASCE/SEI 7-16 have marginally unacceptable probabilities of collapse which can be improved by increasing the displacement capacity of the isolators, (g) seismically isolated structures designed by the minimum criteria of ASCE/SEI 7 and supplemented with minimally designed moat walls have unacceptable probabilities of collapse that are essentially the same as those of similarly designed isolated structures without a moat wall, and (h) seismically isolated structures designed per criteria in item (b) above offer lower mean annual frequencies of exceeding important limits on story drift ratio, residual story drift ratio and peak floor acceleration than comparable non-isolated structures.

ACKNOWLEDGEMENTS

The authors acknowledge Huseyin Darama, Ph.D., PE, Associate, Arup, Los Angeles, CA, Victor Zayas, Ph.D., PE, President, Earthquake Protection Systems, Inc., Vallejo, CA, William J. McVitty, PE, Senior Structural Engineer, Aurecon, Wellington, New Zealand and an anonymous reviewer for providing comments that resulted in substantial changes and improvement of this report. The authors also acknowledge the late Professor Stephen A. Mahin of the University of California, Berkeley and his student Benshun Shao for making available some of their early results on studies of the collapse performance of seismically isolated structures.

TABLE OF CONTENTS

LIST OF FIGURES

LIST OF FIGURES (CONT'D)

LIST OF FIGURES (CONT'D)

LIST OF FIGURES (CONT'D)

LIST OF TABLES

SECTION 1
INTRODUCTION

Many seismically isolated buildings have been designed and analyzed according to the minimum requirements of Chapter 17 of ASCE/SEI 7-10 standard (ASCE, 2010). ASCE/SEI 7-16 (ASCE, 2017) specifies the current ASCE minimum requirements for isolated structures. Both ASCE standards require that the isolation system be detailed to accommodate the displacement demand calculated in the Risk-Targeted Maximum Considered Earthquake (MCE_R), where this displacement is the average of peak values calculated in seven nonlinear response history analyses. Both procedures permit the use of a response modification coefficient (R_I factor) between 1.0 and 2.0 depending on the seismic force-resisting system used. For the case of the ASCE/SEI 7-10 standard, the forces and drifts for the design are based on calculations using the design response (DE) spectrum, which is defined as being 2/3 of the MCE_R spectrum. For the case of the ASCE/SEI 7-16 standard, the forces and drifts for the design are based on calculations using the MCE_R spectrum. Many seismically isolated buildings in the United States have been designed using the ASCE/SEI 7-10 minimum requirements. There are exceptions in which stringent criteria have been employed. Examples are hospitals in California where often project-specific design criteria require the use of an R_I factor of unity for the effects of the DE or MCE_R and larger displacement capacity isolators than the minimum required.

The use of the minimum requirements of the ASCE/SEI 7 standards presumably ensures the minimum acceptable level of safety by preserving the lives of the occupants. It is well recognized that these minimum ASCE design requirements do not serve the resiliency objective of avoiding damage in order to maintain facility functionality. An Executive Order issued in 2016 by the President of the United States (Executive Order 13717, 2016, Hayes et al., 2017) clearly recognizes this fact and states the following: "The Federal Government recognizes that building codes and standards primarily focus on ensuring minimum acceptable levels of earthquake safety for preserving the lives of building occupants. To achieve true resilience against earthquakes, however, new and existing buildings need to exceed those codes and standards to ensure, for example, that the buildings can continue to perform their essential functions following future earthquakes." The Executive Order continues to instruct all federal agencies to "go beyond the codes and standards and ensure that buildings are fully earthquake resilient."

Questions may then arise. (a) Is the probability of collapse of seismically isolated structures designed by the minimum design criteria acceptably low? (b) What should be the criteria for design in terms of R_I and isolator displacement capacity to achieve acceptable probability of collapse? (c) What does isolation achieve in terms of performance measures like peak story drift, residual story drift and floor accelerations?

Some studies have already addressed issues related to these questions. Kikuchi et al. (1995) studied the inelastic response of a two-degree-of-freedom (2-DOF) representation of seismically isolated structures without any consideration for failure of either the structural or the isolation system. The study raised a concern that designs of seismically isolated structures with reduced lateral shear force (equivalently, with a large R factor) can have significant inelastic action and unacceptable behavior. A more recent study (Nakazawa et al, 2011) again made use of the 2-DOF system but enhanced to have non-simulated generic isolation system failure and superstructure failure (assumed to occur at ductility of 4.0) and employed contemporary procedures to determine the collapse margin ratio based on the FEMA P695 procedures (FEMA, 2009). The main contribution of the work was to study the effects of limiting the displacement demand on the isolators by use of moat walls of varied clearance and behavior. Following the Japanese practice of seismic design, the strength of the superstructure was assumed in the range of 0.15 to 0.40 of the superstructure weight (common practice in Japan is the use of 0.3). The study observed that isolated structures have a low level of damage (essentially elastic response) until a certain level of seismic intensity is reached where significant inelastic action occurs for small increases in the seismic intensity.

Studies of Erduran et al (2011) and Sayani et al (2011) compared the inelastic response of conventional and seismically isolated steel braced and moment-resisting 3-story frames designed by the minimum criteria of ASCE 7 (that of 2005) and with unlimited capacity for the isolators. The studies concluded that the seismically isolated frames exhibited lower structural yielding, story drifts, residual story drifts and floor accelerations than comparable conventional frames for seismic events characterized as frequent, design and maximum earthquake. The studies did not provide any information on the collapse of the analyzed structures as the structural model did not have capability of simulating large deformations in the elements of structural systems. However, the studies pointed to interesting observations that (a) allowing for inelastic behavior of the isolated structure limited the displacement demand in the isolators and (b) designing for elastic behavior could have resulted in failure of the isolators if they had limited displacement capacity.

A study of Terzic et al (2012) compared the lifecycle cost of seismically isolated structures designed with different structural systems of various R_I factors. The study demonstrated improved performance and significant reduction of lifecycle cost when the design utilizes an R_I factor of unity in the DE.

The development of the performance assessment methodologies of FEMA P695 (FEMA, 2009) allowed for more rigorous studies of the performance of isolated structures. One of the examples in FEMA P695 involves seismically isolated buildings in which failure of the superstructure was simulated and the isolation system was represented by a generic model together with a displacement-limiting moat wall of various clearances. The structure was a 4-story reinforced concrete building of either a special perimeter moment frame or a special space frame. Concentrating on the code-complaint designs (with R_I=2 in the DE), the study demonstrated acceptable collapse margin ratios, which progressively reduced as the moat wall clearance reduced and the space frame was changed from space to perimeter frame.

A more recent study of Masroor and Mosqueda (2015) utilized models similar to those in the studies of Erduran et al (2011) and Sayani et al (2011) and followed the paradigm of examples of the seismically isolated buildings in FEMA (2009), utilized three-dimensional building models with an improved moat wall model and bi-directional seismic excitation but did not consider failure of the isolators. The results showed that steel intermediate moment frames designed for the DE with an R_I =1.67 and steel ordinary concentrically braced frames designed with R_I =1 had acceptable collapse margin ratios per FEMA (2009) when the size of isolators was sufficiently large to avoid failure of the isolator. Barely acceptable probabilities of collapse were calculated when the moat wall was placed at the minimum required displacement capacity in the MCE_R. The calculations were based on the use of adjusted values of the probability of collapse for accounting for the spectral shape effects (epsilon) using the simplified FEMA P695 procedures (FEMA, 2009). It will be argued in this report that the simplified procedure for the spectral shape effects provided in FEMA P695 does not apply for seismically isolated structures with stiffening behavior and that direct studies, as those used in FEMA P695 for the development of the simplified procedure, are required to properly calculate the effects of spectral shape.

Chimamphant and Kasai (2016) investigated the seismic response of nonstructural components in seismically isolated buildings and compared it to that of comparable conventionally designed buildings by using multi-degree-of-freedom shear-beam models. Failure in the superstructure or the isolation system was ignored and mechanisms that limit the isolator displacement (ex. retaining walls) were not considered. The study used the methodologies described in FEMA P695 (FEMA, 2009) and FEMA P58 (FEMA, 2012[a]) and demonstrated that seismically isolated buildings have better performance than comparable non-isolated buildings but the improvement of performance reduces as the height of the building increases.

Recently, Shao et al. (2017) focused on a 3-story concentrically braced steel frame structure designed for R_I=1 in the MCE$_R$ and investigated the reliability of the ASCE/SEI 7-16 minimum provisions, as well as enhanced designs by providing either increased isolator displacement capacity or providing isolators with hard (moat wall) or soft stopping mechanisms. The main conclusions of the study were that: (a) the isolator displacement capacity needs to be increased by at least 1.8 of the minimum code-prescribed value in order to achieve the code-targeted reliability when no displacement restrainers are provided; (b) smaller displacement capacities can be used when displacement restrainers are utilized but with additional requirements for increased ductility capacity in the superstructure and (c) a total isolator displacement capacity (including the capacity of soft stops) of at least 1.5 times the displacement demand in the MCE$_R$ and an isolator shear strength of at least 3.0 times the base shear in the MCE$_R$ are needed to achieve the required reliability. The study did not consider the spectral shape effects per FEMA P695 (FEMA, 2009) as the simplified method presented in FEMA P695 for considering these effects does not truly apply for seismically isolated structures of large effective period. Accordingly, probabilities of failure must have been overestimated.

This report also investigates the reliability of the ASCE/SEI 7 provisions by concentrating on an archetypical 6-story perimeter frame building that has been previously studied in examples of seismic isolation design and analysis in McVitty and Constantinou (2015). Perimeter steel special concentrically braced frames (SCBF) and special moment resisting frames (SMRF) for this building are designed for a location in California with an R_I factor of 2.0 (per minimum requirements of ASCE/SEI 7-10), 1.5 and 1.0 in the DE and with R_I=2.0 (per minimum requirements of ASCE/SEI 7-16) and 1.0 in the MCE_R when seismically isolated. Also, the case of steel ordinary concentrically braced frames (OCBF) permitted by ASCE/SEI 7-16 with R_I=1.0 is considered. The isolation system for these cases consists of triple Friction Pendulum (FP) isolators having a displacement capacity at initiation of stiffening equal to $1.0D_M$ (per minimum requirements of ASCE/SEI 7-10 and 7-16), $1.25D_M$ and $1.5D_M$, where D_M is the displacement demand in the MCE_R (torsion is not accounted for so the displacement considered is D_M instead of D_{TM}, which would be 1.1 to 1.2 times larger than D_M in the studied systems). For the OCBF the displacement capacity of the isolators at initiation of stiffening is $1.25D_M$, which is permitted by ASCE/SEI 7-16. The stiffening behavior of the triple FP isolators serves as a displacement restrainer for larger displacements than the assumed capacities. Additionally, double concave sliding isolators are considered and designed per minimum criteria and without a displacement restrainer, a practice permitted by the ASCE/SEI 7 standards (and a common practice in Europe, e.g., Ponzo et al, 2017). Moreover, representative results are presented for cases in which a moat wall is used at the minimally allowed distance per ASCE/SEI 7 standards (displacement capacity D_M) and at larger distances. Non-isolated structures, also with braced and moment frame configurations, are designed and studied.

This study presents results on (1) the conditional probability of collapse on the occurrence of the MCE_R of the designed isolated structures and comparable non-isolated structures, and (2) information on the mean annual frequency of exceedance of the peak story drift ratio, the residual story drift ratio and the peak floor and roof acceleration. It is shown that (a) seismically isolated buildings designed by the minimum criteria of ASCE/SEI 7-10 or 7-16 may have unacceptable probability of collapse in the MCE_R, (b) the probability of collapse in the MCE_R is acceptable (and depending on the structural system much less than 10%) and the design may also meet criteria of improved performance in terms of story drift, residual drift and floor acceleration when the structure is designed for R_I=1.0 (either for the DE or the MCE_R) and the isolators have a displacement capacity at initiation of stiffening equal to $1.5D_M$, (c) the behavior described in item (b) is also achieved by the use of moat walls instead of stiffening isolators, also placed at distance $1.5D_M$, (d) reducing the R_I factor may not provide any advantage unless the displacement capacity of the isolators is accordingly increased (as then collapse is due to failure of the isolators), (e) designs that meet the minimum criteria of ASCE/SEI 7-10 or 7-16 and without any displacement restrainer have unacceptably high probabilities of collapse, (f) OCBF designed by the minimum criteria of ASCE/SEI 7-16 have marginally unacceptable probabilities of collapse which can be improved by increasing the displacement capacity of the isolators, (g) seismically isolated structures designed by the minimum criteria of ASCE/SEI 7 and supplemented with moat walls having a gap equal to the displacement demand in the MCE_R as calculated by the procedures of ASCE/SEI 7 have unacceptable probabilities of collapse that are essentially the same as those of similarly designed isolated structures without a moat wall, and (h) seismically isolated structures designed per criteria in item (b) above offer lower mean annual frequencies of exceeding important limits on story drift ratio, residual story drift ratio and peak floor acceleration than comparable non-isolated structures.

SECTION 2
STRUCTURES AND ISOLATION SYSTEMS CONSIDERED

A 6-story archetypical steel building is considered. The building was used in examples in the SEAONC Volume 5 Seismic Design Manual (SEAONC, 2014) and later used in examples of application of the ASCE/SEI 7-16 analysis and design procedures for isolated buildings in McVitty and Constantinou (2015). Figure 2-1 shows plan and view of the building. Its lateral force resisting system consists of four perimeter frames that are configured as special concentrically braced frames (SCBF), or special moment resisting frame (SMF) or ordinary concentrically braced frames (OCBF). The total seismic weight of the building when seismically isolated is 12065.4kip. When non-isolated the weight is 10180.6kip. The building is assumed located on soil class D in San Francisco, CA (Latitude 37.783°, Longitude -122.392°) with MCE_R spectral acceleration values of S_{MS}=1.5g and S_{M1}=0.9g. For the DE, the parameters are S_{DS}=1.0g and S_{D1}=0.6g.

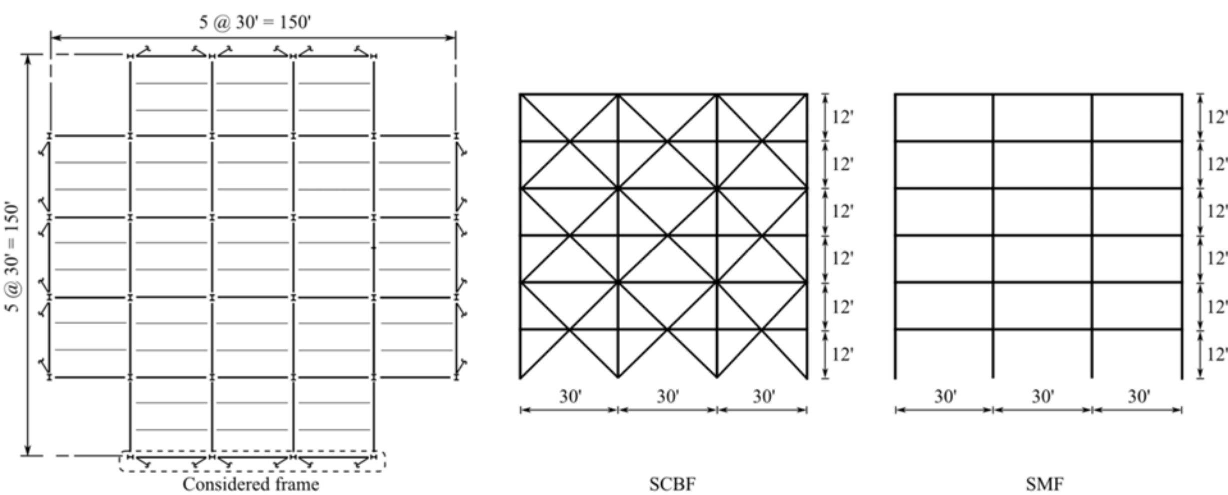

Figure 2-1 Archetypical Building Plan and Views of Braced and Moment Frames

The isolation system consists of triple FP isolators (placed below each column) having the geometric and frictional properties determined in McVitty and Constantinou (2015) but the outer concave plates of the isolators were selected to have three different sizes so that the displacement capacities were varied. Figure 2-2 shows cross sections of the three triple FP isolators considered, having displacement capacities of (a) the minimum required by the criteria of ASCE/SEI 7 (capacity D_M at initiation of stiffening) and (b) increased capacities of 1.25 D_M and 1.5D_M at initiation of stiffening. Note that the internal construction of the three isolators is the same so that their frictional properties are the same for the same conditions of load and motion. The force-displacement relationship for these isolators is shown in Figure 2-3 together with values of the displacement capacity at initiation of stiffening, $D_{Capacity}$, and the ultimate displacement, $D_{Ultimate}$, when the isolator internal parts collapse as calculated on the basis of the theory of Sarlis and Constantinou (2016) in the lower bound friction condition. Note that the isolators may also yield prior to reaching $D_{Ultimate}$ when the lateral force in the stiffening regime of the bearings exceeds the strength of the restrainer ring. While this was modelled in the analysis it did not occur as the shear force did not reach the strength of the ring as calculated using the theory of Sarlis and Constantinou (2016). The displacement capacity provided was D_M (or a multiple of it) and not D_{TM} (which includes the effects of torsion) as the analysis for the reliability assessment was based on two-dimensional representations of the building and torsion was not included.

Two more isolator types were considered without a restrainer ring so that they did not exhibit stiffening behavior. They were designed as Double Concave (DC) isolators (Fenz and Constantinou, 2006) with the same curvature as the triple FP isolators. Both isolators have the same contact area of 11inch as the triple FP isolators. Of the two DC isolators, isolator DC-1 has an ultimate displacement capacity equal to D_M, whereas isolator DC-2 has the same concave plate diameter as the smallest triple FP isolator (TFP-1) and thus a larger ultimate displacement capacity than D_M, determined to be $1.25D_M$ (displacement when the inner slider reaches the edge of the concave plate plus half of the contact diameter of 11inch). Isolators DC-1 is permitted by the ASCE/SEI 7 standards. Isolators with the characteristics of DC-1 and DC-2 have been used in applications in Europe and South America. Force-displacement relationships for these isolators are presented in Figure 2-3.

The frictional properties of the triple FP isolators for high-speed conditions are presented in Table 1 together with values of the property modification factors used to determine the frictional properties (McVitty and Constantinou, 2015). Note that the properties were determined on the basis of prototype test data for similar isolators and use of the procedures in ASCE/SEI 7-16. The values of friction in Table 1 are for high-speed conditions and are different for the interior and exterior isolators due to the different gravity load carried by them. The large difference between the lower and upper bound values of friction reflect (a) the uncertainties due to availability of test data on similar rather than the actual isolators, and (b) the large pressure at which the isolators operate that result in more variability due to heating (McVitty and Constantinou, 2015). For the DC bearings the values of friction coefficient are also presented in Table 1 where are seen to be slightly less than those of the outer surface of the triple FP isolators. The friction force has been calculated as the zero displacement force intercept for the triple FP bearings divided by the normal load. The system property modification factors were assumed to be the same.

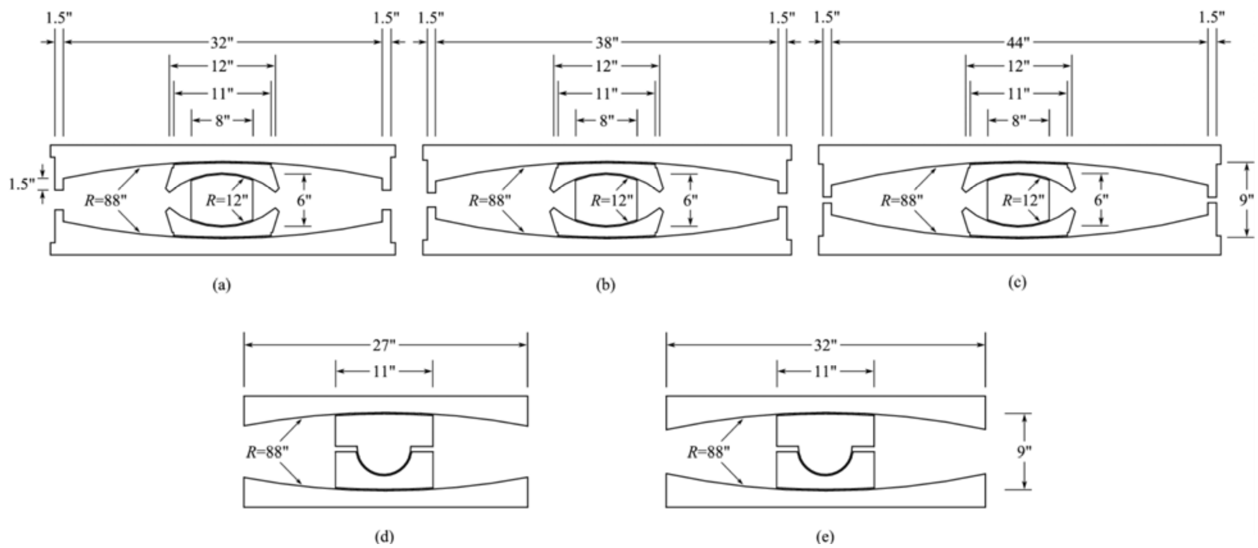

Figure 2-2 Triple FP (TFP) and Double Concave (DC) Isolators of Different Displacement Capacities; (a) TFP-1, (b) TFP-2, (c) TFP-3, (d) DC-1 and (e) DC-2

Table 2-1 Upper and Lower Bound Friction Properties of Triple FP and Double Concave Isolators

		Interior Isolators		Exterior Isolators	
Isolator Type	Sliding Surface	Outer (μ_1=μ_4 or μ)	Inner (μ_2=μ_3)	Outer (μ_1=μ_4 or μ)	Inner (μ_2=μ_3)
Triple Friction Pendulum	Nominal	0.052	0.017	0.073	0.017
	λ_{max}	1.67	1.29	1.39	1.29
	λ_{min}	0.81	0.85	0.58	0.85
	Upper bound	0.087	0.022	0.101	0.022
	Lower bound	0.042	0.015	0.042	0.015
Double Concave	Upper bound	0.080	NA	0.093	NA
	Lower bound	0.039	NA	0.039	NA

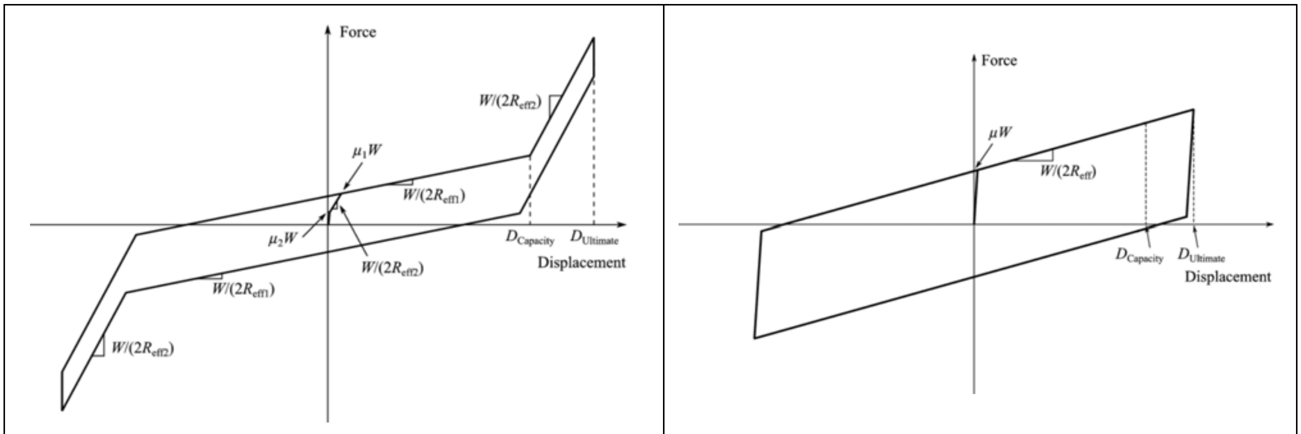

TFP-1 $D_{Capacity}$=20.4in (D_M), $D_{Ultimate}$=26.9in (1.3D_M) TFP-2 $D_{Capacity}$=26.1in (1.25D_M) $D_{Ultimate}$=32.6in (1.6D_M) TFP-3 $D_{Capacity}$=31.8in (1.5D_M) $D_{Ultimate}$=38.3in (1.9D_M)	DC-1 $D_{Capacity}$=20.4in (D_M), $D_{Ultimate}$=20.7in (D_M) DC-2 $D_{Capacity}$=20.4in (D_M), $D_{Ultimate}$=25.4in (1.25D_M)

Figure 2-3 Force-Displacement Relationships of Triple FP (Left) and Double Concave (Right) Isolators

Analyses of the isolated building were conducted per procedures in ASCE/SEI 7 for the MCE_R to determine the isolator displacement demands and the base shear force. Analyses were also conducted for the DE per ASCE/SEI 7-10 in order to calculate the base shear force in the DE. Response History Analysis (RHA) and Equivalent Lateral Force (ELF) procedures were used. For the RHA, the model of analysis was three-dimensional of which details, including details on the motions used and the scaling procedure, are presented in McVitty and Constantinou (2015). Results are summarized in Tables 2 and 3. These results were obtained using seven pairs of amplitude-scaled motions per procedures in ASCE/SEI 7 (both 2010 and 2016). The superstructure was assumed elastic. Torsion was not considered. That is, the calculation of the isolator displacement demand included the effects of bi-directional excitation but not torsional effects. The frame properties used in the RHA and ELF are those in Tables 4 and 5 for SCBF and SMF with R_I=2.0. The effects that the superstructure increased stiffness for the other designs may have had on the isolator displacement demand and base shear force were assumed insignificant.

The tables include design values of base shear per frame and the value of isolator displacement D_M for design based on the criteria of ASCE/SEI 7. There are no or insignificant differences in the calculated isolator displacements and in the base shear force for the two configurations. Accordingly, for both configurations the following values were used in design: isolator displacement D_M=20.7in (average of the two values) and base shear force of 727.6kip in the DE and 883.5kip in the MCE_R (shear force for elastic conditions). Based on these values, frames were designed as follows: (a) per minimum criteria for R_I=2.0 for the DE (per ASCE/SEI 7-10) and for the MCE$_R$ (per ASCE/SEI 7-16), (b) for R_I=1.5 and 1.0 for the DE and (c) for R_I=1 for the MCE$_R$. Also, comparable non-isolated structures were designed with R=6, Ω_0=2, C_d=5 for the SCBF and with R=8, Ω_0=3, C_d=5.5 for the SMF. The design utilized member forces determined in static analysis using the lateral forces prescribed by the ELF procedures of ASCE/SEI 7. Note that for the non-isolated structures the lateral forces were based on the DE (2/3rd of the MCE$_R$) for both versions of the ASCE/SEI 7 standard. The section properties for the beams, columns and braces of the designed frames are presented in Tables 3 and 4. Steel has minimum yield strength F_y equal to 42ksi for braces (round HSS) and 50ksi for columns and beams. The expected yield strengths F_{ye} are 58.8ksi and 55ksi, respectively (American Institute of Steel Construction, 2010).

The results in Tables 2 and 3 demonstrate that the frames meet the drift criteria of the ASCE/SEI 7 standards (ASCE, 2010 and 2016), Section 17.5.6 as the maximum story drift is less than 0.015 of the story height. Note that analysis was performed for the frames designed with R_I=2.0 (the drift is less than the values in Tables 2 and 3 when R_I is less than 2.0). The results of RHA on drift are not presented as the superstructure was assumed elastic and there are no specified limits for such conditions (rather there are limits in Section 17.6.4.4 of ASCE /SEI 7 for analysis using nonlinear force-displacement characteristics for the structural elements).

The SCBF designed with R_I=1.0 in the MCE$_R$ was also analyzed assuming that it behaves as an ordinary concentrically braced frame (OCBF) with isolators having the characteristics of isolators TFP-2 with displacement capacity equal to 1.25D_M and TFP-3 with displacement capacity equal to 1.5D_M. This structural configuration and is permitted per Section 17.2.5.4 of ASCE/SEI 7-16 provided that the isolators have a displacement capacity of at least 1.2D_M. In the RHA for the assessment of performance, the story drift ratio limit at collapse was assumed to be 2% for the OCBF (Masroor and Mosqueda 2015), whereas it was 5% for the SCBF (Sabelli et al., 2013).

Two of the developed designs (SCBF and SMF, R_I=1.0 in the DE, triple FP isolator TFP-3 with $D_{Capacity}$=1.5D_M and $D_{Ultimate}$=1.9D_M, see Figure 2-3) were further analyzed to investigate whether they meet the "Enhanced Structural and Non-structural Design Criteria" of the REDi Rating System (Arup, 2013) for a rating of "Gold" or "Platinum". This enhanced design includes a recommendation to design for an isolator displacement capacity of 1.9D_M, and to have essentially elastic response with a residual drift ratio of less than 0.5% for the "Design Level Earthquake", defined as having a 475 year return period. Analysis of the isolated structures was conducted with the inelastic two-dimensional representation used in the incremental dynamic analysis (to be described later) using the fault-normal (FN) components of the seven motions used in the three-dimensional analysis. These components needed to be scaled by a different factor than in the three-dimensional analysis. (See Table A-1 in McVitty and Constantinou, 2015 where the scale factors are 3.9, 1.7, 3.0, 3.2, 3.9, 3.9 and 3.9 for motions 1 to 7). In the two dimensional analysis, the FN components of these motions were scaled by factors 4.0, 1.3, 1.2, 3.0, 3.5, 5.0 and 5.0, respectively, based on Sections 16.1.3.1 and 17.3.2 of ASCE/SEI 7-10 and 16.2.3 and 17.3.3 of ASCE/SEI 7-16. The analysis resulted in peak drift ratio (average of seven analyses) of 0.15% and a residual drift ratio of 0.01% for the SCBF and in a peak drift ratio of 0.87% and a residual drift ratio of 0.03% for the SMF. Both designs meet the drift criteria of the REDi Rating System (Arup, 2013) for a rating of "gold" or "platinum".

However, it will be shown later in this document that the SMF design has higher mean annual frequencies of exceeding specific residual drift ratio and floor peak acceleration limits than the SCBF design. It will be shown that the SMF design that meets the REDi criteria for gold rating has a 30% probability of exceeding the limit of 0.5% in peak drift ratio and 37% probability of exceeding the peak floor acceleration limit of 0.3g in 50 years. In contrast, the SCBF design that meets the REDi criteria for gold rating has, respectively, probabilities of 2.3% and 6.9%. The SCBF design that has these low probabilities of developing any damage in the lifetime of 50 years also meets the criteria of a seismic isolation standard for continued functionality developed by Zayas et al (2017) and implemented in the design and construction of some hospitals and important structures utilizing triple FP isolators. In this standard, seismically isolated structures meet the REDi "gold" rating when designed with R_I=1 in the DE and the peak story drift ratio is limited to 0.4% and the 5%-damped floor acceleration response spectra are less than 0.6g (in a sense that the median value within the period range of zero to 5sec is less than 0.6g) in the DE. In the same standard the criteria for the REDi "platinum" rating call for limits of 0.3% on peak drift ratio and 0.4g on floor spectral accelerations in the DE. The SCBF design meets the criteria of the standard for continued functionality for "platinum" rating (Zayas, 2017) as it has a peak story drift ratio of 0.15% and a median floor spectral acceleration of 0.3g. The SMF design does not meet the criteria of the standard for continued functionality as the peak story drift ratio is 0.87%.

Table 2-2 Isolator Displacement, Peak Story Drift Ratio and Base Shear Force for Braced Frame

Earthquake	Quantity	Lower Bound Friction	Upper Bound Friction
DE	RHA Base Shear X (kip)	514.8	705.0
	RHA Base Shear Y (kip)	485.1	706.0
	ELF Base Shear (kip)	699.7	799.4
	Design Base Shear (kip) per ASCE/SEI 7-10	727.6	
	ELF Peak Story Drift Ratio	0.0018	
MCE_R	RHA Base Shear X (kip)	796.0	852.7
	RHA Base Shear Y (kip)	687.3	856.5
	ELF Base Shear (kip)	1049.5	1212.5
	Design Base Shear (kip) per ASCE/SEI 7-16	883.5	
	ELF Peak Story Drift Ratio	0.0018	
	RHA Isolator Resultant Displacement (in)	21.1	13.6
	ELF Isolator Displacement (in)	25.1	15.8
	D_M (in)	21.1	
Base shear force is per frame			

Table 2-3 Isolator Displacement, Peak Story Drift Ratio and Base Shear Force for Moment Frame

Earthquake	Quantity	Lower Bound Friction	Upper Bound Friction
DE	RHA Base Shear X (kip)	515.5	726.3
	RHA Base Shear Y (kip)	491.7	656.8
	ELF Base Shear (kip)	699.7	799.4
	Design Base Shear (kip) per ASCE/SEI 7-10	727.6	
	ELF Peak Story Drift Ratio	0.0148	
MCE_R	RHA Base Shear X (kip)	757.7	885.8
	RHA Base Shear Y (kip)	695.7	822.1
	ELF Base Shear (kip)	1049.5	1212.5
	Design Base Shear (kip) per ASCE/SEI 7-16	883.5	
	ELF Peak Story Drift Ratio	0.0144	
	RHA Isolator Resultant Displacement (in)	20.4	13.7
	ELF Isolator Displacement (in)	25.1	15.8
	D_M (in)	20.4	
Base shear force is per frame			

Table 2-4 Sections of Columns and Braces of SCBF and SMF in Isolated and Non-Isolated Buildings

Story		SCBF						SMF					
		Isolated					Non-isolated	Isolated					Non-isolated
		ASCE 7-10			ASCE 7-16			ASCE 7-10			ASCE 7-16		
		R_I=1.0	R_I=1.5	R_I=2.0	R_I=1.0	R_I=2.0	R_I=6.0	R_I=1.0	R_I=1.5	R_I=2.0	R_I=1.0	R_I=2.0	R_I=8.0
6	Column	W12x35	W12x35	W12x35	W12x35	W12x35	W12x35	W24x94	W21x111	W21x93	W24x146	W24x131	W21x147
	Brace	HSS4.5x0.237	HSS4x0.22	HSS4x0.188	HSS4.5x0.337	HSS4x0.237	HSS5x0.25	-	-	-	-	-	-
5	Column	W12x35	W12x35	W12x35	W12x35	W12x35	W16x35	W24x94	W21x111	W21x93	W24x146	W24x131	W21x147
	Brace	HSS6x0.375	HSS5x0.5	HSS5x0.312	HSS6x0.5	HSS5x0.5	HSS6x0.5	-	-	-	-	-	-
4	Column	W12x58	W12x58	W12x58	W12x58	W12x58	W12x58	W24x146	W21x111	W27x129	W24x207	W24x162	W27x194
	Brace	HSS6.875x0.5	HSS6x0.5	HSS6x0.375	HSS7.5x0.5	HSS6x0.5	HSS7x0.5	-	-	-	-	-	-
3	Column	W12x58	W12x58	W12x58	W12x58	W12x58	W12x58	W24x146	W21x111	W27x129	W24x207	W24x162	W27x194
	Brace	HSS6.875x0.5	HSS6x0.5	HSS6x0.375	HSS7.5x0.5	HSS6x0.5	HSS7x0.5	-	-	-	-	-	-
2	Column	W12x96	W12x96	W12x96	W12x96	W12x96	W12x96	W27x235	W27x146	W27x146	W27x307	W27x235	W27x217
	Brace	HSS7.5x0.5	HSS7x0.375	HSS6.875x0.312	HSS8.625x0.5	HSS6.625x0.5	HSS8.625x0.5	-	-	-	-	-	-
1	Column	W12x96	W12x96	W12x96	W12x96	W12x96	W12x96	W27x235	W27x146	W27x146	W27x307	W27x235	W27x217
	Brace	HSS7.5x0.5	HSS7x0.375	HSS6.875x0.312	HSS8.625x0.5	HSS6.625x0.5	HSS8.625x0.5	-	-	-	-	-	-

Table 2-5 Sections of Beams of SCBF and SMF in Isolated and Non-Isolated Buildings

Floor	SCBF						SMF					
	Isolated					Non-isolated	Isolated					Non-isolated
	ASCE 7-10			ASCE 7-16			ASCE 7-10			ASCE 7-16		
	R_I=1.0	R_I=1.5	R_I=2.0	R_I=1.0	R_I=2.0	R_I=6.0	R_I=1.0	R_I=1.5	R_I=2.0	R_I=1.0	R_I=2.0	R_I=8.0
Roof	W16x26	W16x26	W16x26	W16x26	W16x26	W16x26	W18x65	W18x50	W16x45	W18x86	W18x71	W21x62
6	W16x26	W16x26	W16x26	W16x26	W16x26	W16x26	W18x65	W18x50	W16x45	W18x86	W18x71	W21x62
5	W16x26	W16x26	W16x26	W16x31	W16x26	W16x26	W24x117	W24x84	W24x76	W24x176	W24x131	W24x146
4	W16x26	W16x26	W16x26	W16x31	W16x26	W16x26	W24x117	W24x84	W24x76	W24x176	W24x131	W24x146
3	W16x26	W16x26	W16x26	W16x31	W16x26	W16x26	W18x175	W24x103	W24x94	W18x192	W18x175	W24x176
2	W16x26	W16x26	W16x26	W16x31	W16x26	W16x26	W18x175	W24x103	W24x94	W18x192	W18x175	W24x176
1	W18x50	W18x50	W18x50	W18x50	W18x50	-	W21x201	W30x124	W27x129	W21x201	W21x201	-

Figure 2-4 presents representative pushover curves for the analyzed SCBF. The model used is described in Section 3. The results shown represent the base shear force versus the roof displacement of half of the building when the lateral force pattern used in the analysis is proportional to the floor mass times the floor modal displacement. The pushover curves of the non-isolated and six isolated braced frames are shown. The latter apply for the case of isolator TFP-1 with $D_{Capacity}$=20.4in (D_M), $D_{Ultimate}$=26.9in (1.3D_M) (see Figures 2-2 and 2-3) with various values of the R_I factor reflecting increasing strengths in the superstructure per ASCE/SEI 7-10 (R_I=1, 1.5 and 2) and ASCE/SEI 7-16 (R_I=1 and 2). Also, the case of the minimally designed frame (R_I=2) per ASCE/SEI 7-10 and with a moat wall placed at a distance equal to $D_{Capacity}$=20.4in (D_M) is presented. The properties of the isolators are those of the lower bound condition per Table 2-1. The graphs indicate the point when the isolator failed (by collapse of its internal parts). Each pushover curve is shown beyond the isolator collapse point (in dashed line) to denote the behavior when isolators of unlimited ultimate displacement but the same $D_{Capacity}$ (=20.4in) are assumed. Another point on the pushover curves shows the base shear and roof displacement when the maximum story drift reaches the limit of 5%, which is presumed to be the ultimate drift for the braced frame. Quantity x denotes the story at which the maximum drift occurs (first story for all cases).

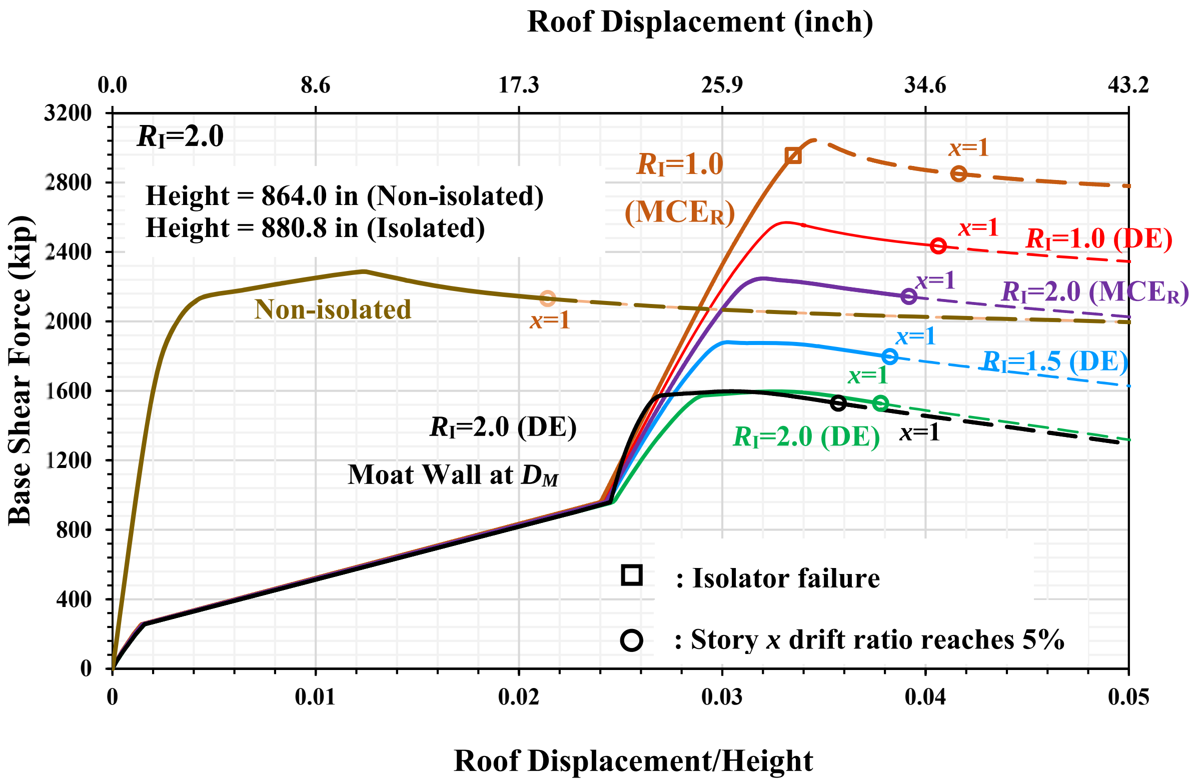

Figure 2-4 Pushover Curves of SCBF in Case of Isolator TFP-1 with $D_{Capacity}$=D_M=20.4in

An immediate observation in these pushover curves is that failure of the isolator occurs prior to failure in the superstructure only in the case of the strongest frame designed for R_I=1 in the MCE$_R$. This behavior is the result of delayed inelastic action in the superstructure as R_I is reduced, which in turn results in increased demand for isolator displacement. When the structure yields, the isolators stop deforming. This demonstrates that increases in the strength of the superstructure must be accompanied by increases in the displacement capacity of the isolators.

An important observation is on the shape of the pushover curves. While the shape of the curve for the non-isolated structure can be reasonably approximated by an elastoplastic representation, the pushover curves of the isolated structures cannot. This observation led the authors to avoid the use of the simplified procedure of FEMA P-695 (FEMA, 2009) for accounting for the spectral shapes effects as that would have required an elastoplastic representation of the pushover curves. Instead, a direct procedure was used for the estimation of the spectral shape effects. We should note that in examples of collapse performance evaluation of isolated structure in FEMA P-695 (FEMA, 2009) and in Masroor and Mosqueda (2015), stiffening behavior as that shown in Figure 2-4 was not considered so that the pushover curves could be used in the application of the simplified procedure for spectral shape effect estimation. While this is inappropriate given the nature of the pushover curves seen in Figure 2-4, errors in the estimation of the spectral shape effects must be small as the spectral shape factors estimates by direct procedures in this report are not very different from those of the aforementioned studies based on the simplified procedure of FEMA P-695.

Important in Figure 2-4 is the behavior of the system with a moat wall, which has a pushover curve that is essentially the same as the pushover curve of the system with just stiffening FP isoaltors. It should be noted that for the analysis the stiffness of the moat wall was assumed to be 1000 times larger than the stiffness of the TFP-1 isolator in the stiffening regime (see Figure 2-3), although use of smaller stiffness values did not produce any notably different results. The reason for this behavior is that inelastic action in the superstructure commences shortly after entering the stiffening regime of the isolator or after engaging the moat wall. This is better illustrated in the pushover curves of additional cases with moat walls that are presented in Figure 2-5. Only cases of R_I=2 in the MCE$_R$ (per ASCE/SEI 7-16) are considered with:

1) The minimally designed isolator TFP-1 without a moat wall and with a moat wall at the minimum distance D_M and then at a distance of 1.25D$_M$. In the latter case, placing the moat wall (at 1.25D_M) which is just short of the ultimate displacement capacity of the isolator (1.3D_M) would appear appropriate. However, it makes no difference in the pushover curves as the superstructure undergoes inelastic action prior to engaging the moat wall and the

isolators stop deforming. That is, the moat wall is not needed. It could have been needed if the superstructure was stronger (R_I factor less than 2) but the location of the wall would have depended on the superstructure strength.

2) The enhanced capacity isolator TFP-2 without a moat wall and with a moat wall placed at a distance of $1.25D_M$, which is the same as the displacement capacity of the isolator at initiation of stiffening.

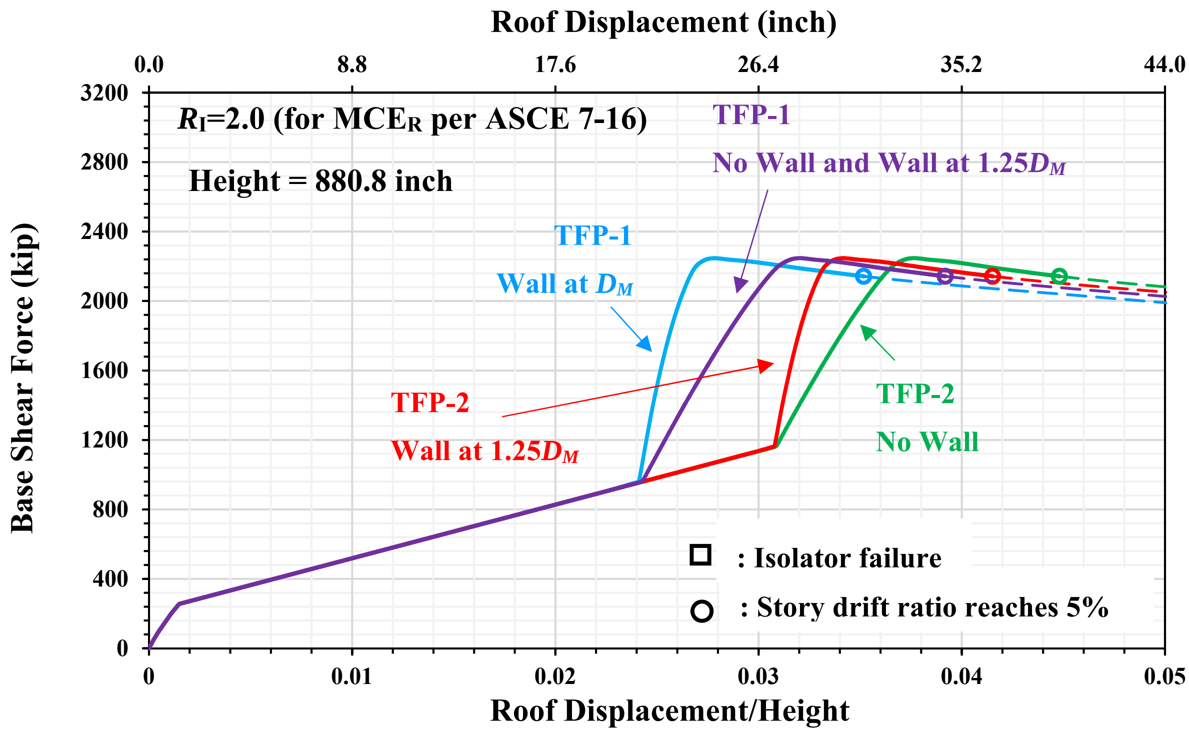

Figure 2-5 Pushover Curves of SCBF in Case of Isolators TFP-1 with $D_{Capacity}$=20.4in (=D_M) and TFP-2 with $D_{Capacity}$=26.1in (=$1.25D_M$) and Moat Walls Placed at Distances D_M and $1.25D_M$

The pushover curves in Figure 2-5 demonstrate that for a design with R_I=2 (for MCE_R) per ASCE/SEI 7-16 (also in Figure 2-4 the pushover curves for designs with the TFP-1 isolator and with and without a moat wall placed at distance at D_M) failure occurs due to excessive deformation in the superstructure and not by failure of the isolators. Also, the pushover curves show small differences when a moat wall is added by comparison to the system without the moat wall provided that the moat wall is placed at a distance equal to $D_{Capacity}$ of the isolator (i.e., isolator TFP-1 with $D_{Capacity}=D_M$ and moat wall at D_M or isolator TFP-2 with $D_{Capacity}=1.25D_M$ and moat wall at $1.25D_M$). Accordingly, we expect that the addition of the moat wall will not significantly affect the probability of collapse by comparison to the use of triple FP isolators with stiffening behavior. Simply the stiffness for displacements beyond $D_{Capacity}$ is different but not substantially different as seen in Figure 2-5. Note that while in the analyses the stiffness of the moat wall was assumed equal to 1000 times that of the FP isolator in the stiffening regime, the difference in stiffness seen in Figures 2-4 and 2-5 is much less. This is due to the fact that the total stiffness is controlled by the stiffness of the yielding superstructure which is much less than that of the moat wall. This behavior is expected to dominate as long as collapse of the structure is not controlled by collapse of the isolators. However, when collapse of the structures is controlled by collapse of the isolators, it is expected that the use of moat walls may reduce the probability of collapse. Examples presented in Section 4 show this to be sometimes the case.

While the results in Figures 2-4 and 2-5 apply for the SCBF, the discussion and conclusions also apply for the SMF. Figure 2-6 shows pushover curves for the SMF. The cases of stiffening isolators and moat walls result in even closer curves than those of the SCBF in Figure 2-5. Nevertheless, results presented in Section 4 show that for the SMF the probability of collapse is reduced when moat walls are used by comparison to the case of the use of equivalent stiffening triple FP isolators. While in the two cases the probabilities of collapse are very low, the difference is due to differences in the mechanisms of collapse: failure of the superstructure in the case of use of moat walls and collapse of the isolators in the case of using stiffening isolators without moat walls. This behavior is exaggerated when the R_I factor is reduced so that inelastic action in the superstructure is delayed and there are larger isolator displacement demands.

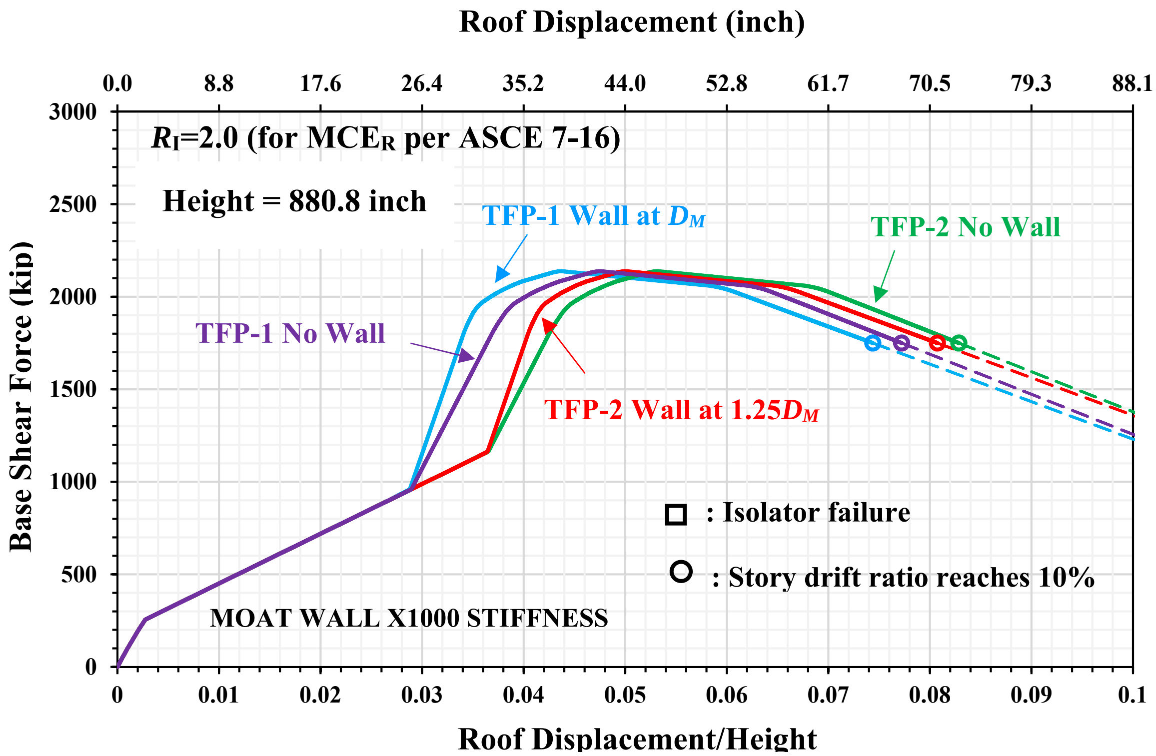

Figure 2-6 Pushover Curves of SMF in Case of Isolators TFP-1 with $D_{Capacity}$=20.4in (=D_M) and TFP-2 with $D_{Capacity}$=26.1in (=1.25D_M) and Moat Walls Placed at Distances D_M and 1.25D_M

SECTION 3
MODELS FOR ANALYSIS

Analysis was performed in program OpenSees (McKenna, 1997) using a two-dimensional representation of the structure as illustrated in Figures 3-1 and 3-2. Figure 3-1 presents the model for the braced isolated building. One of the two seismic force-resisting frames in a principal direction was explicitly modelled with details that will be described below. Each of the columns of the seismic force-resisting frame was supported by one exterior isolator. Half of the remaining building (two rows of columns) was also modelled with all its beams simply connected to the columns but for the connections of the girders on top of the isolators. Each of the columns of the gravity frame was supported by two interior isolators. The gravity and seismic force-resisting frames were placed parallel to each other and interconnected with horizontal rigid links at the locations marked in Figure 3-1 with “H” and with rigid links in the horizontal, vertical and rotational directions at the locations marked “H”, “V” and “R”, respectively. Tributary weights are also shown in the figure. Figure 3-2 presents the model for a non-isolated building where now is possible to locate the columns of the gravity frame at the two sides of the seismic force-resisting frame. The total seismic weight is 6032.7kip for the isolated model and 5090.3kip for the non-isolated model.

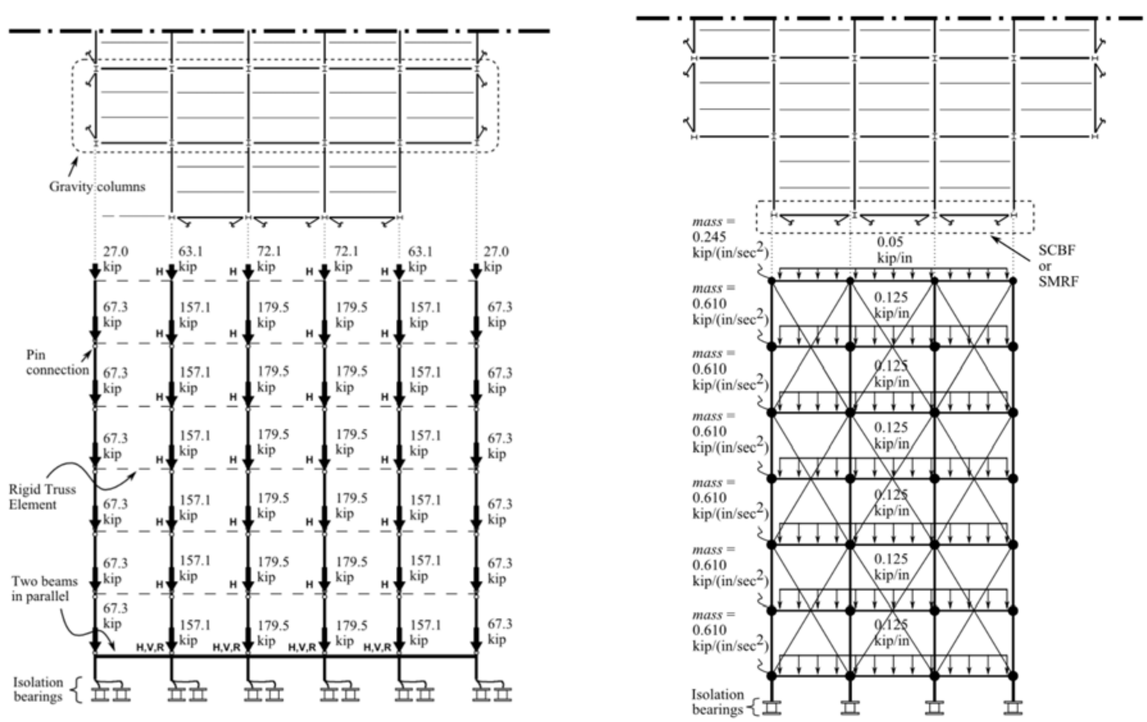

Figure 3-1 Representation of Gravity and Seismic Force-Resisting Frames of Isolated Building

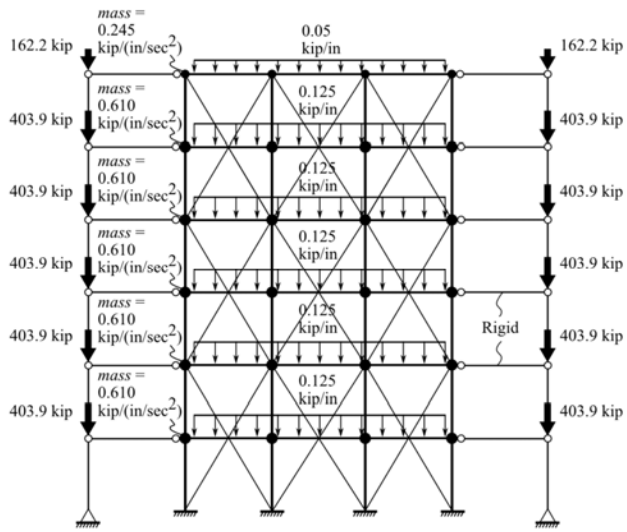

Figure 3-2 Representation of Non-Isolated Building

Columns, girders and braces were modeled based on Uriz and Mahin (2008) and Chen and Mahin (2012). The column and girder sections were modelled with eight fibers for each flange and with eight fibers for the web as shown in Figure 3-3. HSS round hollow tubes used for the braces were modelled with two fibers along the thickness and 16 fibers along the perimeter for a total of 32 fibers. Force-based nonlinear beam-column elements with four integration points were used to model the spread of plasticity across each fiber. The Giuffre-Menegotto-Pinto model ("Steel02" material in OpenSees; Fillippou et al., 1983) was used for the braces, girders and columns to describe smooth bi-linear behavior. The strain-hardening modulus was assigned values of 3% of the elastic modulus for the beams, 0.2% for the columns and 1% for the braces.

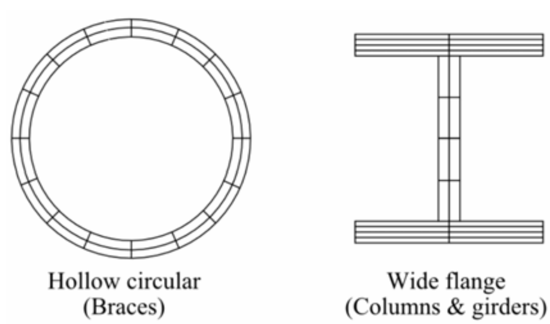

Figure 3-3 Fiber Discretization Used for HSS Brace and Wide Flange Column and Beam

The connections of girders to columns and to braces were modelled as shown in Figure 3-4. The connections between braces and their gusset plates were modeled as pins with zero-length as has been used in the many studies (Erduran et al, 2011, Chen and Mahin, 2012). An initial camber of 1% of the effective brace length (see Figure 3-4 for details) was applied at the brace midpoint to initiate buckling (Figure 3-4, bottom left). Gusset plates ware modeled using the “Elastic Beam Column” element in OpenSees with 10 times the area and moment of inertia of the connecting brace element as recommended by Erduran et al (2011). Panel zones were modeled as essentially rigid by using the “Elastic Beam Column” element with length equal to half the section depth and with 10 times the area and moment of area of the corresponding beam or column element. Member capacities were calculated using the expected yield strength of the materials: 55ksi for beams and columns and 58.8ksi for braces.

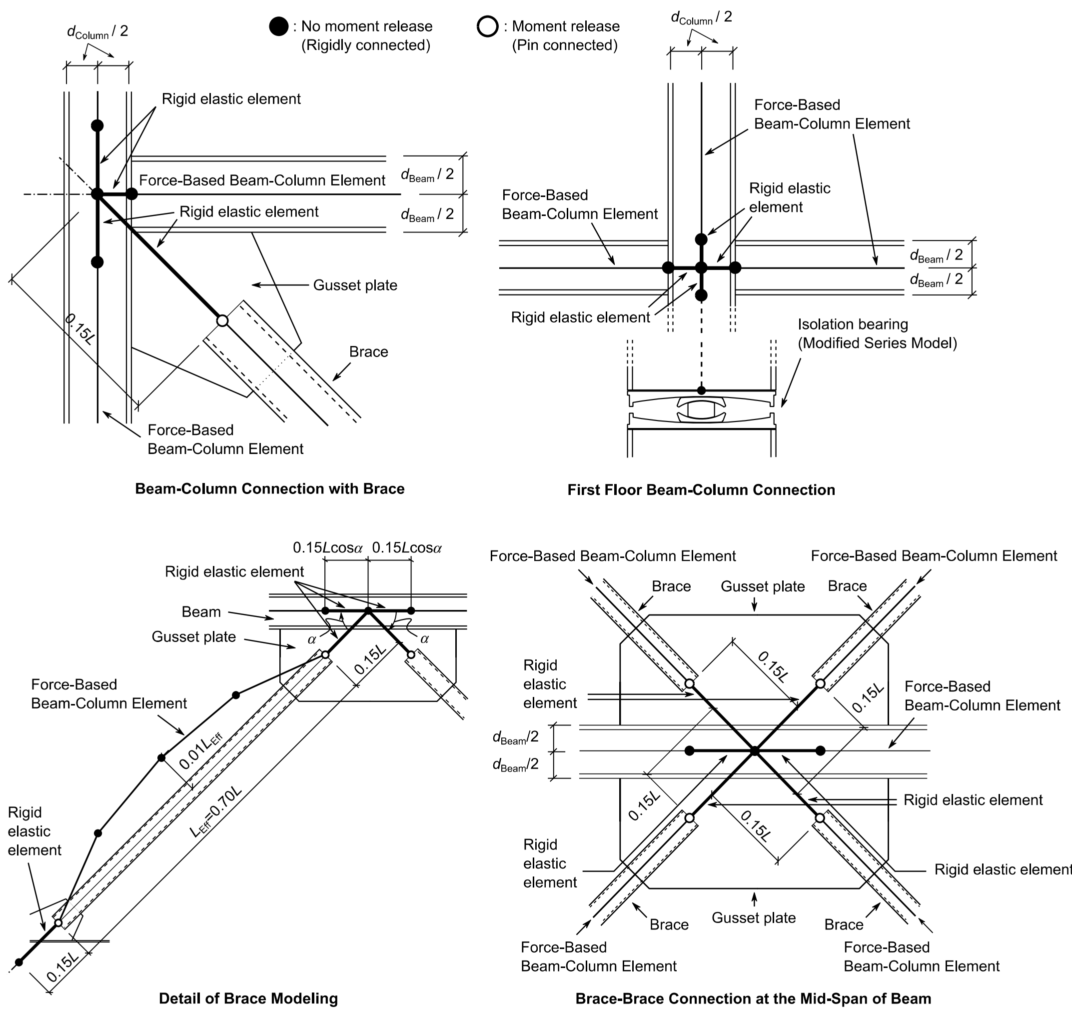

Figure 3-4 Details of Model of Connections

Failure of braces, girders and columns was not explicitly modelled. Rather, the deteriorating behavior of the elements was modelled and failure was implicitly accounted for by considering limits on the story drift.

Inherent damping in the isolated buildings was modelled using the "modal damping" (Chopra and McKenna, 2016) to provide a damping ratio of 0.02 in all modes but the first two ("isolated" modes) for which the damping ratio was set equal to zero per directions in Sarlis and Constantinou (2011). For the non-isolated buildings, the damping ratio was specified as 0.02 in all modes. In the modal damping model, the elastic properties of the structure are used to construct a damping matrix, which is then used in the RHA. The application of the procedure for the isolated building model is complicated by the fact that the isolator models are extremely stiff in the elastic range (the elastic stiffness is the friction force at initiation of motion divided by some very small "yield" displacement which was 0.05in). Instead, the correct stiffness of the isolators for the construction of the damping matrix is the post-elastic stiffness (or the stiffness when friction is disregarded and sliding occurs on the main concave surfaces) (Sarlis and Constantinou, 2011). Accordingly, horizontal, vertical and rotational springs were placed below each isolator element to represent the desired stiffness in the horizontal direction only for the construction of the damping matrix. These springs were restrained to only deflect by 0.001inch so that under inelastic conditions in the nonlinear RHA they do not affect the behavior of the isolators.

The model used in the analysis of the SMF was developed with due considerations for the ultimate behavior of the components and large rotation and displacement effects. Important details of the model follow (more details are presented in Kitayama and Constantinou, 2016): (a) beams and columns were modelled using the Modified Ibarra-Krawinkler bilinear-hysteretic model (Lignos and Krawinkler, 2011), which is capable of simulating deteriorating hysteretic moment-rotation relationship, (b) columns were modeled using a concentrated plasticity bi-linear hysteretic model without strength or stiffness deterioration and with a ratio of elastic to post-elastic stiffness of 0.002 and (c) plastic hinges in columns were located at beam faces and plastic hinges at the column bases were located at a distance equal to the column depth from the base.

The triple FP isolators were modelled using a modification of the series model (Fenz and Constantinou, 2008a) in order to simulate the ultimate behavior of the isolator as predicted by the theory of (Sarlis and Constantinou, 2016), including uplift. Specifically, the modified series model includes the stiffness of the restraining ring k_r and its ultimate capacity. The shear stiffness of the restraining ring was calculated by the following equation, which is based on the shear strength of a 60° wedge of the ring divided by an appropriate value of a yield displacement Y_r:

$$k_r = \frac{\pi\left(b - t_r\right)t_{\mathrm{r}}F_{\mathrm{ry}}}{6Y_r} \tag{3-1}$$

In Equation (3-1), b and t_r are the outside diameter and thickness of the restraining ring, respectively, and Fry is the shear yield stress of the material (25ksi is a representative value for ductile iron per Sarlis and Constantinou, 2016). The strength of the restraining ring is equal to k_rY_r. The value of Y_r was set equal to the thickness t_r. The restrainer is considered acting as long as the restraining ring deformation is less than the thickness t_r. When this displacement is exceeded for the first time, the restraining ring is removed from the model.

The model is assumed valid until the displacement reaches a critical value, which results in collapse or overturning of the internal parts of the bearing. This displacement is denoted as D_{Ultimate} and is equal to the displacement capacity D_{Capacity} as predicted by the theory in (Fenz and Constantinou, 2008[b]) plus half of the diameter of the rigid slider (see Figures 2-2 and 2-3). Note that the model does not explicitly simulate collapse. Simply when this limit of displacement is exceeded, the isolator is considered failed and execution of the program is terminated. Given that collapse is not directly simulated, a user of this model may opt to use a different limit for the ultimate displacement as for example the one calculated by more advanced models in (Sarlis and Constantinou, 2016). Moreover, uplift of the isolators was modelled. The interested reader is referred to (Kitayama et al, 2016) for more details of the modified series model. Note that while there are more detailed models that can simulate failure of the isolator (Sarlis and Constantinou, 2016; Bao et al, 2017), these models are computationally very complex to be used in this study where over 10,000 nonlinear RHA were conducted.

Failure of the analyzed structures was assumed when any of the following conditions occurred: (a) the maximum story drift ratio exceeded 0.02 (Masnoor and Mosqueda, 2015) for buildings with OCBF, 0.05 (Sabelli et al., 2013) for buildings with SCBF and 0.1 (FEMA, 2000) for buildings with SMF, (b) the isolator displacement exceeded D_{Ultimate}, (c) the triple FP isolator uplift displacement exceeded the height of the restraining ring (1.5in), (d) there was instability detected by termination of the analysis program or (e) the slope of the $S_a(T_1)$ vs maximum story drift ratio curve (e.g., the slope of the incremental dynamic analysis or IDA curve) was less than 0.1 times the slope of the same curve in the initial analysis (a condition that indicates a “flat” IDA curve).

It should be noted that the definition of failure of the isolated structure includes the case of failure of the isolators either by excessive lateral displacement or uplift. It may be argued that failure of the isolators does not lead to collapse of the structure if proper detailing is provided to prevent collapse of the structure above the isolators, such as when a large pedestal or foundation area are provided, and provisions are made to raise the structure and replace the isolators. Such cases, while a good practice, are not considered as they are not required by ASCE/SEI-7 and the behavior is not fully understood.

SECTION 4
STRUCTURAL COLLAPSE EVALUATION

Structural collapse of the developed designs was evaluated based on FEMA P695 (2009) using the set of 44 far-field ground motions in this FEMA document. First, IDA (Vamvatsikos and Cornell, 2002) was conducted and data were obtained and used to calculate the collapse capacity. This collapse capacity does not include the spectral shape effects, which are known to be important (Haselton et al, 2011; Baker and Cornell, 2006). While FEMA (2009) includes a simple procedure for accounting for these effects, the procedure is based on the analysis of non-isolated concrete moment frame and wood frame buildings. Application of the procedure to seismically isolated buildings given the behavior depicted in the pushover curves of Figures 2-4 to 2-6 is problematic as discussed in Section 2. A specific study, presented in Appendix A, was conducted to determine the median collapse spectral acceleration at the fundamental period with the spectral shape effects accounted for based on the approach proposed by Haselton et al (2011). The median collapse spectral acceleration at the fundamental period $\widehat{Sa}_{\text{Col,adj}}(T_1)$, as adjusted for the spectral shape effects, is provided by Equation (4-1) in which factors c_0 and c_1 were obtained by regression analysis of IDA data and are presented in Tables 4-1 and 4-2.

$$\widehat{Sa}_{\text{Col,adj}}(T_1)\ \ (units\ \ g) = \exp[c_0 + c_1 \cdot \bar{\varepsilon}_0(T_1)] \tag{4-1}$$

Values of period T_1 were 0.524sec for the non-isolated SCBF, 1.186sec for non-isolated SMF and 3.66sec (=T_M, which is the effective period of the isolated structure in the MCE_R) for all isolated structures. Values of the target epsilon $\bar{\varepsilon}_0(T_1)$ are 1.44 for all isolated structures, 1.46 for the non-isolated SCBF and 1.71 for the non-isolated SMF (see Table A-1).

Tables 4-1 and 4-2 present the results of the collapse evaluation for all considered systems in terms of parameters c_0 and c_1 of Equation (4-1), the median collapse capacity, $\widehat{Sa}_{\text{Col}}(T_1)$, without due consideration for the spectral shape effects (as directly obtained from the IDA results), the median collapse capacity with due consideration for the spectral shape effects per Equation (4-1), $\widehat{Sa}_{\text{Col,adj}}(T_1)$, the dispersion coefficient due to the record-to-record variability (as obtained from the IDA results), β_{RTR}, and the assumed total system collapse uncertainty β_{TOT}. The adjusted collapse margin ratio or *ACMR* per FEMA P695 is given by:

$$ACMR = \frac{\widehat{Sa}_{\text{Col,adj}}(T_1)}{Sa_{\text{MCE}}(T_1)} \tag{4-2}$$

In Equation (4-2), $S_{aMCE}(T_1)$ is the MCE$_R$ spectral acceleration at the fundamental period T_1 (=T_M for isolated structures). Values of $S_{aMCE}(T_1)$ are 1.5g for the non-isolated SCBF structure (T_1=0.524sec), 0.759g for the non-isolated SMF structure (T_1=1.186sec) and 0.246g for all isolated structures (T_1=T_M=3.66sec).

The collapse margin ratio *CMR* without the adjustment for spectra shape effects is given by:

$$CMR = \frac{\widehat{Sa}_{\text{Col}}(T_1)}{Sa_{\text{MCE}}(T_1)} \tag{4-3}$$

The spectral shape factor or *SSF* is given by:

$$SSF = \frac{\widehat{Sa}_{\text{Col,adj}}(T_1)}{\widehat{Sa}_{\text{Col}}(T_1)} = \frac{ACMR}{CMR} \tag{4-4}$$

The total system uncertainty β_{TOT} was calculated using Equation (4-5) per FEMA P695 (2009) where each component of uncertainty is related to a quality rating.

$$\beta_{\text{TOT}} = \sqrt{\beta_{\text{RTR}}^2 + \beta_{\text{DR}}^2 + \beta_{\text{TD}}^2 + \beta_{\text{MDL}}^2} \tag{4-5}$$

In Equation (4-5), β_{DR} is the design requirements-related collapse uncertainty, β_{TD} is the test data-related collapse uncertainty and β_{MDL} is the modeling-related collapse uncertainty. For the seismically isolated structures with SCBF and SMF the following quality ratings and related uncertainties were used: good with β_{MDL}=0.2 for modeling; good with β_{TD}=0.2 for test data and superior with β_{DR}=0.1 for design requirements (same assumptions made in Masroor and Mosqueda, 2015 and FEMA, 2009). For the non-isolated structure with SCBF, β_{MDL}=0.2, β_{TD}=0.2, and β_{DR}=0.2 were used based on Chen and Mahin (2012) and NIST (2010). For the non-isolated structure with SMF, β_{MDL}=0.2, β_{TD}=0.2, and β_{DR}=0.1 were selected based on Elkady and Lignos (2014) and NIST (2010). Note that the assumptions made for the calculation of the total uncertainty in the seismically isolated structures have been also used in the case of analysis with a moat wall for which there is considerable uncertainty on its behavior, primarily on the basis of the observation that analyses with drastically different moat wall stiffness did not result in significant differences. Nevertheless, the interested reader may adjust the values of the uncertainty parameters and recalculate the probabilities of collapse without the need for additional analyses.

Instead of values of the $ACMR$, Tables 5 and 6 present the conditional probability of collapse caused by the MCE_R or $P_{COL,MCE}$, calculated as:

$$P_{\text{COL,MCE}} = \int_0^1 \frac{1}{s\beta_{TOT}\sqrt{2\pi}} \exp\left[-\frac{(\ln s - ACMR)^2}{2\beta_{TOT}^2}\right] ds \tag{4-6}$$

Note that the probability of collapse without the spectral shape effects is also given by Equation (4-6) but with $ACMR$ replaced by CMR. Also, Equation (4-6) may be used for any value of the system uncertainty β by replacing β_{TOT} with β.

The calculated probabilities of collapse depend on the assumed values of uncertainty parameters. For example, if the total uncertainty β_{TOT} is assumed equal to 0.3, as in Shao et al. (2017), the probability of collapse for the isolated SCBF system with R_I=1.0 in the DE and TFP-3 isolator of $D_{Capacity}$=1.5D_M would become 2.7% instead of 4.5% (see Table 4-1). The values of probabilities of collapse in the tables are based on reasonably conservative assumptions on the values of uncertainties. In addition, the results in Tables 4-1 and 4-2 are based on analyses using the lower bound values of friction for the isolators, which systematically resulted in the largest probabilities of collapse. Results are presented for one case using the upper bound values of friction per Table 2-1 to demonstrate the effect. The reason for the reduction in the probability of collapse is the fact that failure is dominated by excessive isolator displacements (they lead to isolator failure or to superstructure collapse after the isolators enter the stiffening regime) and higher values of friction result in smaller displacement demands.

Table 4-1 Results of Collapse Fragility Analysis for Buildings with SCBF and OCBF

System		Coeffs. in Eq. (2) c_0	Coeffs. in Eq. (2) c_1	$Sa_{Col}(T_1)$ (g) (w/o epsilon adjustment)	$Sa_{Col,adj}(T_1)$ (g) (w. epsilon adjustment)	β_{TOT} (β_{RTR})	Prob. Collapse in MCE_R (%)
Designed per ASCE 7-10	R_I=1.0, TFP-1	-1.219	0.146	0.281	0.365	0.366 (0.209)	14.08
	R_I=1.0, TFP-2	-1.083	0.129	0.320	0.408	0.350 (0.181)	7.47
	*R_I=1.0, TFP-3	-0.990	0.115	0.355	0.438	0.341 (0.163)	4.52
	*R_I=1.0, TFP-3, Moat Wall at 1.5D_M (1000xstiffness)	-1.019	0.138	0.347	0.440	0.353 (0.187)	4.98
	*R_I=1.0, TFP-3 (Upper bound friction)	-0.551	0.156	0.557	0.729	0.391 (0.255)	1.23
	R_I=1.5, TFP-1	-1.241	0.121	0.271	0.344	0.352 (0.185)	17.05
	R_I=1.5, TFP-2	-1.138	0.109	0.307	0.375	0.343 (0.166)	10.95
	R_I=1.5, TFP-3	-1.056	0.097	0.331	0.400	0.339 (0.158)	7.59
	R_I=2.0, TFP-1	-1.262	0.123	0.275	0.338	0.348 (0.176)	18.06
	R_I=2.0, TFP-1, Moat Wall at D_M (50xstiffness)	-1.272	0.138	0.272	0.342	0.353 (0.187)	17.57
	R_I=2.0, TFP-1, Moat Wall at D_M (1000xstiffness)	-1.286	0.166	0.262	0.351	0.374 (0.224)	17.13
	R_I=2.0, DC-1 no restraining ring	-1.389	0.148	0.237	0.309	0.378 (0.230)	27.37
	R_I=2.0, DC-2 no restraining ring	-1.228	0.134	0.274	0.356	0.368 (0.213)	15.83
	R_I=2.0, TFP-2	-1.166	0.107	0.293	0.364	0.343 (0.166)	12.74
	R_I=2.0, TFP-2, Moat Wall at 1.25D_M (1000Xstiffness)	-1.196	0.136	0.293	0.368	0.357 (0.194)	12.99
	R_I=2.0, TFP-3	-1.083	0.093	0.323	0.387	0.340 (0.159)	9.09
Designed per ASCE 7-16	R_I=1.0, TFP-1	-1.302	0.129	0.253	0.328	0.356 (0.193)	21.09
	R_I=1.0, TFP-1, Moat Wall at D_M (1000xstiffness)	-1.154	0.186	0.294	0.412	0.395 (0.257)	9.60
	R_I=1.0, TFP-2	-1.140	0.114	0.300	0.377	0.350 (0.181)	11.13
	R_I=1.0, TFP-3	-1.020	0.105	0.341	0.419	0.341 (0.161)	5.87
	R_I=1.0, TFP-2 OCBF	-1.153	0.105	0.299	0.368	0.346 (0.173)	12.31
	R_I=1.0, TFP-3 OCBF	-1.060	0.088	0.332	0.393	0.333 (0.145)	7.96
	R_I=2.0, TFP-1	-1.215	0.139	0.279	0.362	0.357 (0.194)	13.94
	R_I=2.0, TFP-1, Moat Wall	-1.225	0.172	0.281	0.376	0.378	13.07

	at D_M (1000Xstiffness)					(0.230)	
	R_I=2.0, TFP-2	-1.103	0.115	0.312	0.392	0.346 (0.173)	8.93
	R_I=2.0, TFP-2, Moat Wall at 1.25D_M (1000Xstiffness)	-1.145	0.147	0.307	0.393	0.359 (0.198)	9.61
	R_I=2.0, TFP-3	-1.026	0.096	0.343	0.412	0.338 (0.156)	6.38
-	Non-isolated	0.809	0.238	2.821	3.179	0.538 (0.412)	8.15
* Design meets criteria for continued functionality per Zayas et al (2017)							

Table 4-2 Results of Collapse Fragility Analysis for Buildings with SMF

System		Coeffs. in Eq. (2) c_0	c_1	$Sa_{Col}(T_1)$ (g) (w/o epsilon adjustment)	$Sa_{Col,adj}(T_1)$ (g) (w. epsilon adjustment)	β_{TOT} (β_{RTR})	Prob. Collapse in MCE_R (%)
Designed per ASCE 7-10	R_I=1.0, TFP-1	-1.042	0.177	0.331	0.455	0.387 (0.245)	5.58
	R_I=1.0, TFP-2	-0.911	0.164	0.383	0.510	0.372 (0.221)	2.53
	R_I=1.0, TFP-3	-0.827	0.154	0.398	0.546	0.365 (0.208)	1.44
	R_I=1.0, TFP-3 (Upper bound friction)	-0.402	0.190	0.635	0.891	0.428 (0.305)	0.56
	R_I=1.5, TFP-1	-0.996	0.141	0.373	0.453	0.378 (0.230)	5.32
	R_I=1.5, TFP-2	-0.896	0.121	0.393	0.486	0.368 (0.213)	3.20
	R_I=1.5, TFP-3	-0.855	0.098	0.411	0.490	0.360 (0.199)	2.77
	R_I=2.0, TFP-1	-0.998	0.134	0.364	0.447	0.385 (0.241)	6.06
	R_I=2.0, DC-1 no restraining ring	-1.462	0.1053	0.223	0.270	0.360 (0.200)	39.92
	R_I=2.0, DC-2 no restraining ring	-1.307	0.091	0.266	0.309	0.357 (0.194)	26.30
	R_I=2.0, TFP-2	-0.954	0.128	0.390	0.463	0.377 (0.229)	4.67
	R_I=2.0, TFP-3	-0.892	0.091	0.390	0.467	0.358 (0.195)	3.65
Designed per ASCE 7-16	R_I=1.0, TFP-1	-1.143	0.155	0.292	0.398	0.371 (0.218)	9.68
	R_I=1.0, TFP-1, Moat Wall at D_M (1000xstiffness)	-0.619	0.233	0.537	0.753	0.442 (0.325)	0.57
	R_I=1.0, TFP-2	-1.008	0.142	0.327	0.448	0.374 (0.223)	5.46
	R_I=1.0, TFP-3	-0.896	0.131	0.377	0.493	0.369 (0.215)	2.98
	R_I=2.0, TFP-1	-1.037	0.191	0.333	0.467	0.389 (0.247)	4.97

	R_I=2.0, TFP-1, Moat Wall at D_M (1000Xstiffness)	-0.695	0.230	0.476	0.695	0.432 (0.311)	0.81
	R_I=2.0, TFP-2	-0.918	0.176	0.386	0.515	0.376 (0.226)	2.46
	R_I=2.0, TFP-2, Moat Wall at 1.25D_M (1000Xstiffness)	-0.685	0.166	0.498	0.640	0.400 (0.265)	0.85
	R_I=2.0, TFP-3	-0.831	0.153	0.401	0.543	0.363 (0.204)	1.46
-	Non-isolated	0.475	0.242	1.675	2.432	0.448 (0.333)	0.46

Note that the results in Tables 4-1 and 4-2 include cases in which moat walls are used. In Table 4-1 two cases are presented in which the moat wall stiffness is assumed to be 50 times or 1000 times larger than the stiffness of the TFP-1 isolator in the stiffening regime (see Figures 2-2 and 2-3). The two cases result in essentially the same results (see also pushover curves in Figures 2-4 to 2-6 and the related commentary in Section 2 for explanation). Accordingly, other analyses with moat wall make use of the stiffness multiplier of 1000.

In discussing the results of Tables 4-1 and 4-2, the target reliabilities that are stipulated in Section 1.3.1.1 of ASCE 7-16 (ASCE, 2016) can be used. This requires conditional probabilities of collapse caused by the MCE_R not to exceed 10% for typical buildings of risk category I or II, 2.5% for essential buildings of risk category IV and 5% for other structures. The following are observed:

1) SCBF buildings designed by the minimum criteria of ASCE/SEI 7-10 or 7-16 (isolator TFP-1 or DC-1, or TFP-1 with moat wall placed at distance D_M; R_I=2.0) have unacceptable probabilities of collapse in the MCE_R (exceeding 10%). These probabilities of collapse are also larger than that of the non-isolated comparable structure designed by the minimum criteria of ASCE/SEI 7, which has an acceptable probability of collapse in the MCE_R.

2) The probability of collapse decreases with increasing isolator displacement capacity while R_I is fixed. However, the probability of collapse may increase as R_I is reduced while the isolator displacement capacity is fixed. The latter case may appear counterintuitive, as it would be expected that increases in the strength of the superstructure would result in reduction of the probability of collapse. While this is true for non-isolated structures, it is not always true for isolated structures when collapse is dominated by excessive isolator displacement. As the strength of the superstructure is increased, inelastic action in the superstructure is delayed leading to larger isolator displacement demands. Accordingly,

specifications for values of R_I should be consistent with specifications for the displacement capacity of isolators.

3) Use of isolators with $D_{Capacity}$=1.5D_M and $D_{Ultimate}$=1.9D_M (TFP-3), and designed for any acceptable value of parameter R_I have a probability of collapse that is less than 10%, thus acceptable for typical structures of risk category I and II (ASCE, 2016). However, probabilities of collapse less than 5% as required for important structures can be achieved when R_I=1 in the DE per ASCE/SEI 7-10 but not when R_I=1 in the MCE_R per ASCE/SEI 7-16. For the latter case, the isolator displacement capacity should be further increased to be consistent with the strength of the superstructure per comments in item 2 above.

4) The use of moat walls (herein investigated for the cases of (a) R_I=2, isolator TFP-1 with $D_{Capacity}$=D_M and moat wall at D_M or isolator TFP-2 with $D_{Capacity}$=1.25D_M and moat wall at 1.25D_M, and (b) R_I=1, isolator TFP-3 with $D_{Capacity}$=1.5D_M and moat wall at 1.5D_M) resulted in essentially the same results on the probability of collapse as analyzed cases without the moat walls for the SCBF. Apparently and as evident in pushover curves presented in Section 2, the stiffening behavior of the triple FP isolators serves a function similar to a moat wall provided that the isolators do not collapse (that is, there is collapse of the superstructure). This is the case for the SCBF in which collapse is controlled by drift in the superstructure, which is limited (5% drift ratio) for the SCBF.

5) The comment in item 2 above on the need for specifications for values of R_I that are consistent with specifications for the displacement capacity of isolators also applies in the case of the use of moat walls. A clear example is the cases of R_I=1 or 2 and isolator TFP-1 in Table 4-1 for the SCBF designed by the procedures of ASCE/SEI 7-16. For the case of R_I=2, both cases with and without a moat wall placed at D_M result in similar and unacceptable probabilities of collapse of about 13 to 14%. However, when R_I=1, the probability of collapse without the moat wall increases to 21% but reduces to about 10% when a wall is utilized.

6) In the case of the SMF, use of moat wall (herein investigated for the cases of R_I=2, isolator TFP-1 with $D_{Capacity}$=D_M and moat wall at D_M, and isolator TFP-2 with $D_{Capacity}$=1.25D_M and moat wall at 1.25D_M) resulted in a lower probability of collapse than when using the

stiffening isolator, although the probabilities of collapse for both cases are small. Further comments that are presented later in this section attribute the difference to the mode of failure being different in the two cases: collapse of superstructure in the case of the use of moat walls versus collapse of the isolator otherwise. Given that for the SMF the superstructure has significantly larger ability to deform than the SCBF, the probability of collapse is reduced.

7) The importance of the stiffening behavior of the triple FP isolators (or equivalently of some displacement restrainer) is evident in the increase of the probability of collapse when the restrainer ring is removed. (For R_I=2 per ASCE/SEI 7-10, SCBF buildings with TFP-1 and DC-1 isolators have probability of collapse of 18.1% and 27.3%, respectively).

8) The collapse performance of the OCBF design per criteria of ASCE/SEI 7-16 (ASCE, 2016) (R_I=1.0 in MCE$_R$, isolators with $D_{Capacity}$≥1.2D_M) is unacceptable as the probability of collapse exceeds 10%. To achieve acceptable probability of collapse the isolator displacement capacity has to be increased to $D_{Capacity}$=1.5D_M. Note that the study of Masroor and Mosquesda (2015) computed a just acceptable probability of collapse (just over 10%) for a 3-story OCBF building designed by criteria that meet the minimum criteria of ASCE/SEI 7-16. The differences are likely due to the differences in height of the two buildings with the taller building of this study having a larger probability of collapse. This observation is consistent with the results of the study of Chimamphant and Kasai (2016).

9) The results in Table 6 for the SMF are qualitatively similar to those for the SCBF but the probabilities of collapse are lower. This is due to the capability of the SMF to deform more than the SCBF before collapse (assumed 10% story drift ratio for SMF and 5% for SCBF). Nevertheless, SMF designed by the minimum criteria of ASCE/SEI 7-10 without a restrainer ring (R_I=2.0, isolator DC-1) still has unacceptable probability of collapse (39.9%). Even when the displacement capacity is increased (design with isolator DC-2), still the probability of collapse is unacceptable (26.3%).

10) All isolated SMF structures of whatever design details have higher probabilities of collapse than the comparable non-isolated design. A question then arises: what does seismic isolation offer? This will be investigated in the next section where studies of the

performance of the studied structures in terms of peak floor acceleration, peak story drift ratio and peak residual drift ratio are presented.

Explanation for the collapse behavior of the studied isolated structures is provided in the results of Figure 4-1 through 4-4 which present the calculated peak isolator displacement when collapse occurs for the SCBF and SMF in the designs with R_I=1.0, 1.5 and 2.0 (for the DE, per ASCE/SEI 7-10) and 1.0 and 2.0 (for MCE_R per ASCE 7-16) and the three cases of TFP isolators. Note that in these figures each ground motion has the seismic intensity that causes collapse. That is, each ground motions is scaled to a different seismic intensity. Each graph contains two types of lines: a dashed line that denote the displacement capacity $D_{Capacity}$ and a solid line that denote the ultimate displacement capacity $D_{Ultimate}$. Colors are used to distinguish the different size of the considered isolators. Results are presented for each of the 44 motions used in the analysis. The results show that as the R_I factor is increased from the value of 1.0 to 2.0, there is an increasing number of collapses by failure of the superstructure. For example, it may be seen in Figure 4-3 that for the design with R_I=2.0, the percentage of cases when the isolator ultimate capacity is exceeded is about 35% in the design with the minimum displacement capacity isolators TFP-1, is 23% in the design with isolators TFP-2 and is 12% in the design with isolators TFP-3. By comparison for the design with R_I=1.0 in the same figure, all failures are by failure of the isolators. It is apparent that reducing the R_I factor requires also increases in the displacement capacity of the isolators in order to affect the probability of collapse.

The calculated probability of collapse for the 6-story SCBF of the enhanced design with R_I=1.0 and isolators with displacement capacity at initiation of stiffening equal to 1.5D_M and an ultimate displacement capacity of 1.9D_M are very close to those calculated in the study of Shao et al, 2017) for a 3-story SCBF designed by similar procedures. Particularly, Shao et al (2017) calculated a 2.5% probability of collapse in the MCE_R when assuming a dispersion factor of 0.3, whereas this study calculated a 4.5% probability of collapse for a dispersion factor of 0.341 as obtained from the analysis and after adjustment for uncertainties. The probability of collapse is 2.7% when a dispersion factor of 0.3 is assumed, thus essentially the same as that of the Shao et al. (2017) study.

The results of this study demonstrate that designing by the minimum requirements of ASCE/SEI 7 may result in unacceptable probabilities of collapse in the MCE_R. Probabilities of collapse less than 5% in the MCE_R were achieved for designs with R_I=1.0 (either for DE or the MCE_R) and designing triple FP isolators with a displacement capacity at initiation of stiffening equal to 1.5D_M and an ultimate displacement capacity of 1.9D_M. The stiffening behavior of the isolators or equivalently the use of moat walls is important in preventing collapse. Without it, as when using double concave isolators without a restrainer ring or moat walls, there are unacceptably high probabilities of collapse. Also, a design with OCBF that satisfies the minimum criteria of ASCE/SEI 7-16 resulted in a marginally unacceptable probability of collapse in the MCE$_R$, which could be improved to acceptable by using isolators with displacement capacity at initiation of stiffening equal to 1.5D_M instead of 1.2D_M.

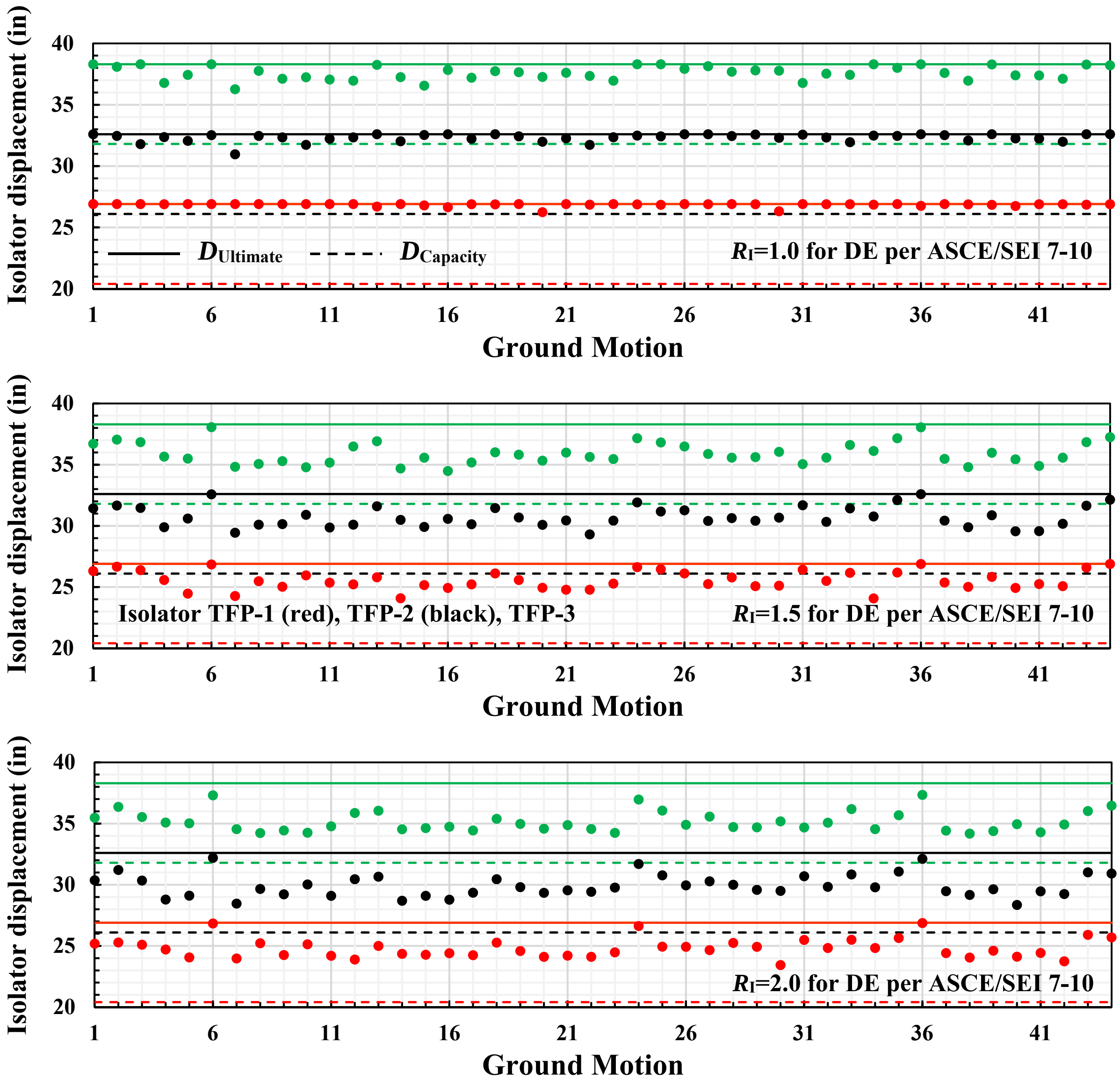

Figure 4-1 Peak Isolator Displacements at Collapse of Buildings with SCBF Designed for the DE per ASCE/SEI 7-10 and without moat walls

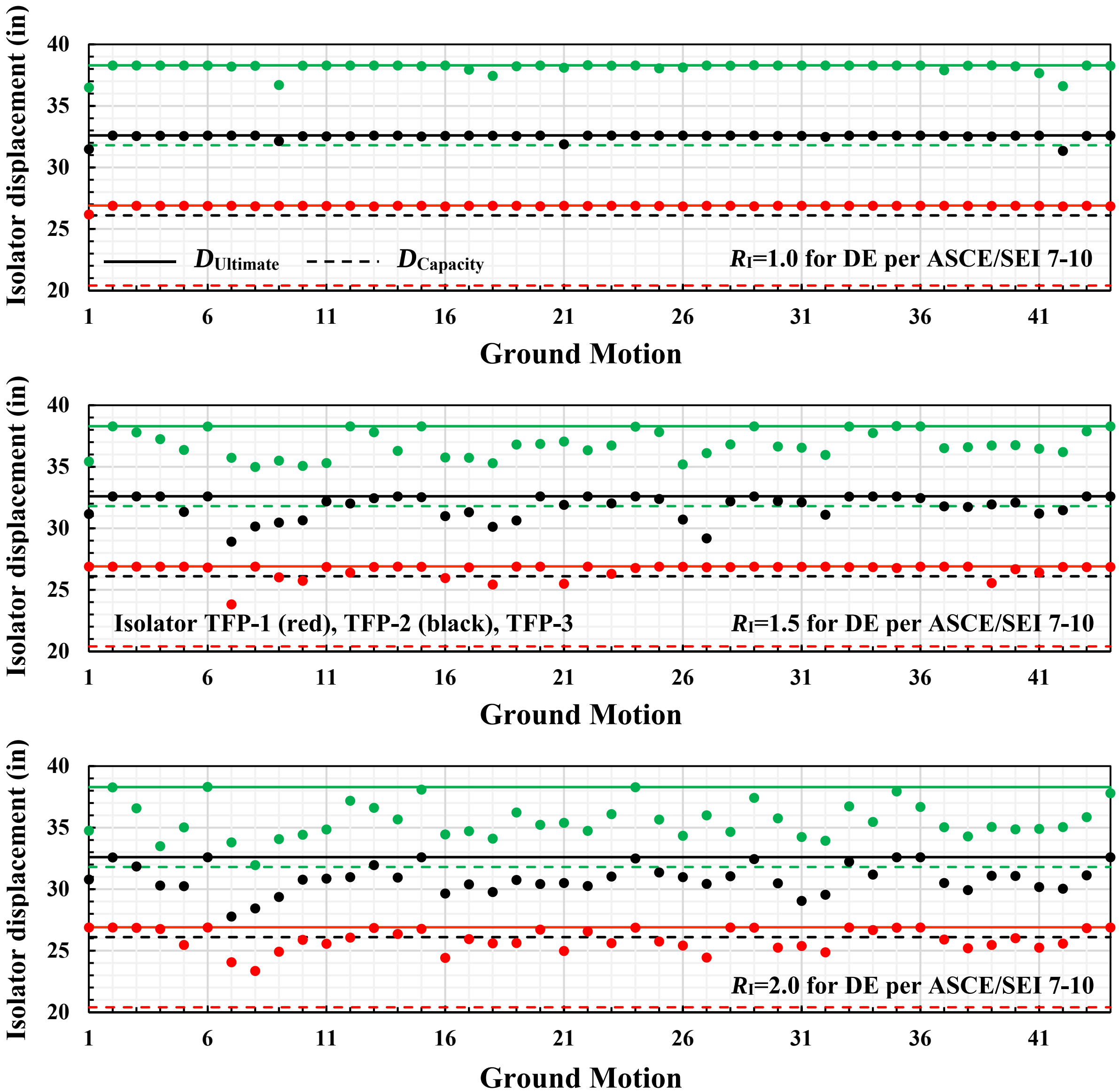

Figure 4-2 Peak Isolator Displacements at Collapse of Buildings with SMF Designed for the DE per ASCE/SEI 7-10 and without moat walls

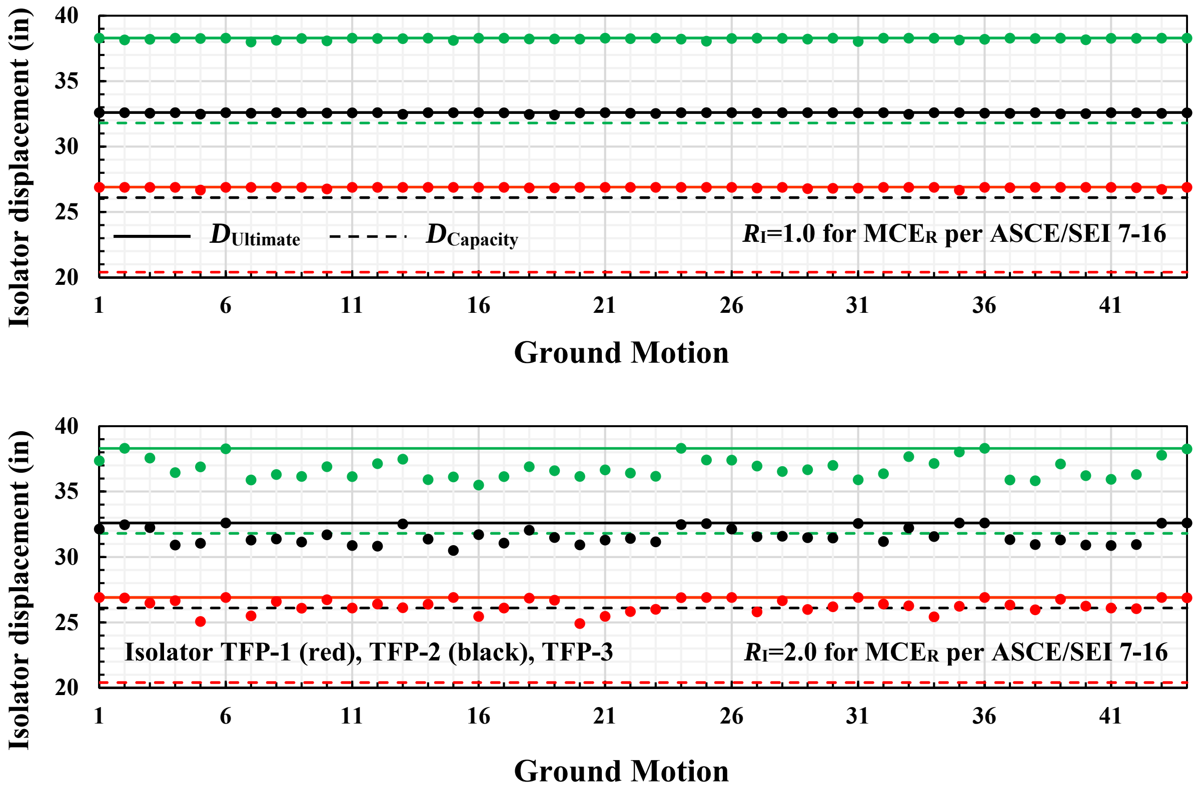

Figure 4-3 Peak Isolator Displacements at Collapse of Buildings with SCBF Designed for the MCE_R per ASCE/SEI 7-16 and without moat walls

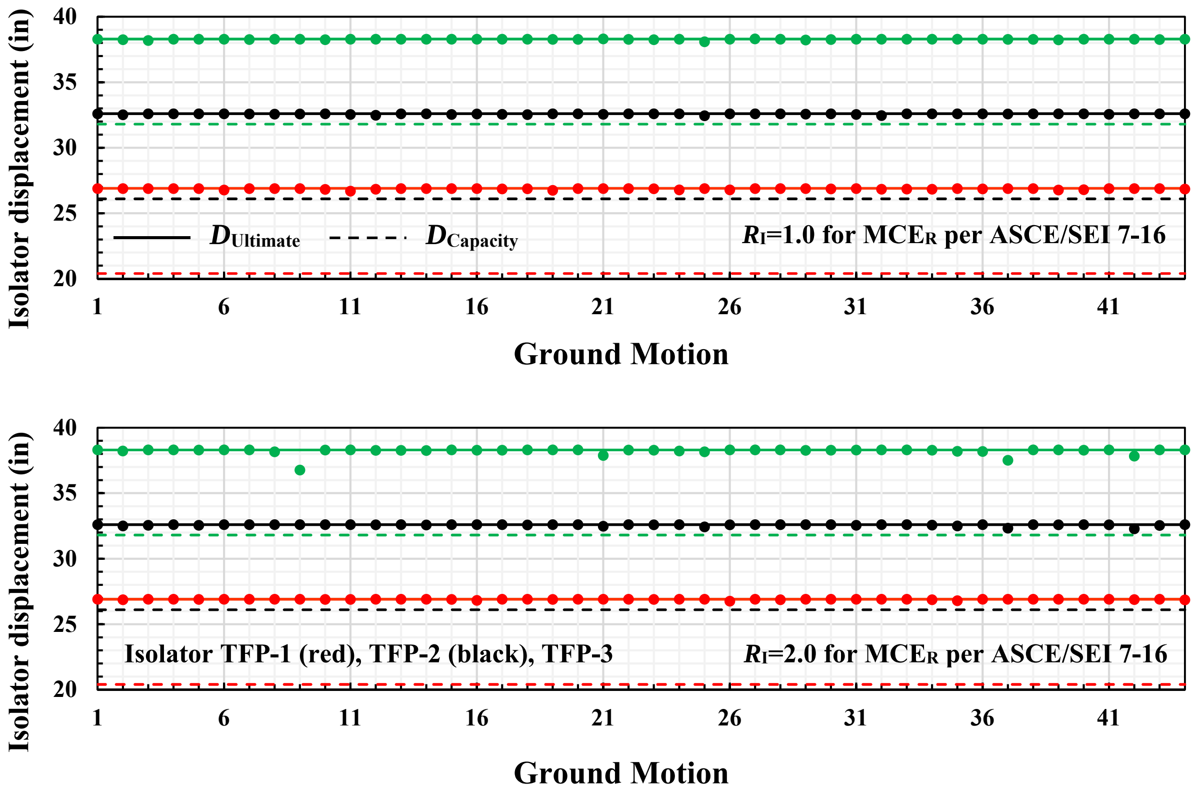

Figure 4-4 Peak Isolator Displacements at Collapse of Buildings with SMF Designed for the MCE_R per ASCE/SEI 7-16 and without moat walls

Of interest is to further investigate and compare the results of the cases with moat wall to those without. Table 4-3 presents extended results that were extracted from the condensed Tables 4-1 and 4-2 using Equations 4-3 to 4-6. An observation to be made in the results is on the values of the spectral shape factor SSF which are about 1.2 to 1.4, thus comparable with results based on the simplified method of FEMA P695 (e.g., FEMA, 2009 reports values of about 1.2 and Masroor and Mosqueda, 2015 report values of about 1.1 to 1.5). While these values are relatively small, they have a significant impact on the probabilities of collapse. Data in Table 4-3 for the probability of collapse in the MCE_R as directly calculated in the incremental dynamic analysis without adjustments for spectral shape effects show large probabilities of collapse which increase when a moat wall is utilized for the SCBF but reduce when a moat wall is utilized for the SMF.

Figures 4-5 to 4-8 provide some additional information on the mode of failure of the systems with and without a moat wall. Like Figures 4-1 to 4-4, the figures present the calculated peak isolator displacement when collapse occurs for each of the 44 motions (each motion is scaled to a different intensity so that it causes collapse). It is noted that all failures of the system with moat wall occur by failure of the superstructure. The SCBF system without a moat wall in Figure 4-5 has 2 out of 44 cases failing due to excessive isolator displacement (design R_I=2 per ASCE 7-10, isolator TFP-1) and 13 out of 44 cases of isolator failure in Figure 4-8 (design R_I=1 per ASCE 7-10, isolator TFP-3).

When the spectral shape effects are considered, the probabilities of collapse drastically reduce but then increased again when uncertainties are accounted for based on Equation 4-5. The data used in the calculation of the spectral acceleration at collapse with due consideration of spectra shape effects are presented in Appendix A. They are described by Equation 4-1 with parameters listed in Table 4-1. A review of the data in Appendix A reveals uncertainties in the lines fitted through the data due to the spread in the data and due to the value of the period T_1-the latter affects the value of quantity $\bar{\varepsilon}_0(T_1)$.

Table 4-3 Extended Results of Fragility Analysis for Selected Systems with and without Moat Walls (all cases of wall with x1000 stiffness)

System	*CMR*	*ACMR*	*SSF*	β_{RTR}	β_{TOT}	Prob. Collapse in MCE_R (%) Without Spectral Shape Effects		Prob. Collapse in MCE_R (%) With Spectral Shape Effects	
						β_{RTR}	β_{TOT}	β_{RTR}	β_{TOT}
SCBF, R_I=1.0, TFP-3 per ASCE 7-10*	1.44	1.78	1.23	0.163	0.341	1.22	14.11	0.02	4.52
SCBF, R_I=1.0, TFP-3 per ASCE 7-10* Moat Wall at 1.5D_M	1.41	1.79	1.27	0.187	0.353	3.29	16.49	0.09	4.98
SCBF, R_I=1.0, TFP-1 per ASCE 7-16	1.03	1.33	1.30	0.193	0.356	44.22	46.86	6.80	21.09
SCBF, R_I=1.0, TFP-1 per ASCE 7-16 Moat Wall at D_M	1.19	1.67	1.40	0.257	0.395	24.50	32.68	2.23	9.60
SCBF, R_I=2.0, TFP-1, per ASCE 7-10	1.12	1.37	1.23	0.176	0.348	26.33	37.43	3.55	18.06
SCBF, R_I=2.0, TFP-1, per ASCE 7-10 Moat Wall at D_M	1.07	1.43	1.34	0.224	0.374	38.87	43.31	5.64	17.13
SCBF, R_I=2.0, TFP-2, per ASCE 7-10	1.19	1.48	1.24	0.166	0.343	14.62	30.52	0.91	12.66
SCBF, R_I=2.0, TFP-2, per ASCE 7-10 Moat Wall at 1.25D_M	1.19	1.49	1.25	0.194	0.357	18.38	31.22	1.90	12.96
SMF, R_I=1.0, TFP-1, per ASCE 7-16 Moat Wall at D_M	2.18	3.06	1.40	0.325	0.442	0.81	3.87	0.03	0.57
SMF, R_I=2.0, TFP-2, per ASCE 7-16	1.57	2.09	1.33	0.226	0.376	2.31	11.54	0.05	2.46
SMF, R_I=2.0, TFP-2, per ASCE 7-16 Moat Wall at 1.25D_M	2.02	2.60	1.29	0.265	0.400	0.39	3.89	0.02	0.85
* Design meets criteria for continued functionality per Zayas et al (2017)									

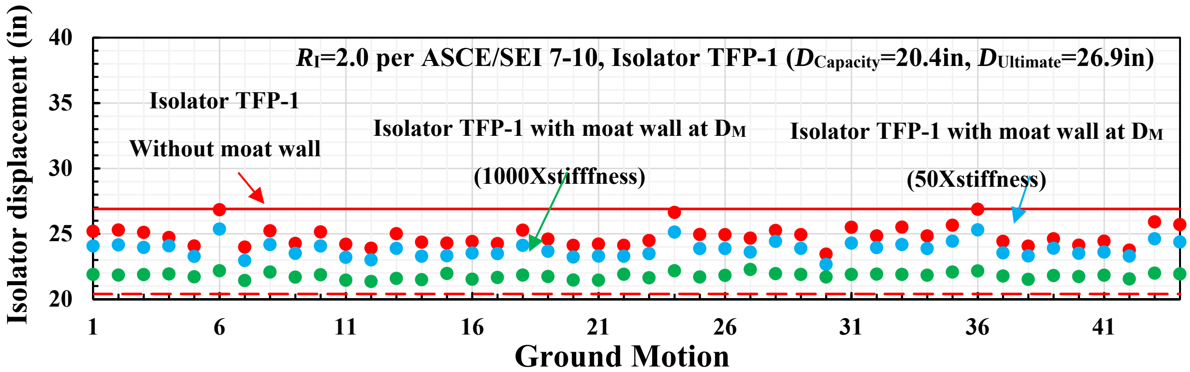

Figure 4-5 Peak Isolator Displacements at Collapse of Buildings with SCBF Designed per ASCE/SEI 7-10, Isolator TFP-1 with and without Moat Wall at Distance D_M

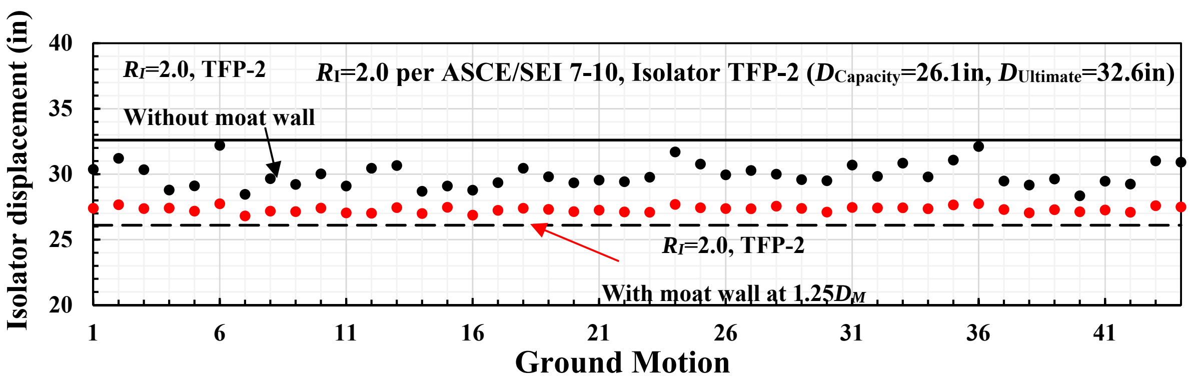

Figure 4-6 Peak Isolator Displacements at Collapse of Buildings with SCBF Designed per ASCE/SEI 7-10, Isolator TFP-2 with and without Moat Wall at Distance 1.25D_M

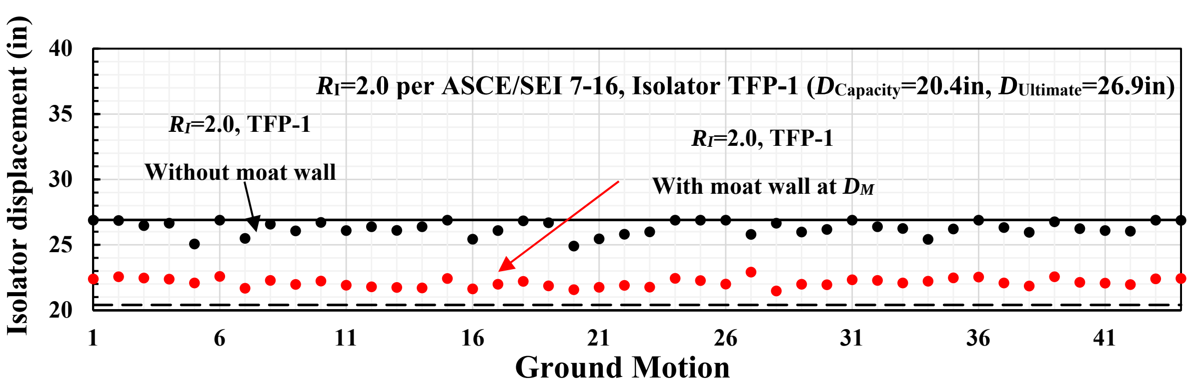

Figure 4-7 Peak Isolator Displacements at Collapse of Buildings with SCBF Designed per ASCE/SEI 7-16, Isolator TFP-1 with and without Moat Wall at Distance D_M

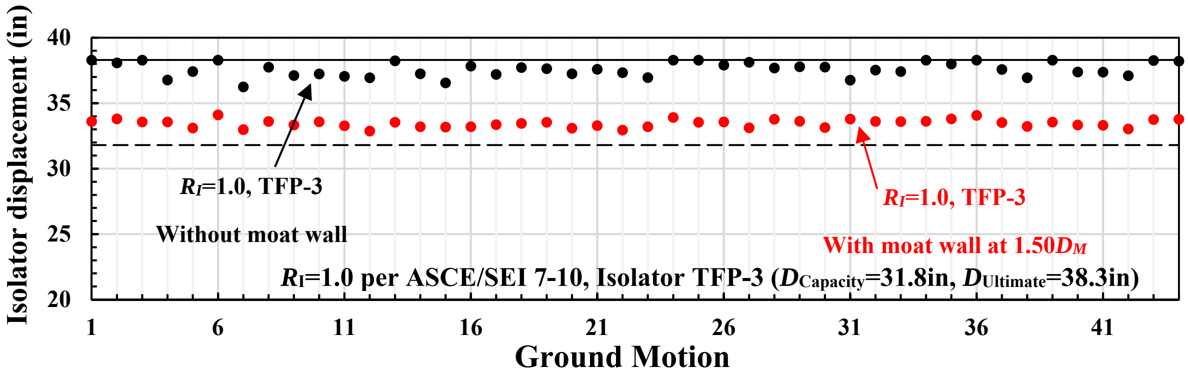

Figure 4-8 Peak Isolator Displacements at Collapse of Buildings with SCBF Designed per ASCE/SEI 7-10, Isolator TFP-3 with and without Moat Wall at Distance 1.5D_M

SECTION 5
PROBABILISTIC ASSESSMENT OF SEISMIC RESPONSE

The seismic performance of the designed isolated and non-isolated buildings is probabilistically assessed in terms of the following engineering demand parameters (EDP): maximum story drift ratio, maximum residual story drift ratio and peak floor acceleration. For the evaluation, the mean annual frequency of exceeding specific limits of these EDP was calculated by considering increasing levels of seismic intensity. The story drift ratio is related to the damage of buildings and is a generally used index of structural damage. It is also related to damage to non-structural components that run vertically (Elenas and Meskouris, 2001; FEMA, 2012[a]). The residual story drift ratio is an important indicator in the decision to repair or demolish damaged buildings (McCormick et al, 2008; FEMA, 2012[a]; Bojorquez and Ruiz-Garcia, 2013). The peak floor acceleration is related to damage of non-structural components attached to floors (suspended ceilings, lighting fixtures, caster-supported furniture, sprinklers, etc.) (FEMA, 2012[a,b]; Furukawa et al, 2013; Soroushian et al, 2015[a,b], Ryu and Reinhorn, 2017). In general, a peak floor acceleration of 0.3g indicates very low or no damage to mechanical, electrical, plumbing, suspended ceilings and sprinklers systems, and to building contents (Elenas and Meskouris, 2001; FEMA, 2012[a]; Furukawa et al, 2013; Soroushian et al, 2015[a,b]; Ryu and Reinhorn, 2017). A maximum story drift ratio of 0.5% indicates the onset of damage for mechanical, electrical and plumbing systems (Elenas and Meskouris, 2001) and content damage and loss of use (Zayas, 2017), and a 0.5% to 1.0% residual drift ratio indicates that it may be more economical to demolish than to repair (McCormick et al, 2008; FEMA, 2012[a]; Bojorquez and Ruiz-Garcia, 2013).

Incremental dynamic analysis is appropriate and useful in assessing the seismic performance of buildings in terms of collapse based on FEMA P695 (FEMA, 2009). However, the use of IDA may not be suitable for the assessment of seismic response other than collapse primarily due to the fact that is based on the use of non-frequent strong earthquake motions (the motions used in the collapse evaluation had magnitude larger than 6.5, peak ground acceleration larger than 0.2g, random epsilon values and scaled up to intensities beyond the MCE_R). Moreover, the adjustment of results of IDA to account for spectral shape effects was shown in Section 4 to include ambiguities and to have a significant effect on the calculated probability of collapse.

For the assessment of seismic response that causes minor or moderate damage under more frequent earthquakes, the selection and scaling of ground motions should be consistent with the local seismic hazard as described in the probabilistic seismic performance procedure of Lin et al (2013[a]) with details on the selection and scaling of motions and a summary of the procedure presented in

NIST (2011). This procedure makes use of conditional spectra. Also, the multiple stripe analysis technique (Jalayer, 2003) was selected to conduct the analyses of this study as it allowed the use of different sets of hazard-consistent ground motions at each intensity level. The results of the study are presented in the form of relationships between the selected EDP and the annual frequency of exceeding specific EDP limits. For the analysis, in total 1,200 motions were selected and scaled to represent ten different earthquake return periods (43 to 10,000 years) and three different building periods (40 motions per return period; 400 motions per building period). Given that the procedure utilizes hazard-consistent ground motions for each considered intensity level, it properly considers spectral shape effects so no corrections are needed. The procedure for the selection and scaling of the motions is described in Appendix B.

The procedure described in Lin et al (2013[a]) and NIST (2011) may also be used to assess the collapse performance for any of the considered seismic intensity levels. This is done in this study in selected cases in order to compare with results obtained by the FEMA P695 procedure. This required some adjustment of the probabilistic assessment procedure to account for uncertainties beyond those inherent in the record-to-record variability of the ground motions. Results of this comparison are presented in Section 6.

Figures 5-1 to 5-9 present the mean annual frequency of exceeding limits on the peak story drift ratio, the peak residual story drift ratio, the peak floor acceleration and the peak roof acceleration, respectively. Results are presented for the non-isolated SCBF and SMF and for the isolated SCBF and SMF structures with R_I=1 and 2 (in the DE or the MCE_R) and with triple FP isolators of the minimum displacement capacity D_M (TFP-1) and the maximum 1.5D_M (TFP-3). Also, the following cases with moat walls (all with 1000xstiffness) are included:

(a) The SCBF with R_I=2 (in the DE), isolator TFP-1 with a moat wall placed at distance D_M and the enhanced design with isolator TFP-2 and a moat wall placed at distance 1.25D_M.
(b) The SCBF with R_I=1 (in the DE), isolator TFP-3 with a moat wall placed at distance 1.5D_M.
(c) The SMF with R_I=2 (in the MCE_R), isolator TFP-1 with a moat wall placed at distance D_M and the enhanced design with isolator TFP-2 and a moat wall placed at distance 1.25D_M.

For the generation of results shown in Figures 5-1 to 5-9, Equation (B-4) was used with $P(EDP > y|(S_a(T_1) = x_i)$ calculated as follows:

1) For the peak story drift ratio (*PSDR*) (*EDP* replaced by *PSDR*) (NIST, 2011; Lin et al, 2013[a]):

$$P(PSDR > y|S_a(T_1) = x_i) = P(C) + \big(1 - P(C)\big)\left(1 - \Phi\left(\frac{lny - \mu_{lnPSDR}}{\sigma_{lnPSDR}}\right)\right) \qquad (5\text{-}1)$$

In Equation (5-1), $P(C)$ is the probability of collapse given $S_a(T_1)=x_i$. It was obtained by first constructing a collapse fragility curve using the method of maximum likelihood (Shinozuka et al, 2000; Baker, 2015) and then obtaining $P(C)$ for x_i. Also, μ_{lnPSDR} and σ_{lnPSDR} are the mean and standard deviation of the $lnPSDR$ values given $S_a(T_1)=x_i$ in which collapse did not occur. Φ is the normal cumulative distribution function given by an expression similar to Equation (4-4) but with the limit of integration extending to "y" instead of 1. Collapse was defined using the same criteria as those used in the structural collapse evaluation. The peak story drift ratio was assumed infinitely large when collapse occurs and was removed from the calculation of term "$\Phi(lny\text{-}\mu_{lnRSDR}/\sigma_{lnPSDR})$" in Equation (4-4).

2) For the case of the peak residual drift ratio (*PRDR*), the same procedure applies with Equation (6) used but *PSDR* replaced by *PRDR*.

3) For the case of the peak floor (*PFA*) Equation (B-4) is used (*EDP* replaced by *PFA*) with $P(PFA>y|S_a(T_1)=x_i)$ calculated by (NIST, 2011; Lin et al, 2013[a]):

$$P(PFA > y|S_a(T_1) = x_i) = 1 - \Phi\left(\frac{lny - \mu_{lnPFA}}{\sigma_{lnPFA}}\right) \qquad (5\text{-}2)$$

Here, μ_{lnPFA} and σ_{lnPFA} are the mean and standard deviation of the $lnPFA$ values given $S_a(T_1)=x_i$.

The results on the mean annual frequency of an *EDP* exceeding a limit y, $\lambda(EDP>y)$, can be used to calculate the probability of exceeding the *EDP* limit y in "N" year, $P(EDP>y)$, by assuming that the earthquake occurrence follows a Poisson distribution so that (FEMA, 2012[a]):

$$P(EDP > y) = 1 - e^{-\lambda(\mathrm{EDP}>y)N} \qquad (5\text{-}3)$$

The results in Figures 5-3 and 5-4 show higher mean annual frequencies for the roof acceleration than the floor acceleration of isolated buildings. Typically, the roof acceleration was higher than that of the floors below in the isolated buildings but not so for the non-isolated buildings. In the discussion that follows some results will be presented that demonstrate the differences.

The results in Figures 5-1 to 5-9 show that: (a) the mean annual frequency of exceeding any acceleration values at the floor or roof level are lower in the isolated buildings of any design than in the comparable non-isolated buildings, (b) isolated buildings have lower mean annual frequencies of exceeding most but not all values of peak story drift ratio and peak residual story drift ratio than comparable non-isolated buildings, (c) isolated buildings designed by the enhanced criteria of R_I=1.0 in the DE (or MCE_R) and stiffening isolators with displacement capacity at initiation of stiffening equal to 1.5D_M have lower mean annual frequencies of exceeding all values of peak story drift ratio and peak residual story drift ratio than comparable non-isolated buildings, and (d) the use of moat walls has generally small effects on the mean annual frequency of exceedance of peak drift ratio and residual drift ratio by comparison to comparable designs with stiffening triple FP isolators without a moat wall. However, the use of moat walls results in systematically higher mean annual frequency of exceedance of high values for the peak floor acceleration. Accordingly, in enhanced designs such as those that meet the criteria in Zayas et al (2017) the use of moat walls do not offer any advantage.

Some sample results in terms of the probability of exceeding specific values of the floor or roof acceleration (0.3g), of the peak story drift ratio (0.5%) and of the residual drift ratio (0.5% and 1%) in 50years (per Equation (5-3)) are presented in Table 5-1. The table also includes the probabilities of collapse in the MCE_R as given in Tables 4-1 and 4-2. The selected EDP limits of 0.3g and 0.5% for peak floor or roof acceleration and peak story drift ratio indicate the onset of damage to non-structural components and to the building contents (Elenas and Meskouris, 2001; Furukawa et al, 2013; Soroushian et al, 2014). The limits of 0.5% to 1.0% for the residual story drift ratio denote that the building will likely have to be demolished as it would be uneconomical to repair (McCormick et al., 2008; FEMA, 2012[a]; Bojorquez and Ruiz-Garcia, 2013).

The results in Table 5-1 show that isolated structures designed with the minimum or by enhanced design criteria have lower probabilities than comparable non-isolated structures to develop, within a lifetime of 50 years, some form of minor damage to non-structural components and building contents or to have large enough residual story drift to require demolition. When isolated structures are designed by the enhanced criteria of R_I=1 in the DE and with stiffening isolators having $D_{Capacity}$=1.5D_M and $D_{Ultimate}$=1.9D_M, there is substantial reduction of the probabilities to develop damage or to require demolition. It is noted that the enhanced braced frame designs (SCBF with R_I=1.0 in the DE and OCBF with R_I=1.0 in the MCE_R and isolators with $D_{Capacity}$=1.5D_M and $D_{Ultimate}$=1.9D_M) have the lowest probabilities to develop minor damage or to require demolition which are noticeably less than those of the isolated moment frames. Characteristic of the two designs is that they have a calculated peak drift ratio of less than 0.2% (for the DE or the MCE_R) per Table 2-2, whereas the enhanced moment frame designs have a drift ratio of less than 1.5% per Table 2-3. This difference is important in controlling damage.

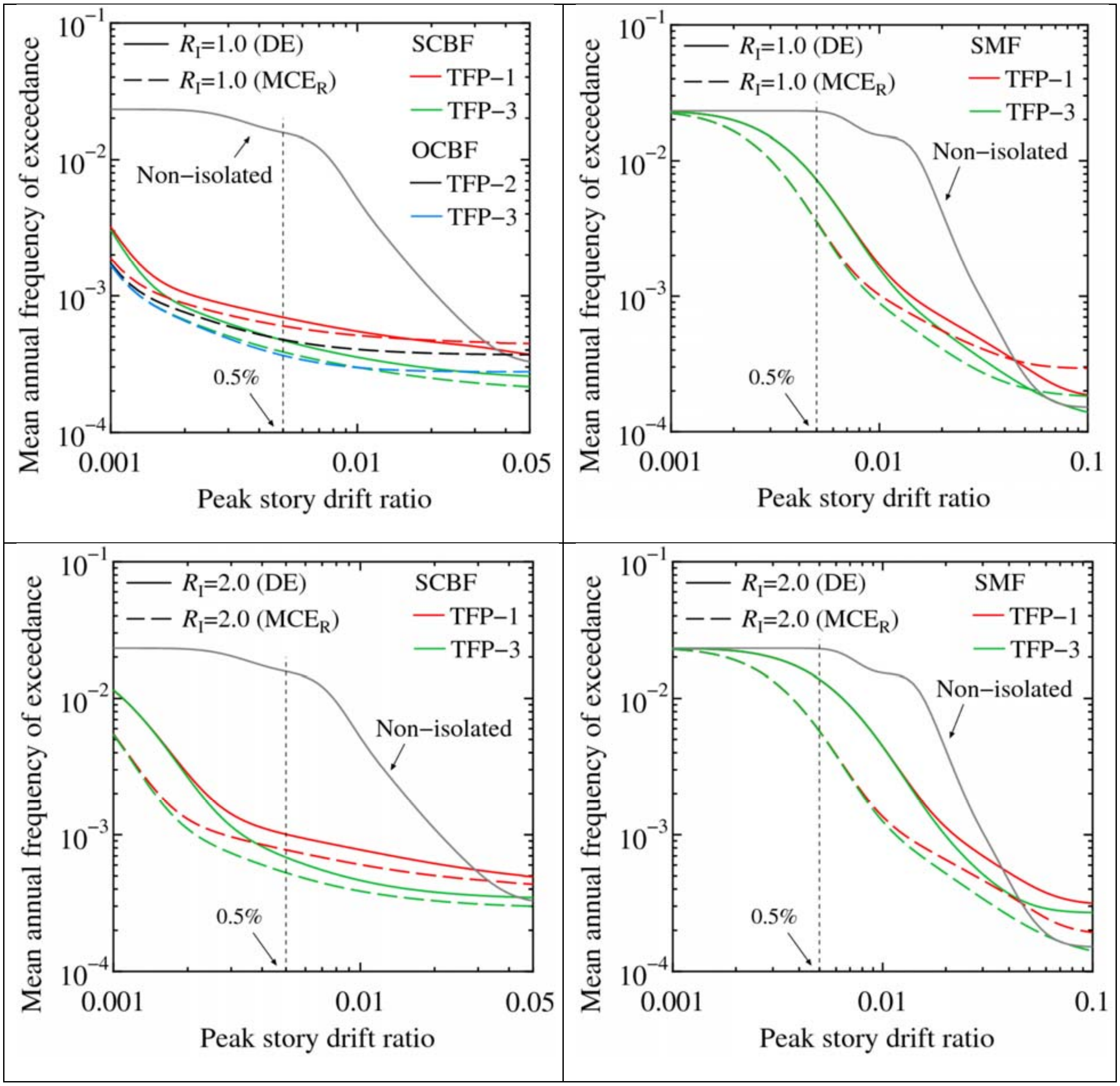

Figure 5-1 Mean Annual Frequency of Exceeding Limits on Peak Story Drift Ratio

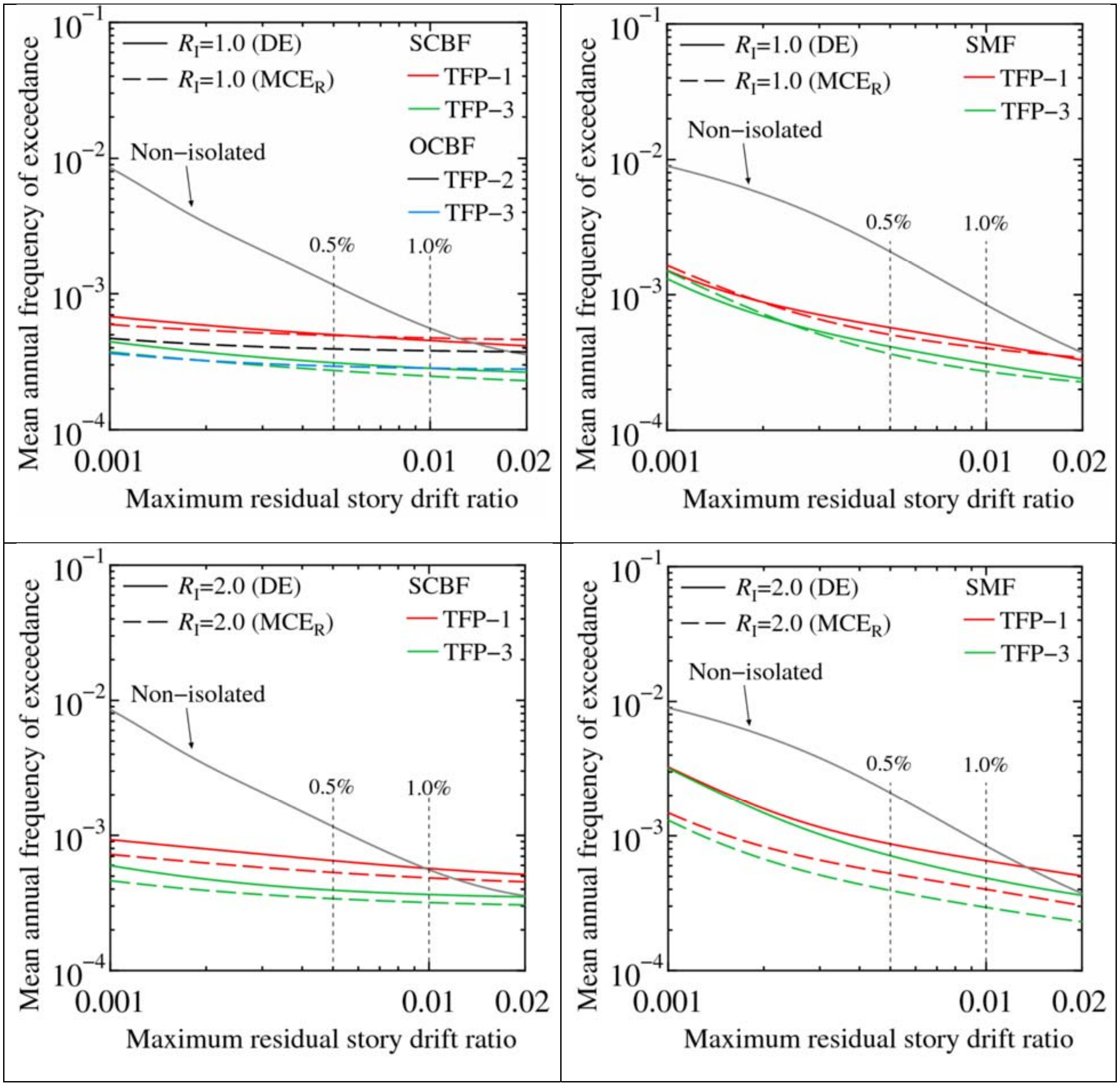

Figure 5-2 Mean Annual Frequency of Exceeding Limits on Peak Residual Story Drift Ratio

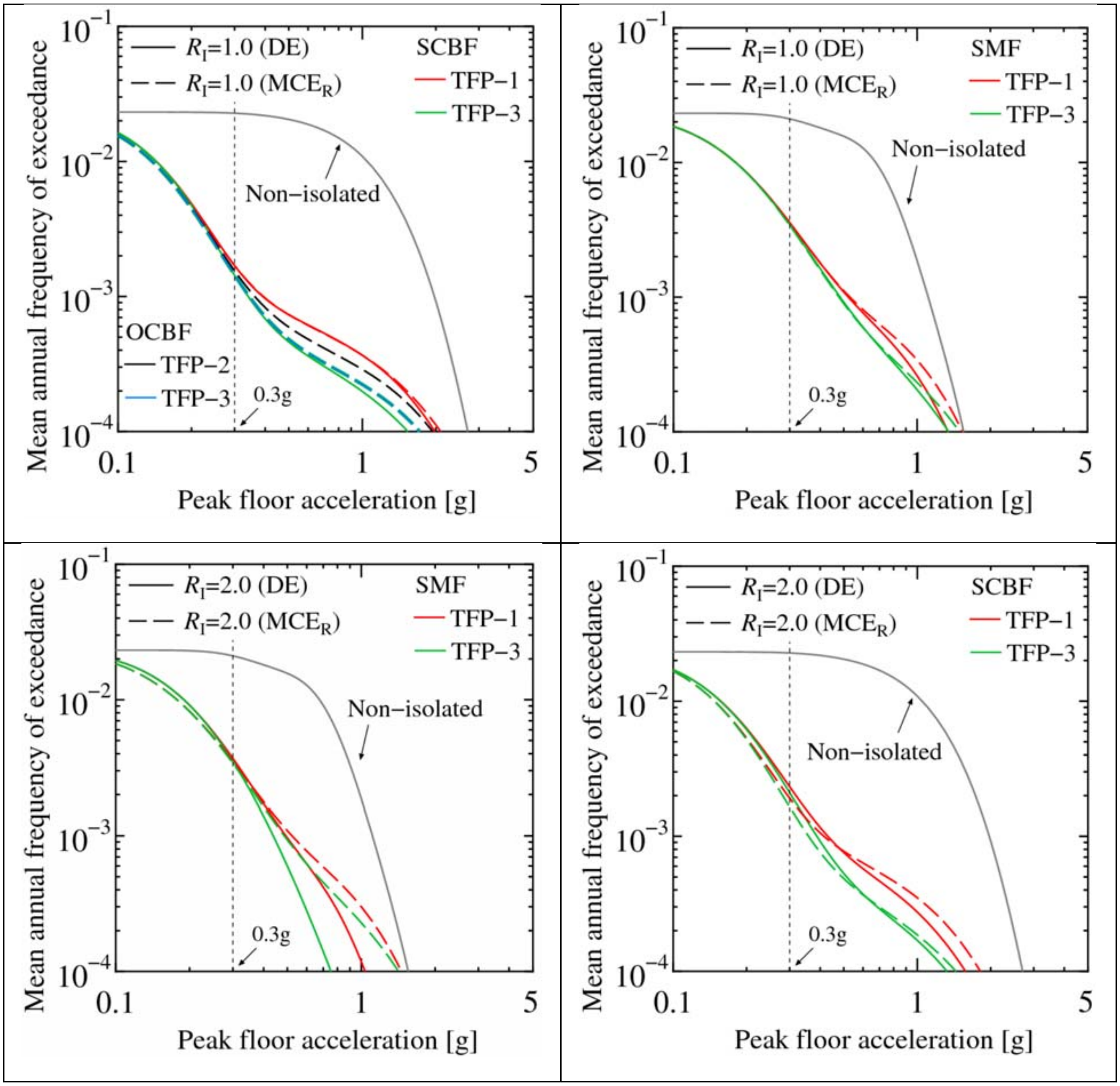

Figure 5-3 Mean Annual Frequency of Exceeding Limits on Floor Acceleration

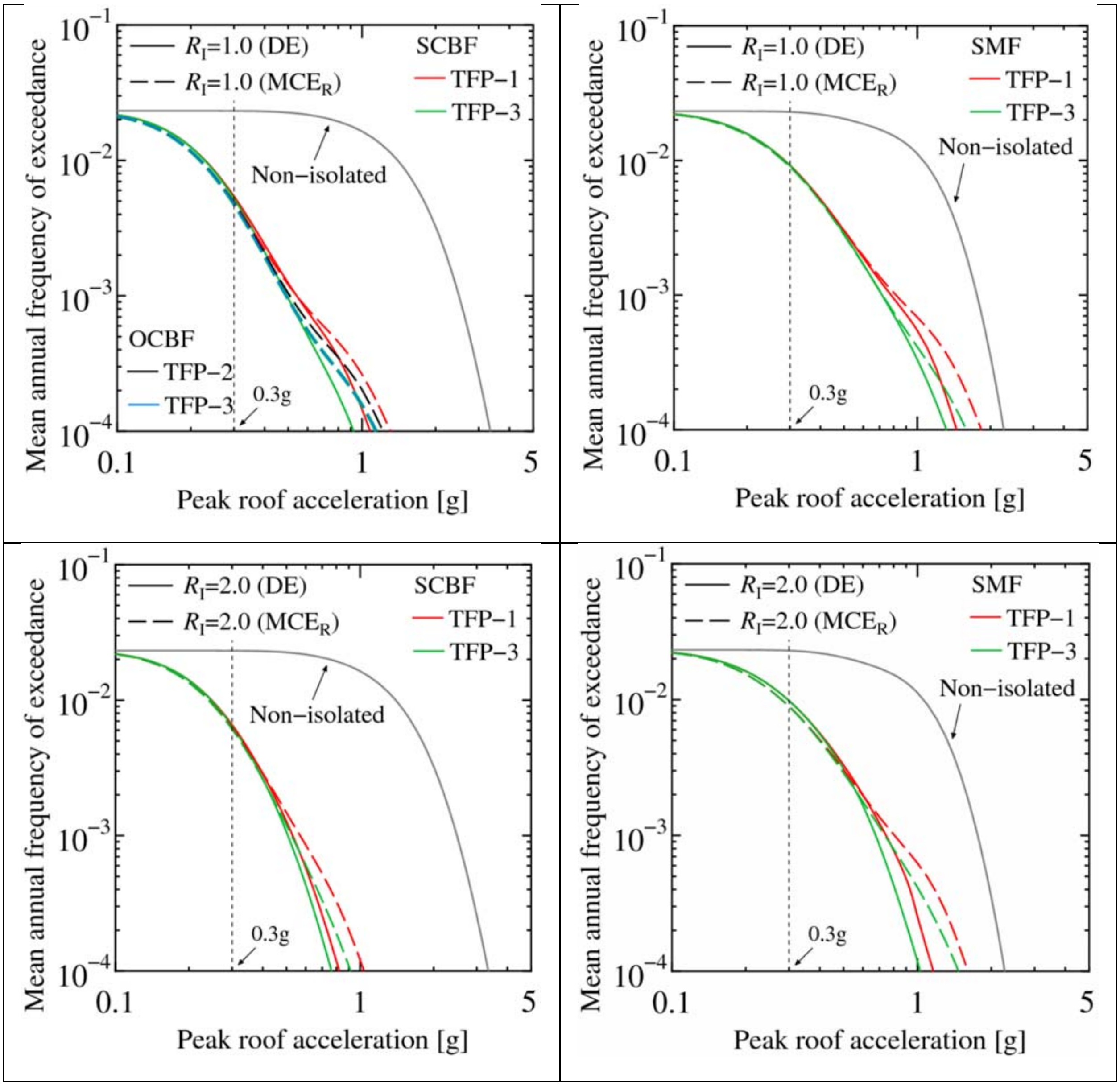

Figure 5-4 Mean Annual Frequency of Exceeding Limits on Roof Acceleration

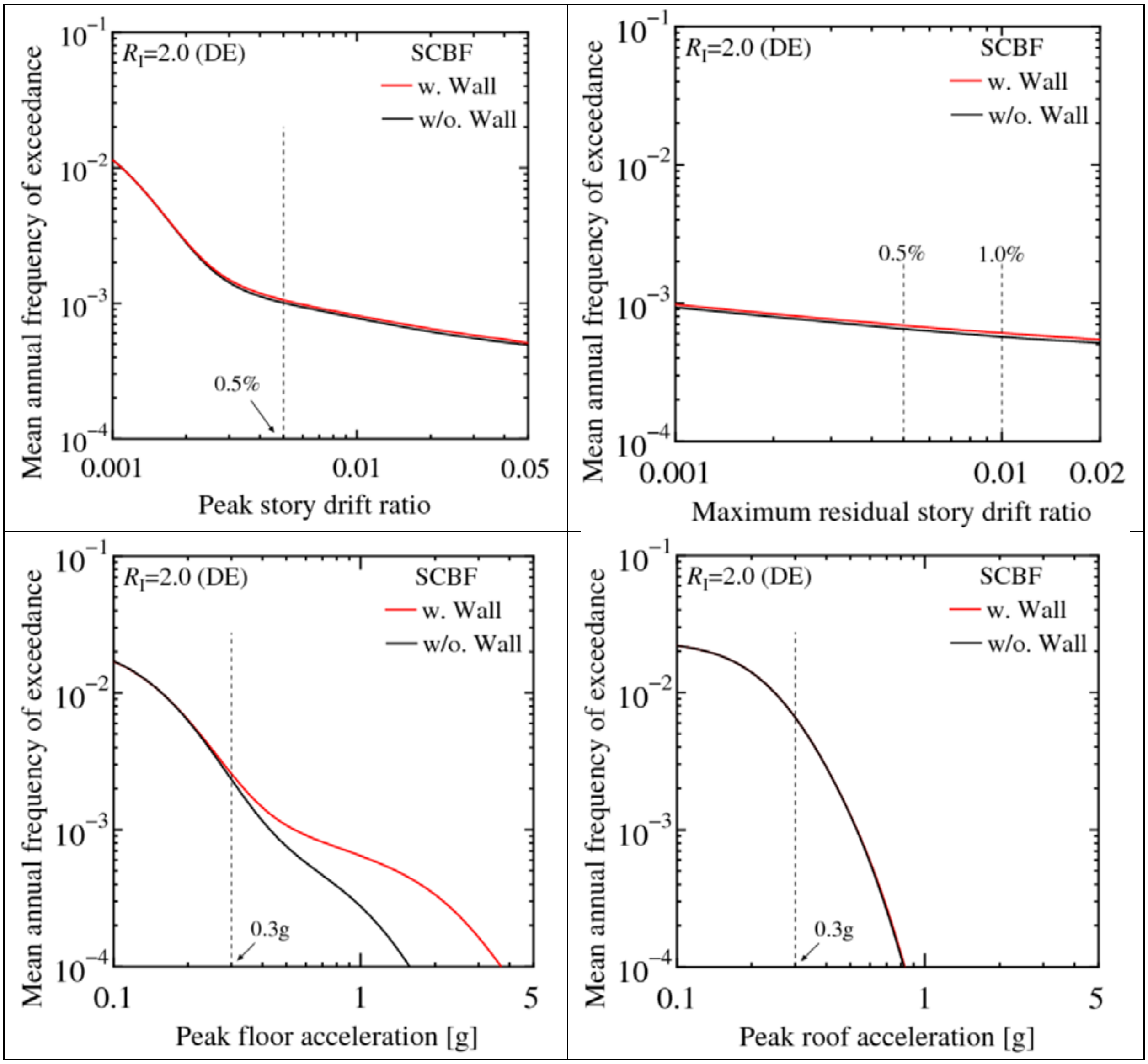

Figure 5-5 Comparisons of Mean Annual Frequency of Exceeding Limits on Drift, Residual Drift and Peak Acceleration for SCBF Designed per Minimum Criteria of ASCE 7-10 (R_I=2, Isolator TFP-1) without and with Moat Wall at D_M

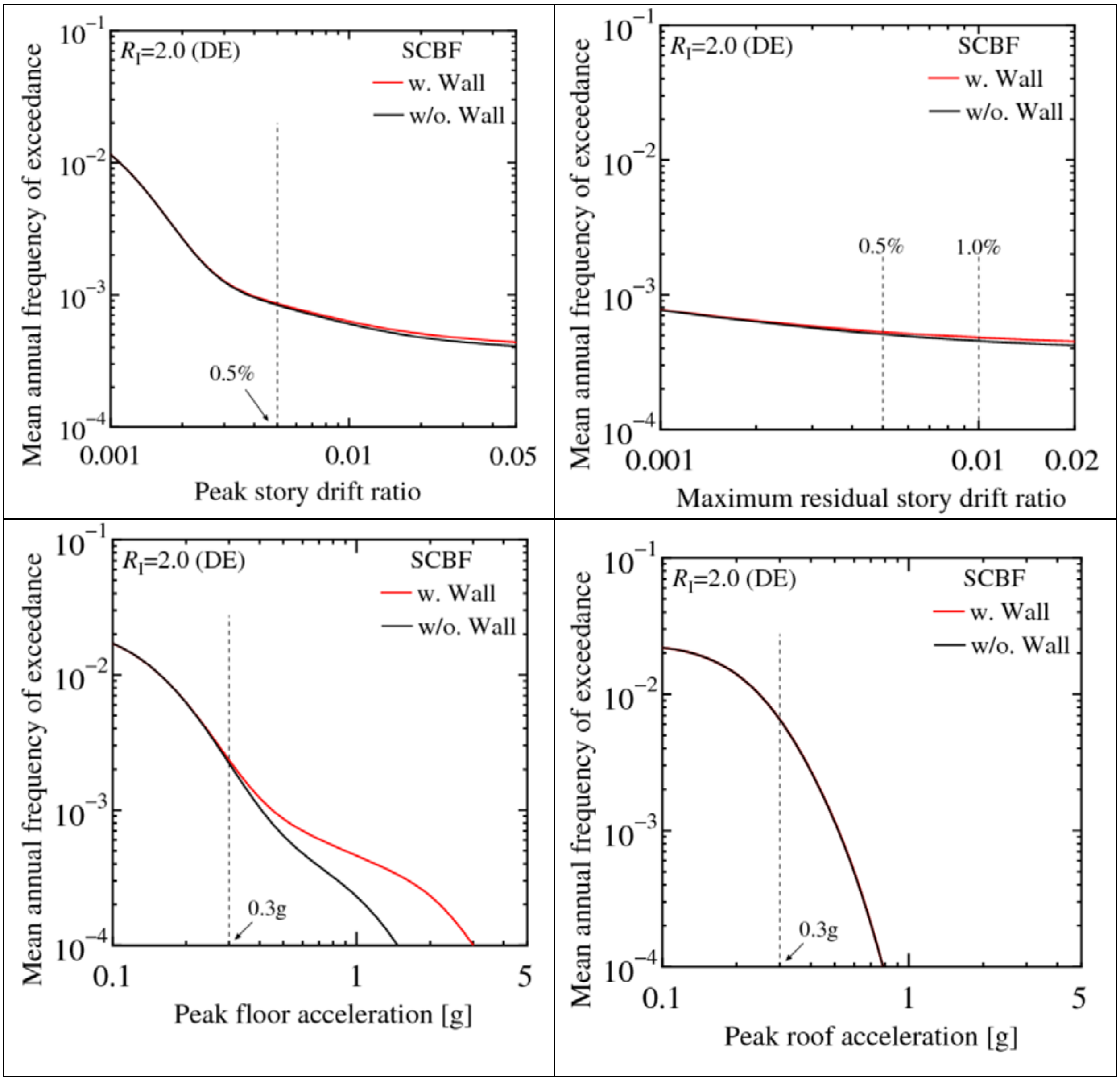

Figure 5-6 Comparisons of Mean Annual Frequency of Exceeding Limits on Drift, Residual Drift and Peak Acceleration for SCBF Designed per ASCE 7-10 for R_I=2, Isolator TFP-2 without and with Moat Wall at 1.25D_M

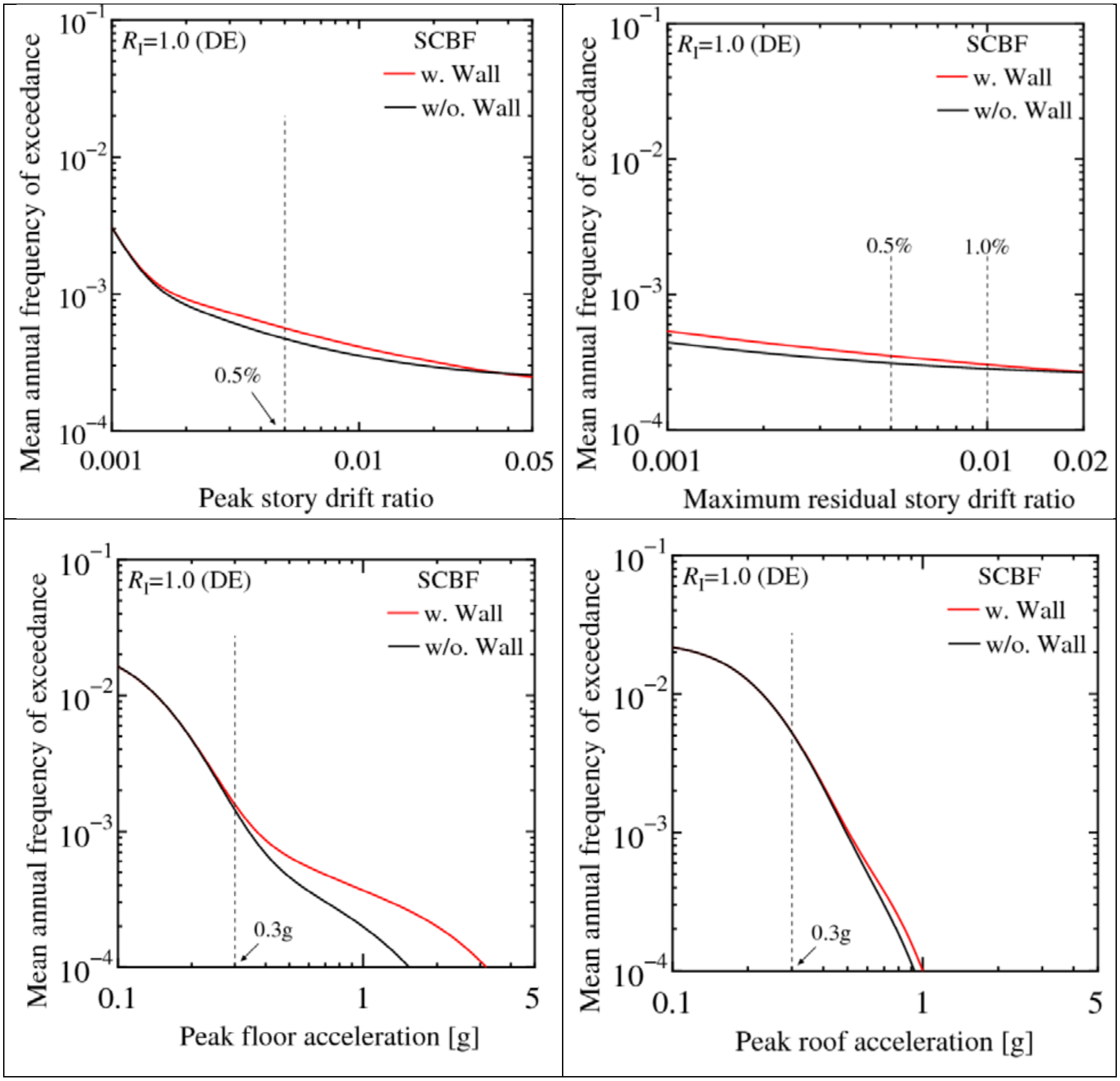

Figure 5-7 Comparisons of Mean Annual Frequency of Exceeding Limits on Drift, Residual Drift and Peak Acceleration for SCBF Designed per ASCE 7-10 for R_I=I, Isolator TFP-3 without and with Moat Wall at 1.50D_M (design without moat wall meets criteria for continued functionality per Zayas et al, 2017)

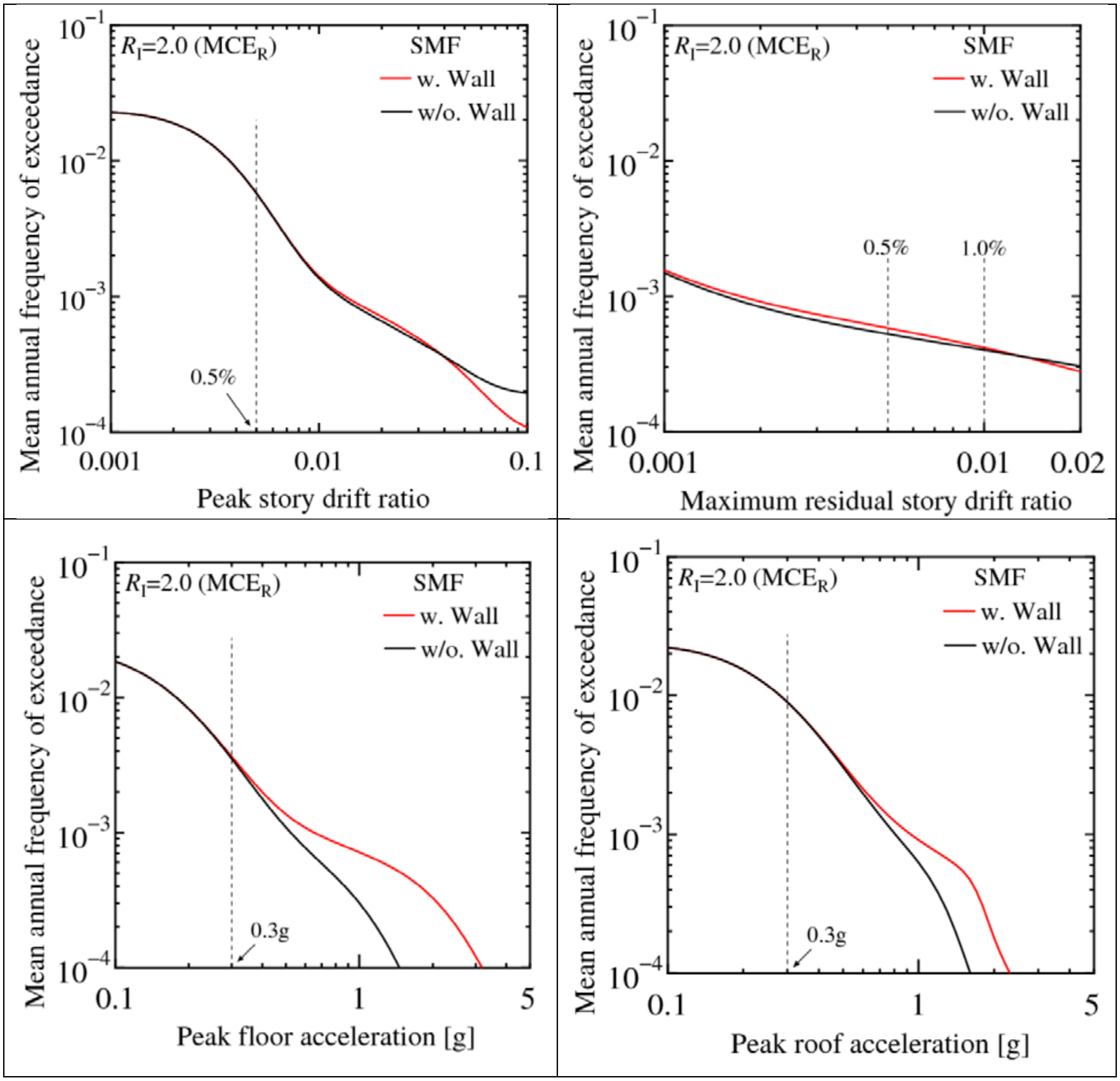

Figure 5-8 Comparisons of Mean Annual Frequency of Exceeding Limits on Drift, Residual Drift and Peak Acceleration for SMF Designed per Minimum Criteria of ASCE 7-16 (R_I=2, Isolator TFP-1) without and with Moat Wall at D_M

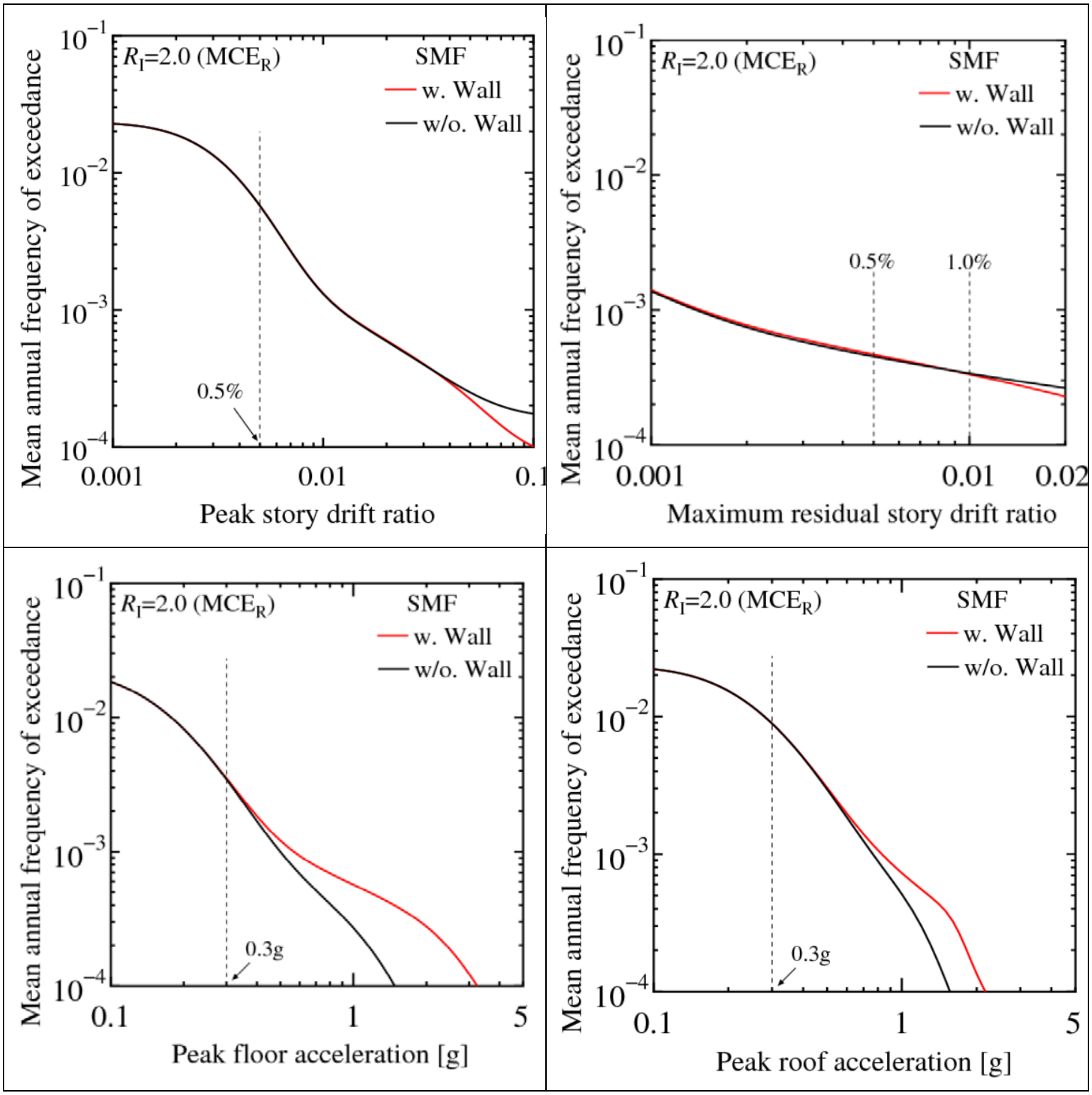

Figure 5-9 Comparisons of Mean Annual Frequency of Exceeding Limits on Drift, Residual Drift and Peak Acceleration for SCBF Designed per ASCE 7-16 for R_I=2, Isolator TFP-2 without and with Moat Wall at 1.25D_M

Table 5-1 Probabilities in % of Collapse in MCE_R and Probabilities of Exceeding in 50 Years Limits on Floor (Roof in Parenthesis) Acceleration, Story Drift Ratio and Residual Drift Ratio for Isolated and Non-Isolated Buildings (PSDR=Peak Story Drift Ratio, PRDR=Peak Residual Drift Ratio, PFA=Peak Floor Acceleration, PRA=Peak Roof Acceleration)

Design Description	Prob. of Collapse in MCE_R (per FEMA P695)	Prob. of Exceeding 0.005 PSDR in 50 years	Prob. of Exceeding 0.005 PRDR in 50 years	Prob. of Exceeding 0.01 PRDR in 50 years	Prob. of Exceeding 0.3g PFA (PRA) in 50 years
Non-isolated SMF, R=8, minimum requirements of ASCE 7-10 and 7-16	0.46	68.4	9.9	4.1	65.1 (68.2)
Isolated SMF, minimum requirements of ASCE 7-10 R_I=2 (DE), TFP-1	6.06	49.7	4.3	3.2	16.9 (38.8)
Isolated SMF, minimum requirements of ASCE 7-16 R_I=2 (MCE_R), TFP-1	4.97	25.0	2.6	2.0	16.1 (36.0)
Isolated SMF, minimum requirements of ASCE 7-16 R_I=2 (MCE_R), TFP-1, moat wall at D_M	0.81	25.1	2.9	2.1	16.7 (36.0)
Isolated SMF, enhanced requirements R_I=1 (DE), TFP-3 $D_{Capacity}$=1.5D_M, $D_{Ultimate}$=1.9D_M	1.44	30.3	2.0	1.5	15.9 (36.7)
Non-isolated SCBF, R=6, minimum requirements of ASCE 7-10 and 7-16	8.15	54.4	5.6	2.7	68.0 (68.6)
Isolated SCBF, minimum requirements of ASCE 7-10 R_I=2 (DE), TFP-1	18.06	4.9	3.2	2.8	11.0 (28.0)
Isolated SCBF, minimum requirements of ASCE/SEI 7-10 R_I=2 (DE), TFP-1, moat wall at D_M	17.13	5.1	3.4	3.0	12.0 (28.1)
Isolated SCBF, minimum requirements of ASCE/SEI 7-10 R_I=2 (DE), TFP-2	12.66	4.1	2.5	2.2	10.5 (27.7)
Isolated SCBF, minimum requirements of ASCE/SEI 7-10 R_I=2 (DE), TFP-2, moat wall at 1.25D_M	12.96	4.2	2.6	2.4	11.1 (27.8)
Isolated SCBF, minimum requirements of ASCE/SEI 7-16 R_I=2 (MCE_R), TFP-1	13.94	3.8	2.6	2.4	9.2 (27.0)
Isolated SCBF, enhanced requirements R_I=1 (DE), TFP-3, $D_{Capacity}$=1.5D_M, $D_{Ultimate}$=1.9D_M	4.52	2.3	1.5	1.4	6.9 (23.0)

Isolated SCBF, enhanced requirements R_I=1 (DE), TFP-3, $D_{Capacity}$=1.5D_M, $D_{Ultimate}$=1.9D_M Moat Wall at 1.5D_M	4.98	2.8	1.7	1.5	7.6 (23.2)
Isolated OCBF, minimum requirements R_I=1 (MCE$_R$),TFP-2, $D_{Capacity}$=1.25D_M, $D_{Ultimate}$=1.6D_M	12.31	2.4	1.9	1.9	7.5 (21.5)
Isolated OCBF, enhanced requirements R_I=1 (MCE$_R$),TFP-3, $D_{Capacity}$=1.5D_M, $D_{Ultimate}$=1.9D_M	7.96	1.8	1.5	1.4	7.0 (21.2)
Isolated SMF, minimum requirements of ASCE 7-16 R_I=2 (MCE$_R$), TFP-2	2.46	25.0	2.2	1.7	15.8 (35.9)
Isolated SMF, minimum requirements of ASCE 7-16 R_I=2 (MCE$_R$), TFP-2 Moat wall at 1.25D_M	0.85	25.0	2.3	1.7	16.1 (35.9)

SECTION 6
COMPARISON OF RESULTS OF COLLAPSE ASSESSMENT OBTAINED BY FEMA P695 PROCEDURE AND BY A PROBABILISTIC APPROACH USING CONDITIONAL SPECTRA

The procedure used in Section 5 to obtain results on the probabilistic response of isolated structures (NIST, 2011; Lin et al, 2013[a]) is also suitable to obtain information on the probability of collapse given a particular level of seismic intensity. This allows comparison of results obtained by this procedure to those obtained using the FEMA P695 procedure (FEMA, 2009) and presented in Section 4.

The probabilistic approach of Section 5 (with additional information in Appendix B) makes use of sets of motions (sample of 40) compatible with conditional spectra for seismic intensities related to return periods in the range of 43 to 10000 years (10 intensities). The motions used for each seismic intensity are different (unlike the IDA procedure used in FEMA P695 which utilizes of the same motions for all seismic intensities). Accordingly, the results of the procedure directly account for the spectral shape effects.

The probabilistic approach involves analysis of each considered structural system with 400 motions. These motions differ depending on the fundamental period of the structural system as the conditional spectra depend on this period. Given that the structural models used in the analysis include features that directly or indirectly detect collapse as described in Section 3, the procedure may be used to obtain results on the probability of collapse as function of the seismic intensity.

Figure 6-1 illustrates the procedure for obtaining results using the probabilistic approach of Section 5 (and Appendix B) and how the results compare with those obtained by use of the FEMA P695 procedure. The results presented in Figure 6-1 apply for the isolated SCBF designed for R_I=2 per ASCE/SEI 7-10 with isolator TFP-1. The top graphs in the figure show the fragility curves as obtained by fitting the data of the IDA analysis following the FEMA P695 procedure and the NIST/Lin analysis using the 400 motions compatible with conditional spectra for ten different return periods. The data of the FEMA P695 analysis are the adjusted for the effect of the spectral shape (*SSF*=1.23) resulting in a fragility curve with the same dispersion factor but a larger median. The fragility curve obtained by the NIST/Lin procedure does not require any adjustment. The two fragility curves are shown again in the bottom graph of the figure in solid lines in which the media and dispersion factors are included in the graphs. Note that the dispersion factor in the fragility curves only accounts for the record-to-record variability in the ground motions (is denoted as β_{RTR}).

The value of the dispersion factor is then adjusted to account for uncertainties as described by Equation 4-5 and the following quality ratings and related uncertainties based on FEMA P695: good with β_{MDL}=0.2 for modeling; good with β_{TD}=0.2 for test data and superior with β_{DR}=0.1 for design requirements. The resulting values of the total dispersion factor β_{TOT} are shown in the figure with the corresponding fragility curves shown in dashed lines.

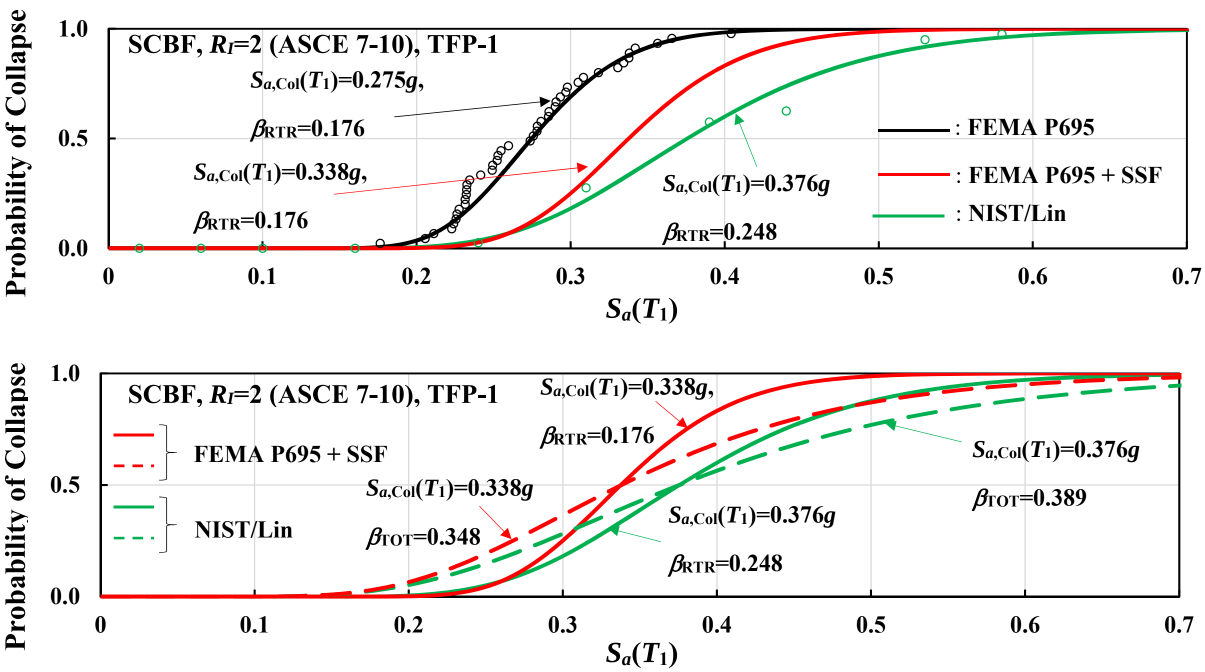

Figure 6-1 Comparison of Fragility Curves for Isolated SCBF, Case R_I=2, Isolator TFP-1 Obtained by Different Methodologies

Table 6-1 presents results of comparison of results obtained for several studied systems using the FEMA P695 and the NIST/Lin methodologies as described above. In calculating the probability of collapse for MCE$_R$ in the table, the value of $S_{aMCE}(T_1)$ as obtained from the MCE$_R$ spectrum was used. This value is equal to 0.246g for the isolated structures (T_1=T_M=3.66sec). The results in the table demonstrate difference in the values of the probabilities but also consistency in how changes in design (in terms of value of R_I , isolator displacement capacity and isolation system characteristics) affect the probability of collapse. The differences in the calculated values of the probability of collapse are relatively small given the significant differences in the two methodologies. This is may be a viewed as validation of the two methodologies.

Table 6-1 Comparison of Probabilities of Collapse of SCBF Obtained by Different Methodologies

Methodology		FEMA P695 (FEMA, 2009) with Direct Evaluation of Spectral Shape Effects			Lin et al (2013[a]), NIST (2011)		
System		$Sa_{Col}(T_1)$ (g)	β_{TOT} (β_{RTR})	Prob. Collapse in MCE_R (%)	$Sa_{Col}(T_1)$ (g)	β_{TOT} (β_{RTR})	Prob. Collapse in MCE_R (%)
Designed per ASCE 7-10	R_I=1.0, TFP-1	0.365	0.366 (0.209)	14.08	0.424	0.434 (0.314)	10.56
	*R_I=1.0, TFP-3	0.438	0.341 (0.163)	4.52	0.453	0.372 (0.219)	5.03
	*R_I=1.0, TFP-3 Moat wall at 1.5D_M	0.440	0.353 (0.187)	4.98	0.466	0.369 (0.215)	4.18
	R_I=2.0, TFP-1	0.338	0.348 (0.176)	18.06	0.376	0.389 (0.248)	13.85
	R_I=2.0, TFP-1 Moat wall at D_M	0.351	0.374 (0.224)	17.13	0.377	0.411 (0.281)	14.94
	R_I=2.0, TFP-2 Moat wall at 1.25D_M	0.368	0.357 (0.194)	12.99	0.390	0.403 (0.269)	12.68
	R_I=2.0, TFP-3	0.387	0.340 (0.159)	9.09	0.419	0.409 (0.278)	9.61
Designed per ASCE 7-16	R_I=1.0, TFP-1	0.328	0.356 (0.193)	21.09	0.382	0.408 (0.276)	14.02
	R_I=1.0, TFP-3	0.419	0.341 (0.161)	5.87	0.471	0.355 (0.189)	3.34
	R_I=2.0, TFP-1	0.362	0.357 (0.194)	13.94	0.386	0.376 (0.226)	11.58
	R_I=2.0, TFP-3	0.412	0.338 (0.156)	6.38	0.435	0.391 (0.250)	7.21
* Design meets criteria for continued functionality per Zayas et al (2017)							

Table 6-2 Comparison of Probabilities of Collapse of SMF Obtained by Different Methodologies

Methodology		FEMA P695 (FEMA, 2009) with Direct Evaluation of Spectral Shape Effects			Lin et al (2013[a]), NIST (2011)		
System		$Sa_{Col}(T_1)$ (g)	β_{TOT} (β_{RTR})	Prob. Collapse in MCE_R (%)	$Sa_{Col}(T_1)$ (g)	β_{TOT} (β_{RTR})	Prob. Collapse in MCE_R (%)
Designed per ASCE 7-10	R_I=1.0, TFP-1	0.455	0.387 (0.245)	5.58	0.504	0.394 (0.256)	3.44
	R_I=1.0, TFP-3	0.546	0.365 (0.208)	1.44	0.533	0.366 (0.210)	1.73
	R_I=2.0, TFP-1	0.447	0.385 (0.241)	6.60	0.441	0.427 (0.304)	8.61
	R_I=2.0, TFP-3	0.467	0.358 (0.195)	3.65	0.466	0.440 (0.322)	7.34
Designed per ASCE 7-16	R_I=1.0, TFP-1	0.398	0.371 (0.218)	9.68	0.435	0.387 (0.245)	7.05
	R_I=1.0, TFP-3	0.493	0.369 (0.215)	2.98	0.489	0.368 (0.213)	3.08
	R_I=2.0, TFP-1	0.467	0.389 (0.247)	4.97	0.500	0.396 (0.258)	3.67
	R_I=2.0, TFP-1 Moat wall at 1.00D_M	0.695	0.432 (0.311)	0.81	0.625	0.444 (0.327)	1.78
	R_I=2.0, TFP-2 Moat wall at 1.25D_M	0.640	0.400 (0.265)	0.85	0.592	0.386 (0.243)	1.15
	R_I=2.0, TFP-3	0.543	0.363 (0.204)	1.46	0.529	0.368 (0.212)	1.86

SECTION 7
CONCLUSIONS AND DISCUSSION

It has been shown that seismically isolated structures designed by the minimum criteria of ASCE/SEI 7-10 or 7-16 (ASCE, 2010 or 2016) may have unacceptable probabilities of collapse in the MCE_R, whereas comparable non-isolated structures, also designed by the minimum criteria of ASCE/SEI 7, have acceptable probabilities of collapse. Improvement of the collapse performance is achieved by designing for an R_I=1.0 in the DE and providing isolators with stiffening behavior and with a displacement capacity at initiation of stiffening equal to 1.5D_M and ultimate displacement capacity of 1.9D_M, where D_M is the displacement capacity in the MCE_R as stipulated by the minimum criteria of ASCE/SEI 7. In general, increasing the strength of seismically isolated structures (by reducing R_I) does not result in improvement of the collapse performance unless the displacement capacity of the isolators is proportionally increased. The reason for this behavior is that by increasing the strength, inelastic action in the superstructure is delayed so that the isolator displacement demand is increased leading to collapse by failure of the isolators.

The significance of providing isolator displacement restraint through the use of stiffening isolators or the use of moat walls was demonstrated by the substantial increase in the probability of collapse when the restrainer ring of the isolators was removed and no moat walls were used. For example, the probability of collapse in the MCE_R of the isolated SMF designed by the minimum criteria of ASCE/SEI 7-10 and triple FP isolators (TFP-1) was 6.1%. It was 39.9% when the isolator restrainer ring was removed and the isolators were converted to double concave with the minimum displacement capacity per ASCE/SEI 7-10 (DC-1) (the probabilities were 18.1% and 27.4%, respectively, for the SCBF designed by the minimum criteria of ASCE/SEI 7-10).

The use of moat walls was shown to result in essentially the same collapse behavior as similarly designed buildings with triple FP isolators that exhibit stiffening behavior. For example, minimally designed SCBF per ASCE/SEI 7-10 (R_I=2) had essentially the same probability of collapse in the MCE_R when the minimum size isolator TFP-1 was used (displacement capacity at initiation of stiffening equal to D_M and ultimate displacement capacity of 1.3D_M, where D_M is the displacement capacity in the MCE_R as stipulated by the minimum criteria of ASCE/SEI 7) and when a moat wall was placed at distance D_M or when the moat wall was removed. Use of the moat wall was shown to result in essentially the same pushover curves as when stiffening triple FP isolators were used, thus explaining the close results on the probability of collapse for the two cases. Increasing the gap in moat walls beyond the minimum required distance of D_M resulted in reduction of the probability of collapse similarly to the use of triple FP isolators of larger displacement capacity at initiation of stiffening. It should be noted that analysis without consideration of the spectral shape effects and considering only record-to-record uncertainties (as produced directly by incremental dynamic analysis) resulted in substantially larger probabilities of collapse when moat walls were used than when stiffening triple FP isolators were used. The differences in the probabilities of collapse diminished when the spectral shape effects and uncertainties were considered.

Moreover, it has been observed that the use of moat walls may improve the collapse performance by comparison to comparable designs with stiffening isolators in cases where collapse is dominated by failure of the isolators due to excessive displacement demand. This is the case when the design utilizes inconsistent combinations of superstructure strength (small R_I, say 1.0) and minimal displacement capacity isolators (say isolator TFP-1).

The conclusions of this study in terms of requirements for the superstructure design and the isolator displacement capacity to achieve acceptable collapse performance are consistent with the results of a similar study conducted for 3-story isolated structures (Shao et al, 2017).

Nearly all studied isolated structures of whatever design details had higher probabilities of collapse than the comparable non-isolated designs (actually all isolated SMF but not all other buildings had higher probability of collapse). Given this fact, studies of the performance of the designed isolated and non-isolated structures in terms of peak floor acceleration, peak story drift ratio and peak residual drift ratio were conducted in order to clarify any advantages offered by seismic isolation. These studies showed that isolated structures designed by any design criteria (minimum or enhanced) have lower probabilities than comparable non-isolated structures to develop, within a lifetime of 50 years, some form of minor damage to non-structural components and building contents or to have large enough residual story drift to require demolition. When isolated structures are designed by the enhanced criteria of R_I=1 in the DE and with stiffening isolators having $D_{Capacity}$=1.5D_M and $D_{Ultimate}$=1.9D_M, there is substantial reduction of the probabilities to develop damage or to require demolition. Best performance was obtained with the enhanced braced frame designs (SCBF with R_I=1.0 in the DE or OCBF with R_I=1.0 in the MCE_R and isolators with $D_{Capacity}$=1.5D_M and $D_{Ultimate}$=1.9D_M). These designs had noticeably less probabilities to develop minor damage or to require demolition than the isolated moment frames. Characteristic of the braced frame designs was a peak drift ratio of 0.2%, whereas the moment frame designs have a drift ratio of 1.5% - a difference of important in controlling damage. Also, these enhanced braced frame designs met the criteria of a standard for continued functionality developed by Zayas et al (2017). These enhanced brace frame designs have been shown to exhibit a reduction in effectiveness (in terms of increases in the mean annual probability of exceedance of floor peak acceleration) when moat walls were used.

The study also demonstrated the significance of utilizing restraint in the isolation system to limit displacements and prevent collapse of the isolators. The use of stiffening triple FP isolators is one of the options available. The other is the use of moat walls. However, the displacement capacity of the isolators and the location of the moat wall should be consistent with the superstructure design (value of R_I). Designs based on the minimum criteria of ASCE/SEI 7 and with a moat wall placed at the MCE_R displacement does not ensure an acceptable probability of collapse. Moreover, the lack of any restraint, either in the form of stiffening isolators or moat walls, ensures an unacceptable probability of collapse.

The presented studies were limited to examples of perimeter braced and moment 6-story steel frames with sliding isolators at one particular location in California. A study of Shao et al. (2017) included similar 3-story braced frames, also with sliding isolators. Neither of the two studies considered the effect of vertical ground shaking. There is a need to extend these studies to taller structures and to other structural systems (e.g., concrete space frames) in order to cover a wider range of structures of interest in seismic isolation. Moreover, these studies have been limited to the analysis of two-dimensional representations of isolated structures, whereas three-dimensional representations would have likely resulted in the prediction of higher probabilities of collapse. Similarly, consideration of the vertical ground shaking should result in even higher probabilities of collapse.

Nevertheless, the results of these studies clearly show a need to re-visit the ASCE/SEI 7 criteria for the design of seismically isolated structures. Ideally, the specified R_I factor, the minimum displacement capacity of the isolators and the isolator stiffening characteristics should be dependent on the seismic force-resisting system. In the absence of such detailed studies, it justified to require designs with R_I=1.0 and isolators with D_{Capacity}=1.5D_{M} and D_{Ultimate}=1.9D_{M} in order to ensure acceptable collapse performance for important structures. Such a design also offers additional benefits in terms reduction of the probability to develop minor damage to non-structural components and the building contents, and in reducing the probability of having to demolish the building in its lifetime. These benefits become substantial when additional requirements on drift and floor acceleration are imposed, such as the limits of 0.3% or 0.4% on the peak drift and 0.4g or 0.6g on the floor spectral acceleration (median in period range of zero to 5sec). An option for achieving this desired performance is to apply the provisions of ASCE/SEI 7-16 (ASCE, 2017) together with the criteria of the standard for continued functionality developed by Zayas (2017). This may ensure acceptable probabilities of collapse and also sufficiently limit building damage to qualify for the Arup (2013) REDi platinum or gold rating on seismic resiliency.

SECTION 8
REFERENCES

American Institute of Steel Construction. (2010). “Steel Construction Manual”, 14th Ed., Third Printing. AISC: Chicago, IL.

Arup. (2013). “Resilience-based Earthquake Design Initiative (REDi^{TM}) Rating System”. Version 1.0.

ASCE/SEI 7. (2010). “Minimum Design Loads for Buildings and Other Structures.” American Society of Civil Engineers: VA, U.S.A.

ASCE/SEI 7. (2017). “Minimum Design Loads for Buildings and Other Structures.” American Society of Civil Engineers: VA, U.S.A.

Baker JW, Cornell CA. (2006). “Spectral Shape, Epsilon and Record Selection.” *Earthquake Engineering and Structural Engineering*. 35(9), 1077-1095.

Baker JW, Jayaram N. (2008). “Correlation of Spectral Acceleration Values from NGA Ground Motion Models.” *Earthquake Spectra*. 24(1), 299-317.

Baker JW. (2011). “Conditional Mean Spectrum: Tool for Ground-Motion Selection.” *Journal of Structural Engineering*. 137(3), 332-344.

Baker JW. (2015). “Efficient Analytical Fragility Function Fitting Using Dynamic Structural Analysis.” *Earthquake Spectra*. 31 (1). 579-599.

Baker JW, Lee C. (2017). “An Improved Algorithm for Selecting Ground Motions to Match a Conditional Spectrum.” *Journal of Earthquake Engineering*. DOI: 10.1080/13632469.2016.1264334.

Bao Y, Becker TC, Hamaguchi H. (2016). “Failure of Double Friction Pendulum Bearings under Pulse-Type Motions.” *Earthquake Engineering and Structural Dynamics*, 46(5), 715–732. DOI: 10.1002/eqe.2827.

Bojorquez E, Ruiz-Garcia J. (2013). “Residual Drift Demands in Moment-Resisting Steel Frames Subjected to Narrow-Band Earthquake Ground Motions.” *Earthquake Engineering and Structural Dynamics*, 42(11), 1583–1598.

Boore DM, Stewart JP, Seyhan E, Atkinson GM. (2014). NGA-West2 Equations for Predicting PGA, PGV, and 5% damped PSA for Shallow Crustal Earthquake.” *Earthquake Spectra*. 30(3), 1057-1085.

Chen CH, Mahin SA. (2012). “Performance-Based Seismic Demands Assessment of Concentrically Braced Steel Frame Buildings.” *PEER 2012/103*, December, Pacific Earthquake Engineering Research Center, PEER.

Chimamphant S., Kasai K. (2016). “Comparative Response and Performance of Base-Isolated and Fixed-Base Structures.” *Earthquake Engineering and Structural Dynamics*, 45(1), 5-27. DOI: 10.1002/eqe.2612.

Chopra AK, McKenna F. (2016). “Modeling Viscous Damping in Nonlinear Response History Analysis of Buildings for Earthquake Excitation.” *Earthquake Engineering and Structural Dynamics*, 45(2), 193–211. DOI: 10.1002/eqe.2622.

Elenas A, Meskouris K. (2001). “Correlation Study between Seismic Acceleration Parameters and Damage Indices of Structures.” *Engineering Structures*. 23 (6). 698-704.

Elkady A, Lignos DG. (2014). “Modeling of the Composite Action in Fully Restrained Beam-to-Column Connections: Implications in the Seismic Design and Collapse Capacity of Steel Special Moment Frames.” *Earthquake Engineering and Structural Dynamics*, 43(13), 1935-1954.

Erduran E, Dao ND, Ryan KL. “Comparative Response Assessment of Minimally Compliant Low-Rise Conventional and Base-Isolated Steel Frames.” *Earthquake Engineering and Structural Dynamics* 2010; **40**(10): 1123–1141.

Executive Order 13717, “Establishing a Federal Earthquake Risk Management Standard.” February 2, 2016.

FEMA. (2000). “Recommended Seismic Design Criteria for New Steel Moment-Frame Buildings.” *Report FEMA 350*, Federal Emergency Management Agency, Washington DC, USA, 2009.

FEMA. (2009). “Quantification of Building Seismic Performance Factors.” *Report FEMA P695*, Federal Emergency Management Agency, Washington DC, USA, 2009.

FEMA. (2012[a]). “Seismic Performance Assessment of Buildings.” Report FEMA P-58, Federal Emergency Management Agency, Washington DC, U.S.A., 2012.

FEMA. (2012[b]). “Reducing the Risks of Nonstructural Earthquake Damage – A Practical Guide.” Report FEMA E-74, Federal Emergency Management Agency, Washington DC, U.S.A., 2012.

Fenz DM, Constantinou MC. (2006). “Behaviour of the Double Concave Friction Pendulum bearing.” *Earthquake Engineering and Structural Dynamics*, 35(11), 1403–1424.

Fenz DM, Constantinou MC. (2008[a]). “Modeling Triple Friction Pendulum Bearing for Response-History Analysis.” *Earthquake Spectra* 2008; **24** (4): 1011-1028. DOI: http://dx.doi.org/10.1193/1.2982531.

Fenz DM, Constantinou MC. (2008[b]). “Spherical Sliding Isolation Bearings with Adaptive Behavior: Theory.” *Earthquake Engineering and Structural Dynamics*, 37(2), 163–183.

Field EH, Jordan TH, Cornell CA. (2003). “OpenSHA: Adeveloping Community-Modeling Environment for Seismic Hazard Analysis.” *Seismological Research Letters*, 74 (4), 406-419.

Filippou FC, Popov EP, Bertero VV. (1983). “Effects of Bond Deterioration on Hysteretic Behavior of Reinforced Concrete Joints.” *Report EERC 83-19*, Earthquake Engineering Research Center, University of California, Berkeley.

Furukawa S, Sato E, Shi Y, Becker T, Nakashima M. (2013). “Full-Scale Shaking Table Test of a Base-Isolated Medical Facility Subjected to Vertical Motions.” *Earthquake Engineering and Structural Dynamics*, 42(13), 1931-1949.

Haselton CB, Baker JW, Liel AB, Deierlein GG. (2011). "Accounting for Ground-Motion Spectral Shape Characteristics in Structural Collapse Assessment Through an Adjustment for Epsilon." *Journal of Structural Engineering*, 137(3), 332-344.

Hayes J, McCabe SL. Mahoney M. (2017). "ICSSC Recommended Practice (RP) 9. Implementation Guidelines for Executive Order 13717: Establishing a Federal Earthquake Risk Management Standard." *National Institute of Standards and Technology (NIST) Technical Note 1922*. DOI: https://doi.org/10.6028/NIST.TN.1922.

Hsiao PC, Lehman DE, Roeder CW. (2012). "Improved Analytical Model for Special Concentrically Braced Frames." *ASCE Journal of Constructional Steel Research*, 73: 80-94.

Jalayer F. (2003). "Direct Probabilistic Seismic Analysis: Implementing Non-Linear Dynamic Assessments." *PhD Thesis*, Stanford University.

Jayaram N, Lin T, Baker JW. (2011). "A Computationally Efficient Ground-Motion Selection Algorithm for Matching a Target Response Spectrum Mean and Variance." *Earthquake Spectra*. 27 (3), 797-815.

Kikuchi M, Tamura K, Wada A. (1995). "Safety Evaluation of Base-Isolated Structures." *J. Struct. Constr. Eng*., AIJ, No. 470, 65-73, Apr. (in Japanese).

Kitayama S, Constantinou MC. (2016). "Probabilistic Collapse Resistance and Residual Drift Assessment of Buildings with Fluidic Self-Centering Systems." *Earthquake Engineering and Structural Engineering*, 45(12), 1935–1953. DOI: 10.1002/eqe.2733.

Kitayama S, Constantinou MC, Lee D. (2016). "Procedures and Results of Assessment of Seismic Performance of Seismically Isolated Electrical Transformers with due Consideration for Vertical Isolation and Vertical Ground Motion Effects." *MCEER-16-0010*; Multidisciplinary Center for Earthquake Engineering Research, Buffalo, NY.

Kohrangi M, Bazzurro P, Vamvatsikos D, Spillatura A. (2017). Conditional spectrum-based ground motion record selection using average spectral acceleration. *Earthquake Engineering and Structural Engineering*, 46 (10), 1667-1685.

Lignos DG, Krawinkler H. (2011). "Deterioration Modeling of Steel Components in Support of Collapse Prediction of Steel Moment Frames under Earthquake Loading." *Journal of Structural Engineering*, 137(11), 1291–1302. DOI:10.1061/(ASCE)ST.1943-541X.0000376.

Lin T, Haselton CB, Baker JW. (2013[a]). "Conditional Spectrum-Based Ground Motion Selection. Part I: Hazard Consistency for Risk-Based Assessments." *Earthquake Engineering and Structural Engineering*, 42 (12), 1847-1865.

Lin T, Harmsen SC, Baker JW, Luco N. (2013[b]). Conditional spectrum computation incorporating multiple causal earthquakes and ground-motion prediction models. *Bulletin of the Seismological Society of America*, 103 (2A), 1103-1116.

Masroor A., Mosqueda G. (2015). "Assessing the Collapse Probability of Base-Isolated Buildings Considering Pounding to Moat Walls using the FEMA P695 Methodology." *Earthquake Spectra*. 31(4). 2069-2086.

McCormick J, Aburano H, Ikenaga M, Nakashima M. (2008). "Permissible Residual Deformation Levels for Building Structures Considering both Safety and Human Elements." Proceedings of the 14th World Conference on Earthquake Engineering. Auckland New Zealand, Paper number 2421.

McKenna FT. (1997). "Object-Oriented Finite Element Programming: Frameworks for Analysis, Algorithms and Parallel Computing." *Ph.D. Thesis*. Department of Civil and Environmental Engineering, University of California, Berkeley.

McVitty WJ, Constantinou MC. (2015). "Property Modification Factors for Seismic Isolators: Design Guidance for Buildings." *MCEER-15-0005*, Multidisciplinary Center for Earthquake Engineering Research, Buffalo, NY.

Nakazawa N, Kishiki S, Qu Z, Miyoshi A, Wada A. (2011). "Fundamental Study on Probabilistic Evaluation of the Ultimate State of Base Isolated Structures." *8CUEE Conference Proceedings*, 8th International Conference on Urban Earthquake Engineering, March 7-8, 2011, Tokyo Institute of Technology, Tokyo, Japan.

Neter J, Kutner M, Wasserman W, Nachtsheim C. (1996). *Applied linear statistical models*, 4th edition, McGraw-Hill/Irwin.

NIST. (2010). “Evaluation of the FEMA P-695 Methodology for Quantification of Building Seismic Performance Factors.” *NIST GCR 10-917-8*. Technical Report, prepared by the NEHRP Consultants Joint Venture for the National Institute of Standards and Technology: Gaithersburg, Maryland.

NIST. (2011). “Selecting and Scaling Earthquake Ground Motions for Performing Response-History Analysis.” *NIST GCR 11-917-15*. Technical Report, prepared by the NEHRP Consultants Joint Venture for the National Institute of Standards and Technology: Gaithersburg, Maryland.

Ponzo FC, Cesare AD, Leccese G, Nigro D. (2017). “Shake Table Testing on Restoring Capability of Double Concave Friction Pendulum Seismic Isolation Systems.” *Earthquake Engineering and Structural Dynamics*. 46 (14). DOI: 10.1002/eqe.2907.

Ryu KP, Reinhorn AM. (2017) “Experimental Study of Large Area Suspended Ceilings.” *Journal of Earthquake Engineering*. DOI: 10.1080/13632469.2017.1342294

Sabelli R, Roeder CW, Hajjar JF. (2013). “Seismic Design of Steel Special Concentrically Braced Frame Systems – A guide for Practicing Engineers.” NEHRP Seismic Design Technical Brief No. 8, NIST GCR 13-917-24.

Sarlis AA, Constantinou MC. (2011). “Modeling Triple Friction Pendulum Isolators in Program SAP2000.” *Personal communication*.

Sarlis AA, Constantinou MC. (2016). “A Model of Triple Friction Pendulum Bearing for General Geometric and Frictional Parameters.” *Earthquake Engineering and Structural Dynamics*, 45 (11): 1837-1853. DOI: 10.1002/eqe.2738.

Sayani PJ, Erduran E, Ryan KL. “Comparative Response Assessment of Minimally Compliant Low-Rise Base-Isolated and Conventional Steel Moment-Resisting Frame Buildings.” *Journal of Structural Engineering*, 137(10), 1118-1131.

Shao B, Mahin SA, Zayas V. (2017). “Member Capacity Factors for Seismic Isolators as Required to Limit Isolated Structure Collapse Risks to within ASCE 7 Stipulated Structure Collapse Risk Limits.” *Project draft report*. Structural Engineering, Mechanics and Materials Department of Civil and Environmental Engineering University of California, Berkeley June 24, 2017.

Shinozuka M, Feng MQ, Lee J, Naganuma T. (2000). “Statistical Analysis of Fragility Curves.” *Journal of Engineering Mechanics*. 126 (12). 1224-1231.

Soroushian S, Maragakis EM, Jenkins C. (2015[a]). “Capacity Evaluation of Suspended Ceiling Components, Part 1: Experimental studies.” *Journal of Earthquake Engineering*. 19 (5). 784-804.

Soroushian S, Zaghi AE, Maragakis EM, Echevarria A, Tian Y, Filiatrault A. (2015[b]). “Seismic Fragility Study of Fire Sprinkler Piping Systems with Grooved Fit Joints”. *Journal of Structural Engineering*, 141(6), 04014157.

Structural Engineers Association of California. (2012). “SEAOC Structural/Seismic Design Manual. Volume 5: Examples for Seismically Isolated Buildings and Buildings with Supplemental Damping.” Published January 2014.

Terzic V, Mahin SA, Comerio MC. (2012). “Lifecycle Cost Comparisons for Different Structural Systems Designed for the Same Location.” *Proceedings of the 10th National Conference in Earthquake Engineering*, Earthquake Engineering Research Institute, Anchorage, AK.

Uriz P, Mahin SA. (2008). “Toward Earthquake-Resistant Design of Concentrically Braced Steel-Frame Structures.” *PEER 2008/08*, November 2008, Pacific Earthquake Engineering Research Center, PEER.

Vamvatsikos D, Cornell CA. (2002). “Incremental Dynamic Analysis.” *Earthquake Engineering and Structural Dynamics*, 31(3), 491–514.

Zayas V, Mahin SA, Constantinou MC. (2017). Seismic Isolation Standard for Continued Functionality. Department of Civil and Environmental Engineering, University of California, Berkeley, https://goo.gl/h82Fnk .

Zayas V, Mahin SA, Constantinou MC. (2017). Commentary to the Seismic Isolation Standard for Continued Functionality. Department of Civil and Environmental Engineering, University of California, Berkeley, https://goo.gl/r6sdwL .

APPENDIX A
PROCEDURE FOR CALCULATING THE MEDIAN COLLAPSE SPECTRAL ACCELERATION WHEN CONSIDERING SPECTRAL SHAPE EFFECTS

The procedure involves the following steps:

1. Obtain the target epsilon $\bar{\varepsilon}_0(T_1)$, magnitude M, and distance R from de-aggregation of the ground motion hazard (probabilistic seismic hazard analysis) for the specific location of the structure (longitude and latitude), site class (average shear-wave velocity V_{s30}=259 m/sec for class D), spectral period and return period. The return period of 2475 years (corresponding to a probability of exceedance of 2% in 50 years) is used based on Haselton et al (2011) because the primary purpose of collapse evaluation is to compute the conditional collapse probability for a 2% in 50 years ground motion. Information was obtained from the USGS website (https://earthquake.usgs.gov/hazards/interactive/ accessed on July 16, 2017) where results of de-aggregation for period of 0.2, 1.0 and 2.0 second were available. Linear interpolation and extrapolation in logarithmic space of the seismic hazard curves (annual frequency of exceedance vs spectral acceleration) was used for other values of period (T_1=0.524sec for non-isolated SCBF, T_1=1.186sec for non-isolated SMF and T_1=T_M =3.66sec for all isolated structures).

2. Perform incremental dynamic analysis (IDA) (Vamvatsikos and Cornell, 2012) (for this study the 44 ground motions of FEMA P695) to obtain the collapse capacity in terms of the spectral acceleration at fundamental period T_1 at collapse for each ground motion, $Sa_{Col,j}(T_1)$ (T_M in case of base-isolated structures and j is the identification number for the ground motions; j = 1 to 44).

3. Calculate epsilon at T_1, $\varepsilon_j(T_1)$ for the j^{th} ground motion (j=1 to 44), defined as the number of standard deviations by which the natural logarithm of $S_{aj}(T_1)$, ln[$S_{aj}(T_1)$], differs from the mean predicted ln[$S_a(T_1)$] for a given magnitude and distance (Baker, 2011):

$$\varepsilon_j(T_1) = \frac{\ln[Sa_j(T_1)] - \mu_{\ln Sa}(M,R,T_1)}{\sigma_{\ln Sa}(T_1)} \tag{A-1}$$

In Equation (A-1), $\mu_{\ln Sa}(M,R,T_1)$ is the predicted mean of $\ln[S_a(T_1)]$ at a given magnitude M, distance R and period T_1, and $\sigma_{\ln Sa}(T_1)$ is the predicted standard deviation of $\ln[S_a(T_1)]$ at a given M, R and T_1. Note that $\mu_{\ln Sa}(M,R,T_1)$ and $\sigma_{\ln Sa}(T_1)$ are obtained from any ground motion prediction model (herein the model of Abrahamson and Silva, 1997 was used, which was also used by Haselton et al, 2011). Quantity $\ln[S_{aj}(T_1)]$ in Equation (A-1) is the natural logarithm of the spectral acceleration at T_1 of each of 44 original (before scaling) ground motions.

4. Perform a linear regression analysis between $\ln[S_{a\mathrm{Col},j}(T_1)]$ and $\varepsilon_j(T_1)$ and determine parameters c_0 and c_1 based on the following equation:

$$\ln[S_{a\mathrm{Col}}(T_1)] \;\; = c_0 + c_1 \cdot \varepsilon(T_1) \tag{A-2}$$

   Note that based on Appendix B of FEMA (2009), for establishing a relationship between the $\ln[S_{a\mathrm{Col}}(T_1)]$ and $\varepsilon(T_1)$, the p-value (Neter et al, 1996) must be less than 0.05 for the trend to be statistically defensible.

5. Replace $\varepsilon(T_1)$ with $\bar{\varepsilon}_0(T_1)$ in Equation (A-2) and solve to obtain the adjusted mean collapse capacity, $\widehat{Sa}_{\mathrm{Col,adj}}(T_1)$:

$$\widehat{Sa}_{\mathrm{Col,adj}}(T_1) \;\; (units \;\; g) = \exp[c_0 + c_1 \cdot \bar{\varepsilon}_0(T_1)] \tag{A-3}$$

   The record-to-record dispersion coefficient, β_{RTR}, is calculated as the standard deviation of the natural logarithm of $S_{a\mathrm{Col}j}(T_1)$ of the 44 motions without any further adjustment. Note that Haselton et al (2011) described a procedure for further reduction of the dispersion using the residuals of the regression analysis but the effect was found to be insignificant in this study and was not included in the presented results.

Values of the target epsilon $\bar{\varepsilon}_0(T_1)$, magnitude M and distance R for return period of 2475 years obtained by de-aggregation of the seismic hazard are presented in Table A-1.

Table A-1 Values of $\bar{\varepsilon}_0(T_1)$, M and R for Considered Site and 2475 Years Return Period

	$\bar{\varepsilon}_0(T_1)$	M	R(km)
Isolated	1.44	7.96	16.0
Non-isolated (SCBF)	1.46	7.35	16.0
Non-isolated (SMF)	1.71	7.63	16.0

Using the ground motion prediction model of Abrahamson and Silva (1997) the median 5%-damped response spectra were constructed for isolated and non-isolated structures and are presented in Figure A-1 together with the spectra of the 44 ground motions used in the IDA. Program OpenSHA (Field et al, 2003) was used to construct the spectra using the Abrahamson and Silva prediction model. The same model also predicted the standard deviation, which is presented in Figure A-2. The standard deviation is the same for the isolated and non-isolated structures.

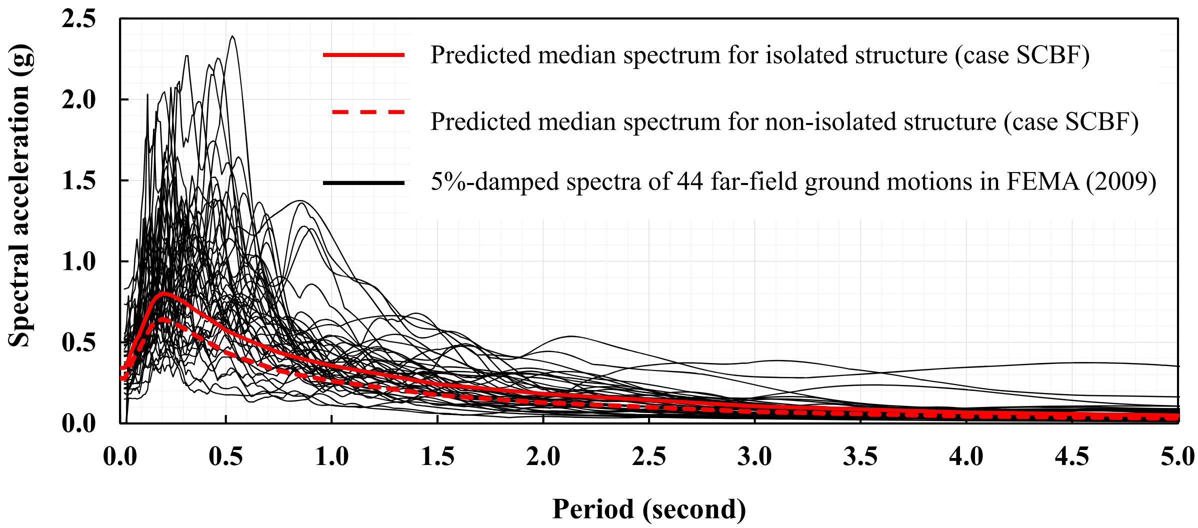

Figure A-1 Response Spectra of FEMA Far-Field Motions and Predicted Median Spectra

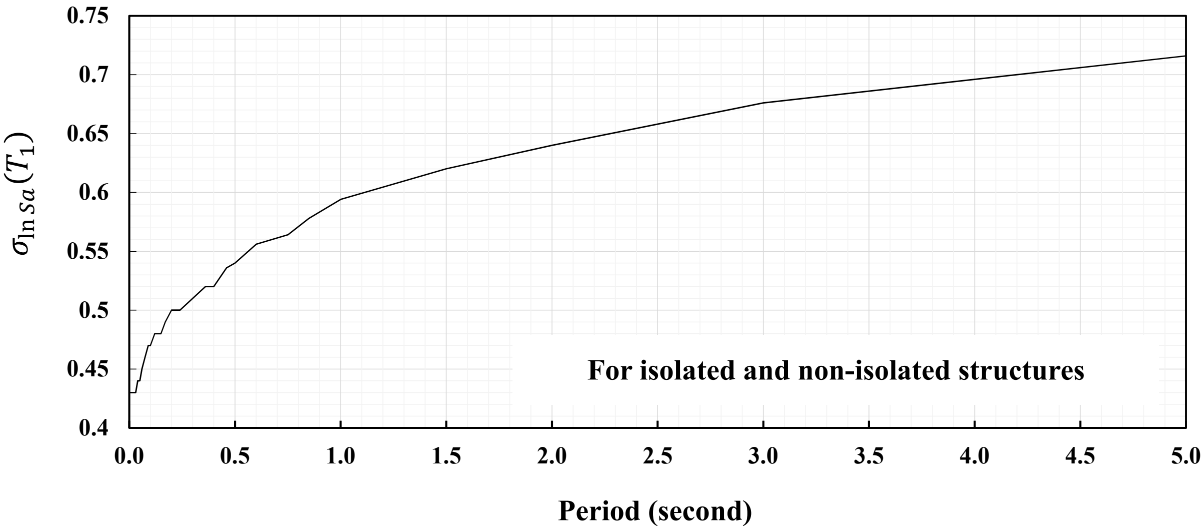

Figure A-2 Standard Deviation of Natural Logarithm of Spectral Acceleration

The values of $\varepsilon_j(T_1)$ for each of the 44 ground motions (j=1 to 44) for the isolated and non-isolated structures where then calculated by use of Equation (A-1) and are presented in Figure A-3 for the case of the SCBF where it is seen that the values of epsilon are higher for the non-isolated structure.

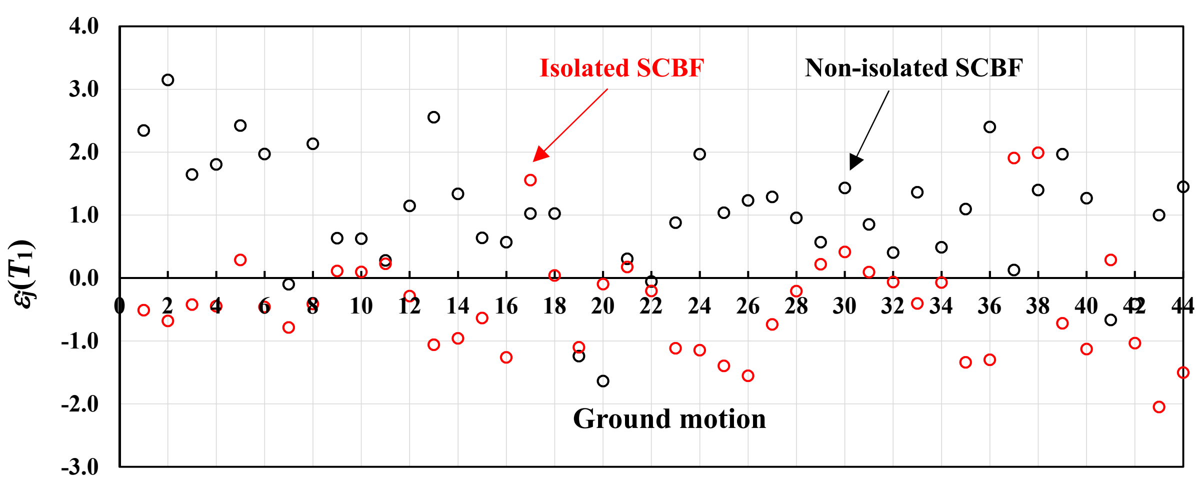

Figure A-3 Calculated Values of $\varepsilon_j(T_1)$ for Each of 44 Ground Motions (Isolated SCBF: R_I=1.0 (DE), TFP-1)

Based on the results of IDA and the information on $\varepsilon_j(T_1)$ in Figure A-3, linear regression analysis was performed to establish the relationship between the $\ln[S_{a\mathrm{Col},j}(T_1)]$ and $\varepsilon_j(T_1)$. Figures A-4 present the relationship between $\ln[S_{a\mathrm{Col},j}(T_1)]$ and $\varepsilon_j(T_1)$ for all cases considered. The figures also present the fitted linear regression model of Equation (A-2) for each case. The calculated p-values (Neter et al, 1996) were less than 10^{-3}, thus statistically meaningful (less than 0.05). Also, Figures A-5 to A-7 compare the relationships between $\ln[Sa_{\mathrm{Col,j}}(T_1)]$ and $\varepsilon_j(T_1)$ for the analyzed isolated SCBF buildings with and without moat walls.

$$\ln[S_{a\mathrm{COL}}\,(T_1)] = -1.2193 + 0.1458 \cdot \varepsilon(T_1)$$

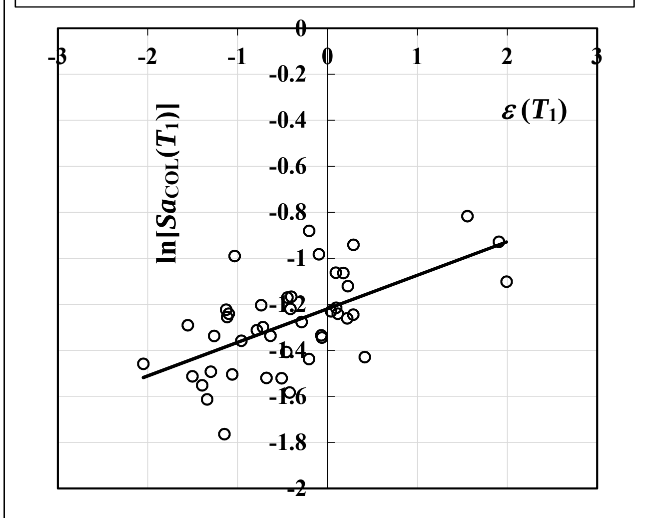

Isolated SCBF structure (TFP-1, R_{I}=1.0 in DE)

$$\ln[S_{a\mathrm{COL}}\,(T_1)] = -1.0416 + 0.1772 \cdot \varepsilon(T_1)$$

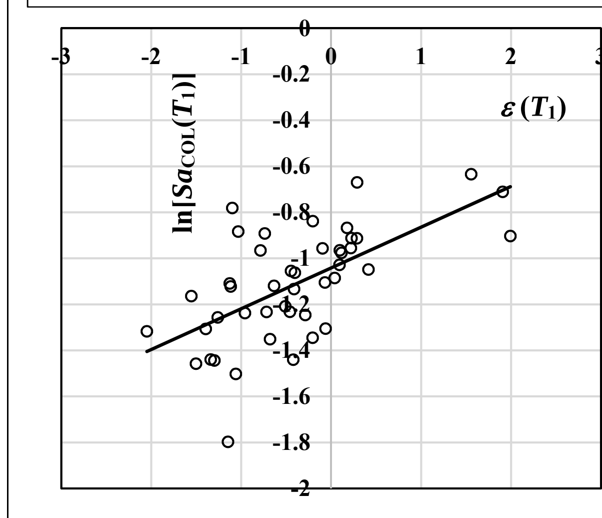

Isolated SMF structure (TFP-1, R_{I}=1.0 in DE)

$$\ln[S_{a\mathrm{COL}}\,(T_1)] = -1.0832 + 0.129 \cdot \varepsilon(T_1)$$

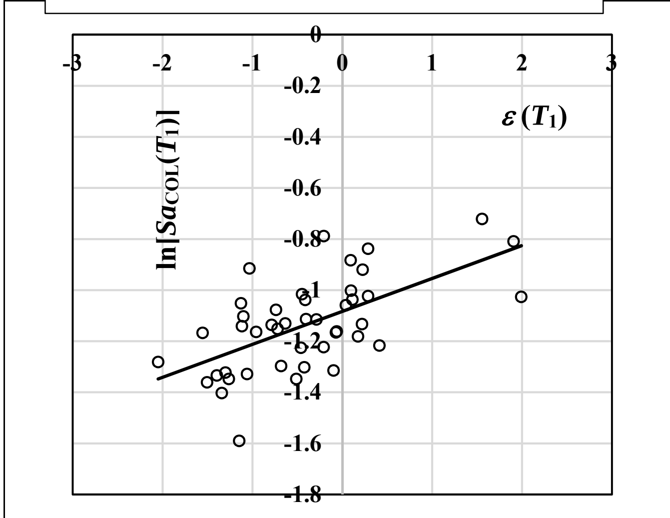

Isolated SCBF structure (TFP-2, R_{I}=1.0 in DE)

$$\ln[S_{a\mathrm{COL}}\,(T_1)] = -0.9105 + 0.1641 \cdot \varepsilon(T_1)$$

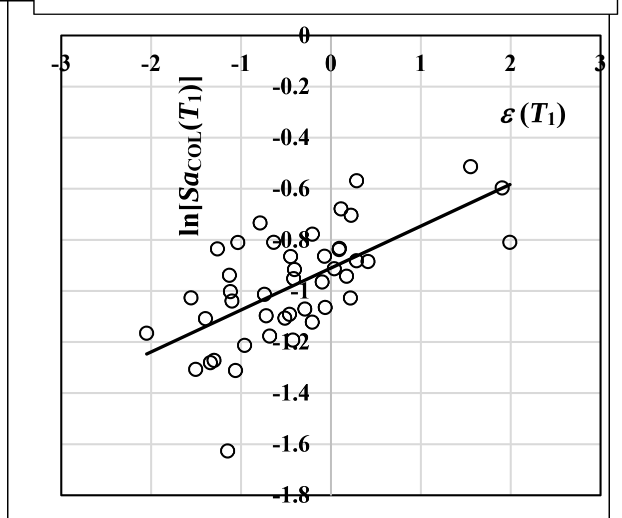

Isolated SMF structure (TFP-2, R_{I}=1.0 in DE)

Figure A-4 Relationship between $\ln[S_{a\mathrm{Col},j}(T_1)]$ and $\varepsilon_j(T_1)$ for Buildings without Moat Wall

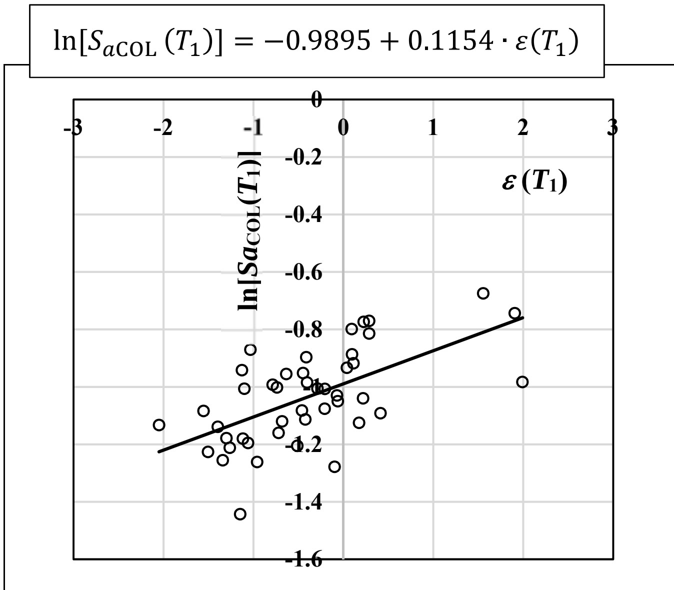

Isolated SCBF structure (TFP-3, R_I=1.0 in DE)

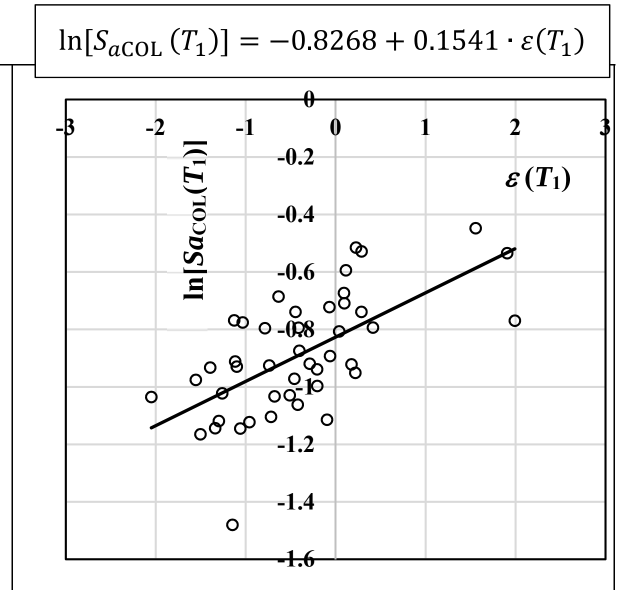

Isolated SMF structure (TFP-3, R_I=1.0 in DE)

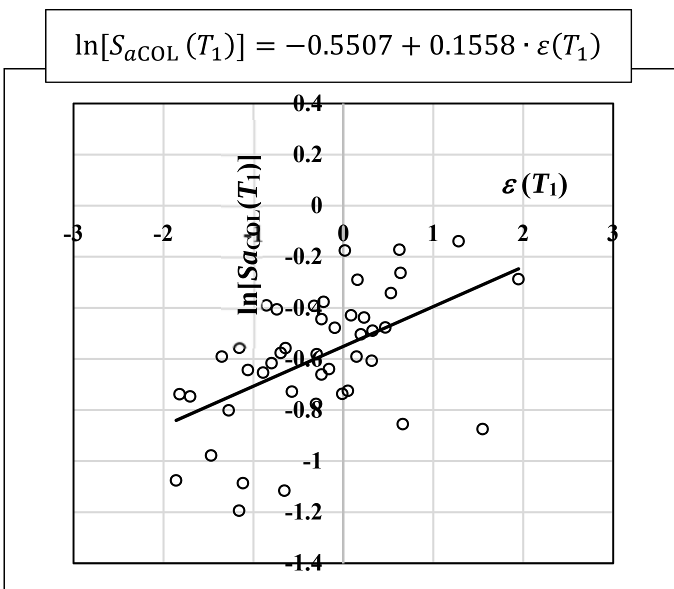

Isolated SCBF structure (TFP-3, R_I=1.0 in DE, Upper Bound)

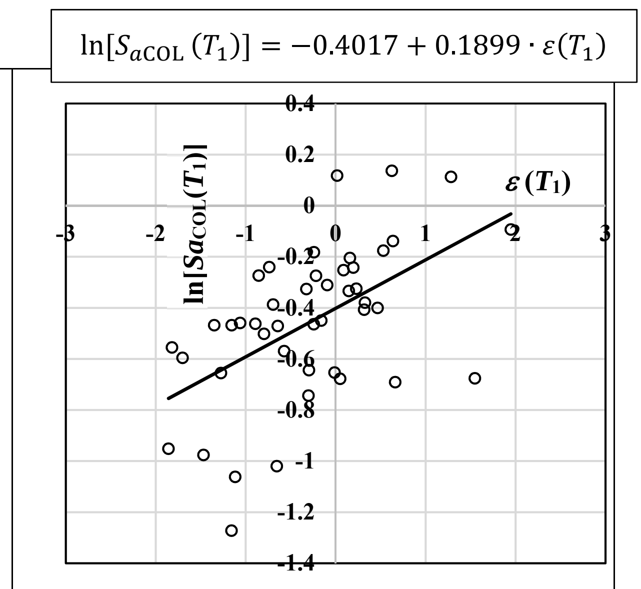

Isolated SMF structure (TFP-3, R_I=1.0 in DE, Upper Bound)

Figure A-4 Continued

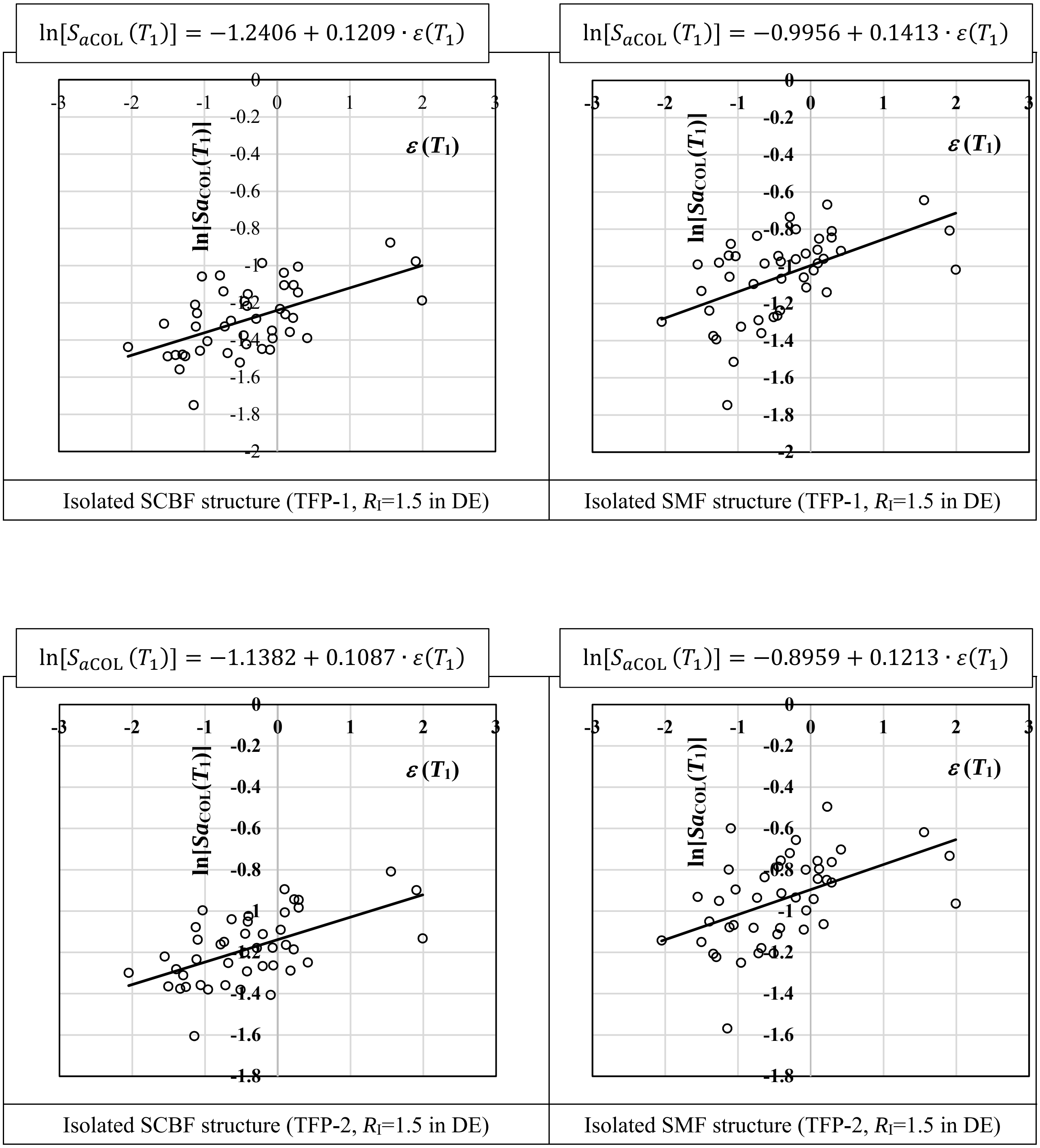

Isolated SCBF structure (TFP-1, R_I=1.5 in DE)

Isolated SMF structure (TFP-1, R_I=1.5 in DE)

Isolated SCBF structure (TFP-2, R_I=1.5 in DE)

Isolated SMF structure (TFP-2, R_I=1.5 in DE)

Figure A-4 Continued

$$\ln[S_{a\mathrm{COL}}\,(T_1)] = -1.0555 + 0.0966 \cdot \varepsilon(T_1)$$

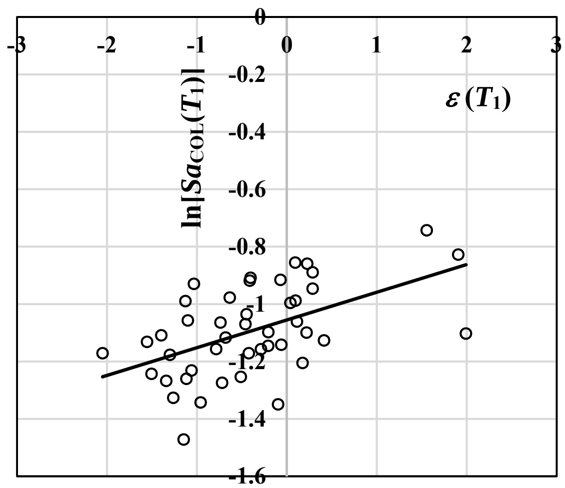

Isolated SCBF structure (TFP-3, R_{I}=1.5 in DE)

$$\ln[S_{a\mathrm{COL}}\,(T_1)] = -0.8548 + 0.0984 \cdot \varepsilon(T_1)$$

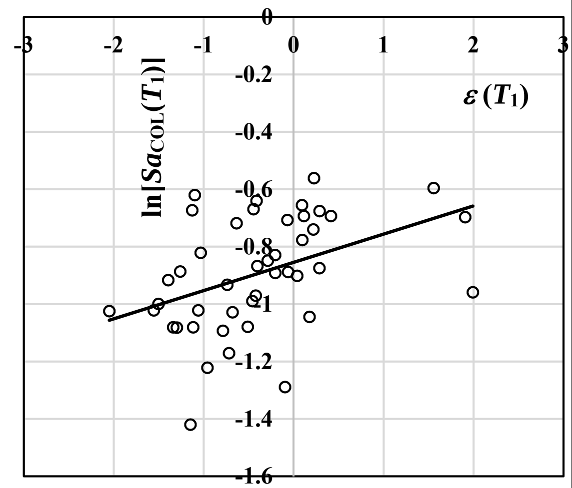

Isolated SMF structure (TFP-3, R_{I}=1.5 in DE)

$$\ln[S_{a\mathrm{COL}}\,(T_1)] = -1.262 + 0.1225 \cdot \varepsilon(T_1)$$

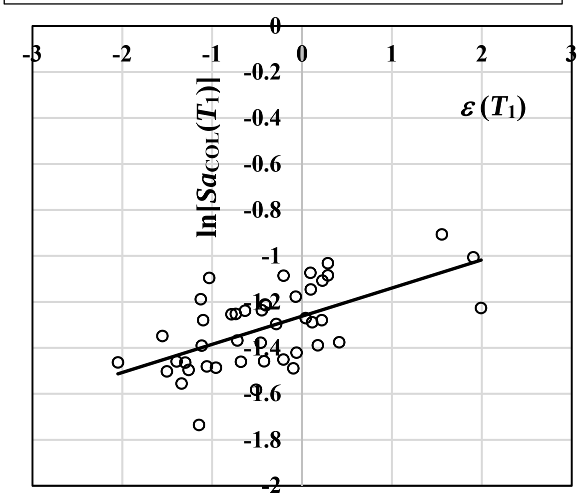

Isolated SCBF structure (TFP-1, R_{I}=2.0 in DE)

$$\ln[S_{a\mathrm{COL}}\,(T_1)] = -0.9983 + 0.1336 \cdot \varepsilon(T_1)$$

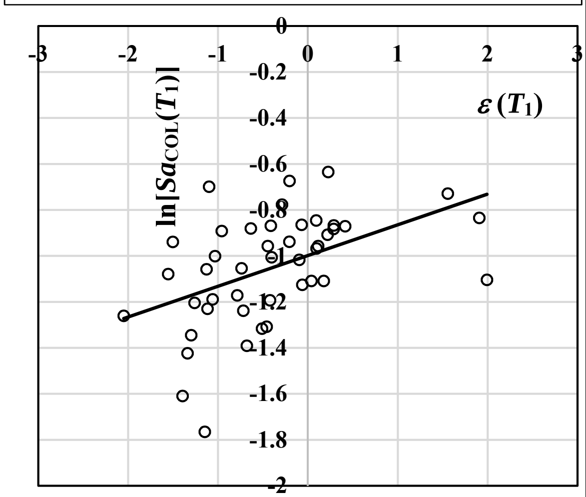

Isolated SMF structure (TFP-1, R_{I}=2.0 in DE)

Figure A-4 Continued

$\ln[S_{a\mathrm{COL}}\,(T_1)] = -1.1661 + 0.1068 \cdot \varepsilon(T_1)$

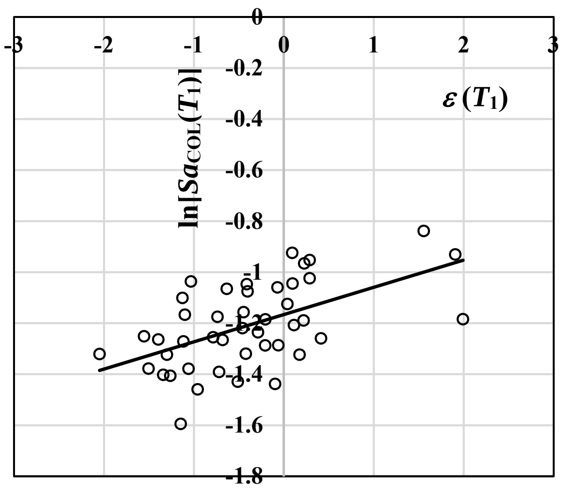

Isolated SCBF structure (TFP-2, R_I=2.0 in DE)

$\ln[S_{a\mathrm{COL}}\,(T_1)] = -0.9542 + 0.1284 \cdot \varepsilon(T_1)$

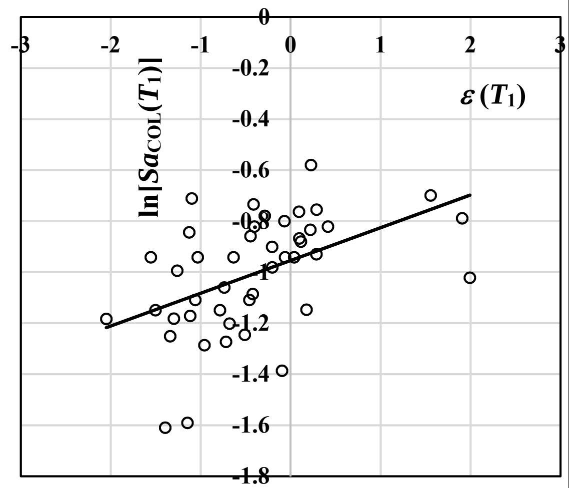

Isolated SMF structure (TFP-2, R_I=2.0 in DE)

$\ln[S_{a\mathrm{COL}}\,(T_1)] = -1.0831 + 0.0927 \cdot \varepsilon(T_1)$

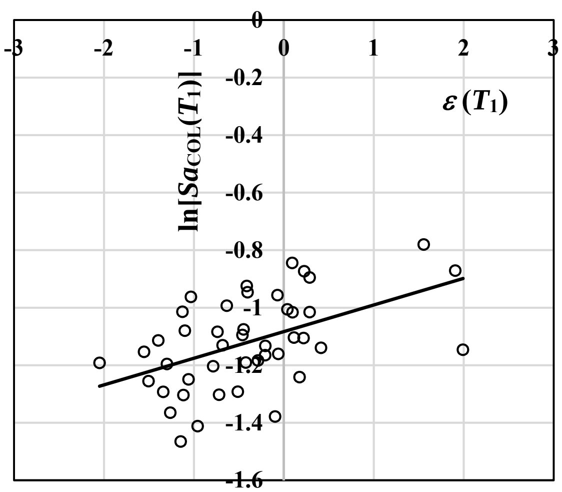

Isolated SCBF structure (TFP-3, R_I=2.0 in DE)

$\ln[S_{a\mathrm{COL}}\,(T_1)] = -0.9542 + 0.1284 \cdot \varepsilon(T_1)$

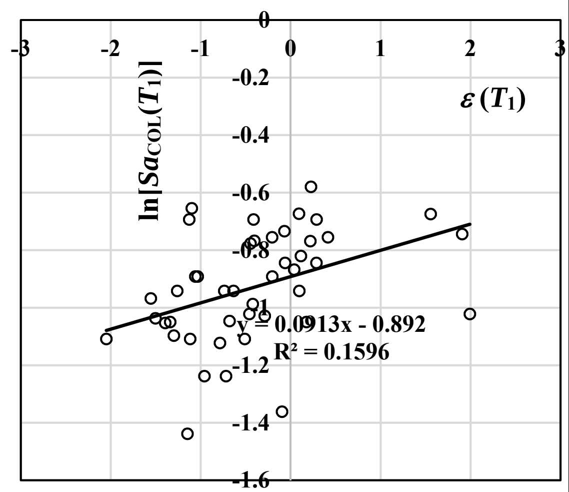

Isolated SMF structure (TFP-3, R_I=2.0 in DE)

Figure A-4 Continued

$\ln[S_{a\mathrm{COL}}\,(T_1)] = -1.3887 + 0.1484 \cdot \varepsilon(T_1)$

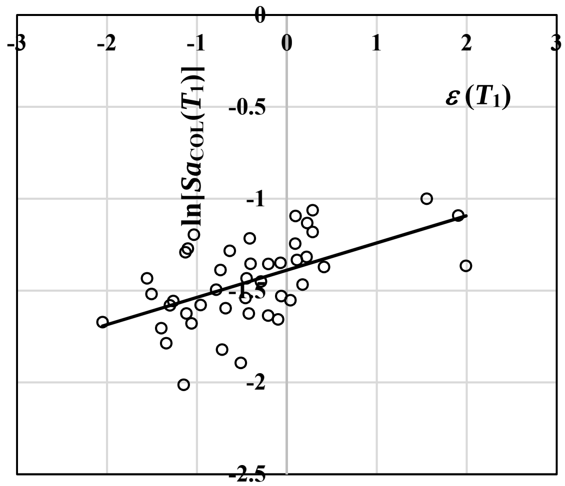

Isolated SCBF structure (R_{I}=2.0, DC-1 no restraining ring)

$\ln[S_{a\mathrm{COL}}\,(T_1)] = -1.462 + 0.1053 \cdot \varepsilon(T_1)$

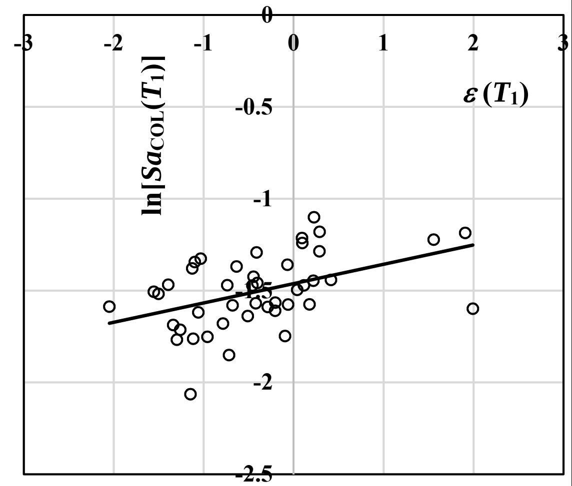

Isolated SMF structure (R_{I}=2.0, DC-1 no restraining ring)

$\ln[S_{a\mathrm{COL}}\,(T_1)] = -1.2276 + 0.1343 \cdot \varepsilon(T_1)$

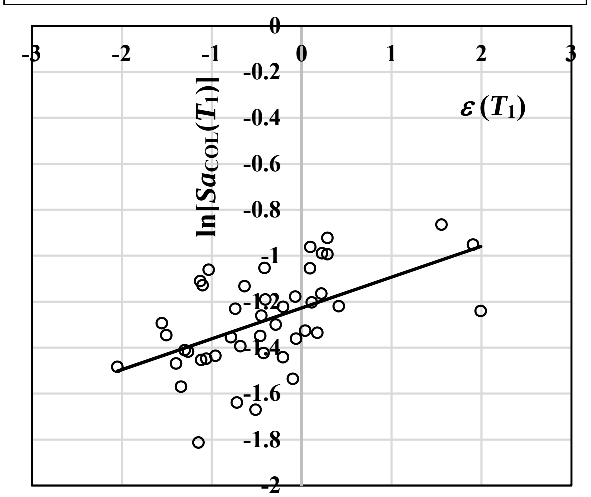

Isolated SCBF structure (R_{I}=2.0, DC-2 no restraining ring)

$\ln[S_{a\mathrm{COL}}\,(T_1)] = -1.3069 + 0.091 \cdot \varepsilon(T_1)$

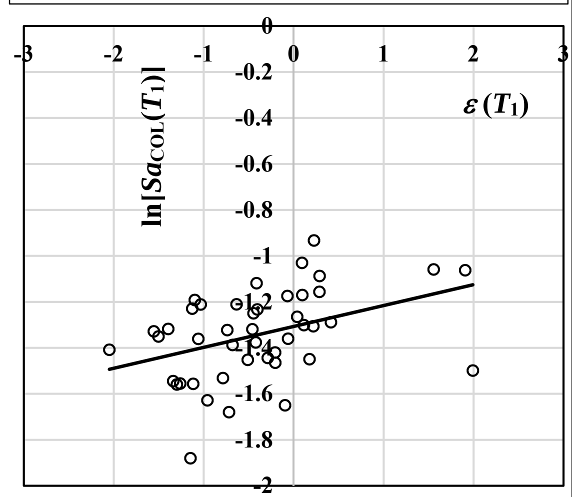

Isolated SMF structure (R_{I}=2.0, DC-2 no restraining ring)

Figure A-4 Continued

$\ln[S_{a\mathrm{COL}}\,(T_1)] = 0.8091 + 0.2378 \cdot \varepsilon(T_1)$

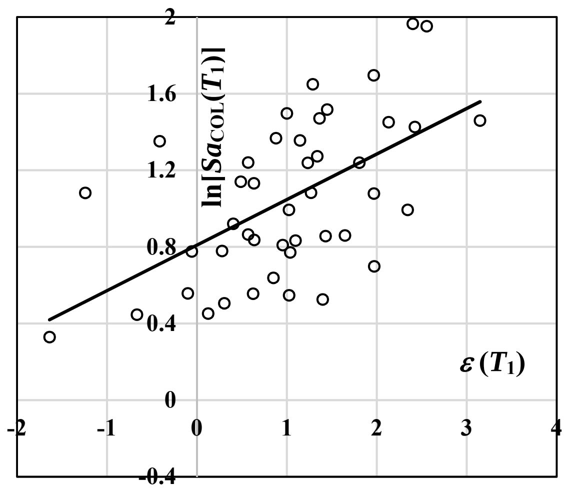

Isolated SCBF structure (Non-Isolated)

$\ln[S_{a\mathrm{COL}}\,(T_1)] = 0.475 + 0.242 \cdot \varepsilon(T_1)$

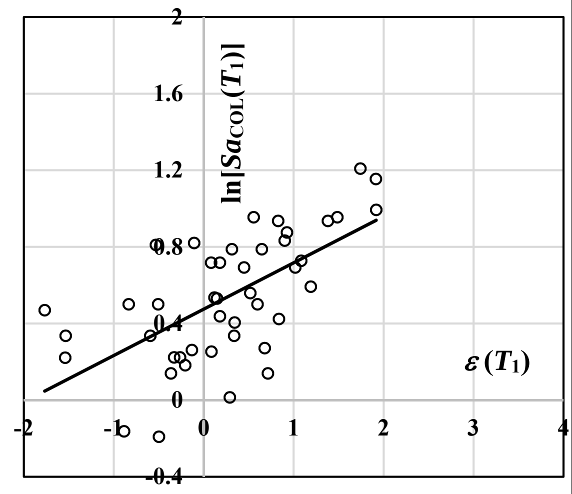

Isolated SMF structure (Non-Isolated)

$\ln[S_{a\mathrm{COL}}\,(T_1)] = -1.3017 + 0.1289 \cdot \varepsilon(T_1)$

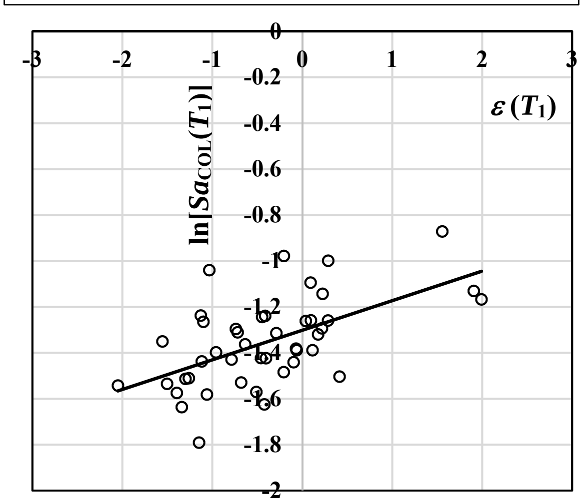

Isolated SCBF structure (TFP-1, R_I=1.0 in MCE_R)

$\ln[S_{a\mathrm{COL}}\,(T_1)] = -1.1431 + 0.1547 \cdot \varepsilon(T_1)$

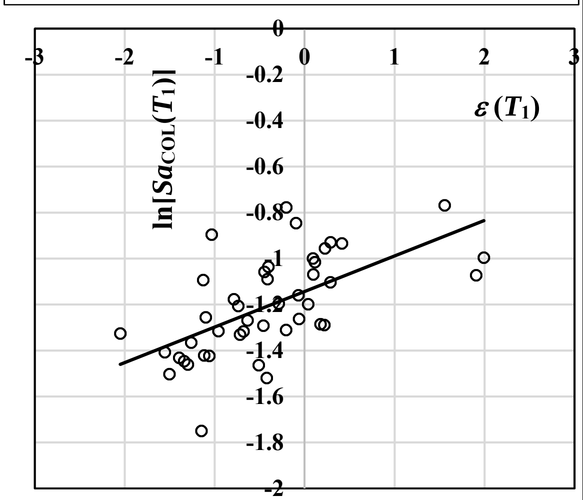

Isolated SMF structure (TFP-1, R_I=1.0 in MCE_R)

Figure A-4 Continued

$$\ln[S_{a\mathrm{COL}}\,(T_1)] = -1.1393 + 0.1141 \cdot \varepsilon(T_1)$$

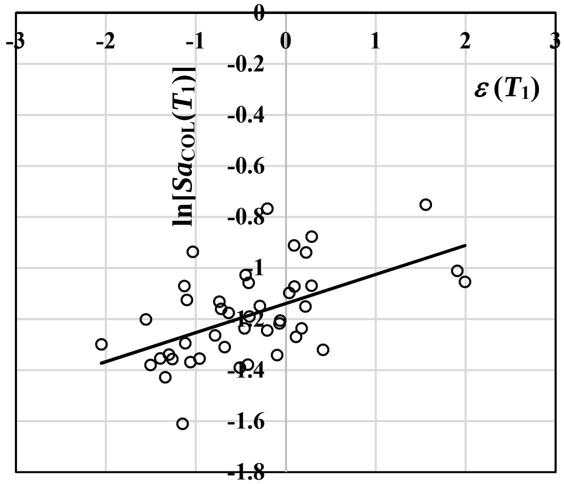

Isolated SCBF structure (TFP-2, R_I=1.0 in MCE_R)

$$\ln[S_{a\mathrm{COL}}\,(T_1)] = -1.0083 + 0.1424 \cdot \varepsilon(T_1)$$

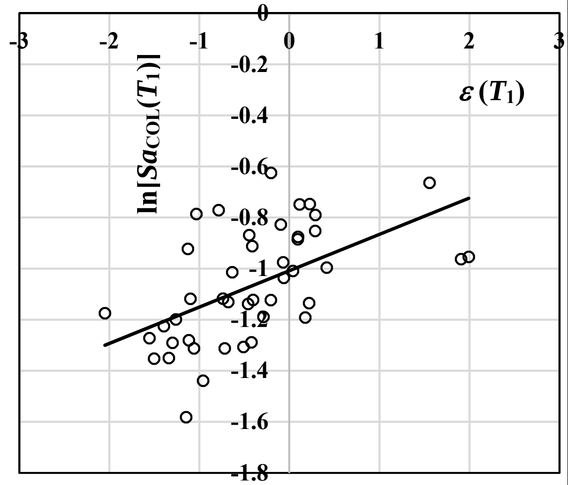

Isolated SMF structure (TFP-2, R_I=1.0 in MCE_R)

$$\ln[S_{a\mathrm{COL}}\,(T_1)] = -1.0198 + 0.1047 \cdot \varepsilon(T_1)$$

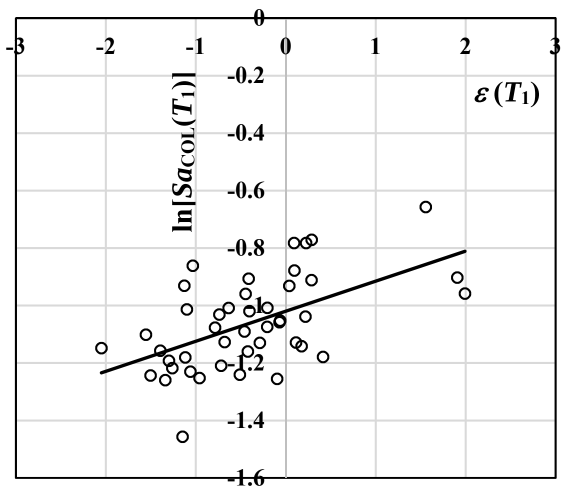

Isolated SCBF structure (TFP-3, R_I=1.0 in MCE_R)

$$\ln[S_{a\mathrm{COL}}\,(T_1)] = -0.896 + 0.1312 \cdot \varepsilon(T_1)$$

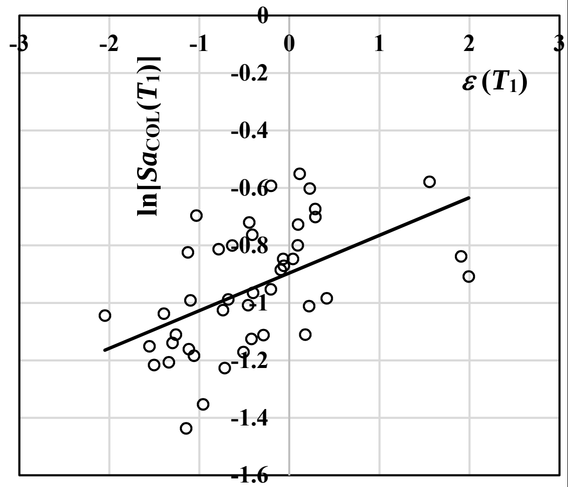

Isolated SMF structure (TFP-3, R_I=1.0 in MCE_R)

Figure A-4 Continued

$$\ln[S_{a\mathrm{COL}}\,(T_1)] = -1.2153 + 0.1387 \cdot \varepsilon(T_1)$$

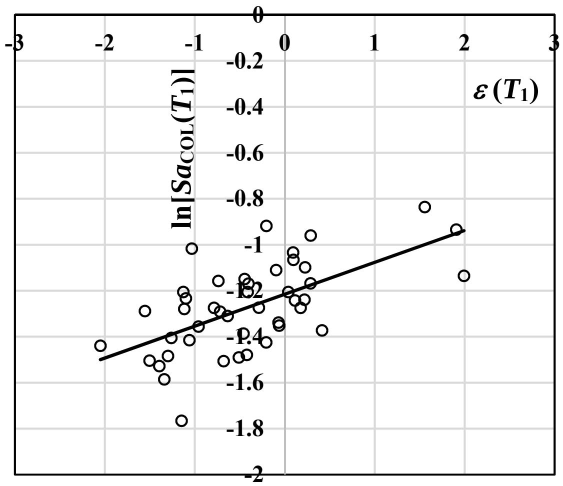

Isolated SCBF structure (TFP-1, R_{I}=2.0 in $\mathrm{MCE_R}$)

$$\ln[S_{a\mathrm{COL}}\,(T_1)] = -1.0366 + 0.1907 \cdot \varepsilon(T_1)$$

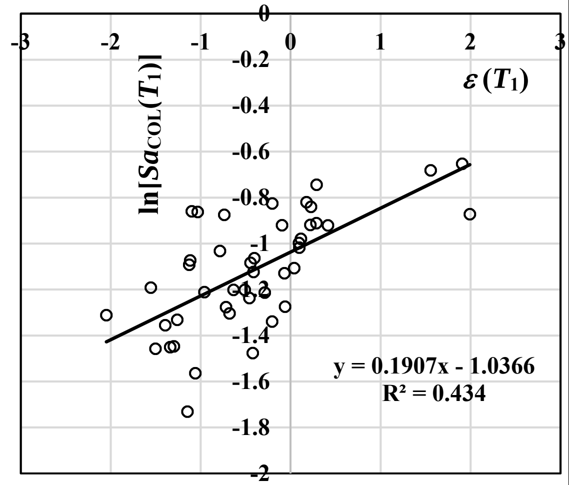

Isolated SMF structure (TFP-1, R_{I}=2.0 in $\mathrm{MCE_R}$)

$$\ln[S_{a\mathrm{COL}}\,(T_1)] = -1.1027 + 0.1153 \cdot \varepsilon(T_1)$$

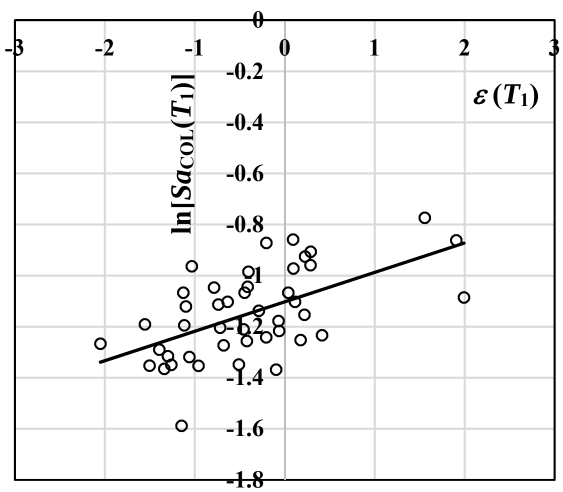

Isolated SCBF structure (TFP-2, R_{I}=2.0 in $\mathrm{MCE_R}$)

$$\ln[S_{a\mathrm{COL}}\,(T_1)] = -1.0366 + 0.1907 \cdot \varepsilon(T_1)$$

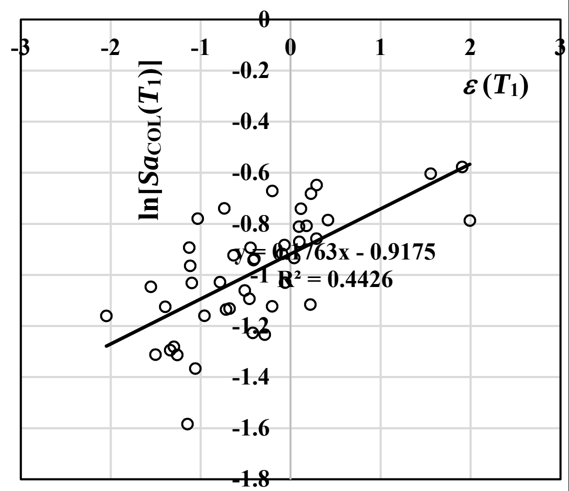

Isolated SMF structure (TFP-2, R_{I}=2.0 in $\mathrm{MCE_R}$)

Figure A-4 Continued

$\ln[S_{a\mathrm{COL}}\,(T_1)] = -1.026 + 0.0962 \cdot \varepsilon(T_1)$

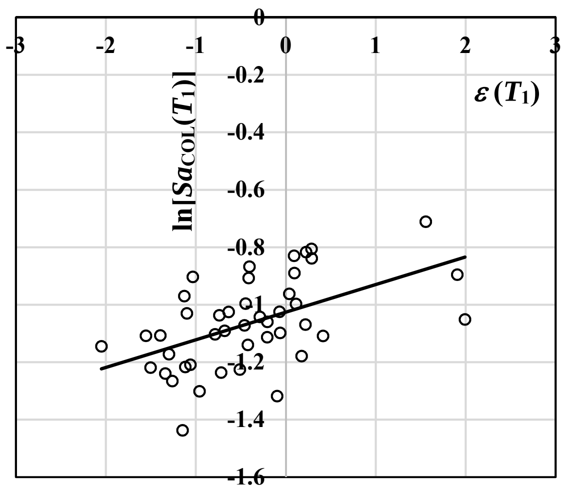

Isolated SCBF structure (TFP-3, R_I=2.0 in MCE_R)

$\ln[S_{a\mathrm{COL}}\,(T_1)] = -0.8309 + 0.1526 \cdot \varepsilon(T_1)$

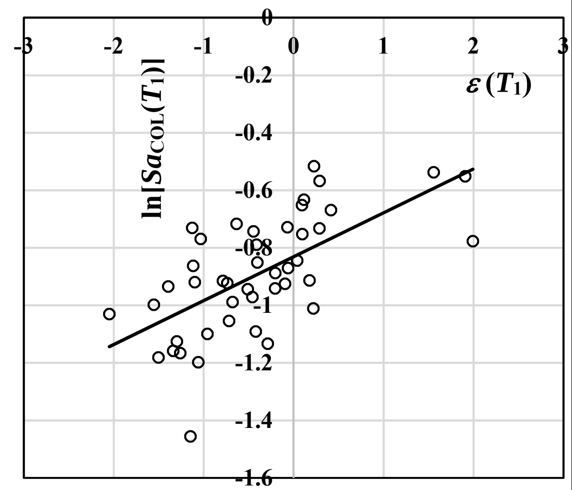

Isolated SMF structure (TFP-3, R_I=2.0 in MCE_R)

$\ln[S_{a\mathrm{COL}}\,(T_1)] = -1.1527 + 0.1054 \cdot \varepsilon(T_1)$

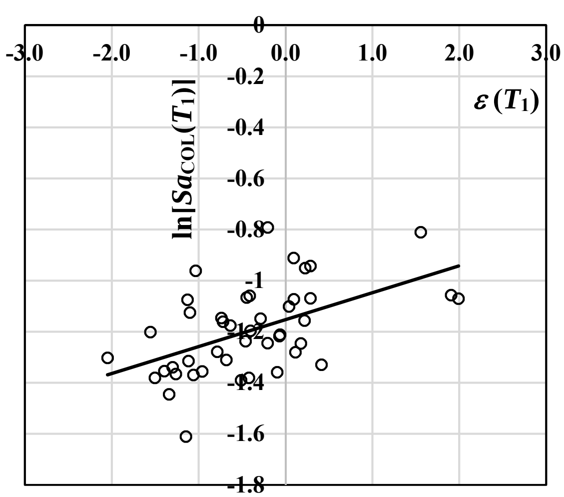

Isolated OCBF structure (TFP-2, R_I=1.0 in MCE_R)

$\ln[S_{a\mathrm{COL}}\,(T_1)] = -1.0604 + 0.0883 \cdot \varepsilon(T_1)$

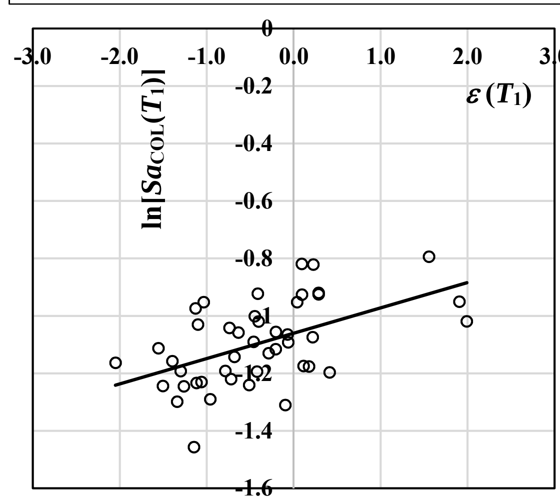

Isolated OCBF structure (TFP-3, R_I=1.0 in MCE_R)

Figure A-4 Continued

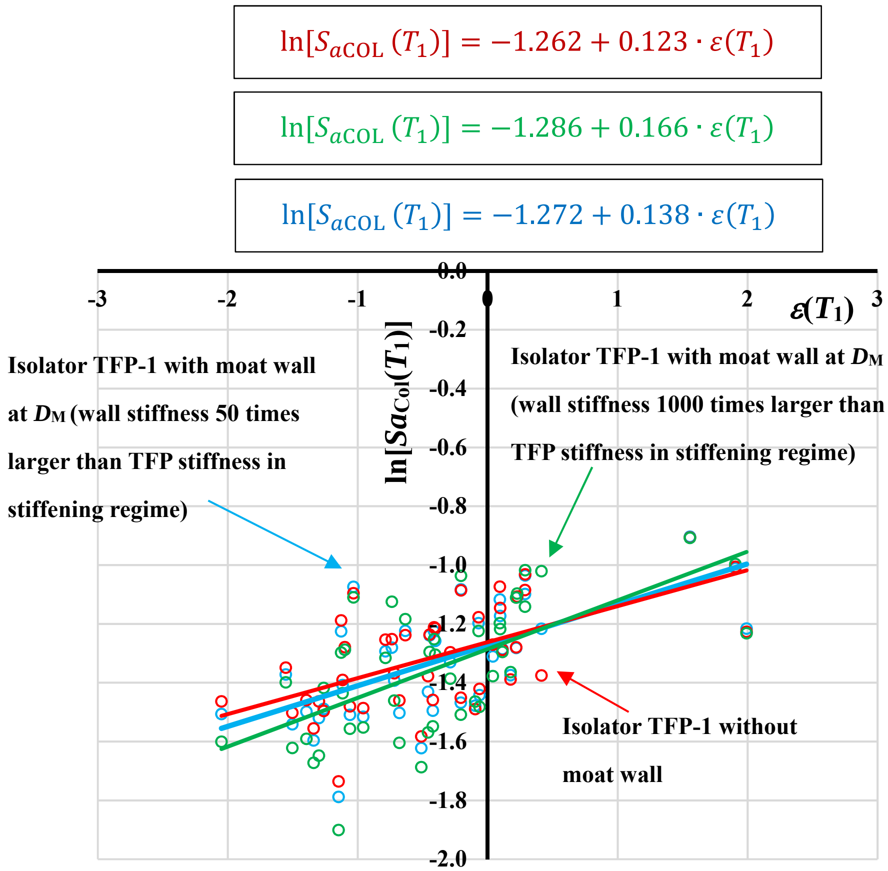

Figure A-5 Relationship between $\ln[Sa_{\mathrm{Col,j}}(T_1)]$ and $\varepsilon_j(T_1)$ for Isolated Buildings with SCBF Designed for R_I=2.0 per ASCE/SEI 7-10 and Isolator TFP-1 (D_{Capacity}=20.4in, D_{Ultimate}=26.9inch) with and without Moat Wall

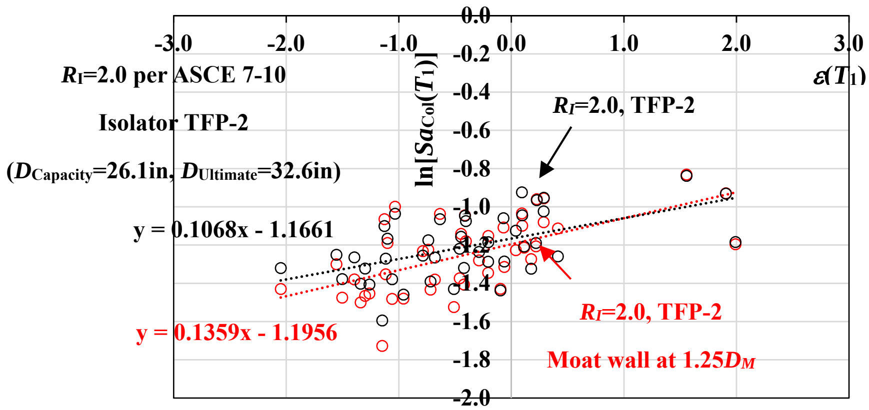

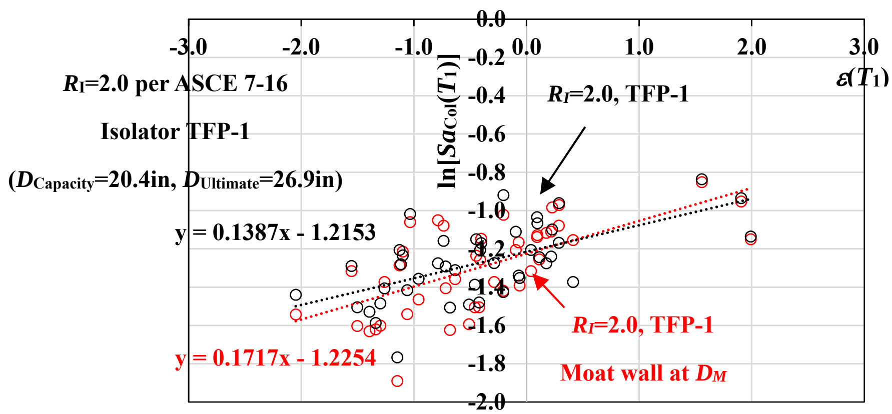

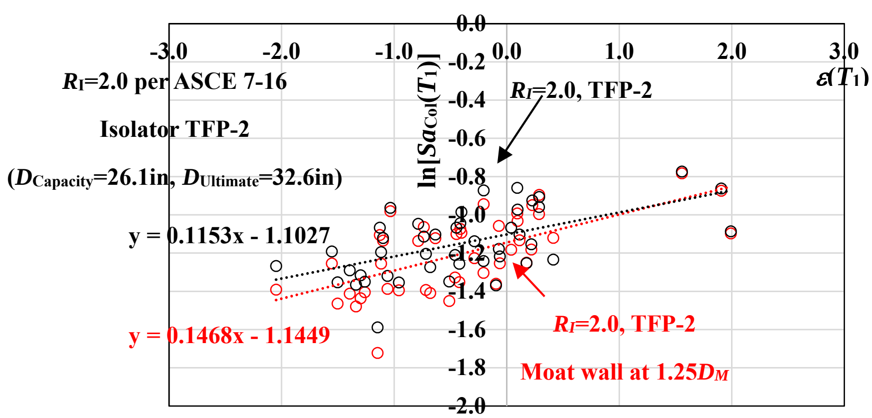

Figure A-6 Relationship between $\ln[Sa_{\mathrm{Col,j}}(T_1)]$ and $\varepsilon_j(T_1)$ for Isolated Buildings with SCBF Designed for R_I=2.0 and Isolator TFP-1 (D_{Capacity}=20.4in, D_{Ultimate}=26.9inch) or Isolator TFP-2 (D_{Capacity}=26.1in, D_{Ultimate}=32.6inch) with and without Moat Wall

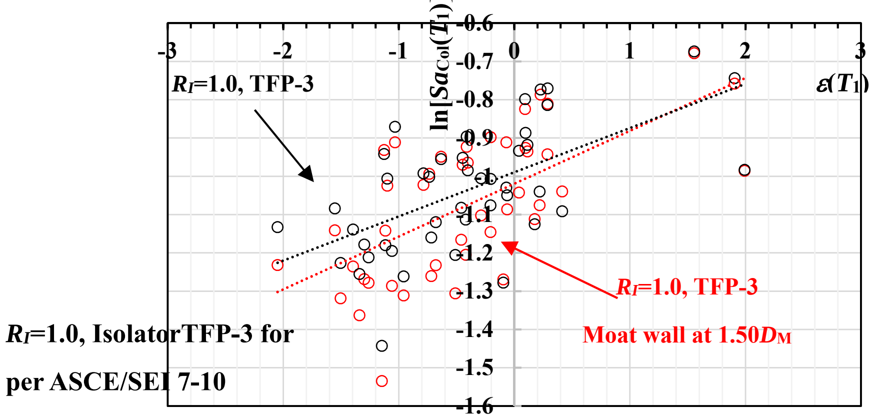

Figure A-7 Relationship between ln[$Sa_{Col,j}(T_1)$] and $\varepsilon_j(T_1)$ for Isolated Buildings with SCBF Designed for R_I=1.0 per ASCE/SEI 7-10 and Isolator TFP-3 ($D_{Capacity}$=31.8in, $D_{Ultimate}$=38.3inch) with and without Moat Wall

APPENDIX B

PROCEDURE FOR THE PROBABILISTIC SEISMIC PERFORMANCE ASSESSMENT

The procedure involves the following steps:

1. Obtain magnitude M and distance R from de-aggregation of the ground motion hazard for the specific location of the structure (longitude and latitude), site class (Vs_{30}), spectral period and selected return period. This step is identical to step 1 of Appendix A but there are several return periods. Obtain the seismic hazard curves for each building period T_1. Obtain the spectral acceleration $S_a(T_1)$ for each of the return periods selected. In this work the return periods of 43, 144, 289, 475, 949, 1485, 2475, 3899, 7462 and 10000 years were selected (corresponding to the probabilities of exceedance ranging from 50% in 30 years to 2% in 200 years).

2. Construct a Conditional Mean Spectrum (CMS) (Baker, 2011) for each of the selected return periods using a ground motion predictive model. In this work, the model of Boore et al. (2014) was used in conjunction with Baker and Jayaram (2008).

3. Select and scale ground motions to match the target Conditional Spectra (CS) for each hazard level. Note that CS includes conditional standard deviation in addition to conditional mean (CMS). In this work 40 motions (one directional as the analysis is for plane frames) were selected and scaled. For this purpose, publicly available computer programs can be used (e.g., Jayaram et al, 2011; Baker and Lee, 2017). Check that the selected ground motions are consistent with the seismic hazard curves at the relevant periods (Lin et al., 2013[a]). For the evaluation of the "hazard consistency" of the selected ground motions, the rate of exceedance of $S_a(T)$ implied by the ground motions selected conditional on $S_a(T_1)$ is calculated by the following equation (Lin et al, 2013[a]):

$$\lambda(S_a(T) > y) = \sum_{i=1}^{n} P(S_a(T) > y | S_a(T_1) = x_i)\lambda(S_a(T_1) = x_i) \qquad \text{(B-1)}$$

   In this equation, n is the number of considered $S_a(T_1)$ amplitudes and $P(S_a(T)>y|S_a(T_1)=x_i)$ is the probability that a ground motion selected and scaled to have $S_a(T_1)=x_i$ has an spectral acceleration at period T that is greater than y. Here this probability is estimated as the fraction of the 40 ground motions with $S_a(T_1)=x_i$ that have $S_a(T)>y$. The calculated rate of exceedance $\lambda(S_a(T)>y)$ is compared with the seismic hazard curve. If the selected ground motion does not satisfy the hazard consistency criteria, the selection of motions is repeated based on NIST (2011) and Lin et al. (2013[a]).

4. Conduct seismic response analysis and calculate Engineering Response Parameters (EDP) of interest (in this study EDP are the maximum story drift ratio, the maximum residual story drift ratio and the maximum floor and roof accelerations). The mean annual rate of EDP exceeding y, λ(EDP>y), is then calculated. This is mathematically expressed as:

$$\lambda(\mathrm{EDP} > y) = \sum_{i=1}^{n} P(EDP > y|(S_a(T_1) = x_i)\lambda(S_a(T_1) = x_i) \qquad \text{(B-2)}$$

where $P(\mathrm{EDP}>y|S_a(T_1)=x_i)$ is the probability of EDP exceeding y given a ground motion with $S_a(T_1)=x_i$ and seismic hazard curve $\lambda(S_a(T_1) = x_i)$.

The seismic hazard curves are shown in Figure B-1 for building period T_1 equal to 0.524, 1.186 and 3.660 seconds. The mean causal earthquake magnitude M and distance R for the location of the building and for V_{s30}=259 m/sec were obtained for the selected values of return period and are shown in Figure B-2.

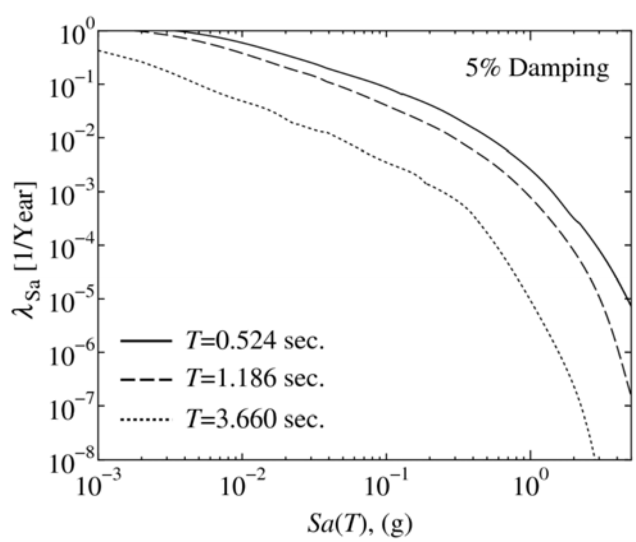

Figure B-1 Seismic Hazard Curves for T_1=0.524, 1.186 and 3.660 Seconds

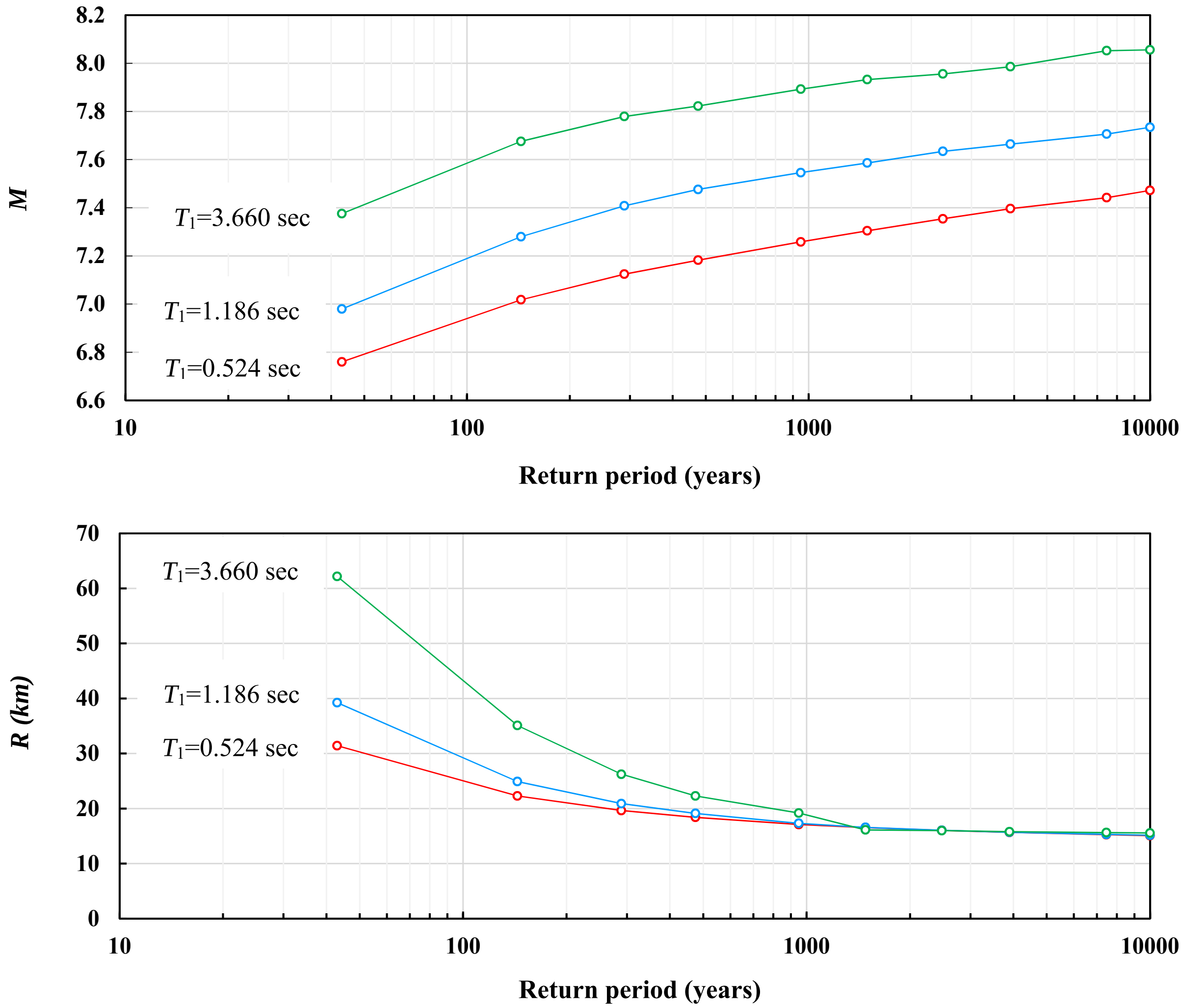

Figure B-2 Mean Causal Earthquake Magnitude M and Distance R as Function of Return Period

Conditional mean spectra for each of the three periods T_1 are presented in Figure B-3. Note that there are 10 spectra, one for each of the considered return periods.

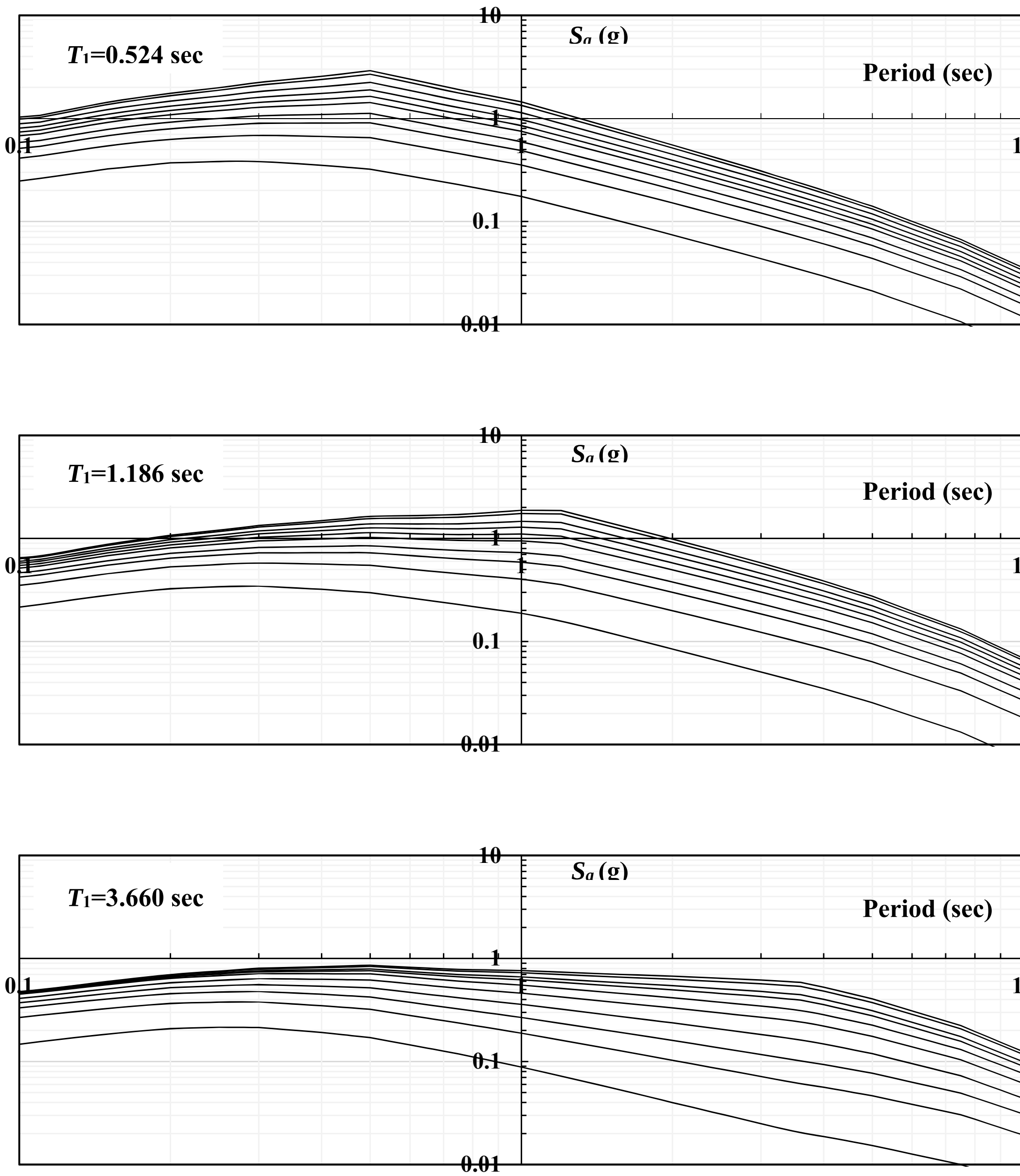

Figure B-3 Conditional Mean Spectra for Return Period of 43, 144, 289, 475, 949, 1485, 2475, 3899, 7462 and 10000 Year and for Building Period T_1=0.524, 1.186 and 3.660 Second

The algorithm developed by Baker and Lee (2017) were used for the selection and scaling of ground motions. Forty ground motions were selected and scaled for each return period (total 1200 different ground motions for the three building period cases). Scaling was only in amplitude with a maximum scale factor of 5. Figures B-4 to B-13present the response spectra of 40 scaled ground motions for each of the 10 return periods, their mean values and the mean values ± two standard deviations (mean±2σ). The graphs also show the target CMS and the

CMS±2σ.

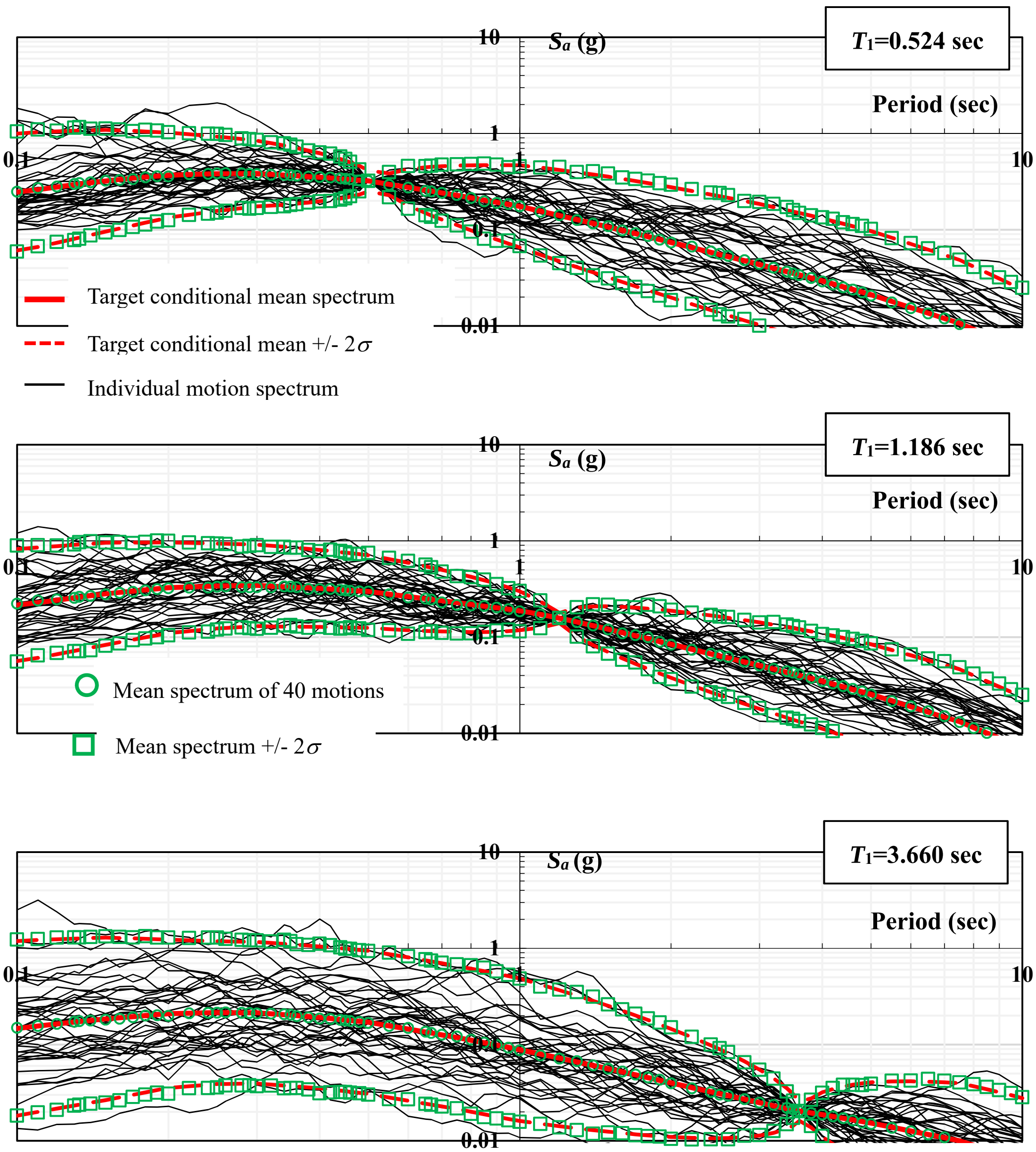

Figure B-4 Spectra of Scaled Motions and Conditional Spectra for Return Period of 43 Years and Period T_1 Equal to 0.524, 1.186 and 3.660 Seconds

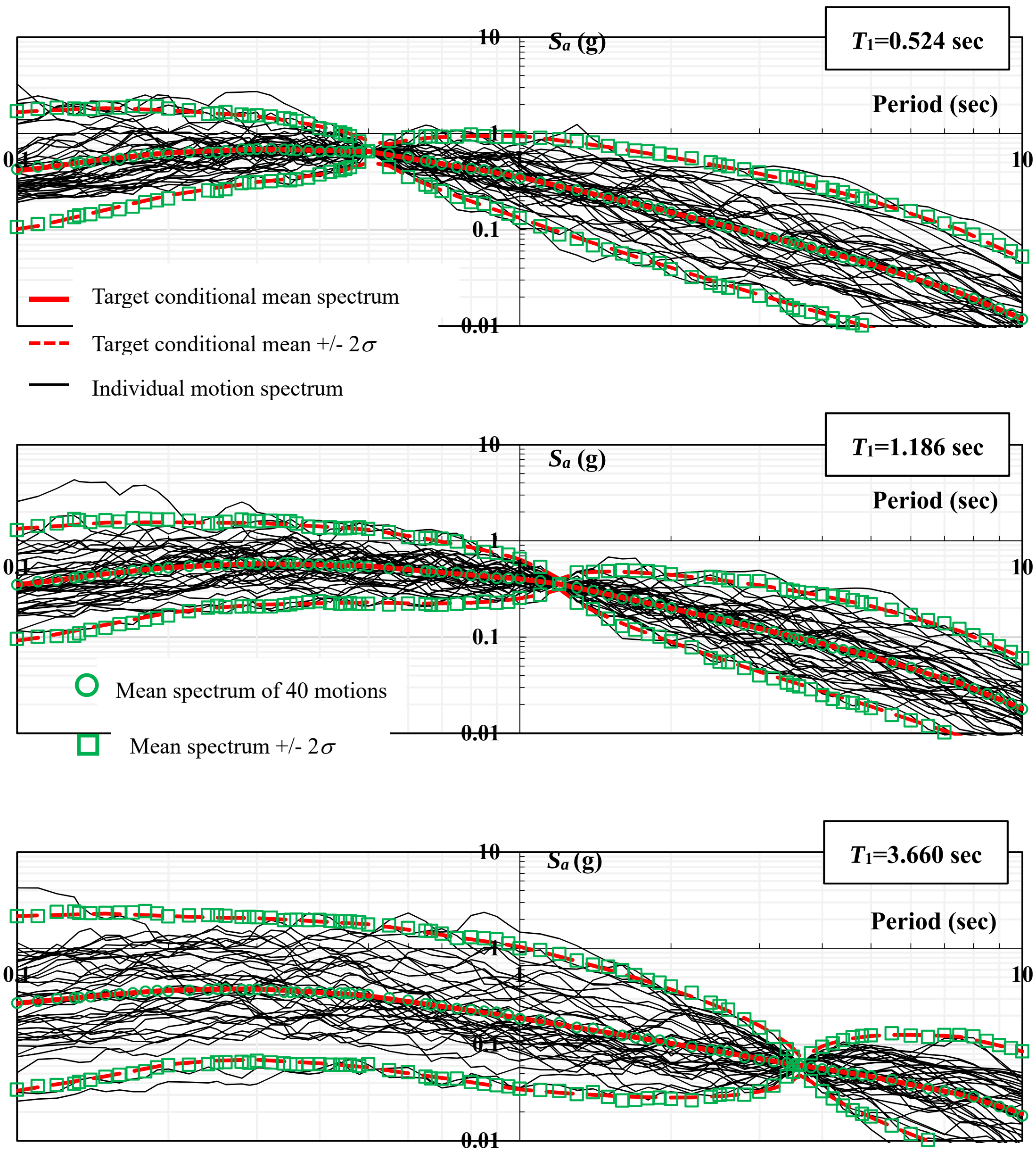

Figure B-5 Spectra of Scaled Motions and Conditional Spectra for Return Period of 144 Years and Period T_1 Equal to 0.524, 1.186 and 3.660 Seconds

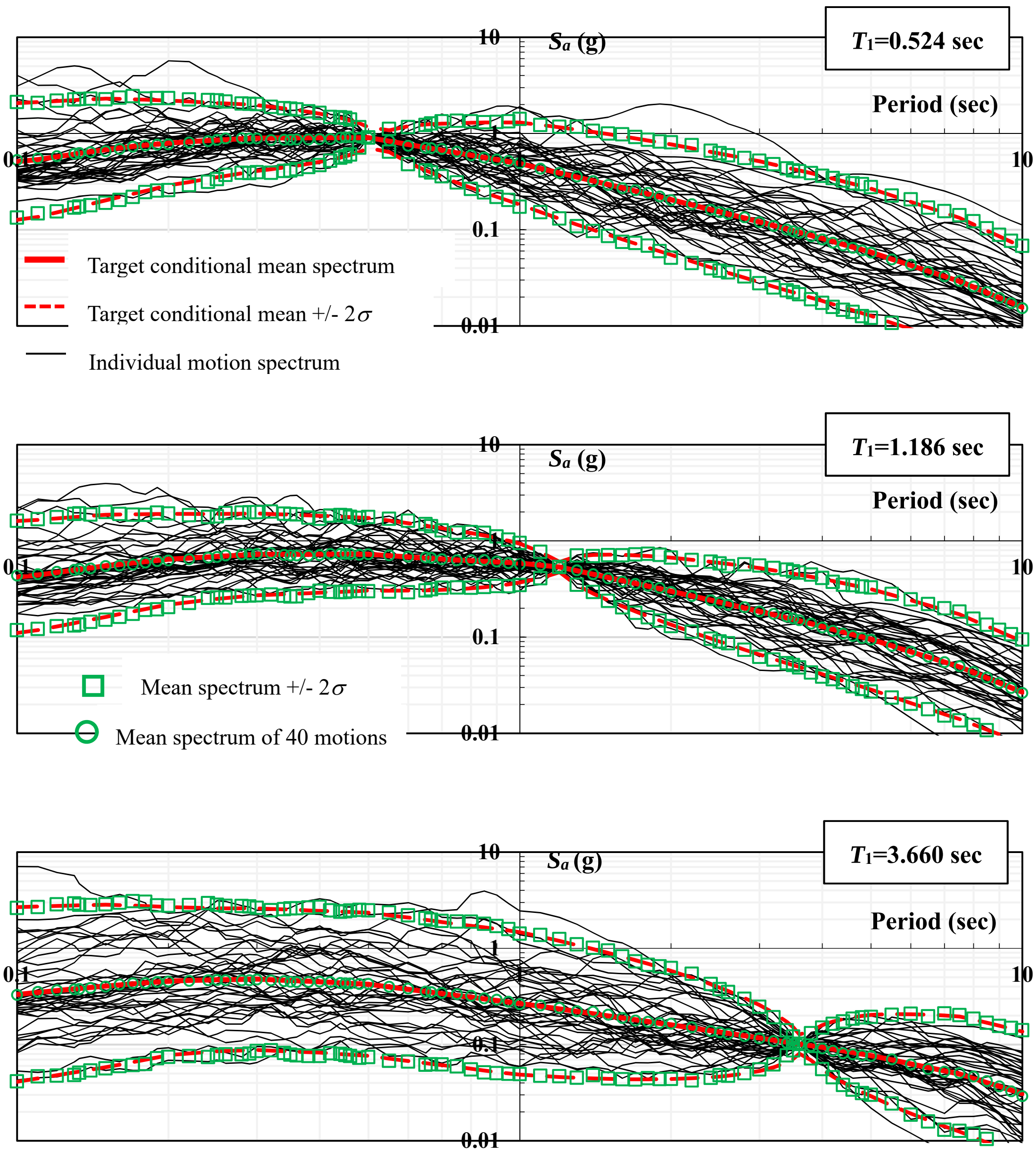

Figure B-6 Spectra of Scaled Motions and Conditional Spectra for Return Period of 289 Years and Period T_1 Equal to 0.524, 1.186 and 3.660 Seconds

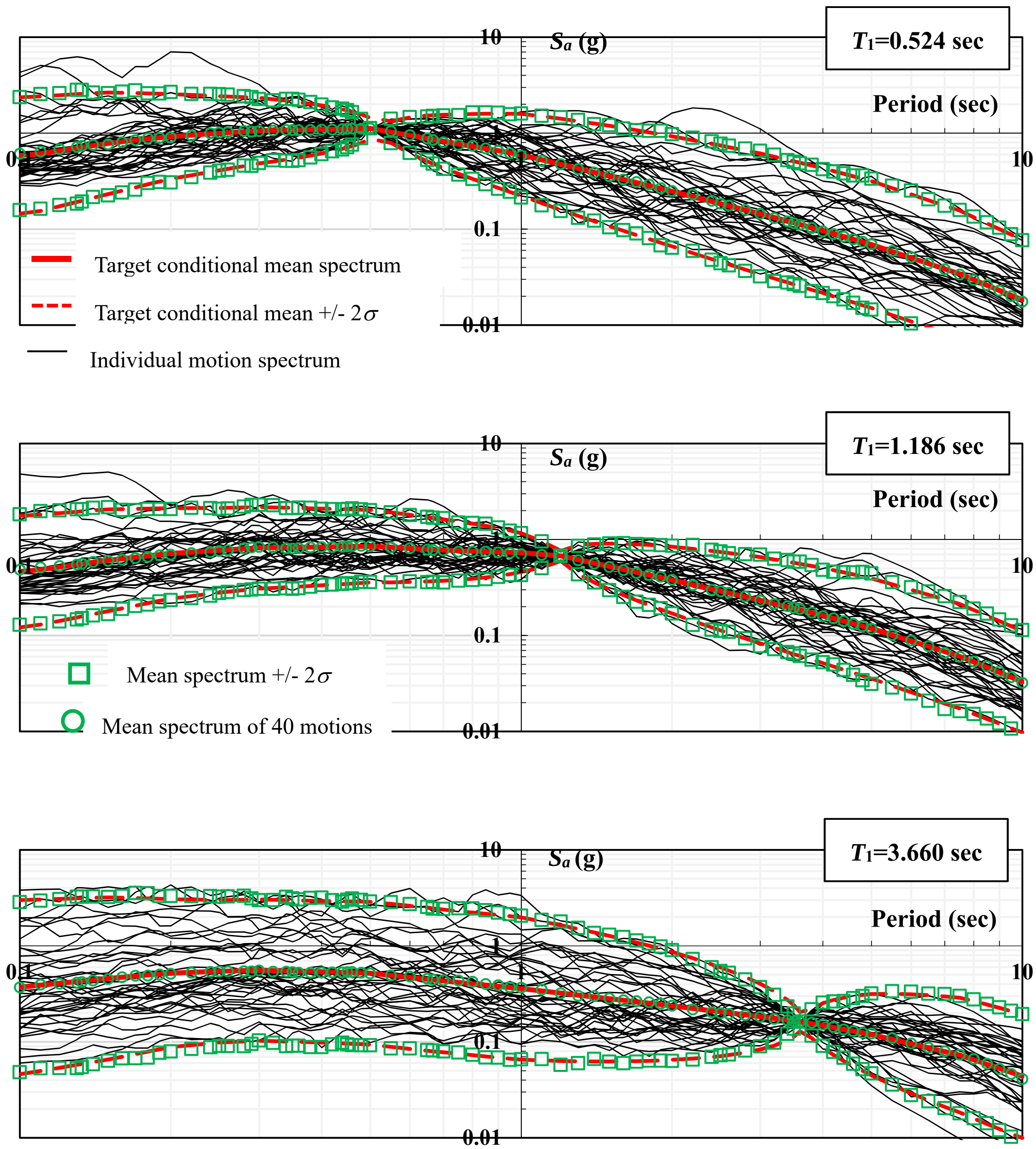

Figure B-7 Spectra of Scaled Motions and Conditional Spectra for Return Period of 475 Years and Period T_1 Equal to 0.524, 1.186 and 3.660 Seconds

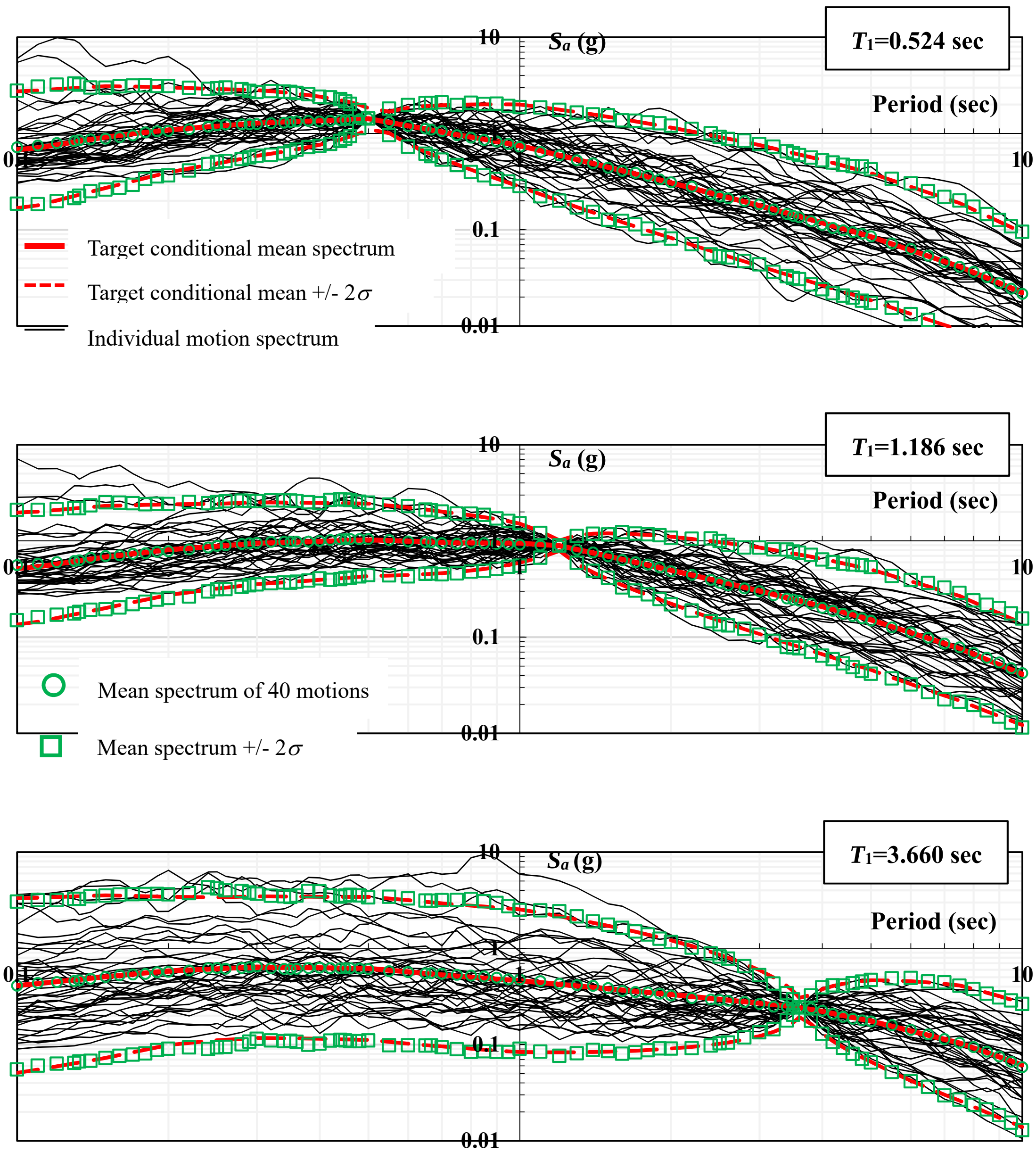

Figure B-8 Spectra of Scaled Motions and Conditional Spectra for Return Period of 949 Years and Period T_1 Equal to 0.524, 1.186 and 3.660 Seconds

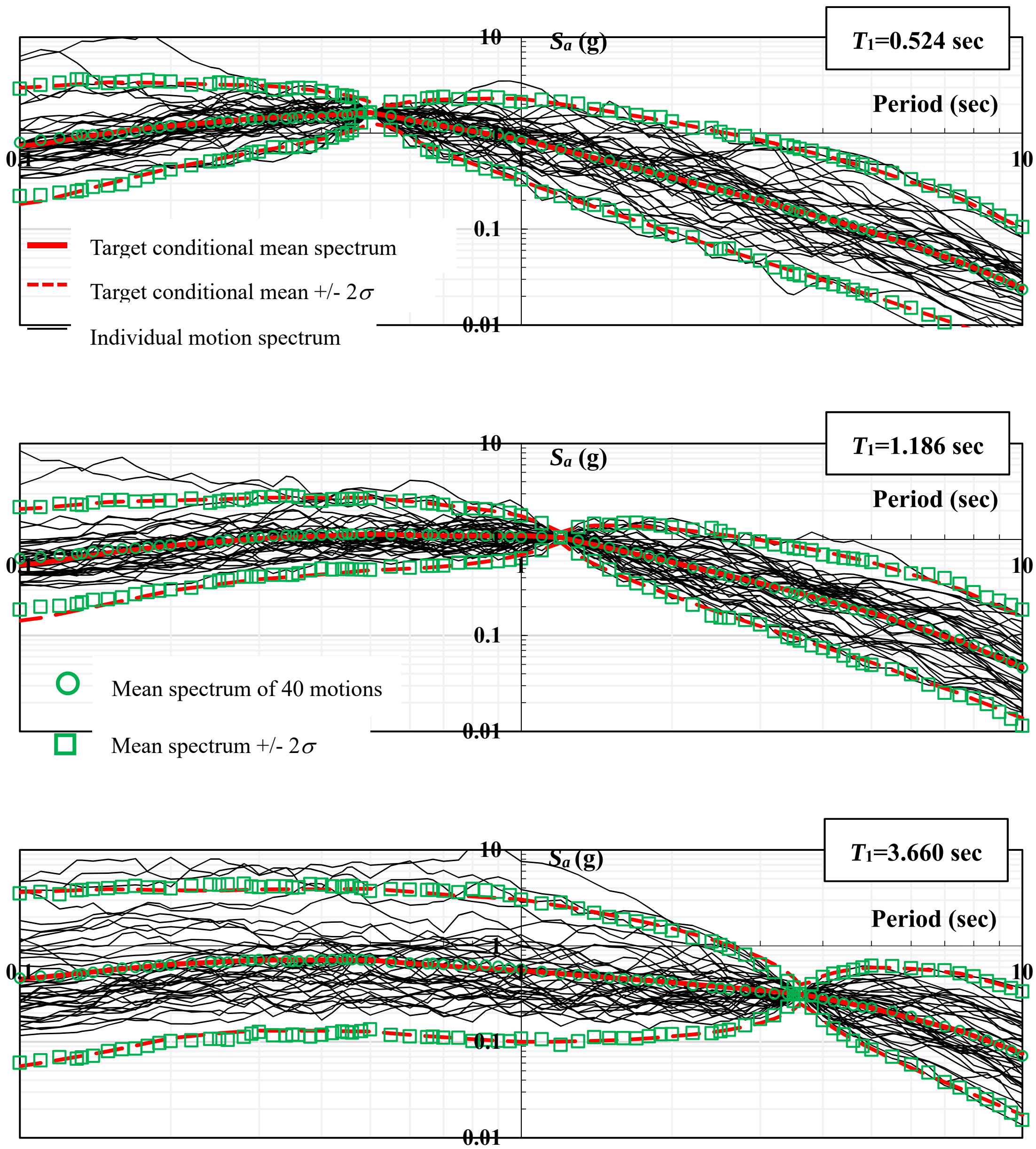

Figure B-9 Spectra of Scaled Motions and Conditional Spectra for Return Period of 1485 Years and Period T_1 Equal to 0.524, 1.186 and 3.660 Seconds

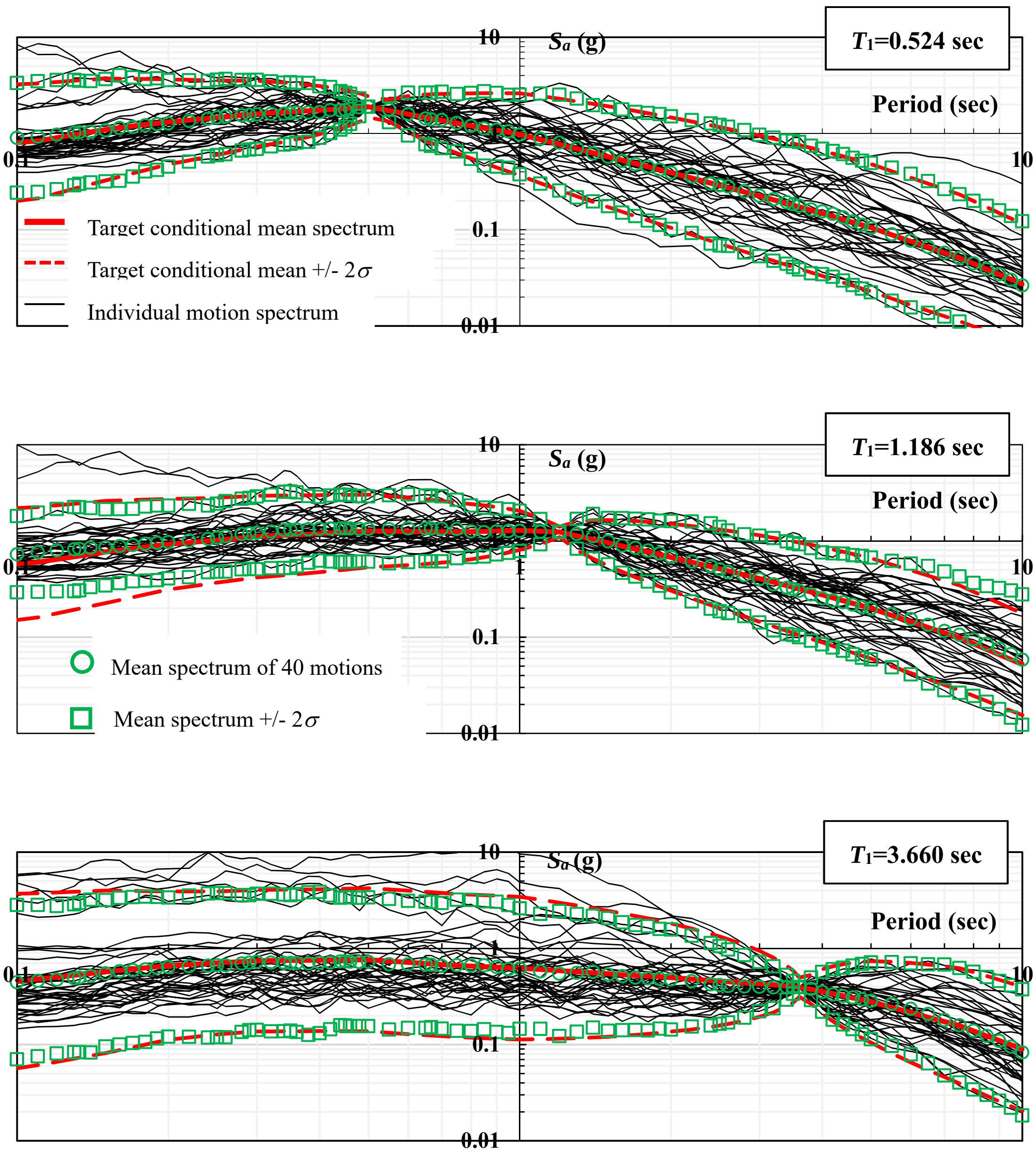

Figure B-10 Spectra of Scaled Motions and Conditional Spectra for Return Period of 2475 Years and Period T_1 Equal to 0.524, 1.186 and 3.660 Seconds

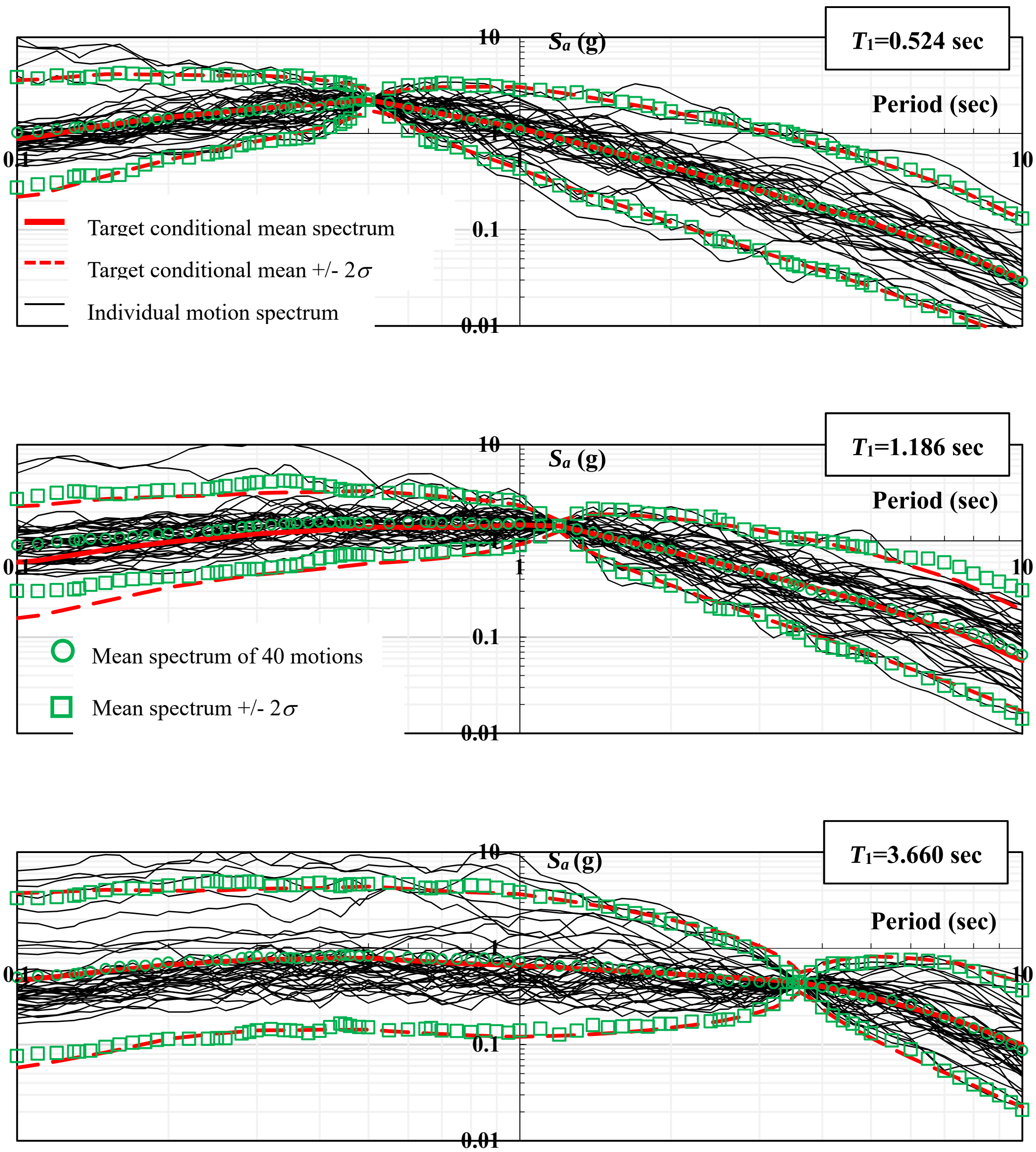

Figure B-11 Spectra of Scaled Motions and Conditional Spectra for Return Period of 3899 Years and Period T_1 Equal to 0.524, 1.186 and 3.660 Seconds

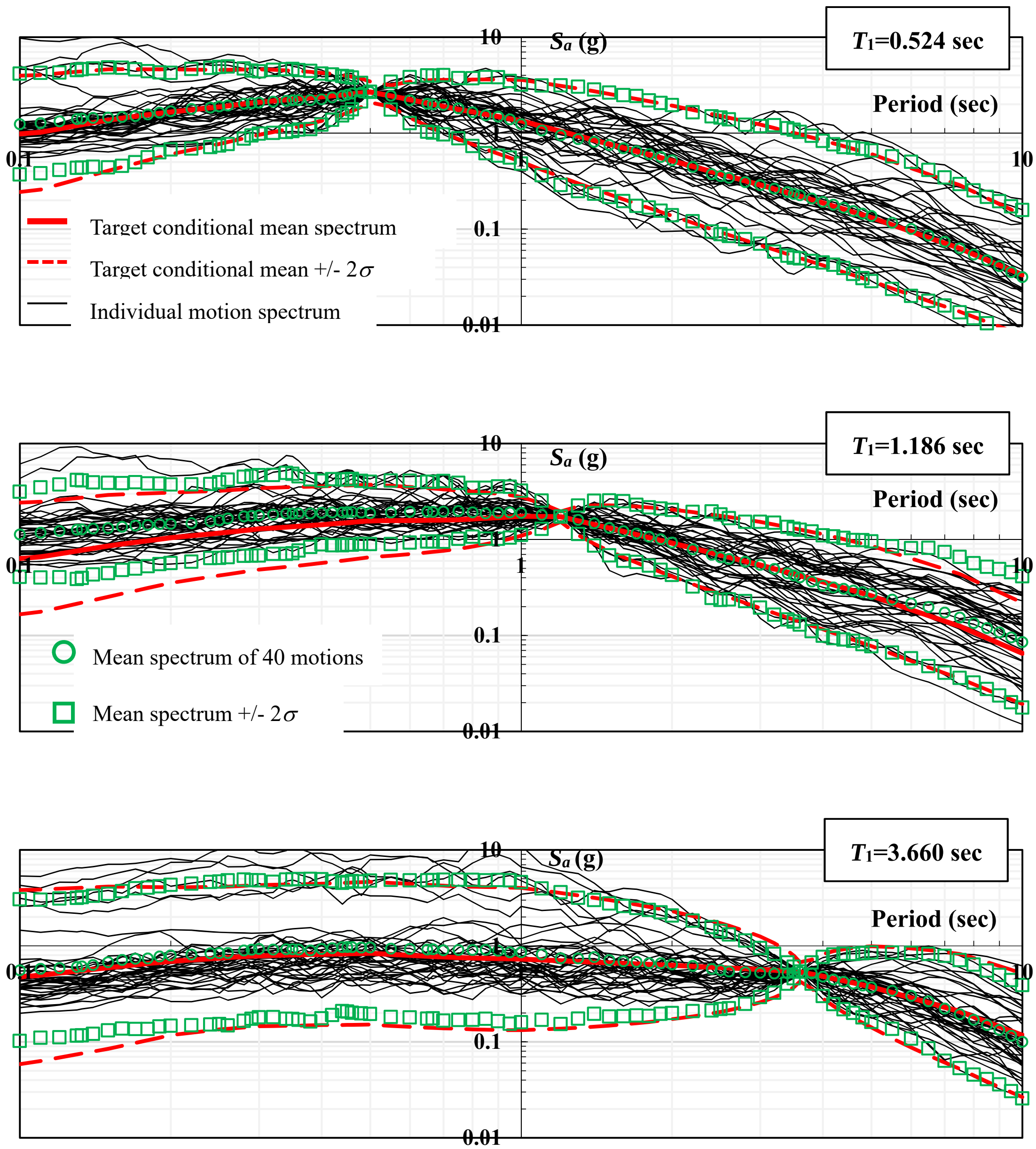

Figure B-12 Spectra of Scaled Motions and Conditional Spectra for Return Period of 7462 Years and Period T_1 Equal to 0.524, 1.186 and 3.660 Seconds

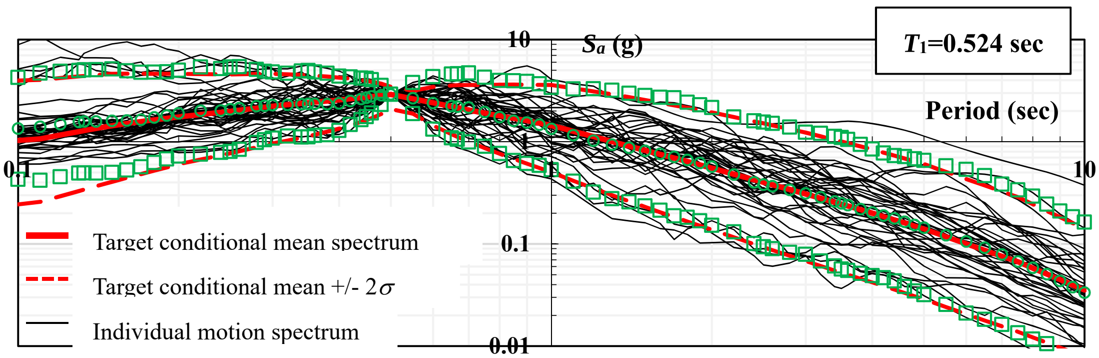

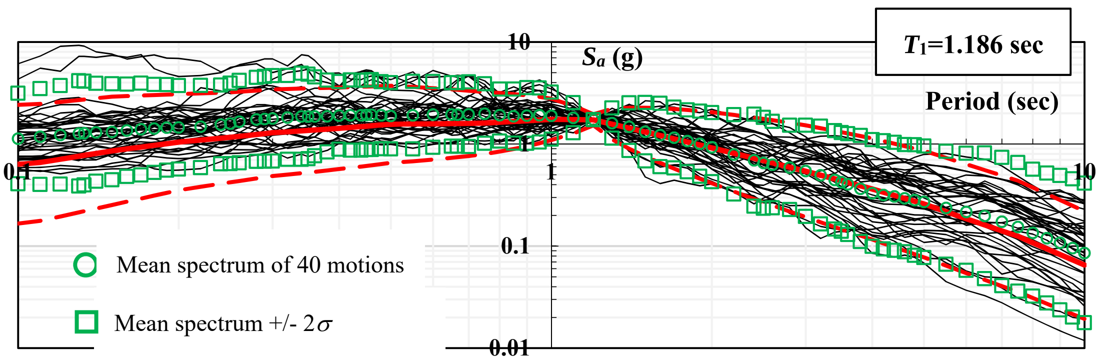

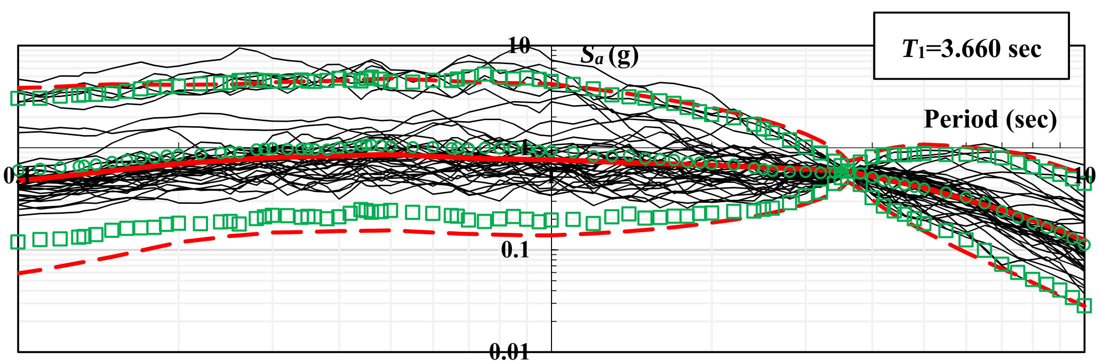

Figure B-13 Spectra of Scaled Motions and Conditional Spectra for Return Period of 10000 Years and Period T_1 Equal to 0.524, 1.186 and 3.660 Seconds

The selected and scaled ground motions used for the probabilistic evaluation must be representative of those that would be experienced in the future (Kohrangi et al, 2017). To ensure this the selected motions are evaluated for "hazard consistency". For the evaluation the rate of exceedance of $S_a(T)$ by the selected ground motions, conditional on $S_a(T_1)$, is calculated by the following equation (NIST, 2011; Lin et al., 2013[a]):

$$\lambda(Sa(T) > y) = \sum_{i=1}^{n} P(Sa(T) > y|Sa(T_1) = x_i)\lambda(Sa(T_1) = x_i) \qquad \text{(B-3)}$$

In Equation (B-3) n is the number of considered $S_a(T_1)$ amplitudes. Also, $P(S_a(T)>y|S_a(T_1)=x_i)$ is the probability that a ground motion selected and scaled to have $S_a(T_1)=x_i$ has a spectral acceleration at period T that is greater than y. This probability was estimated as the fraction of the 40 ground motions with $S_a(T_1)=x_i$ that have $S_a(T)>y$. Note that $\lambda(Sa(T_1) = x_i)$ can be calculated as follows (NIST, 2011; Lin et al., 2013[a]):

$$\lambda(Sa(T_1) = x_i) = \frac{\lambda(Sa(T_1)>x_{i-1}) - \lambda(Sa(T_1)>x_{i+1})}{2} \qquad \text{(B-4)}$$

For the hazard consistency, the calculated rate of exceedance $\lambda(S_a(T)>y)$ as function of $S_a(T_1)$ is compared with the seismic hazard curve obtained for the site from USGS (https://earthquake.usgs.gov/hazards/interactive/), with the two curves expected to be in close agreement. If the curves are not sufficiently close, the selected ground motions are assumed to violate hazard consistency and the process is re-started with new motions.

Figure B-14 compares the rates of exceedance with the seismic hazard curves obtained from the USGS website (https://earthquake.usgs.gov/hazards/interactive/) for the three values of period T_1 corresponding to the considered isolated structures ($T_1=T_M=3.66$sec), the non-isolated SMF structure ($T_1=1.866$sec) and the non-isolated SCBF structure ($T_1=0.524$sec). The seismic hazard curves in Figure B-14 were constructed for different periods T depending on the structure analyzed. Specifically, for the case of the seismically isolated structures (Fig. B-14(a)), the three periods were T=3.66, 0.989 and 0.377seconds. The periods are the fundamental period (=3.66sec), the second period for the case of the isolated SMF (=0.989sec) and the second period for the case of the isolated SCBF (=0.377sec) obtained by modal analysis for the frames designed with $R_I=1.5$ and with the isolators represented by the effective properties in the MCE_R. (The second and third period values for the isolated frames designed for $R_I=1.0$ and 2.0 were within 10% of period values in the curves of Figure B-14). The curves in Figure B-14(b) apply for the case of the non-isolated SMF building. The three values of period T are the fundamental

(1.186sec), the second period (0.437sec) and a value twice the fundamental period (2T=2.372sec). Similarly, the curves in Figure B-14(c) apply for the case of the non-isolated SCBF building, with the three values of period T being the fundamental (0.524sec), the second period (0.195sec) and a value twice the fundamental period (2T=1.048sec).) Note that these ranges of period are examined because the goal of the analysis is to compute values of the maximum story drift ratio, the residual story drift ratio and the peak floor acceleration which are sensitive to motions of different frequency content. The shorter periods are examined because the peak floor acceleration is sensitive to motions of large frequencies (short period). The longer periods (2T values) are examined because the maximum story drift and the residual story drift are sensitive to motions containing components with large periods that may be close to the lengthened period of the analyzed buildings when they undergo inelastic action in strong ground motions (NIST, 2011; Lin et al., 2013[a]).

The computed curves for the mean annual rate of exceedance for the selected ground motions are in good agreement with the seismic hazard curves obtained from USGS for the site except for the case of the isolated structures (Fig. B-14(a)) and for the lower periods (T=0.377 and 0.989sec). In these cases the computed rates are less than those of the seismic hazard curves, suggesting that the computed mean annual frequencies of exceedance for the floor accelerations of the isolated buildings are somehow underestimated (as they are affected by motions with low period content). Nonetheless, the selection of ground motions was deemed acceptable given that the fidelity of the computed curves for the mean annual rate of exceedance of the selected ground motions (as compared to the seismic hazard curves obtained from USGS) was comparable to those presented in other studies (NIST, 2011; Lin et al, 2013[a]; Kohrangi et al, 2017).

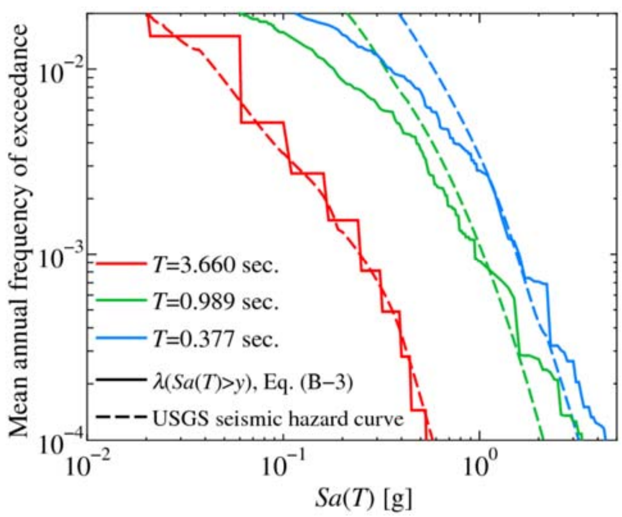

(a)

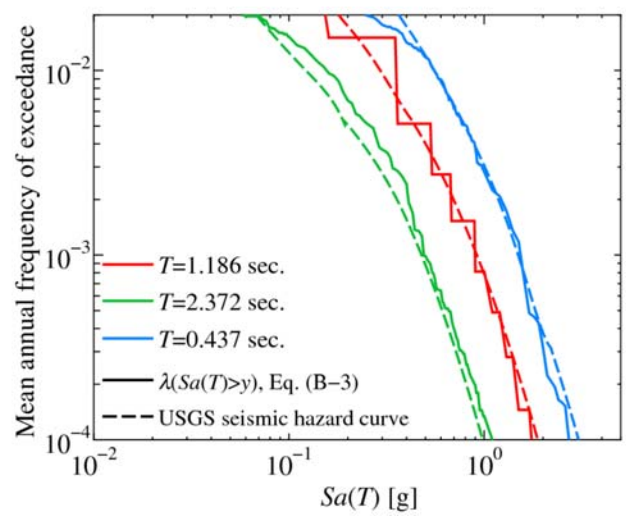

(b)

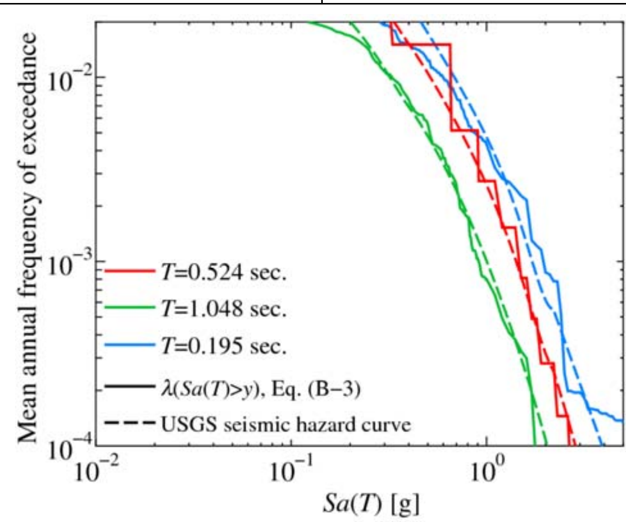

(c)

Figure B-14 Comparison of Calculated Mean Annual Frequency Rates Based on Selected Ground Motions (Solid Lines) and USGS Seismic Hazard Curves Dashed Lines) for (a) Isolated Buildings, (b) Non-isolated SMF Building and (c) Non-isolated SCBF Building

MCEER Technical Reports

MCEER publishes technical reports on a variety of subjects written by authors funded through MCEER. These reports can be downloaded from the MCEER website at http://www.buffalo.edu/mceer. They can also be requested through NTIS, P.O. Box 1425, Springfield, Virginia 22151. NTIS accession numbers are shown in parenthesis, if available.

NCEER-87-0001 "First-Year Program in Research, Education and Technology Transfer," 3/5/87, (PB88-134275, A04, MF-A01).

NCEER-87-0002 "Experimental Evaluation of Instantaneous Optimal Algorithms for Structural Control," by R.C. Lin, T.T. Soong and A.M. Reinhorn, 4/20/87, (PB88-134341, A04, MF-A01).

NCEER-87-0003 "Experimentation Using the Earthquake Simulation Facilities at University at Buffalo," by A.M. Reinhorn and R.L. Ketter, not available.

NCEER-87-0004 "The System Characteristics and Performance of a Shaking Table," by J.S. Hwang, K.C. Chang and G.C. Lee, 6/1/87, (PB88-134259, A03, MF-A01). This report is available only through NTIS (see address given above).

NCEER-87-0005 "A Finite Element Formulation for Nonlinear Viscoplastic Material Using a Q Model," by O. Gyebi and G. Dasgupta, 11/2/87, (PB88-213764, A08, MF-A01).

NCEER-87-0006 "Symbolic Manipulation Program (SMP) - Algebraic Codes for Two and Three Dimensional Finite Element Formulations," by X. Lee and G. Dasgupta, 11/9/87, (PB88-218522, A05, MF-A01).

NCEER-87-0007 "Instantaneous Optimal Control Laws for Tall Buildings Under Seismic Excitations," by J.N. Yang, A. Akbarpour and P. Ghaemmaghami, 6/10/87, (PB88-134333, A06, MF-A01). This report is only available through NTIS (see address given above).

NCEER-87-0008 "IDARC: Inelastic Damage Analysis of Reinforced Concrete Frame - Shear-Wall Structures," by Y.J. Park, A.M. Reinhorn and S.K. Kunnath, 7/20/87, (PB88-134325, A09, MF-A01). This report is only available through NTIS (see address given above).

NCEER-87-0009 "Liquefaction Potential for New York State: A Preliminary Report on Sites in Manhattan and Buffalo," by M. Budhu, V. Vijayakumar, R.F. Giese and L. Baumgras, 8/31/87, (PB88-163704, A03, MF-A01). This report is available only through NTIS (see address given above).

NCEER-87-0010 "Vertical and Torsional Vibration of Foundations in Inhomogeneous Media," by A.S. Veletsos and K.W. Dotson, 6/1/87, (PB88-134291, A03, MF-A01). This report is only available through NTIS (see address given above).

NCEER-87-0011 "Seismic Probabilistic Risk Assessment and Seismic Margins Studies for Nuclear Power Plants," by Howard H.M. Hwang, 6/15/87, (PB88-134267, A03, MF-A01). This report is only available through NTIS (see address given above).

NCEER-87-0012 "Parametric Studies of Frequency Response of Secondary Systems Under Ground-Acceleration Excitations," by Y. Yong and Y.K. Lin, 6/10/87, (PB88-134309, A03, MF-A01). This report is only available through NTIS (see address given above).

NCEER-87-0013 "Frequency Response of Secondary Systems Under Seismic Excitation," by J.A. HoLung, J. Cai and Y.K. Lin, 7/31/87, (PB88-134317, A05, MF-A01). This report is only available through NTIS (see address given above).

NCEER-87-0014 "Modelling Earthquake Ground Motions in Seismically Active Regions Using Parametric Time Series Methods," by G.W. Ellis and A.S. Cakmak, 8/25/87, (PB88-134283, A08, MF-A01). This report is only available through NTIS (see address given above).

NCEER-87-0015 "Detection and Assessment of Seismic Structural Damage," by E. DiPasquale and A.S. Cakmak, 8/25/87, (PB88-163712, A05, MF-A01). This report is only available through NTIS (see address given above).

NCEER-87-0016 "Pipeline Experiment at Parkfield, California," by J. Isenberg and E. Richardson, 9/15/87, (PB88-163720, A03, MF-A01). This report is available only through NTIS (see address given above).

NCEER-87-0017 "Digital Simulation of Seismic Ground Motion," by M. Shinozuka, G. Deodatis and T. Harada, 8/31/87, (PB88-155197, A04, MF-A01). This report is available only through NTIS (see address given above).

NCEER-87-0018 "Practical Considerations for Structural Control: System Uncertainty, System Time Delay and Truncation of Small Control Forces," J.N. Yang and A. Akbarpour, 8/10/87, (PB88-163738, A08, MF-A01). This report is only available through NTIS (see address given above).

NCEER-87-0019 "Modal Analysis of Nonclassically Damped Structural Systems Using Canonical Transformation," by J.N. Yang, S. Sarkani and F.X. Long, 9/27/87, (PB88-187851, A04, MF-A01).

NCEER-87-0020 "A Nonstationary Solution in Random Vibration Theory," by J.R. Red-Horse and P.D. Spanos, 11/3/87, (PB88-163746, A03, MF-A01).

NCEER-87-0021 "Horizontal Impedances for Radially Inhomogeneous Viscoelastic Soil Layers," by A.S. Veletsos and K.W. Dotson, 10/15/87, (PB88-150859, A04, MF-A01).

NCEER-87-0022 "Seismic Damage Assessment of Reinforced Concrete Members," by Y.S. Chung, C. Meyer and M. Shinozuka, 10/9/87, (PB88-150867, A05, MF-A01). This report is available only through NTIS (see address given above).

NCEER-87-0023 "Active Structural Control in Civil Engineering," by T.T. Soong, 11/11/87, (PB88-187778, A03, MF-A01).

NCEER-87-0024 "Vertical and Torsional Impedances for Radially Inhomogeneous Viscoelastic Soil Layers," by K.W. Dotson and A.S. Veletsos, 12/87, (PB88-187786, A03, MF-A01).

NCEER-87-0025 "Proceedings from the Symposium on Seismic Hazards, Ground Motions, Soil-Liquefaction and Engineering Practice in Eastern North America," October 20-22, 1987, edited by K.H. Jacob, 12/87, (PB88-188115, A23, MF-A01). This report is available only through NTIS (see address given above).

NCEER-87-0026 "Report on the Whittier-Narrows, California, Earthquake of October 1, 1987," by J. Pantelic and A. Reinhorn, 11/87, (PB88-187752, A03, MF-A01). This report is available only through NTIS (see address given above).

NCEER-87-0027 "Design of a Modular Program for Transient Nonlinear Analysis of Large 3-D Building Structures," by S. Srivastav and J.F. Abel, 12/30/87, (PB88-187950, A05, MF-A01). This report is only available through NTIS (see address given above).

NCEER-87-0028 "Second-Year Program in Research, Education and Technology Transfer," 3/8/88, (PB88-219480, A04, MF-A01).

NCEER-88-0001 "Workshop on Seismic Computer Analysis and Design of Buildings With Interactive Graphics," by W. McGuire, J.F. Abel and C.H. Conley, 1/18/88, (PB88-187760, A03, MF-A01). This report is only available through NTIS (see address given above).

NCEER-88-0002 "Optimal Control of Nonlinear Flexible Structures," by J.N. Yang, F.X. Long and D. Wong, 1/22/88, (PB88-213772, A06, MF-A01).

NCEER-88-0003 "Substructuring Techniques in the Time Domain for Primary-Secondary Structural Systems," by G.D. Manolis and G. Juhn, 2/10/88, (PB88-213780, A04, MF-A01).

NCEER-88-0004 "Iterative Seismic Analysis of Primary-Secondary Systems," by A. Singhal, L.D. Lutes and P.D. Spanos, 2/23/88, (PB88-213798, A04, MF-A01).

NCEER-88-0005 "Stochastic Finite Element Expansion for Random Media," by P.D. Spanos and R. Ghanem, 3/14/88, (PB88-213806, A03, MF-A01).

NCEER-88-0006 "Combining Structural Optimization and Structural Control," by F.Y. Cheng and C.P. Pantelides, 1/10/88, (PB88-213814, A05, MF-A01).

NCEER-88-0007 "Seismic Performance Assessment of Code-Designed Structures," by H.H-M. Hwang, J-W. Jaw and H-J. Shau, 3/20/88, (PB88-219423, A04, MF-A01). This report is only available through NTIS (see address given above).

NCEER-88-0008 "Reliability Analysis of Code-Designed Structures Under Natural Hazards," by H.H-M. Hwang, H. Ushiba and M. Shinozuka, 2/29/88, (PB88-229471, A07, MF-A01). This report is only available through NTIS (see address given above).

NCEER-88-0009 "Seismic Fragility Analysis of Shear Wall Structures," by J-W Jaw and H.H-M. Hwang, 4/30/88, (PB89-102867, A04, MF-A01).

NCEER-88-0010 "Base Isolation of a Multi-Story Building Under a Harmonic Ground Motion - A Comparison of Performances of Various Systems," by F-G Fan, G. Ahmadi and I.G. Tadjbakhsh, 5/18/88, (PB89-122238, A06, MF-A01). This report is only available through NTIS (see address given above).

NCEER-88-0011 "Seismic Floor Response Spectra for a Combined System by Green's Functions," by F.M. Lavelle, L.A. Bergman and P.D. Spanos, 5/1/88, (PB89-102875, A03, MF-A01).

NCEER-88-0012 "A New Solution Technique for Randomly Excited Hysteretic Structures," by G.Q. Cai and Y.K. Lin, 5/16/88, (PB89-102883, A03, MF-A01).

NCEER-88-0013 "A Study of Radiation Damping and Soil-Structure Interaction Effects in the Centrifuge," by K. Weissman, supervised by J.H. Prevost, 5/24/88, (PB89-144703, A06, MF-A01).

NCEER-88-0014 "Parameter Identification and Implementation of a Kinematic Plasticity Model for Frictional Soils," by J.H. Prevost and D.V. Griffiths, not available.

NCEER-88-0015 "Two- and Three- Dimensional Dynamic Finite Element Analyses of the Long Valley Dam," by D.V. Griffiths and J.H. Prevost, 6/17/88, (PB89-144711, A04, MF-A01).

NCEER-88-0016 "Damage Assessment of Reinforced Concrete Structures in Eastern United States," by A.M. Reinhorn, M.J. Seidel, S.K. Kunnath and Y.J. Park, 6/15/88, (PB89-122220, A04, MF-A01). This report is only available through NTIS (see address given above).

NCEER-88-0017 "Dynamic Compliance of Vertically Loaded Strip Foundations in Multilayered Viscoelastic Soils," by S. Ahmad and A.S.M. Israil, 6/17/88, (PB89-102891, A04, MF-A01).

NCEER-88-0018 "An Experimental Study of Seismic Structural Response With Added Viscoelastic Dampers," by R.C. Lin, Z. Liang, T.T. Soong and R.H. Zhang, 6/30/88, (PB89-122212, A05, MF-A01). This report is available only through NTIS (see address given above).

NCEER-88-0019 "Experimental Investigation of Primary - Secondary System Interaction," by G.D. Manolis, G. Juhn and A.M. Reinhorn, 5/27/88, (PB89-122204, A04, MF-A01).

NCEER-88-0020 "A Response Spectrum Approach For Analysis of Nonclassically Damped Structures," by J.N. Yang, S. Sarkani and F.X. Long, 4/22/88, (PB89-102909, A04, MF-A01).

NCEER-88-0021 "Seismic Interaction of Structures and Soils: Stochastic Approach," by A.S. Veletsos and A.M. Prasad, 7/21/88, (PB89-122196, A04, MF-A01). This report is only available through NTIS (see address given above).

NCEER-88-0022 "Identification of the Serviceability Limit State and Detection of Seismic Structural Damage," by E. DiPasquale and A.S. Cakmak, 6/15/88, (PB89-122188, A05, MF-A01). This report is available only through NTIS (see address given above).

NCEER-88-0023 "Multi-Hazard Risk Analysis: Case of a Simple Offshore Structure," by B.K. Bhartia and E.H. Vanmarcke, 7/21/88, (PB89-145213, A05, MF-A01).

NCEER-88-0024 "Automated Seismic Design of Reinforced Concrete Buildings," by Y.S. Chung, C. Meyer and M. Shinozuka, 7/5/88, (PB89-122170, A06, MF-A01). This report is available only through NTIS (see address given above).

NCEER-88-0025 "Experimental Study of Active Control of MDOF Structures Under Seismic Excitations," by L.L. Chung, R.C. Lin, T.T. Soong and A.M. Reinhorn, 7/10/88, (PB89-122600, A04, MF-A01).

NCEER-88-0026 "Earthquake Simulation Tests of a Low-Rise Metal Structure," by J.S. Hwang, K.C. Chang, G.C. Lee and R.L. Ketter, 8/1/88, (PB89-102917, A04, MF-A01).

NCEER-88-0027 "Systems Study of Urban Response and Reconstruction Due to Catastrophic Earthquakes," by F. Kozin and H.K. Zhou, 9/22/88, (PB90-162348, A04, MF-A01).

NCEER-88-0028 "Seismic Fragility Analysis of Plane Frame Structures," by H.H-M. Hwang and Y.K. Low, 7/31/88, (PB89-131445, A06, MF-A01).

NCEER-88-0029 "Response Analysis of Stochastic Structures," by A. Kardara, C. Bucher and M. Shinozuka, 9/22/88, (PB89-174429, A04, MF-A01).

NCEER-88-0030 "Nonnormal Accelerations Due to Yielding in a Primary Structure," by D.C.K. Chen and L.D. Lutes, 9/19/88, (PB89-131437, A04, MF-A01).

NCEER-88-0031 "Design Approaches for Soil-Structure Interaction," by A.S. Veletsos, A.M. Prasad and Y. Tang, 12/30/88, (PB89-174437, A03, MF-A01). This report is available only through NTIS (see address given above).

NCEER-88-0032 "A Re-evaluation of Design Spectra for Seismic Damage Control," by C.J. Turkstra and A.G. Tallin, 11/7/88, (PB89-145221, A05, MF-A01).

NCEER-88-0033 "The Behavior and Design of Noncontact Lap Splices Subjected to Repeated Inelastic Tensile Loading," by V.E. Sagan, P. Gergely and R.N. White, 12/8/88, (PB89-163737, A08, MF-A01).

NCEER-88-0034 "Seismic Response of Pile Foundations," by S.M. Mamoon, P.K. Banerjee and S. Ahmad, 11/1/88, (PB89-145239, A04, MF-A01).

NCEER-88-0035 "Modeling of R/C Building Structures With Flexible Floor Diaphragms (IDARC2)," by A.M. Reinhorn, S.K. Kunnath and N. Panahshahi, 9/7/88, (PB89-207153, A07, MF-A01).

NCEER-88-0036 "Solution of the Dam-Reservoir Interaction Problem Using a Combination of FEM, BEM with Particular Integrals, Modal Analysis, and Substructuring," by C-S. Tsai, G.C. Lee and R.L. Ketter, 12/31/88, (PB89-207146, A04, MF-A01).

NCEER-88-0037 "Optimal Placement of Actuators for Structural Control," by F.Y. Cheng and C.P. Pantelides, 8/15/88, (PB89-162846, A05, MF-A01).

NCEER-88-0038 "Teflon Bearings in Aseismic Base Isolation: Experimental Studies and Mathematical Modeling," by A. Mokha, M.C. Constantinou and A.M. Reinhorn, 12/5/88, (PB89-218457, A10, MF-A01). This report is available only through NTIS (see address given above).

NCEER-88-0039 "Seismic Behavior of Flat Slab High-Rise Buildings in the New York City Area," by P. Weidlinger and M. Ettouney, 10/15/88, (PB90-145681, A04, MF-A01).

NCEER-88-0040 "Evaluation of the Earthquake Resistance of Existing Buildings in New York City," by P. Weidlinger and M. Ettouney, 10/15/88, not available.

NCEER-88-0041 "Small-Scale Modeling Techniques for Reinforced Concrete Structures Subjected to Seismic Loads," by W. Kim, A. El-Attar and R.N. White, 11/22/88, (PB89-189625, A05, MF-A01).

NCEER-88-0042 "Modeling Strong Ground Motion from Multiple Event Earthquakes," by G.W. Ellis and A.S. Cakmak, 10/15/88, (PB89-174445, A03, MF-A01).

NCEER-88-0043 "Nonstationary Models of Seismic Ground Acceleration," by M. Grigoriu, S.E. Ruiz and E. Rosenblueth, 7/15/88, (PB89-189617, A04, MF-A01).

NCEER-88-0044 "SARCF User's Guide: Seismic Analysis of Reinforced Concrete Frames," by Y.S. Chung, C. Meyer and M. Shinozuka, 11/9/88, (PB89-174452, A08, MF-A01).

NCEER-88-0045 "First Expert Panel Meeting on Disaster Research and Planning," edited by J. Pantelic and J. Stoyle, 9/15/88, (PB89-174460, A05, MF-A01).

NCEER-88-0046 "Preliminary Studies of the Effect of Degrading Infill Walls on the Nonlinear Seismic Response of Steel Frames," by C.Z. Chrysostomou, P. Gergely and J.F. Abel, 12/19/88, (PB89-208383, A05, MF-A01).

NCEER-88-0047 "Reinforced Concrete Frame Component Testing Facility - Design, Construction, Instrumentation and Operation," by S.P. Pessiki, C. Conley, T. Bond, P. Gergely and R.N. White, 12/16/88, (PB89-174478, A04, MF-A01).

NCEER-89-0001 "Effects of Protective Cushion and Soil Compliancy on the Response of Equipment Within a Seismically Excited Building," by J.A. HoLung, 2/16/89, (PB89-207179, A04, MF-A01).

NCEER-89-0002 "Statistical Evaluation of Response Modification Factors for Reinforced Concrete Structures," by H.H-M. Hwang and J-W. Jaw, 2/17/89, (PB89-207187, A05, MF-A01).

NCEER-89-0003 "Hysteretic Columns Under Random Excitation," by G-Q. Cai and Y.K. Lin, 1/9/89, (PB89-196513, A03, MF-A01).

NCEER-89-0004 "Experimental Study of `Elephant Foot Bulge' Instability of Thin-Walled Metal Tanks," by Z-H. Jia and R.L. Ketter, 2/22/89, (PB89-207195, A03, MF-A01).

NCEER-89-0005 "Experiment on Performance of Buried Pipelines Across San Andreas Fault," by J. Isenberg, E. Richardson and T.D. O'Rourke, 3/10/89, (PB89-218440, A04, MF-A01). This report is available only through NTIS (see address given above).

NCEER-89-0006 "A Knowledge-Based Approach to Structural Design of Earthquake-Resistant Buildings," by M. Subramani, P. Gergely, C.H. Conley, J.F. Abel and A.H. Zaghw, 1/15/89, (PB89-218465, A06, MF-A01).

NCEER-89-0007 "Liquefaction Hazards and Their Effects on Buried Pipelines," by T.D. O'Rourke and P.A. Lane, 2/1/89, (PB89-218481, A09, MF-A01).

NCEER-89-0008 "Fundamentals of System Identification in Structural Dynamics," by H. Imai, C-B. Yun, O. Maruyama and M. Shinozuka, 1/26/89, (PB89-207211, A04, MF-A01).

NCEER-89-0009 "Effects of the 1985 Michoacan Earthquake on Water Systems and Other Buried Lifelines in Mexico," by A.G. Ayala and M.J. O'Rourke, 3/8/89, (PB89-207229, A06, MF-A01).

NCEER-89-R010 "NCEER Bibliography of Earthquake Education Materials," by K.E.K. Ross, Second Revision, 9/1/89, (PB90-125352, A05, MF-A01). This report is replaced by NCEER-92-0018.

NCEER-89-0011 "Inelastic Three-Dimensional Response Analysis of Reinforced Concrete Building Structures (IDARC-3D), Part I - Modeling," by S.K. Kunnath and A.M. Reinhorn, 4/17/89, (PB90-114612, A07, MF-A01). This report is available only through NTIS (see address given above).

NCEER-89-0012 "Recommended Modifications to ATC-14," by C.D. Poland and J.O. Malley, 4/12/89, (PB90-108648, A15, MF-A01).

NCEER-89-0013 "Repair and Strengthening of Beam-to-Column Connections Subjected to Earthquake Loading," by M. Corazao and A.J. Durrani, 2/28/89, (PB90-109885, A06, MF-A01).

NCEER-89-0014 "Program EXKAL2 for Identification of Structural Dynamic Systems," by O. Maruyama, C-B. Yun, M. Hoshiya and M. Shinozuka, 5/19/89, (PB90-109877, A09, MF-A01).

NCEER-89-0015 "Response of Frames With Bolted Semi-Rigid Connections, Part I - Experimental Study and Analytical Predictions," by P.J. DiCorso, A.M. Reinhorn, J.R. Dickerson, J.B. Radziminski and W.L. Harper, 6/1/89, not available.

NCEER-89-0016 "ARMA Monte Carlo Simulation in Probabilistic Structural Analysis," by P.D. Spanos and M.P. Mignolet, 7/10/89, (PB90-109893, A03, MF-A01).

NCEER-89-P017 "Preliminary Proceedings from the Conference on Disaster Preparedness - The Place of Earthquake Education in Our Schools," Edited by K.E.K. Ross, 6/23/89, (PB90-108606, A03, MF-A01).

NCEER-89-0017 "Proceedings from the Conference on Disaster Preparedness - The Place of Earthquake Education in Our Schools," Edited by K.E.K. Ross, 12/31/89, (PB90-207895, A012, MF-A02). This report is available only through NTIS (see address given above).

NCEER-89-0018 "Multidimensional Models of Hysteretic Material Behavior for Vibration Analysis of Shape Memory Energy Absorbing Devices, by E.J. Graesser and F.A. Cozzarelli, 6/7/89, (PB90-164146, A04, MF-A01).

NCEER-89-0019 "Nonlinear Dynamic Analysis of Three-Dimensional Base Isolated Structures (3D-BASIS)," by S. Nagarajaiah, A.M. Reinhorn and M.C. Constantinou, 8/3/89, (PB90-161936, A06, MF-A01). This report has been replaced by NCEER-93-0011.

NCEER-89-0020 "Structural Control Considering Time-Rate of Control Forces and Control Rate Constraints," by F.Y. Cheng and C.P. Pantelides, 8/3/89, (PB90-120445, A04, MF-A01).

NCEER-89-0021 "Subsurface Conditions of Memphis and Shelby County," by K.W. Ng, T-S. Chang and H-H.M. Hwang, 7/26/89, (PB90-120437, A03, MF-A01).

NCEER-89-0022 "Seismic Wave Propagation Effects on Straight Jointed Buried Pipelines," by K. Elhmadi and M.J. O'Rourke, 8/24/89, (PB90-162322, A10, MF-A02).

NCEER-89-0023 "Workshop on Serviceability Analysis of Water Delivery Systems," edited by M. Grigoriu, 3/6/89, (PB90-127424, A03, MF-A01).

NCEER-89-0024 "Shaking Table Study of a 1/5 Scale Steel Frame Composed of Tapered Members," by K.C. Chang, J.S. Hwang and G.C. Lee, 9/18/89, (PB90-160169, A04, MF-A01).

NCEER-89-0025 "DYNA1D: A Computer Program for Nonlinear Seismic Site Response Analysis - Technical Documentation," by Jean H. Prevost, 9/14/89, (PB90-161944, A07, MF-A01). This report is available only through NTIS (see address given above).

NCEER-89-0026 "1:4 Scale Model Studies of Active Tendon Systems and Active Mass Dampers for Aseismic Protection," by A.M. Reinhorn, T.T. Soong, R.C. Lin, Y.P. Yang, Y. Fukao, H. Abe and M. Nakai, 9/15/89, (PB90-173246, A10, MF-A02). This report is available only through NTIS (see address given above).

NCEER-89-0027 "Scattering of Waves by Inclusions in a Nonhomogeneous Elastic Half Space Solved by Boundary Element Methods," by P.K. Hadley, A. Askar and A.S. Cakmak, 6/15/89, (PB90-145699, A07, MF-A01).

NCEER-89-0028 "Statistical Evaluation of Deflection Amplification Factors for Reinforced Concrete Structures," by H.H.M. Hwang, J-W. Jaw and A.L. Ch'ng, 8/31/89, (PB90-164633, A05, MF-A01).

NCEER-89-0029 "Bedrock Accelerations in Memphis Area Due to Large New Madrid Earthquakes," by H.H.M. Hwang, C.H.S. Chen and G. Yu, 11/7/89, (PB90-162330, A04, MF-A01).

NCEER-89-0030 "Seismic Behavior and Response Sensitivity of Secondary Structural Systems," by Y.Q. Chen and T.T. Soong, 10/23/89, (PB90-164658, A08, MF-A01).

NCEER-89-0031 "Random Vibration and Reliability Analysis of Primary-Secondary Structural Systems," by Y. Ibrahim, M. Grigoriu and T.T. Soong, 11/10/89, (PB90-161951, A04, MF-A01).

NCEER-89-0032 "Proceedings from the Second U.S. - Japan Workshop on Liquefaction, Large Ground Deformation and Their Effects on Lifelines, September 26-29, 1989," Edited by T.D. O'Rourke and M. Hamada, 12/1/89, (PB90-209388, A22, MF-A03).

NCEER-89-0033 "Deterministic Model for Seismic Damage Evaluation of Reinforced Concrete Structures," by J.M. Bracci, A.M. Reinhorn, J.B. Mander and S.K. Kunnath, 9/27/89, (PB91-108803, A06, MF-A01).

NCEER-89-0034 "On the Relation Between Local and Global Damage Indices," by E. DiPasquale and A.S. Cakmak, 8/15/89, (PB90-173865, A05, MF-A01).

NCEER-89-0035 "Cyclic Undrained Behavior of Nonplastic and Low Plasticity Silts," by A.J. Walker and H.E. Stewart, 7/26/89, (PB90-183518, A10, MF-A01).

NCEER-89-0036 "Liquefaction Potential of Surficial Deposits in the City of Buffalo, New York," by M. Budhu, R. Giese and L. Baumgrass, 1/17/89, (PB90-208455, A04, MF-A01).

NCEER-89-0037 "A Deterministic Assessment of Effects of Ground Motion Incoherence," by A.S. Veletsos and Y. Tang, 7/15/89, (PB90-164294, A03, MF-A01).

NCEER-89-0038 "Workshop on Ground Motion Parameters for Seismic Hazard Mapping," July 17-18, 1989, edited by R.V. Whitman, 12/1/89, (PB90-173923, A04, MF-A01).

NCEER-89-0039 "Seismic Effects on Elevated Transit Lines of the New York City Transit Authority," by C.J. Costantino, C.A. Miller and E. Heymsfield, 12/26/89, (PB90-207887, A06, MF-A01).

NCEER-89-0040 "Centrifugal Modeling of Dynamic Soil-Structure Interaction," by K. Weissman, Supervised by J.H. Prevost, 5/10/89, (PB90-207879, A07, MF-A01).

NCEER-89-0041 "Linearized Identification of Buildings With Cores for Seismic Vulnerability Assessment," by I-K. Ho and A.E. Aktan, 11/1/89, (PB90-251943, A07, MF-A01).

NCEER-90-0001 "Geotechnical and Lifeline Aspects of the October 17, 1989 Loma Prieta Earthquake in San Francisco," by T.D. O'Rourke, H.E. Stewart, F.T. Blackburn and T.S. Dickerman, 1/90, (PB90-208596, A05, MF-A01).

NCEER-90-0002 "Nonnormal Secondary Response Due to Yielding in a Primary Structure," by D.C.K. Chen and L.D. Lutes, 2/28/90, (PB90-251976, A07, MF-A01).

NCEER-90-0003 "Earthquake Education Materials for Grades K-12," by K.E.K. Ross, 4/16/90, (PB91-251984, A05, MF-A05). This report has been replaced by NCEER-92-0018.

NCEER-90-0004 "Catalog of Strong Motion Stations in Eastern North America," by R.W. Busby, 4/3/90, (PB90-251984, A05, MF-A01).

NCEER-90-0005 "NCEER Strong-Motion Data Base: A User Manual for the GeoBase Release (Version 1.0 for the Sun3)," by P. Friberg and K. Jacob, 3/31/90 (PB90-258062, A04, MF-A01).

NCEER-90-0006 "Seismic Hazard Along a Crude Oil Pipeline in the Event of an 1811-1812 Type New Madrid Earthquake," by H.H.M. Hwang and C-H.S. Chen, 4/16/90, (PB90-258054, A04, MF-A01).

NCEER-90-0007 "Site-Specific Response Spectra for Memphis Sheahan Pumping Station," by H.H.M. Hwang and C.S. Lee, 5/15/90, (PB91-108811, A05, MF-A01).

NCEER-90-0008 "Pilot Study on Seismic Vulnerability of Crude Oil Transmission Systems," by T. Ariman, R. Dobry, M. Grigoriu, F. Kozin, M. O'Rourke, T. O'Rourke and M. Shinozuka, 5/25/90, (PB91-108837, A06, MF-A01).

NCEER-90-0009 "A Program to Generate Site Dependent Time Histories: EQGEN," by G.W. Ellis, M. Srinivasan and A.S. Cakmak, 1/30/90, (PB91-108829, A04, MF-A01).

NCEER-90-0010 "Active Isolation for Seismic Protection of Operating Rooms," by M.E. Talbott, Supervised by M. Shinozuka, 6/8/9, (PB91-110205, A05, MF-A01).

NCEER-90-0011 "Program LINEARID for Identification of Linear Structural Dynamic Systems," by C-B. Yun and M. Shinozuka, 6/25/90, (PB91-110312, A08, MF-A01).

NCEER-90-0012 "Two-Dimensional Two-Phase Elasto-Plastic Seismic Response of Earth Dams," by A.N. Yiagos, Supervised by J.H. Prevost, 6/20/90, (PB91-110197, A13, MF-A02).

NCEER-90-0013 "Secondary Systems in Base-Isolated Structures: Experimental Investigation, Stochastic Response and Stochastic Sensitivity," by G.D. Manolis, G. Juhn, M.C. Constantinou and A.M. Reinhorn, 7/1/90, (PB91-110320, A08, MF-A01).

NCEER-90-0014 "Seismic Behavior of Lightly-Reinforced Concrete Column and Beam-Column Joint Details," by S.P. Pessiki, C.H. Conley, P. Gergely and R.N. White, 8/22/90, (PB91-108795, A11, MF-A02).

NCEER-90-0015 "Two Hybrid Control Systems for Building Structures Under Strong Earthquakes," by J.N. Yang and A. Danielians, 6/29/90, (PB91-125393, A04, MF-A01).

NCEER-90-0016 "Instantaneous Optimal Control with Acceleration and Velocity Feedback," by J.N. Yang and Z. Li, 6/29/90, (PB91-125401, A03, MF-A01).

NCEER-90-0017 "Reconnaissance Report on the Northern Iran Earthquake of June 21, 1990," by M. Mehrain, 10/4/90, (PB91-125377, A03, MF-A01).

NCEER-90-0018 "Evaluation of Liquefaction Potential in Memphis and Shelby County," by T.S. Chang, P.S. Tang, C.S. Lee and H. Hwang, 8/10/90, (PB91-125427, A09, MF-A01).

NCEER-90-0019 "Experimental and Analytical Study of a Combined Sliding Disc Bearing and Helical Steel Spring Isolation System," by M.C. Constantinou, A.S. Mokha and A.M. Reinhorn, 10/4/90, (PB91-125385, A06, MF-A01). This report is available only through NTIS (see address given above).

NCEER-90-0020 "Experimental Study and Analytical Prediction of Earthquake Response of a Sliding Isolation System with a Spherical Surface," by A.S. Mokha, M.C. Constantinou and A.M. Reinhorn, 10/11/90, (PB91-125419, A05, MF-A01).

NCEER-90-0021 "Dynamic Interaction Factors for Floating Pile Groups," by G. Gazetas, K. Fan, A. Kaynia and E. Kausel, 9/10/90, (PB91-170381, A05, MF-A01).

NCEER-90-0022 "Evaluation of Seismic Damage Indices for Reinforced Concrete Structures," by S. Rodriguez-Gomez and A.S. Cakmak, 9/30/90, PB91-171322, A06, MF-A01).

NCEER-90-0023 "Study of Site Response at a Selected Memphis Site," by H. Desai, S. Ahmad, E.S. Gazetas and M.R. Oh, 10/11/90, (PB91-196857, A03, MF-A01).

NCEER-90-0024 "A User's Guide to Strongmo: Version 1.0 of NCEER's Strong-Motion Data Access Tool for PCs and Terminals," by P.A. Friberg and C.A.T. Susch, 11/15/90, (PB91-171272, A03, MF-A01).

NCEER-90-0025 "A Three-Dimensional Analytical Study of Spatial Variability of Seismic Ground Motions," by L-L. Hong and A.H.-S. Ang, 10/30/90, (PB91-170399, A09, MF-A01).

NCEER-90-0026 "MUMOID User's Guide - A Program for the Identification of Modal Parameters," by S. Rodriguez-Gomez and E. DiPasquale, 9/30/90, (PB91-171298, A04, MF-A01).

NCEER-90-0027 "SARCF-II User's Guide - Seismic Analysis of Reinforced Concrete Frames," by S. Rodriguez-Gomez, Y.S. Chung and C. Meyer, 9/30/90, (PB91-171280, A05, MF-A01).

NCEER-90-0028 "Viscous Dampers: Testing, Modeling and Application in Vibration and Seismic Isolation," by N. Makris and M.C. Constantinou, 12/20/90 (PB91-190561, A06, MF-A01).

NCEER-90-0029 "Soil Effects on Earthquake Ground Motions in the Memphis Area," by H. Hwang, C.S. Lee, K.W. Ng and T.S. Chang, 8/2/90, (PB91-190751, A05, MF-A01).

NCEER-91-0001 "Proceedings from the Third Japan-U.S. Workshop on Earthquake Resistant Design of Lifeline Facilities and Countermeasures for Soil Liquefaction, December 17-19, 1990," edited by T.D. O'Rourke and M. Hamada, 2/1/91, (PB91-179259, A99, MF-A04).

NCEER-91-0002 "Physical Space Solutions of Non-Proportionally Damped Systems," by M. Tong, Z. Liang and G.C. Lee, 1/15/91, (PB91-179242, A04, MF-A01).

NCEER-91-0003 "Seismic Response of Single Piles and Pile Groups," by K. Fan and G. Gazetas, 1/10/91, (PB92-174994, A04, MF-A01).

NCEER-91-0004 "Damping of Structures: Part 1 - Theory of Complex Damping," by Z. Liang and G. Lee, 10/10/91, (PB92-197235, A12, MF-A03).

NCEER-91-0005 "3D-BASIS - Nonlinear Dynamic Analysis of Three Dimensional Base Isolated Structures: Part II," by S. Nagarajaiah, A.M. Reinhorn and M.C. Constantinou, 2/28/91, (PB91-190553, A07, MF-A01). This report has been replaced by NCEER-93-0011.

NCEER-91-0006 "A Multidimensional Hysteretic Model for Plasticity Deforming Metals in Energy Absorbing Devices," by E.J. Graesser and F.A. Cozzarelli, 4/9/91, (PB92-108364, A04, MF-A01).

NCEER-91-0007 "A Framework for Customizable Knowledge-Based Expert Systems with an Application to a KBES for Evaluating the Seismic Resistance of Existing Buildings," by E.G. Ibarra-Anaya and S.J. Fenves, 4/9/91, (PB91-210930, A08, MF-A01).

NCEER-91-0008 "Nonlinear Analysis of Steel Frames with Semi-Rigid Connections Using the Capacity Spectrum Method," by G.G. Deierlein, S-H. Hsieh, Y-J. Shen and J.F. Abel, 7/2/91, (PB92-113828, A05, MF-A01).

NCEER-91-0009 "Earthquake Education Materials for Grades K-12," by K.E.K. Ross, 4/30/91, (PB91-212142, A06, MF-A01). This report has been replaced by NCEER-92-0018.

NCEER-91-0010 "Phase Wave Velocities and Displacement Phase Differences in a Harmonically Oscillating Pile," by N. Makris and G. Gazetas, 7/8/91, (PB92-108356, A04, MF-A01).

NCEER-91-0011 "Dynamic Characteristics of a Full-Size Five-Story Steel Structure and a 2/5 Scale Model," by K.C. Chang, G.C. Yao, G.C. Lee, D.S. Hao and Y.C. Yeh," 7/2/91, (PB93-116648, A06, MF-A02).

NCEER-91-0012 "Seismic Response of a 2/5 Scale Steel Structure with Added Viscoelastic Dampers," by K.C. Chang, T.T. Soong, S-T. Oh and M.L. Lai, 5/17/91, (PB92-110816, A05, MF-A01).

NCEER-91-0013 "Earthquake Response of Retaining Walls; Full-Scale Testing and Computational Modeling," by S. Alampalli and A-W.M. Elgamal, 6/20/91, not available.

NCEER-91-0014 "3D-BASIS-M: Nonlinear Dynamic Analysis of Multiple Building Base Isolated Structures," by P.C. Tsopelas, S. Nagarajaiah, M.C. Constantinou and A.M. Reinhorn, 5/28/91, (PB92-113885, A09, MF-A02).

NCEER-91-0015 "Evaluation of SEAOC Design Requirements for Sliding Isolated Structures," by D. Theodossiou and M.C. Constantinou, 6/10/91, (PB92-114602, A11, MF-A03).

NCEER-91-0016 "Closed-Loop Modal Testing of a 27-Story Reinforced Concrete Flat Plate-Core Building," by H.R. Somaprasad, T. Toksoy, H. Yoshiyuki and A.E. Aktan, 7/15/91, (PB92-129980, A07, MF-A02).

NCEER-91-0017 "Shake Table Test of a 1/6 Scale Two-Story Lightly Reinforced Concrete Building," by A.G. El-Attar, R.N. White and P. Gergely, 2/28/91, (PB92-222447, A06, MF-A02).

NCEER-91-0018 "Shake Table Test of a 1/8 Scale Three-Story Lightly Reinforced Concrete Building," by A.G. El-Attar, R.N. White and P. Gergely, 2/28/91, (PB93-116630, A08, MF-A02).

NCEER-91-0019 "Transfer Functions for Rigid Rectangular Foundations," by A.S. Veletsos, A.M. Prasad and W.H. Wu, 7/31/91, not available.

NCEER-91-0020 "Hybrid Control of Seismic-Excited Nonlinear and Inelastic Structural Systems," by J.N. Yang, Z. Li and A. Danielians, 8/1/91, (PB92-143171, A06, MF-A02).

NCEER-91-0021 "The NCEER-91 Earthquake Catalog: Improved Intensity-Based Magnitudes and Recurrence Relations for U.S. Earthquakes East of New Madrid," by L. Seeber and J.G. Armbruster, 8/28/91, (PB92-176742, A06, MF-A02).

NCEER-91-0022 "Proceedings from the Implementation of Earthquake Planning and Education in Schools: The Need for Change - The Roles of the Changemakers," by K.E.K. Ross and F. Winslow, 7/23/91, (PB92-129998, A12, MF-A03).

NCEER-91-0023 "A Study of Reliability-Based Criteria for Seismic Design of Reinforced Concrete Frame Buildings," by H.H.M. Hwang and H-M. Hsu, 8/10/91, (PB92-140235, A09, MF-A02).

NCEER-91-0024 "Experimental Verification of a Number of Structural System Identification Algorithms," by R.G. Ghanem, H. Gavin and M. Shinozuka, 9/18/91, (PB92-176577, A18, MF-A04).

NCEER-91-0025 "Probabilistic Evaluation of Liquefaction Potential," by H.H.M. Hwang and C.S. Lee," 11/25/91, (PB92-143429, A05, MF-A01).

NCEER-91-0026 "Instantaneous Optimal Control for Linear, Nonlinear and Hysteretic Structures - Stable Controllers," by J.N. Yang and Z. Li, 11/15/91, (PB92-163807, A04, MF-A01).

NCEER-91-0027 "Experimental and Theoretical Study of a Sliding Isolation System for Bridges," by M.C. Constantinou, A. Kartoum, A.M. Reinhorn and P. Bradford, 11/15/91, (PB92-176973, A10, MF-A03).

NCEER-92-0001 "Case Studies of Liquefaction and Lifeline Performance During Past Earthquakes, Volume 1: Japanese Case Studies," Edited by M. Hamada and T. O'Rourke, 2/17/92, (PB92-197243, A18, MF-A04).

NCEER-92-0002 "Case Studies of Liquefaction and Lifeline Performance During Past Earthquakes, Volume 2: United States Case Studies," Edited by T. O'Rourke and M. Hamada, 2/17/92, (PB92-197250, A20, MF-A04).

NCEER-92-0003 "Issues in Earthquake Education," Edited by K. Ross, 2/3/92, (PB92-222389, A07, MF-A02).

NCEER-92-0004 "Proceedings from the First U.S. - Japan Workshop on Earthquake Protective Systems for Bridges," Edited by I.G. Buckle, 2/4/92, (PB94-142239, A99, MF-A06).

NCEER-92-0005 "Seismic Ground Motion from a Haskell-Type Source in a Multiple-Layered Half-Space," A.P. Theoharis, G. Deodatis and M. Shinozuka, 1/2/92, not available.

NCEER-92-0006 "Proceedings from the Site Effects Workshop," Edited by R. Whitman, 2/29/92, (PB92-197201, A04, MF-A01).

NCEER-92-0007 "Engineering Evaluation of Permanent Ground Deformations Due to Seismically-Induced Liquefaction," by M.H. Baziar, R. Dobry and A-W.M. Elgamal, 3/24/92, (PB92-222421, A13, MF-A03).

NCEER-92-0008 "A Procedure for the Seismic Evaluation of Buildings in the Central and Eastern United States," by C.D. Poland and J.O. Malley, 4/2/92, (PB92-222439, A20, MF-A04).

NCEER-92-0009 "Experimental and Analytical Study of a Hybrid Isolation System Using Friction Controllable Sliding Bearings," by M.Q. Feng, S. Fujii and M. Shinozuka, 5/15/92, (PB93-150282, A06, MF-A02).

NCEER-92-0010 "Seismic Resistance of Slab-Column Connections in Existing Non-Ductile Flat-Plate Buildings," by A.J. Durrani and Y. Du, 5/18/92, (PB93-116812, A06, MF-A02).

NCEER-92-0011 "The Hysteretic and Dynamic Behavior of Brick Masonry Walls Upgraded by Ferrocement Coatings Under Cyclic Loading and Strong Simulated Ground Motion," by H. Lee and S.P. Prawel, 5/11/92, not available.

NCEER-92-0012 "Study of Wire Rope Systems for Seismic Protection of Equipment in Buildings," by G.F. Demetriades, M.C. Constantinou and A.M. Reinhorn, 5/20/92, (PB93-116655, A08, MF-A02).

NCEER-92-0013 "Shape Memory Structural Dampers: Material Properties, Design and Seismic Testing," by P.R. Witting and F.A. Cozzarelli, 5/26/92, (PB93-116663, A05, MF-A01).

NCEER-92-0014 "Longitudinal Permanent Ground Deformation Effects on Buried Continuous Pipelines," by M.J. O'Rourke, and C. Nordberg, 6/15/92, (PB93-116671, A08, MF-A02).

NCEER-92-0015 "A Simulation Method for Stationary Gaussian Random Functions Based on the Sampling Theorem," by M. Grigoriu and S. Balopoulou, 6/11/92, (PB93-127496, A05, MF-A01).

NCEER-92-0016 "Gravity-Load-Designed Reinforced Concrete Buildings: Seismic Evaluation of Existing Construction and Detailing Strategies for Improved Seismic Resistance," by G.W. Hoffmann, S.K. Kunnath, A.M. Reinhorn and J.B. Mander, 7/15/92, (PB94-142007, A08, MF-A02).

NCEER-92-0017 "Observations on Water System and Pipeline Performance in the Limón Area of Costa Rica Due to the April 22, 1991 Earthquake," by M. O'Rourke and D. Ballantyne, 6/30/92, (PB93-126811, A06, MF-A02).

NCEER-92-0018 "Fourth Edition of Earthquake Education Materials for Grades K-12," Edited by K.E.K. Ross, 8/10/92, (PB93-114023, A07, MF-A02).

NCEER-92-0019 "Proceedings from the Fourth Japan-U.S. Workshop on Earthquake Resistant Design of Lifeline Facilities and Countermeasures for Soil Liquefaction," Edited by M. Hamada and T.D. O'Rourke, 8/12/92, (PB93-163939, A99, MF-E11).

NCEER-92-0020 "Active Bracing System: A Full Scale Implementation of Active Control," by A.M. Reinhorn, T.T. Soong, R.C. Lin, M.A. Riley, Y.P. Wang, S. Aizawa and M. Higashino, 8/14/92, (PB93-127512, A06, MF-A02).

NCEER-92-0021 "Empirical Analysis of Horizontal Ground Displacement Generated by Liquefaction-Induced Lateral Spreads," by S.F. Bartlett and T.L. Youd, 8/17/92, (PB93-188241, A06, MF-A02).

NCEER-92-0022 "IDARC Version 3.0: Inelastic Damage Analysis of Reinforced Concrete Structures," by S.K. Kunnath, A.M. Reinhorn and R.F. Lobo, 8/31/92, (PB93-227502, A07, MF-A02).

NCEER-92-0023 "A Semi-Empirical Analysis of Strong-Motion Peaks in Terms of Seismic Source, Propagation Path and Local Site Conditions, by M. Kamiyama, M.J. O'Rourke and R. Flores-Berrones, 9/9/92, (PB93-150266, A08, MF-A02).

NCEER-92-0024 "Seismic Behavior of Reinforced Concrete Frame Structures with Nonductile Details, Part I: Summary of Experimental Findings of Full Scale Beam-Column Joint Tests," by A. Beres, R.N. White and P. Gergely, 9/30/92, (PB93-227783, A05, MF-A01).

NCEER-92-0025 "Experimental Results of Repaired and Retrofitted Beam-Column Joint Tests in Lightly Reinforced Concrete Frame Buildings," by A. Beres, S. El-Borgi, R.N. White and P. Gergely, 10/29/92, (PB93-227791, A05, MF-A01).

NCEER-92-0026 "A Generalization of Optimal Control Theory: Linear and Nonlinear Structures," by J.N. Yang, Z. Li and S. Vongchavalitkul, 11/2/92, (PB93-188621, A05, MF-A01).

NCEER-92-0027 "Seismic Resistance of Reinforced Concrete Frame Structures Designed Only for Gravity Loads: Part I - Design and Properties of a One-Third Scale Model Structure," by J.M. Bracci, A.M. Reinhorn and J.B. Mander, 12/1/92, (PB94-104502, A08, MF-A02).

NCEER-92-0028 "Seismic Resistance of Reinforced Concrete Frame Structures Designed Only for Gravity Loads: Part II - Experimental Performance of Subassemblages," by L.E. Aycardi, J.B. Mander and A.M. Reinhorn, 12/1/92, (PB94-104510, A08, MF-A02).

NCEER-92-0029 "Seismic Resistance of Reinforced Concrete Frame Structures Designed Only for Gravity Loads: Part III - Experimental Performance and Analytical Study of a Structural Model," by J.M. Bracci, A.M. Reinhorn and J.B. Mander, 12/1/92, (PB93-227528, A09, MF-A01).

NCEER-92-0030 "Evaluation of Seismic Retrofit of Reinforced Concrete Frame Structures: Part I - Experimental Performance of Retrofitted Subassemblages," by D. Choudhuri, J.B. Mander and A.M. Reinhorn, 12/8/92, (PB93-198307, A07, MF-A02).

NCEER-92-0031 "Evaluation of Seismic Retrofit of Reinforced Concrete Frame Structures: Part II - Experimental Performance and Analytical Study of a Retrofitted Structural Model," by J.M. Bracci, A.M. Reinhorn and J.B. Mander, 12/8/92, (PB93-198315, A09, MF-A03).

NCEER-92-0032 "Experimental and Analytical Investigation of Seismic Response of Structures with Supplemental Fluid Viscous Dampers," by M.C. Constantinou and M.D. Symans, 12/21/92, (PB93-191435, A10, MF-A03). This report is available only through NTIS (see address given above).

NCEER-92-0033 "Reconnaissance Report on the Cairo, Egypt Earthquake of October 12, 1992," by M. Khater, 12/23/92, (PB93-188621, A03, MF-A01).

NCEER-92-0034 "Low-Level Dynamic Characteristics of Four Tall Flat-Plate Buildings in New York City," by H. Gavin, S. Yuan, J. Grossman, E. Pekelis and K. Jacob, 12/28/92, (PB93-188217, A07, MF-A02).

NCEER-93-0001 "An Experimental Study on the Seismic Performance of Brick-Infilled Steel Frames With and Without Retrofit," by J.B. Mander, B. Nair, K. Wojtkowski and J. Ma, 1/29/93, (PB93-227510, A07, MF-A02).

NCEER-93-0002 "Social Accounting for Disaster Preparedness and Recovery Planning," by S. Cole, E. Pantoja and V. Razak, 2/22/93, (PB94-142114, A12, MF-A03).

NCEER-93-0003 "Assessment of 1991 NEHRP Provisions for Nonstructural Components and Recommended Revisions," by T.T. Soong, G. Chen, Z. Wu, R-H. Zhang and M. Grigoriu, 3/1/93, (PB93-188639, A06, MF-A02).

NCEER-93-0004 "Evaluation of Static and Response Spectrum Analysis Procedures of SEAOC/UBC for Seismic Isolated Structures," by C.W. Winters and M.C. Constantinou, 3/23/93, (PB93-198299, A10, MF-A03).

NCEER-93-0005 "Earthquakes in the Northeast - Are We Ignoring the Hazard? A Workshop on Earthquake Science and Safety for Educators," edited by K.E.K. Ross, 4/2/93, (PB94-103066, A09, MF-A02).

NCEER-93-0006 "Inelastic Response of Reinforced Concrete Structures with Viscoelastic Braces," by R.F. Lobo, J.M. Bracci, K.L. Shen, A.M. Reinhorn and T.T. Soong, 4/5/93, (PB93-227486, A05, MF-A02).

NCEER-93-0007 "Seismic Testing of Installation Methods for Computers and Data Processing Equipment," by K. Kosar, T.T. Soong, K.L. Shen, J.A. HoLung and Y.K. Lin, 4/12/93, (PB93-198299, A07, MF-A02).

NCEER-93-0008 "Retrofit of Reinforced Concrete Frames Using Added Dampers," by A. Reinhorn, M. Constantinou and C. Li, not available.

NCEER-93-0009 "Seismic Behavior and Design Guidelines for Steel Frame Structures with Added Viscoelastic Dampers," by K.C. Chang, M.L. Lai, T.T. Soong, D.S. Hao and Y.C. Yeh, 5/1/93, (PB94-141959, A07, MF-A02).

NCEER-93-0010 "Seismic Performance of Shear-Critical Reinforced Concrete Bridge Piers," by J.B. Mander, S.M. Waheed, M.T.A. Chaudhary and S.S. Chen, 5/12/93, (PB93-227494, A08, MF-A02).

NCEER-93-0011 "3D-BASIS-TABS: Computer Program for Nonlinear Dynamic Analysis of Three Dimensional Base Isolated Structures," by S. Nagarajaiah, C. Li, A.M. Reinhorn and M.C. Constantinou, 8/2/93, (PB94-141819, A09, MF-A02).

NCEER-93-0012 "Effects of Hydrocarbon Spills from an Oil Pipeline Break on Ground Water," by O.J. Helweg and H.H.M. Hwang, 8/3/93, (PB94-141942, A06, MF-A02).

NCEER-93-0013 "Simplified Procedures for Seismic Design of Nonstructural Components and Assessment of Current Code Provisions," by M.P. Singh, L.E. Suarez, E.E. Matheu and G.O. Maldonado, 8/4/93, (PB94-141827, A09, MF-A02).

NCEER-93-0014 "An Energy Approach to Seismic Analysis and Design of Secondary Systems," by G. Chen and T.T. Soong, 8/6/93, (PB94-142767, A11, MF-A03).

NCEER-93-0015 "Proceedings from School Sites: Becoming Prepared for Earthquakes - Commemorating the Third Anniversary of the Loma Prieta Earthquake," Edited by F.E. Winslow and K.E.K. Ross, 8/16/93, (PB94-154275, A16, MF-A02).

NCEER-93-0016 "Reconnaissance Report of Damage to Historic Monuments in Cairo, Egypt Following the October 12, 1992 Dahshur Earthquake," by D. Sykora, D. Look, G. Croci, E. Karaesmen and E. Karaesmen, 8/19/93, (PB94-142221, A08, MF-A02).

NCEER-93-0017 "The Island of Guam Earthquake of August 8, 1993," by S.W. Swan and S.K. Harris, 9/30/93, (PB94-141843, A04, MF-A01).

NCEER-93-0018 "Engineering Aspects of the October 12, 1992 Egyptian Earthquake," by A.W. Elgamal, M. Amer, K. Adalier and A. Abul-Fadl, 10/7/93, (PB94-141983, A05, MF-A01).

NCEER-93-0019 "Development of an Earthquake Motion Simulator and its Application in Dynamic Centrifuge Testing," by I. Krstelj, Supervised by J.H. Prevost, 10/23/93, (PB94-181773, A-10, MF-A03).

NCEER-93-0020 "NCEER-Taisei Corporation Research Program on Sliding Seismic Isolation Systems for Bridges: Experimental and Analytical Study of a Friction Pendulum System (FPS)," by M.C. Constantinou, P. Tsopelas, Y-S. Kim and S. Okamoto, 11/1/93, (PB94-142775, A08, MF-A02).

NCEER-93-0021 "Finite Element Modeling of Elastomeric Seismic Isolation Bearings," by L.J. Billings, Supervised by R. Shepherd, 11/8/93, not available.

NCEER-93-0022 "Seismic Vulnerability of Equipment in Critical Facilities: Life-Safety and Operational Consequences," by K. Porter, G.S. Johnson, M.M. Zadeh, C. Scawthorn and S. Eder, 11/24/93, (PB94-181765, A16, MF-A03).

NCEER-93-0023 "Hokkaido Nansei-oki, Japan Earthquake of July 12, 1993, by P.I. Yanev and C.R. Scawthorn, 12/23/93, (PB94-181500, A07, MF-A01).

NCEER-94-0001 "An Evaluation of Seismic Serviceability of Water Supply Networks with Application to the San Francisco Auxiliary Water Supply System," by I. Markov, Supervised by M. Grigoriu and T. O'Rourke, 1/21/94, (PB94-204013, A07, MF-A02).

NCEER-94-0002 "NCEER-Taisei Corporation Research Program on Sliding Seismic Isolation Systems for Bridges: Experimental and Analytical Study of Systems Consisting of Sliding Bearings, Rubber Restoring Force Devices and Fluid Dampers," Volumes I and II, by P. Tsopelas, S. Okamoto, M.C. Constantinou, D. Ozaki and S. Fujii, 2/4/94, (PB94-181740, A09, MF-A02 and PB94-181757, A12, MF-A03).

NCEER-94-0003 "A Markov Model for Local and Global Damage Indices in Seismic Analysis," by S. Rahman and M. Grigoriu, 2/18/94, (PB94-206000, A12, MF-A03).

NCEER-94-0004 "Proceedings from the NCEER Workshop on Seismic Response of Masonry Infills," edited by D.P. Abrams, 3/1/94, (PB94-180783, A07, MF-A02).

NCEER-94-0005 "The Northridge, California Earthquake of January 17, 1994: General Reconnaissance Report," edited by J.D. Goltz, 3/11/94, (PB94-193943, A10, MF-A03).

NCEER-94-0006 "Seismic Energy Based Fatigue Damage Analysis of Bridge Columns: Part I - Evaluation of Seismic Capacity," by G.A. Chang and J.B. Mander, 3/14/94, (PB94-219185, A11, MF-A03).

NCEER-94-0007 "Seismic Isolation of Multi-Story Frame Structures Using Spherical Sliding Isolation Systems," by T.M. Al-Hussaini, V.A. Zayas and M.C. Constantinou, 3/17/94, (PB94-193745, A09, MF-A02).

NCEER-94-0008 "The Northridge, California Earthquake of January 17, 1994: Performance of Highway Bridges," edited by I.G. Buckle, 3/24/94, (PB94-193851, A06, MF-A02).

NCEER-94-0009 "Proceedings of the Third U.S.-Japan Workshop on Earthquake Protective Systems for Bridges," edited by I.G. Buckle and I. Friedland, 3/31/94, (PB94-195815, A99, MF-A06).

NCEER-94-0010 "3D-BASIS-ME: Computer Program for Nonlinear Dynamic Analysis of Seismically Isolated Single and Multiple Structures and Liquid Storage Tanks," by P.C. Tsopelas, M.C. Constantinou and A.M. Reinhorn, 4/12/94, (PB94-204922, A09, MF-A02).

NCEER-94-0011 "The Northridge, California Earthquake of January 17, 1994: Performance of Gas Transmission Pipelines," by T.D. O'Rourke and M.C. Palmer, 5/16/94, (PB94-204989, A05, MF-A01).

NCEER-94-0012 "Feasibility Study of Replacement Procedures and Earthquake Performance Related to Gas Transmission Pipelines," by T.D. O'Rourke and M.C. Palmer, 5/25/94, (PB94-206638, A09, MF-A02).

NCEER-94-0013 "Seismic Energy Based Fatigue Damage Analysis of Bridge Columns: Part II - Evaluation of Seismic Demand," by G.A. Chang and J.B. Mander, 6/1/94, (PB95-18106, A08, MF-A02).

NCEER-94-0014 "NCEER-Taisei Corporation Research Program on Sliding Seismic Isolation Systems for Bridges: Experimental and Analytical Study of a System Consisting of Sliding Bearings and Fluid Restoring Force/Damping Devices," by P. Tsopelas and M.C. Constantinou, 6/13/94, (PB94-219144, A10, MF-A03).

NCEER-94-0015 "Generation of Hazard-Consistent Fragility Curves for Seismic Loss Estimation Studies," by H. Hwang and J-R. Huo, 6/14/94, (PB95-181996, A09, MF-A02).

NCEER-94-0016 "Seismic Study of Building Frames with Added Energy-Absorbing Devices," by W.S. Pong, C.S. Tsai and G.C. Lee, 6/20/94, (PB94-219136, A10, A03).

NCEER-94-0017 "Sliding Mode Control for Seismic-Excited Linear and Nonlinear Civil Engineering Structures," by J. Yang, J. Wu, A. Agrawal and Z. Li, 6/21/94, (PB95-138483, A06, MF-A02).

NCEER-94-0018 "3D-BASIS-TABS Version 2.0: Computer Program for Nonlinear Dynamic Analysis of Three Dimensional Base Isolated Structures," by A.M. Reinhorn, S. Nagarajaiah, M.C. Constantinou, P. Tsopelas and R. Li, 6/22/94, (PB95-182176, A08, MF-A02).

NCEER-94-0019 "Proceedings of the International Workshop on Civil Infrastructure Systems: Application of Intelligent Systems and Advanced Materials on Bridge Systems," Edited by G.C. Lee and K.C. Chang, 7/18/94, (PB95-252474, A20, MF-A04).

NCEER-94-0020 "Study of Seismic Isolation Systems for Computer Floors," by V. Lambrou and M.C. Constantinou, 7/19/94, (PB95-138533, A10, MF-A03).

NCEER-94-0021 "Proceedings of the U.S.-Italian Workshop on Guidelines for Seismic Evaluation and Rehabilitation of Unreinforced Masonry Buildings," Edited by D.P. Abrams and G.M. Calvi, 7/20/94, (PB95-138749, A13, MF-A03).

NCEER-94-0022 "NCEER-Taisei Corporation Research Program on Sliding Seismic Isolation Systems for Bridges: Experimental and Analytical Study of a System Consisting of Lubricated PTFE Sliding Bearings and Mild Steel Dampers," by P. Tsopelas and M.C. Constantinou, 7/22/94, (PB95-182184, A08, MF-A02).

NCEER-94-0023 “Development of Reliability-Based Design Criteria for Buildings Under Seismic Load,” by Y.K. Wen, H. Hwang and M. Shinozuka, 8/1/94, (PB95-211934, A08, MF-A02).

NCEER-94-0024 “Experimental Verification of Acceleration Feedback Control Strategies for an Active Tendon System,” by S.J. Dyke, B.F. Spencer, Jr., P. Quast, M.K. Sain, D.C. Kaspari, Jr. and T.T. Soong, 8/29/94, (PB95-212320, A05, MF-A01).

NCEER-94-0025 “Seismic Retrofitting Manual for Highway Bridges,” Edited by I.G. Buckle and I.F. Friedland, published by the Federal Highway Administration (PB95-212676, A15, MF-A03).

NCEER-94-0026 “Proceedings from the Fifth U.S.-Japan Workshop on Earthquake Resistant Design of Lifeline Facilities and Countermeasures Against Soil Liquefaction,” Edited by T.D. O’Rourke and M. Hamada, 11/7/94, (PB95-220802, A99, MF-E08).

NCEER-95-0001 "Experimental and Analytical Investigation of Seismic Retrofit of Structures with Supplemental Damping: Part 1 - Fluid Viscous Damping Devices," by A.M. Reinhorn, C. Li and M.C. Constantinou, 1/3/95, (PB95-266599, A09, MF-A02).

NCEER-95-0002 "Experimental and Analytical Study of Low-Cycle Fatigue Behavior of Semi-Rigid Top-And-Seat Angle Connections," by G. Pekcan, J.B. Mander and S.S. Chen, 1/5/95, (PB95-220042, A07, MF-A02).

NCEER-95-0003 "NCEER-ATC Joint Study on Fragility of Buildings," by T. Anagnos, C. Rojahn and A.S. Kiremidjian, 1/20/95, (PB95-220026, A06, MF-A02).

NCEER-95-0004 "Nonlinear Control Algorithms for Peak Response Reduction," by Z. Wu, T.T. Soong, V. Gattulli and R.C. Lin, 2/16/95, (PB95-220349, A05, MF-A01).

NCEER-95-0005 "Pipeline Replacement Feasibility Study: A Methodology for Minimizing Seismic and Corrosion Risks to Underground Natural Gas Pipelines," by R.T. Eguchi, H.A. Seligson and D.G. Honegger, 3/2/95, (PB95-252326, A06, MF-A02).

NCEER-95-0006 "Evaluation of Seismic Performance of an 11-Story Frame Building During the 1994 Northridge Earthquake," by F. Naeim, R. DiSulio, K. Benuska, A. Reinhorn and C. Li, not available.

NCEER-95-0007 "Prioritization of Bridges for Seismic Retrofitting," by N. Basöz and A.S. Kiremidjian, 4/24/95, (PB95-252300, A08, MF-A02).

NCEER-95-0008 "Method for Developing Motion Damage Relationships for Reinforced Concrete Frames," by A. Singhal and A.S. Kiremidjian, 5/11/95, (PB95-266607, A06, MF-A02).

NCEER-95-0009 "Experimental and Analytical Investigation of Seismic Retrofit of Structures with Supplemental Damping: Part II - Friction Devices," by C. Li and A.M. Reinhorn, 7/6/95, (PB96-128087, A11, MF-A03).

NCEER-95-0010 "Experimental Performance and Analytical Study of a Non-Ductile Reinforced Concrete Frame Structure Retrofitted with Elastomeric Spring Dampers," by G. Pekcan, J.B. Mander and S.S. Chen, 7/14/95, (PB96-137161, A08, MF-A02).

NCEER-95-0011 "Development and Experimental Study of Semi-Active Fluid Damping Devices for Seismic Protection of Structures," by M.D. Symans and M.C. Constantinou, 8/3/95, (PB96-136940, A23, MF-A04).

NCEER-95-0012 "Real-Time Structural Parameter Modification (RSPM): Development of Innervated Structures," by Z. Liang, M. Tong and G.C. Lee, 4/11/95, (PB96-137153, A06, MF-A01).

NCEER-95-0013 "Experimental and Analytical Investigation of Seismic Retrofit of Structures with Supplemental Damping: Part III - Viscous Damping Walls," by A.M. Reinhorn and C. Li, 10/1/95, (PB96-176409, A11, MF-A03).

NCEER-95-0014 "Seismic Fragility Analysis of Equipment and Structures in a Memphis Electric Substation," by J-R. Huo and H.H.M. Hwang, 8/10/95, (PB96-128087, A09, MF-A02).

NCEER-95-0015 "The Hanshin-Awaji Earthquake of January 17, 1995: Performance of Lifelines," Edited by M. Shinozuka, 11/3/95, (PB96-176383, A15, MF-A03).

NCEER-95-0016 "Highway Culvert Performance During Earthquakes," by T.L. Youd and C.J. Beckman, available as NCEER-96-0015.

NCEER-95-0017 "The Hanshin-Awaji Earthquake of January 17, 1995: Performance of Highway Bridges," Edited by I.G. Buckle, 12/1/95, not available.

NCEER-95-0018 "Modeling of Masonry Infill Panels for Structural Analysis," by A.M. Reinhorn, A. Madan, R.E. Valles, Y. Reichmann and J.B. Mander, 12/8/95, (PB97-110886, MF-A01, A06).

NCEER-95-0019 "Optimal Polynomial Control for Linear and Nonlinear Structures," by A.K. Agrawal and J.N. Yang, 12/11/95, (PB96-168737, A07, MF-A02).

NCEER-95-0020 "Retrofit of Non-Ductile Reinforced Concrete Frames Using Friction Dampers," by R.S. Rao, P. Gergely and R.N. White, 12/22/95, (PB97-133508, A10, MF-A02).

NCEER-95-0021 "Parametric Results for Seismic Response of Pile-Supported Bridge Bents," by G. Mylonakis, A. Nikolaou and G. Gazetas, 12/22/95, (PB97-100242, A12, MF-A03).

NCEER-95-0022 "Kinematic Bending Moments in Seismically Stressed Piles," by A. Nikolaou, G. Mylonakis and G. Gazetas, 12/23/95, (PB97-113914, MF-A03, A13).

NCEER-96-0001 "Dynamic Response of Unreinforced Masonry Buildings with Flexible Diaphragms," by A.C. Costley and D.P. Abrams," 10/10/96, (PB97-133573, MF-A03, A15).

NCEER-96-0002 "State of the Art Review: Foundations and Retaining Structures," by I. Po Lam, not available.

NCEER-96-0003 "Ductility of Rectangular Reinforced Concrete Bridge Columns with Moderate Confinement," by N. Wehbe, M. Saiidi, D. Sanders and B. Douglas, 11/7/96, (PB97-133557, A06, MF-A02).

NCEER-96-0004 "Proceedings of the Long-Span Bridge Seismic Research Workshop," edited by I.G. Buckle and I.M. Friedland, not available.

NCEER-96-0005 "Establish Representative Pier Types for Comprehensive Study: Eastern United States," by J. Kulicki and Z. Prucz, 5/28/96, (PB98-119217, A07, MF-A02).

NCEER-96-0006 "Establish Representative Pier Types for Comprehensive Study: Western United States," by R. Imbsen, R.A. Schamber and T.A. Osterkamp, 5/28/96, (PB98-118607, A07, MF-A02).

NCEER-96-0007 "Nonlinear Control Techniques for Dynamical Systems with Uncertain Parameters," by R.G. Ghanem and M.I. Bujakov, 5/27/96, (PB97-100259, A17, MF-A03).

NCEER-96-0008 "Seismic Evaluation of a 30-Year Old Non-Ductile Highway Bridge Pier and Its Retrofit," by J.B. Mander, B. Mahmoodzadegan, S. Bhadra and S.S. Chen, 5/31/96, (PB97-110902, MF-A03, A10).

NCEER-96-0009 "Seismic Performance of a Model Reinforced Concrete Bridge Pier Before and After Retrofit," by J.B. Mander, J.H. Kim and C.A. Ligozio, 5/31/96, (PB97-110910, MF-A02, A10).

NCEER-96-0010 "IDARC2D Version 4.0: A Computer Program for the Inelastic Damage Analysis of Buildings," by R.E. Valles, A.M. Reinhorn, S.K. Kunnath, C. Li and A. Madan, 6/3/96, (PB97-100234, A17, MF-A03).

NCEER-96-0011 "Estimation of the Economic Impact of Multiple Lifeline Disruption: Memphis Light, Gas and Water Division Case Study," by S.E. Chang, H.A. Seligson and R.T. Eguchi, 8/16/96, (PB97-133490, A11, MF-A03).

NCEER-96-0012 "Proceedings from the Sixth Japan-U.S. Workshop on Earthquake Resistant Design of Lifeline Facilities and Countermeasures Against Soil Liquefaction, Edited by M. Hamada and T. O'Rourke, 9/11/96, (PB97-133581, A99, MF-A06).

NCEER-96-0013 "Chemical Hazards, Mitigation and Preparedness in Areas of High Seismic Risk: A Methodology for Estimating the Risk of Post-Earthquake Hazardous Materials Release," by H.A. Seligson, R.T. Eguchi, K.J. Tierney and K. Richmond, 11/7/96, (PB97-133565, MF-A02, A08).

NCEER-96-0014 "Response of Steel Bridge Bearings to Reversed Cyclic Loading," by J.B. Mander, D-K. Kim, S.S. Chen and G.J. Premus, 11/13/96, (PB97-140735, A12, MF-A03).

NCEER-96-0015 "Highway Culvert Performance During Past Earthquakes," by T.L. Youd and C.J. Beckman, 11/25/96, (PB97-133532, A06, MF-A01).

NCEER-97-0001 "Evaluation, Prevention and Mitigation of Pounding Effects in Building Structures," by R.E. Valles and A.M. Reinhorn, 2/20/97, (PB97-159552, A14, MF-A03).

NCEER-97-0002 "Seismic Design Criteria for Bridges and Other Highway Structures," by C. Rojahn, R. Mayes, D.G. Anderson, J. Clark, J.H. Hom, R.V. Nutt and M.J. O'Rourke, 4/30/97, (PB97-194658, A06, MF-A03).

NCEER-97-0003 “Proceedings of the U.S.-Italian Workshop on Seismic Evaluation and Retrofit,” Edited by D.P. Abrams and G.M. Calvi, 3/19/97, (PB97-194666, A13, MF-A03).

NCEER-97-0004 "Investigation of Seismic Response of Buildings with Linear and Nonlinear Fluid Viscous Dampers," by A.A. Seleemah and M.C. Constantinou, 5/21/97, (PB98-109002, A15, MF-A03).

NCEER-97-0005 "Proceedings of the Workshop on Earthquake Engineering Frontiers in Transportation Facilities," edited by G.C. Lee and I.M. Friedland, 8/29/97, (PB98-128911, A25, MR-A04).

NCEER-97-0006 "Cumulative Seismic Damage of Reinforced Concrete Bridge Piers," by S.K. Kunnath, A. El-Bahy, A. Taylor and W. Stone, 9/2/97, (PB98-108814, A11, MF-A03).

NCEER-97-0007 "Structural Details to Accommodate Seismic Movements of Highway Bridges and Retaining Walls," by R.A. Imbsen, R.A. Schamber, E. Thorkildsen, A. Kartoum, B.T. Martin, T.N. Rosser and J.M. Kulicki, 9/3/97, (PB98-108996, A09, MF-A02).

NCEER-97-0008 "A Method for Earthquake Motion-Damage Relationships with Application to Reinforced Concrete Frames," by A. Singhal and A.S. Kiremidjian, 9/10/97, (PB98-108988, A13, MF-A03).

NCEER-97-0009 "Seismic Analysis and Design of Bridge Abutments Considering Sliding and Rotation," by K. Fishman and R. Richards, Jr., 9/15/97, (PB98-108897, A06, MF-A02).

NCEER-97-0010 "Proceedings of the FHWA/NCEER Workshop on the National Representation of Seismic Ground Motion for New and Existing Highway Facilities," edited by I.M. Friedland, M.S. Power and R.L. Mayes, 9/22/97, (PB98-128903, A21, MF-A04).

NCEER-97-0011 "Seismic Analysis for Design or Retrofit of Gravity Bridge Abutments," by K.L. Fishman, R. Richards, Jr. and R.C. Divito, 10/2/97, (PB98-128937, A08, MF-A02).

NCEER-97-0012 "Evaluation of Simplified Methods of Analysis for Yielding Structures," by P. Tsopelas, M.C. Constantinou, C.A. Kircher and A.S. Whittaker, 10/31/97, (PB98-128929, A10, MF-A03).

NCEER-97-0013 "Seismic Design of Bridge Columns Based on Control and Repairability of Damage," by C-T. Cheng and J.B. Mander, 12/8/97, (PB98-144249, A11, MF-A03).

NCEER-97-0014 "Seismic Resistance of Bridge Piers Based on Damage Avoidance Design," by J.B. Mander and C-T. Cheng, 12/10/97, (PB98-144223, A09, MF-A02).

NCEER-97-0015 “Seismic Response of Nominally Symmetric Systems with Strength Uncertainty,” by S. Balopoulou and M. Grigoriu, 12/23/97, (PB98-153422, A11, MF-A03).

NCEER-97-0016 “Evaluation of Seismic Retrofit Methods for Reinforced Concrete Bridge Columns,” by T.J. Wipf, F.W. Klaiber and F.M. Russo, 12/28/97, (PB98-144215, A12, MF-A03).

NCEER-97-0017 “Seismic Fragility of Existing Conventional Reinforced Concrete Highway Bridges,” by C.L. Mullen and A.S. Cakmak, 12/30/97, (PB98-153406, A08, MF-A02).

NCEER-97-0018 “Loss Asssessment of Memphis Buildings,” edited by D.P. Abrams and M. Shinozuka, 12/31/97, (PB98-144231, A13, MF-A03).

NCEER-97-0019 “Seismic Evaluation of Frames with Infill Walls Using Quasi-static Experiments,” by K.M. Mosalam, R.N. White and P. Gergely, 12/31/97, (PB98-153455, A07, MF-A02).

NCEER-97-0020 “Seismic Evaluation of Frames with Infill Walls Using Pseudo-dynamic Experiments,” by K.M. Mosalam, R.N. White and P. Gergely, 12/31/97, (PB98-153430, A07, MF-A02).

NCEER-97-0021 “Computational Strategies for Frames with Infill Walls: Discrete and Smeared Crack Analyses and Seismic Fragility,” by K.M. Mosalam, R.N. White and P. Gergely, 12/31/97, (PB98-153414, A10, MF-A02).

NCEER-97-0022 "Proceedings of the NCEER Workshop on Evaluation of Liquefaction Resistance of Soils," edited by T.L. Youd and I.M. Idriss, 12/31/97, (PB98-155617, A15, MF-A03).

MCEER-98-0001 "Extraction of Nonlinear Hysteretic Properties of Seismically Isolated Bridges from Quick-Release Field Tests," by Q. Chen, B.M. Douglas, E.M. Maragakis and I.G. Buckle, 5/26/98, (PB99-118838, A06, MF-A01).

MCEER-98-0002 "Methodologies for Evaluating the Importance of Highway Bridges," by A. Thomas, S. Eshenaur and J. Kulicki, 5/29/98, (PB99-118846, A10, MF-A02).

MCEER-98-0003 "Capacity Design of Bridge Piers and the Analysis of Overstrength," by J.B. Mander, A. Dutta and P. Goel, 6/1/98, (PB99-118853, A09, MF-A02).

MCEER-98-0004 "Evaluation of Bridge Damage Data from the Loma Prieta and Northridge, California Earthquakes," by N. Basoz and A. Kiremidjian, 6/2/98, (PB99-118861, A15, MF-A03).

MCEER-98-0005 "Screening Guide for Rapid Assessment of Liquefaction Hazard at Highway Bridge Sites," by T. L. Youd, 6/16/98, (PB99-118879, A06, not available on microfiche).

MCEER-98-0006 "Structural Steel and Steel/Concrete Interface Details for Bridges," by P. Ritchie, N. Kauhl and J. Kulicki, 7/13/98, (PB99-118945, A06, MF-A01).

MCEER-98-0007 "Capacity Design and Fatigue Analysis of Confined Concrete Columns," by A. Dutta and J.B. Mander, 7/14/98, (PB99-118960, A14, MF-A03).

MCEER-98-0008 "Proceedings of the Workshop on Performance Criteria for Telecommunication Services Under Earthquake Conditions," edited by A.J. Schiff, 7/15/98, (PB99-118952, A08, MF-A02).

MCEER-98-0009 "Fatigue Analysis of Unconfined Concrete Columns," by J.B. Mander, A. Dutta and J.H. Kim, 9/12/98, (PB99-123655, A10, MF-A02).

MCEER-98-0010 "Centrifuge Modeling of Cyclic Lateral Response of Pile-Cap Systems and Seat-Type Abutments in Dry Sands," by A.D. Gadre and R. Dobry, 10/2/98, (PB99-123606, A13, MF-A03).

MCEER-98-0011 "IDARC-BRIDGE: A Computational Platform for Seismic Damage Assessment of Bridge Structures," by A.M. Reinhorn, V. Simeonov, G. Mylonakis and Y. Reichman, 10/2/98, (PB99-162919, A15, MF-A03).

MCEER-98-0012 "Experimental Investigation of the Dynamic Response of Two Bridges Before and After Retrofitting with Elastomeric Bearings," by D.A. Wendichansky, S.S. Chen and J.B. Mander, 10/2/98, (PB99-162927, A15, MF-A03).

MCEER-98-0013 "Design Procedures for Hinge Restrainers and Hinge Sear Width for Multiple-Frame Bridges," by R. Des Roches and G.L. Fenves, 11/3/98, (PB99-140477, A13, MF-A03).

MCEER-98-0014 "Response Modification Factors for Seismically Isolated Bridges," by M.C. Constantinou and J.K. Quarshie, 11/3/98, (PB99-140485, A14, MF-A03).

MCEER-98-0015 "Proceedings of the U.S.-Italy Workshop on Seismic Protective Systems for Bridges," edited by I.M. Friedland and M.C. Constantinou, 11/3/98, (PB2000-101711, A22, MF-A04).

MCEER-98-0016 "Appropriate Seismic Reliability for Critical Equipment Systems: Recommendations Based on Regional Analysis of Financial and Life Loss," by K. Porter, C. Scawthorn, C. Taylor and N. Blais, 11/10/98, (PB99-157265, A08, MF-A02).

MCEER-98-0017 "Proceedings of the U.S. Japan Joint Seminar on Civil Infrastructure Systems Research," edited by M. Shinozuka and A. Rose, 11/12/98, (PB99-156713, A16, MF-A03).

MCEER-98-0018 "Modeling of Pile Footings and Drilled Shafts for Seismic Design," by I. PoLam, M. Kapuskar and D. Chaudhuri, 12/21/98, (PB99-157257, A09, MF-A02).

MCEER-99-0001 "Seismic Evaluation of a Masonry Infilled Reinforced Concrete Frame by Pseudodynamic Testing," by S.G. Buonopane and R.N. White, 2/16/99, (PB99-162851, A09, MF-A02).

MCEER-99-0002 "Response History Analysis of Structures with Seismic Isolation and Energy Dissipation Systems: Verification Examples for Program SAP2000," by J. Scheller and M.C. Constantinou, 2/22/99, (PB99-162869, A08, MF-A02).

MCEER-99-0003 "Experimental Study on the Seismic Design and Retrofit of Bridge Columns Including Axial Load Effects," by A. Dutta, T. Kokorina and J.B. Mander, 2/22/99, (PB99-162877, A09, MF-A02).

MCEER-99-0004 "Experimental Study of Bridge Elastomeric and Other Isolation and Energy Dissipation Systems with Emphasis on Uplift Prevention and High Velocity Near-source Seismic Excitation," by A. Kasalanati and M. C. Constantinou, 2/26/99, (PB99-162885, A12, MF-A03).

MCEER-99-0005 "Truss Modeling of Reinforced Concrete Shear-flexure Behavior," by J.H. Kim and J.B. Mander, 3/8/99, (PB99-163693, A12, MF-A03).

MCEER-99-0006 "Experimental Investigation and Computational Modeling of Seismic Response of a 1:4 Scale Model Steel Structure with a Load Balancing Supplemental Damping System," by G. Pekcan, J.B. Mander and S.S. Chen, 4/2/99, (PB99-162893, A11, MF-A03).

MCEER-99-0007 "Effect of Vertical Ground Motions on the Structural Response of Highway Bridges," by M.R. Button, C.J. Cronin and R.L. Mayes, 4/10/99, (PB2000-101411, A10, MF-A03).

MCEER-99-0008 "Seismic Reliability Assessment of Critical Facilities: A Handbook, Supporting Documentation, and Model Code Provisions," by G.S. Johnson, R.E. Sheppard, M.D. Quilici, S.J. Eder and C.R. Scawthorn, 4/12/99, (PB2000-101701, A18, MF-A04).

MCEER-99-0009 "Impact Assessment of Selected MCEER Highway Project Research on the Seismic Design of Highway Structures," by C. Rojahn, R. Mayes, D.G. Anderson, J.H. Clark, D'Appolonia Engineering, S. Gloyd and R.V. Nutt, 4/14/99, (PB99-162901, A10, MF-A02).

MCEER-99-0010 "Site Factors and Site Categories in Seismic Codes," by R. Dobry, R. Ramos and M.S. Power, 7/19/99, (PB2000-101705, A08, MF-A02).

MCEER-99-0011 "Restrainer Design Procedures for Multi-Span Simply-Supported Bridges," by M.J. Randall, M. Saiidi, E. Maragakis and T. Isakovic, 7/20/99, (PB2000-101702, A10, MF-A02).

MCEER-99-0012 "Property Modification Factors for Seismic Isolation Bearings," by M.C. Constantinou, P. Tsopelas, A. Kasalanati and E. Wolff, 7/20/99, (PB2000-103387, A11, MF-A03).

MCEER-99-0013 "Critical Seismic Issues for Existing Steel Bridges," by P. Ritchie, N. Kauhl and J. Kulicki, 7/20/99, (PB2000-101697, A09, MF-A02).

MCEER-99-0014 "Nonstructural Damage Database," by A. Kao, T.T. Soong and A. Vender, 7/24/99, (PB2000-101407, A06, MF-A01).

MCEER-99-0015 "Guide to Remedial Measures for Liquefaction Mitigation at Existing Highway Bridge Sites," by H.G. Cooke and J. K. Mitchell, 7/26/99, (PB2000-101703, A11, MF-A03).

MCEER-99-0016 "Proceedings of the MCEER Workshop on Ground Motion Methodologies for the Eastern United States," edited by N. Abrahamson and A. Becker, 8/11/99, (PB2000-103385, A07, MF-A02).

MCEER-99-0017 "Quindío, Colombia Earthquake of January 25, 1999: Reconnaissance Report," by A.P. Asfura and P.J. Flores, 10/4/99, (PB2000-106893, A06, MF-A01).

MCEER-99-0018 "Hysteretic Models for Cyclic Behavior of Deteriorating Inelastic Structures," by M.V. Sivaselvan and A.M. Reinhorn, 11/5/99, (PB2000-103386, A08, MF-A02).

MCEER-99-0019 "Proceedings of the 7th U.S.- Japan Workshop on Earthquake Resistant Design of Lifeline Facilities and Countermeasures Against Soil Liquefaction," edited by T.D. O'Rourke, J.P. Bardet and M. Hamada, 11/19/99, (PB2000-103354, A99, MF-A06).

MCEER-99-0020 "Development of Measurement Capability for Micro-Vibration Evaluations with Application to Chip Fabrication Facilities," by G.C. Lee, Z. Liang, J.W. Song, J.D. Shen and W.C. Liu, 12/1/99, (PB2000-105993, A08, MF-A02).

MCEER-99-0021 "Design and Retrofit Methodology for Building Structures with Supplemental Energy Dissipating Systems," by G. Pekcan, J.B. Mander and S.S. Chen, 12/31/99, (PB2000-105994, A11, MF-A03).

MCEER-00-0001 "The Marmara, Turkey Earthquake of August 17, 1999: Reconnaissance Report," edited by C. Scawthorn; with major contributions by M. Bruneau, R. Eguchi, T. Holzer, G. Johnson, J. Mander, J. Mitchell, W. Mitchell, A. Papageorgiou, C. Scaethorn, and G. Webb, 3/23/00, (PB2000-106200, A11, MF-A03).

MCEER-00-0002 "Proceedings of the MCEER Workshop for Seismic Hazard Mitigation of Health Care Facilities," edited by G.C. Lee, M. Ettouney, M. Grigoriu, J. Hauer and J. Nigg, 3/29/00, (PB2000-106892, A08, MF-A02).

MCEER-00-0003 "The Chi-Chi, Taiwan Earthquake of September 21, 1999: Reconnaissance Report," edited by G.C. Lee and C.H. Loh, with major contributions by G.C. Lee, M. Bruneau, I.G. Buckle, S.E. Chang, P.J. Flores, T.D. O'Rourke, M. Shinozuka, T.T. Soong, C-H. Loh, K-C. Chang, Z-J. Chen, J-S. Hwang, M-L. Lin, G-Y. Liu, K-C. Tsai, G.C. Yao and C-L. Yen, 4/30/00, (PB2001-100980, A10, MF-A02).

MCEER-00-0004 "Seismic Retrofit of End-Sway Frames of Steel Deck-Truss Bridges with a Supplemental Tendon System: Experimental and Analytical Investigation," by G. Pekcan, J.B. Mander and S.S. Chen, 7/1/00, (PB2001-100982, A10, MF-A02).

MCEER-00-0005 "Sliding Fragility of Unrestrained Equipment in Critical Facilities," by W.H. Chong and T.T. Soong, 7/5/00, (PB2001-100983, A08, MF-A02).

MCEER-00-0006 "Seismic Response of Reinforced Concrete Bridge Pier Walls in the Weak Direction," by N. Abo-Shadi, M. Saiidi and D. Sanders, 7/17/00, (PB2001-100981, A17, MF-A03).

MCEER-00-0007 "Low-Cycle Fatigue Behavior of Longitudinal Reinforcement in Reinforced Concrete Bridge Columns," by J. Brown and S.K. Kunnath, 7/23/00, (PB2001-104392, A08, MF-A02).

MCEER-00-0008 "Soil Structure Interaction of Bridges for Seismic Analysis," I. PoLam and H. Law, 9/25/00, (PB2001-105397, A08, MF-A02).

MCEER-00-0009 "Proceedings of the First MCEER Workshop on Mitigation of Earthquake Disaster by Advanced Technologies (MEDAT-1), edited by M. Shinozuka, D.J. Inman and T.D. O'Rourke, 11/10/00, (PB2001-105399, A14, MF-A03).

MCEER-00-0010 "Development and Evaluation of Simplified Procedures for Analysis and Design of Buildings with Passive Energy Dissipation Systems, Revision 01," by O.M. Ramirez, M.C. Constantinou, C.A. Kircher, A.S. Whittaker, M.W. Johnson, J.D. Gomez and C. Chrysostomou, 11/16/01, (PB2001-105523, A23, MF-A04).

MCEER-00-0011 "Dynamic Soil-Foundation-Structure Interaction Analyses of Large Caissons," by C-Y. Chang, C-M. Mok, Z-L. Wang, R. Settgast, F. Waggoner, M.A. Ketchum, H.M. Gonnermann and C-C. Chin, 12/30/00, (PB2001-104373, A07, MF-A02).

MCEER-00-0012 "Experimental Evaluation of Seismic Performance of Bridge Restrainers," by A.G. Vlassis, E.M. Maragakis and M. Saiid Saiidi, 12/30/00, (PB2001-104354, A09, MF-A02).

MCEER-00-0013 "Effect of Spatial Variation of Ground Motion on Highway Structures," by M. Shinozuka, V. Saxena and G. Deodatis, 12/31/00, (PB2001-108755, A13, MF-A03).

MCEER-00-0014 "A Risk-Based Methodology for Assessing the Seismic Performance of Highway Systems," by S.D. Werner, C.E. Taylor, J.E. Moore, II, J.S. Walton and S. Cho, 12/31/00, (PB2001-108756, A14, MF-A03).

MCEER-01-0001 "Experimental Investigation of P-Delta Effects to Collapse During Earthquakes," by D. Vian and M. Bruneau, 6/25/01, (PB2002-100534, A17, MF-A03).

MCEER-01-0002 "Proceedings of the Second MCEER Workshop on Mitigation of Earthquake Disaster by Advanced Technologies (MEDAT-2)," edited by M. Bruneau and D.J. Inman, 7/23/01, (PB2002-100434, A16, MF-A03).

MCEER-01-0003 "Sensitivity Analysis of Dynamic Systems Subjected to Seismic Loads," by C. Roth and M. Grigoriu, 9/18/01, (PB2003-100884, A12, MF-A03).

MCEER-01-0004 "Overcoming Obstacles to Implementing Earthquake Hazard Mitigation Policies: Stage 1 Report," by D.J. Alesch and W.J. Petak, 12/17/01, (PB2002-107949, A07, MF-A02).

MCEER-01-0005 "Updating Real-Time Earthquake Loss Estimates: Methods, Problems and Insights," by C.E. Taylor, S.E. Chang and R.T. Eguchi, 12/17/01, (PB2002-107948, A05, MF-A01).

MCEER-01-0006 "Experimental Investigation and Retrofit of Steel Pile Foundations and Pile Bents Under Cyclic Lateral Loadings," by A. Shama, J. Mander, B. Blabac and S. Chen, 12/31/01, (PB2002-107950, A13, MF-A03).

MCEER-02-0001 "Assessment of Performance of Bolu Viaduct in the 1999 Duzce Earthquake in Turkey" by P.C. Roussis, M.C. Constantinou, M. Erdik, E. Durukal and M. Dicleli, 5/8/02, (PB2003-100883, A08, MF-A02).

MCEER-02-0002 "Seismic Behavior of Rail Counterweight Systems of Elevators in Buildings," by M.P. Singh, Rildova and L.E. Suarez, 5/27/02. (PB2003-100882, A11, MF-A03).

MCEER-02-0003 "Development of Analysis and Design Procedures for Spread Footings," by G. Mylonakis, G. Gazetas, S. Nikolaou and A. Chauncey, 10/02/02, (PB2004-101636, A13, MF-A03, CD-A13).

MCEER-02-0004 "Bare-Earth Algorithms for Use with SAR and LIDAR Digital Elevation Models," by C.K. Huyck, R.T. Eguchi and B. Houshmand, 10/16/02, (PB2004-101637, A07, CD-A07).

MCEER-02-0005 "Review of Energy Dissipation of Compression Members in Concentrically Braced Frames," by K.Lee and M. Bruneau, 10/18/02, (PB2004-101638, A10, CD-A10).

MCEER-03-0001 "Experimental Investigation of Light-Gauge Steel Plate Shear Walls for the Seismic Retrofit of Buildings" by J. Berman and M. Bruneau, 5/2/03, (PB2004-101622, A10, MF-A03, CD-A10).

MCEER-03-0002 "Statistical Analysis of Fragility Curves," by M. Shinozuka, M.Q. Feng, H. Kim, T. Uzawa and T. Ueda, 6/16/03, (PB2004-101849, A09, CD-A09).

MCEER-03-0003 "Proceedings of the Eighth U.S.-Japan Workshop on Earthquake Resistant Design f Lifeline Facilities and Countermeasures Against Liquefaction," edited by M. Hamada, J.P. Bardet and T.D. O'Rourke, 6/30/03, (PB2004-104386, A99, CD-A99).

MCEER-03-0004 "Proceedings of the PRC-US Workshop on Seismic Analysis and Design of Special Bridges," edited by L.C. Fan and G.C. Lee, 7/15/03, (PB2004-104387, A14, CD-A14).

MCEER-03-0005 "Urban Disaster Recovery: A Framework and Simulation Model," by S.B. Miles and S.E. Chang, 7/25/03, (PB2004-104388, A07, CD-A07).

MCEER-03-0006 "Behavior of Underground Piping Joints Due to Static and Dynamic Loading," by R.D. Meis, M. Maragakis and R. Siddharthan, 11/17/03, (PB2005-102194, A13, MF-A03, CD-A00).

MCEER-04-0001 "Experimental Study of Seismic Isolation Systems with Emphasis on Secondary System Response and Verification of Accuracy of Dynamic Response History Analysis Methods," by E. Wolff and M. Constantinou, 1/16/04 (PB2005-102195, A99, MF-E08, CD-A00).

MCEER-04-0002 "Tension, Compression and Cyclic Testing of Engineered Cementitious Composite Materials," by K. Kesner and S.L. Billington, 3/1/04, (PB2005-102196, A08, CD-A08).

MCEER-04-0003 "Cyclic Testing of Braces Laterally Restrained by Steel Studs to Enhance Performance During Earthquakes," by O.C. Celik, J.W. Berman and M. Bruneau, 3/16/04, (PB2005-102197, A13, MF-A03, CD-A00).

MCEER-04-0004 "Methodologies for Post Earthquake Building Damage Detection Using SAR and Optical Remote Sensing: Application to the August 17, 1999 Marmara, Turkey Earthquake," by C.K. Huyck, B.J. Adams, S. Cho, R.T. Eguchi, B. Mansouri and B. Houshmand, 6/15/04, (PB2005-104888, A10, CD-A00).

MCEER-04-0005 "Nonlinear Structural Analysis Towards Collapse Simulation: A Dynamical Systems Approach," by M.V. Sivaselvan and A.M. Reinhorn, 6/16/04, (PB2005-104889, A11, MF-A03, CD-A00).

MCEER-04-0006 "Proceedings of the Second PRC-US Workshop on Seismic Analysis and Design of Special Bridges," edited by G.C. Lee and L.C. Fan, 6/25/04, (PB2005-104890, A16, CD-A00).

MCEER-04-0007 "Seismic Vulnerability Evaluation of Axially Loaded Steel Built-up Laced Members," by K. Lee and M. Bruneau, 6/30/04, (PB2005-104891, A16, CD-A00).

MCEER-04-0008 "Evaluation of Accuracy of Simplified Methods of Analysis and Design of Buildings with Damping Systems for Near-Fault and for Soft-Soil Seismic Motions," by E.A. Pavlou and M.C. Constantinou, 8/16/04, (PB2005-104892, A08, MF-A02, CD-A00).

MCEER-04-0009 "Assessment of Geotechnical Issues in Acute Care Facilities in California," by M. Lew, T.D. O'Rourke, R. Dobry and M. Koch, 9/15/04, (PB2005-104893, A08, CD-A00).

MCEER-04-0010 "Scissor-Jack-Damper Energy Dissipation System," by A.N. Sigaher-Boyle and M.C. Constantinou, 12/1/04 (PB2005-108221).

MCEER-04-0011 "Seismic Retrofit of Bridge Steel Truss Piers Using a Controlled Rocking Approach," by M. Pollino and M. Bruneau, 12/20/04 (PB2006-105795).

MCEER-05-0001 "Experimental and Analytical Studies of Structures Seismically Isolated with an Uplift-Restraint Isolation System," by P.C. Roussis and M.C. Constantinou, 1/10/05 (PB2005-108222).

MCEER-05-0002 "A Versatile Experimentation Model for Study of Structures Near Collapse Applied to Seismic Evaluation of Irregular Structures," by D. Kusumastuti, A.M. Reinhorn and A. Rutenberg, 3/31/05 (PB2006-101523).

MCEER-05-0003 "Proceedings of the Third PRC-US Workshop on Seismic Analysis and Design of Special Bridges," edited by L.C. Fan and G.C. Lee, 4/20/05, (PB2006-105796).

MCEER-05-0004 "Approaches for the Seismic Retrofit of Braced Steel Bridge Piers and Proof-of-Concept Testing of an Eccentrically Braced Frame with Tubular Link," by J.W. Berman and M. Bruneau, 4/21/05 (PB2006-101524).

MCEER-05-0005 "Simulation of Strong Ground Motions for Seismic Fragility Evaluation of Nonstructural Components in Hospitals," by A. Wanitkorkul and A. Filiatrault, 5/26/05 (PB2006-500027).

MCEER-05-0006 "Seismic Safety in California Hospitals: Assessing an Attempt to Accelerate the Replacement or Seismic Retrofit of Older Hospital Facilities," by D.J. Alesch, L.A. Arendt and W.J. Petak, 6/6/05 (PB2006-105794).

MCEER-05-0007 "Development of Seismic Strengthening and Retrofit Strategies for Critical Facilities Using Engineered Cementitious Composite Materials," by K. Kesner and S.L. Billington, 8/29/05 (PB2006-111701).

MCEER-05-0008 "Experimental and Analytical Studies of Base Isolation Systems for Seismic Protection of Power Transformers," by N. Murota, M.Q. Feng and G-Y. Liu, 9/30/05 (PB2006-111702).

MCEER-05-0009 "3D-BASIS-ME-MB: Computer Program for Nonlinear Dynamic Analysis of Seismically Isolated Structures," by P.C. Tsopelas, P.C. Roussis, M.C. Constantinou, R. Buchanan and A.M. Reinhorn, 10/3/05 (PB2006-111703).

MCEER-05-0010 "Steel Plate Shear Walls for Seismic Design and Retrofit of Building Structures," by D. Vian and M. Bruneau, 12/15/05 (PB2006-111704).

MCEER-05-0011 "The Performance-Based Design Paradigm," by M.J. Astrella and A. Whittaker, 12/15/05 (PB2006-111705).

MCEER-06-0001 "Seismic Fragility of Suspended Ceiling Systems," H. Badillo-Almaraz, A.S. Whittaker, A.M. Reinhorn and G.P. Cimellaro, 2/4/06 (PB2006-111706).

MCEER-06-0002 "Multi-Dimensional Fragility of Structures," by G.P. Cimellaro, A.M. Reinhorn and M. Bruneau, 3/1/06 (PB2007-106974, A09, MF-A02, CD A00).

MCEER-06-0003 "Built-Up Shear Links as Energy Dissipators for Seismic Protection of Bridges," by P. Dusicka, A.M. Itani and I.G. Buckle, 3/15/06 (PB2006-111708).

MCEER-06-0004 "Analytical Investigation of the Structural Fuse Concept," by R.E. Vargas and M. Bruneau, 3/16/06 (PB2006-111709).

MCEER-06-0005 "Experimental Investigation of the Structural Fuse Concept," by R.E. Vargas and M. Bruneau, 3/17/06 (PB2006-111710).

MCEER-06-0006 "Further Development of Tubular Eccentrically Braced Frame Links for the Seismic Retrofit of Braced Steel Truss Bridge Piers," by J.W. Berman and M. Bruneau, 3/27/06 (PB2007-105147).

MCEER-06-0007 "REDARS Validation Report," by S. Cho, C.K. Huyck, S. Ghosh and R.T. Eguchi, 8/8/06 (PB2007-106983).

MCEER-06-0008 "Review of Current NDE Technologies for Post-Earthquake Assessment of Retrofitted Bridge Columns," by J.W. Song, Z. Liang and G.C. Lee, 8/21/06 (PB2007-106984).

MCEER-06-0009 "Liquefaction Remediation in Silty Soils Using Dynamic Compaction and Stone Columns," by S. Thevanayagam, G.R. Martin, R. Nashed, T. Shenthan, T. Kanagalingam and N. Ecemis, 8/28/06 (PB2007-106985).

MCEER-06-0010 "Conceptual Design and Experimental Investigation of Polymer Matrix Composite Infill Panels for Seismic Retrofitting," by W. Jung, M. Chiewanichakorn and A.J. Aref, 9/21/06 (PB2007-106986).

MCEER-06-0011 "A Study of the Coupled Horizontal-Vertical Behavior of Elastomeric and Lead-Rubber Seismic Isolation Bearings," by G.P. Warn and A.S. Whittaker, 9/22/06 (PB2007-108679).

MCEER-06-0012 "Proceedings of the Fourth PRC-US Workshop on Seismic Analysis and Design of Special Bridges: Advancing Bridge Technologies in Research, Design, Construction and Preservation," Edited by L.C. Fan, G.C. Lee and L. Ziang, 10/12/06 (PB2007-109042).

MCEER-06-0013 "Cyclic Response and Low Cycle Fatigue Characteristics of Plate Steels," by P. Dusicka, A.M. Itani and I.G. Buckle, 11/1/06 06 (PB2007-106987).

MCEER-06-0014 "Proceedings of the Second US-Taiwan Bridge Engineering Workshop," edited by W.P. Yen, J. Shen, J-Y. Chen and M. Wang, 11/15/06 (PB2008-500041).

MCEER-06-0015 "User Manual and Technical Documentation for the REDARS™ Import Wizard," by S. Cho, S. Ghosh, C.K. Huyck and S.D. Werner, 11/30/06 (PB2007-114766).

MCEER-06-0016 "Hazard Mitigation Strategy and Monitoring Technologies for Urban and Infrastructure Public Buildings: Proceedings of the China-US Workshops," edited by X.Y. Zhou, A.L. Zhang, G.C. Lee and M. Tong, 12/12/06 (PB2008-500018).

MCEER-07-0001 "Static and Kinetic Coefficients of Friction for Rigid Blocks," by C. Kafali, S. Fathali, M. Grigoriu and A.S. Whittaker, 3/20/07 (PB2007-114767).

MCEER-07-0002 "Hazard Mitigation Investment Decision Making: Organizational Response to Legislative Mandate," by L.A. Arendt, D.J. Alesch and W.J. Petak, 4/9/07 (PB2007-114768).

MCEER-07-0003 "Seismic Behavior of Bidirectional-Resistant Ductile End Diaphragms with Unbonded Braces in Straight or Skewed Steel Bridges," by O. Celik and M. Bruneau, 4/11/07 (PB2008-105141).

MCEER-07-0004 "Modeling Pile Behavior in Large Pile Groups Under Lateral Loading," by A.M. Dodds and G.R. Martin, 4/16/07(PB2008-105142).

MCEER-07-0005 "Experimental Investigation of Blast Performance of Seismically Resistant Concrete-Filled Steel Tube Bridge Piers," by S. Fujikura, M. Bruneau and D. Lopez-Garcia, 4/20/07 (PB2008-105143).

MCEER-07-0006 "Seismic Analysis of Conventional and Isolated Liquefied Natural Gas Tanks Using Mechanical Analogs," by I.P. Christovasilis and A.S. Whittaker, 5/1/07, not available.

MCEER-07-0007 "Experimental Seismic Performance Evaluation of Isolation/Restraint Systems for Mechanical Equipment – Part 1: Heavy Equipment Study," by S. Fathali and A. Filiatrault, 6/6/07 (PB2008-105144).

MCEER-07-0008 "Seismic Vulnerability of Timber Bridges and Timber Substructures," by A.A. Sharma, J.B. Mander, I.M. Friedland and D.R. Allicock, 6/7/07 (PB2008-105145).

MCEER-07-0009 "Experimental and Analytical Study of the XY-Friction Pendulum (XY-FP) Bearing for Bridge Applications," by C.C. Marin-Artieda, A.S. Whittaker and M.C. Constantinou, 6/7/07 (PB2008-105191).

MCEER-07-0010 "Proceedings of the PRC-US Earthquake Engineering Forum for Young Researchers," Edited by G.C. Lee and X.Z. Qi, 6/8/07 (PB2008-500058).

MCEER-07-0011 "Design Recommendations for Perforated Steel Plate Shear Walls," by R. Purba and M. Bruneau, 6/18/07, (PB2008-105192).

MCEER-07-0012 "Performance of Seismic Isolation Hardware Under Service and Seismic Loading," by M.C. Constantinou, A.S. Whittaker, Y. Kalpakidis, D.M. Fenz and G.P. Warn, 8/27/07, (PB2008-105193).

MCEER-07-0013 "Experimental Evaluation of the Seismic Performance of Hospital Piping Subassemblies," by E.R. Goodwin, E. Maragakis and A.M. Itani, 9/4/07, (PB2008-105194).

MCEER-07-0014 "A Simulation Model of Urban Disaster Recovery and Resilience: Implementation for the 1994 Northridge Earthquake," by S. Miles and S.E. Chang, 9/7/07, (PB2008-106426).

MCEER-07-0015 "Statistical and Mechanistic Fragility Analysis of Concrete Bridges," by M. Shinozuka, S. Banerjee and S-H. Kim, 9/10/07, (PB2008-106427).

MCEER-07-0016 "Three-Dimensional Modeling of Inelastic Buckling in Frame Structures," by M. Schachter and AM. Reinhorn, 9/13/07, (PB2008-108125).

MCEER-07-0017 "Modeling of Seismic Wave Scattering on Pile Groups and Caissons," by I. Po Lam, H. Law and C.T. Yang, 9/17/07 (PB2008-108150).

MCEER-07-0018 "Bridge Foundations: Modeling Large Pile Groups and Caissons for Seismic Design," by I. Po Lam, H. Law and G.R. Martin (Coordinating Author), 12/1/07 (PB2008-111190).

MCEER-07-0019 "Principles and Performance of Roller Seismic Isolation Bearings for Highway Bridges," by G.C. Lee, Y.C. Ou, Z. Liang, T.C. Niu and J. Song, 12/10/07 (PB2009-110466).

MCEER-07-0020 "Centrifuge Modeling of Permeability and Pinning Reinforcement Effects on Pile Response to Lateral Spreading," by L.L Gonzalez-Lagos, T. Abdoun and R. Dobry, 12/10/07 (PB2008-111191).

MCEER-07-0021 "Damage to the Highway System from the Pisco, Perú Earthquake of August 15, 2007," by J.S. O'Connor, L. Mesa and M. Nykamp, 12/10/07, (PB2008-108126).

MCEER-07-0022 "Experimental Seismic Performance Evaluation of Isolation/Restraint Systems for Mechanical Equipment – Part 2: Light Equipment Study," by S. Fathali and A. Filiatrault, 12/13/07 (PB2008-111192).

MCEER-07-0023 "Fragility Considerations in Highway Bridge Design," by M. Shinozuka, S. Banerjee and S.H. Kim, 12/14/07 (PB2008-111193).

MCEER-07-0024 "Performance Estimates for Seismically Isolated Bridges," by G.P. Warn and A.S. Whittaker, 12/30/07 (PB2008-112230).

MCEER-08-0001 "Seismic Performance of Steel Girder Bridge Superstructures with Conventional Cross Frames," by L.P. Carden, A.M. Itani and I.G. Buckle, 1/7/08, (PB2008-112231).

MCEER-08-0002 "Seismic Performance of Steel Girder Bridge Superstructures with Ductile End Cross Frames with Seismic Isolators," by L.P. Carden, A.M. Itani and I.G. Buckle, 1/7/08 (PB2008-112232).

MCEER-08-0003 "Analytical and Experimental Investigation of a Controlled Rocking Approach for Seismic Protection of Bridge Steel Truss Piers," by M. Pollino and M. Bruneau, 1/21/08 (PB2008-112233).

MCEER-08-0004 "Linking Lifeline Infrastructure Performance and Community Disaster Resilience: Models and Multi-Stakeholder Processes," by S.E. Chang, C. Pasion, K. Tatebe and R. Ahmad, 3/3/08 (PB2008-112234).

MCEER-08-0005 "Modal Analysis of Generally Damped Linear Structures Subjected to Seismic Excitations," by J. Song, Y-L. Chu, Z. Liang and G.C. Lee, 3/4/08 (PB2009-102311).

MCEER-08-0006 "System Performance Under Multi-Hazard Environments," by C. Kafali and M. Grigoriu, 3/4/08 (PB2008-112235).

MCEER-08-0007 "Mechanical Behavior of Multi-Spherical Sliding Bearings," by D.M. Fenz and M.C. Constantinou, 3/6/08 (PB2008-112236).

MCEER-08-0008 "Post-Earthquake Restoration of the Los Angeles Water Supply System," by T.H.P. Tabucchi and R.A. Davidson, 3/7/08 (PB2008-112237).

MCEER-08-0009 "Fragility Analysis of Water Supply Systems," by A. Jacobson and M. Grigoriu, 3/10/08 (PB2009-105545).

MCEER-08-0010 "Experimental Investigation of Full-Scale Two-Story Steel Plate Shear Walls with Reduced Beam Section Connections," by B. Qu, M. Bruneau, C-H. Lin and K-C. Tsai, 3/17/08 (PB2009-106368).

MCEER-08-0011 "Seismic Evaluation and Rehabilitation of Critical Components of Electrical Power Systems," S. Ersoy, B. Feizi, A. Ashrafi and M. Ala Saadeghvaziri, 3/17/08 (PB2009-105546).

MCEER-08-0012 "Seismic Behavior and Design of Boundary Frame Members of Steel Plate Shear Walls," by B. Qu and M. Bruneau, 4/26/08 . (PB2009-106744).

MCEER-08-0013 "Development and Appraisal of a Numerical Cyclic Loading Protocol for Quantifying Building System Performance," by A. Filiatrault, A. Wanitkorkul and M. Constantinou, 4/27/08 (PB2009-107906).

MCEER-08-0014 "Structural and Nonstructural Earthquake Design: The Challenge of Integrating Specialty Areas in Designing Complex, Critical Facilities," by W.J. Petak and D.J. Alesch, 4/30/08 (PB2009-107907).

MCEER-08-0015 "Seismic Performance Evaluation of Water Systems," by Y. Wang and T.D. O'Rourke, 5/5/08 (PB2009-107908).

MCEER-08-0016 "Seismic Response Modeling of Water Supply Systems," by P. Shi and T.D. O'Rourke, 5/5/08 (PB2009-107910).

MCEER-08-0017 "Numerical and Experimental Studies of Self-Centering Post-Tensioned Steel Frames," by D. Wang and A. Filiatrault, 5/12/08 (PB2009-110479).

MCEER-08-0018 "Development, Implementation and Verification of Dynamic Analysis Models for Multi-Spherical Sliding Bearings," by D.M. Fenz and M.C. Constantinou, 8/15/08 (PB2009-107911).

MCEER-08-0019 "Performance Assessment of Conventional and Base Isolated Nuclear Power Plants for Earthquake Blast Loadings," by Y.N. Huang, A.S. Whittaker and N. Luco, 10/28/08 (PB2009-107912).

MCEER-08-0020 "Remote Sensing for Resilient Multi-Hazard Disaster Response – Volume I: Introduction to Damage Assessment Methodologies," by B.J. Adams and R.T. Eguchi, 11/17/08 (PB2010-102695).

MCEER-08-0021 "Remote Sensing for Resilient Multi-Hazard Disaster Response – Volume II: Counting the Number of Collapsed Buildings Using an Object-Oriented Analysis: Case Study of the 2003 Bam Earthquake," by L. Gusella, C.K. Huyck and B.J. Adams, 11/17/08 (PB2010-100925).

MCEER-08-0022 "Remote Sensing for Resilient Multi-Hazard Disaster Response – Volume III: Multi-Sensor Image Fusion Techniques for Robust Neighborhood-Scale Urban Damage Assessment," by B.J. Adams and A. McMillan, 11/17/08 (PB2010-100926).

MCEER-08-0023 "Remote Sensing for Resilient Multi-Hazard Disaster Response – Volume IV: A Study of Multi-Temporal and Multi-Resolution SAR Imagery for Post-Katrina Flood Monitoring in New Orleans," by A. McMillan, J.G. Morley, B.J. Adams and S. Chesworth, 11/17/08 (PB2010-100927).

MCEER-08-0024 "Remote Sensing for Resilient Multi-Hazard Disaster Response – Volume V: Integration of Remote Sensing Imagery and VIEWS™ Field Data for Post-Hurricane Charley Building Damage Assessment," by J.A. Womble, K. Mehta and B.J. Adams, 11/17/08 (PB2009-115532).

MCEER-08-0025 "Building Inventory Compilation for Disaster Management: Application of Remote Sensing and Statistical Modeling," by P. Sarabandi, A.S. Kiremidjian, R.T. Eguchi and B. J. Adams, 11/20/08 (PB2009-110484).

MCEER-08-0026 "New Experimental Capabilities and Loading Protocols for Seismic Qualification and Fragility Assessment of Nonstructural Systems," by R. Retamales, G. Mosqueda, A. Filiatrault and A. Reinhorn, 11/24/08 (PB2009-110485).

MCEER-08-0027 "Effects of Heating and Load History on the Behavior of Lead-Rubber Bearings," by I.V. Kalpakidis and M.C. Constantinou, 12/1/08 (PB2009-115533).

MCEER-08-0028 "Experimental and Analytical Investigation of Blast Performance of Seismically Resistant Bridge Piers," by S.Fujikura and M. Bruneau, 12/8/08 (PB2009-115534).

MCEER-08-0029 "Evolutionary Methodology for Aseismic Decision Support," by Y. Hu and G. Dargush, 12/15/08.

MCEER-08-0030 "Development of a Steel Plate Shear Wall Bridge Pier System Conceived from a Multi-Hazard Perspective," by D. Keller and M. Bruneau, 12/19/08 (PB2010-102696).

MCEER-09-0001 "Modal Analysis of Arbitrarily Damped Three-Dimensional Linear Structures Subjected to Seismic Excitations," by Y.L. Chu, J. Song and G.C. Lee, 1/31/09 (PB2010-100922).

MCEER-09-0002 "Air-Blast Effects on Structural Shapes," by G. Ballantyne, A.S. Whittaker, A.J. Aref and G.F. Dargush, 2/2/09 (PB2010-102697).

MCEER-09-0003 "Water Supply Performance During Earthquakes and Extreme Events," by A.L. Bonneau and T.D. O'Rourke, 2/16/09 (PB2010-100923).

MCEER-09-0004 "Generalized Linear (Mixed) Models of Post-Earthquake Ignitions," by R.A. Davidson, 7/20/09 (PB2010-102698).

MCEER-09-0005 "Seismic Testing of a Full-Scale Two-Story Light-Frame Wood Building: NEESWood Benchmark Test," by I.P. Christovasilis, A. Filiatrault and A. Wanitkorkul, 7/22/09 (PB2012-102401).

MCEER-09-0006 "IDARC2D Version 7.0: A Program for the Inelastic Damage Analysis of Structures," by A.M. Reinhorn, H. Roh, M. Sivaselvan, S.K. Kunnath, R.E. Valles, A. Madan, C. Li, R. Lobo and Y.J. Park, 7/28/09 (PB2010-103199).

MCEER-09-0007 "Enhancements to Hospital Resiliency: Improving Emergency Planning for and Response to Hurricanes," by D.B. Hess and L.A. Arendt, 7/30/09 (PB2010-100924).

MCEER-09-0008 "Assessment of Base-Isolated Nuclear Structures for Design and Beyond-Design Basis Earthquake Shaking," by Y.N. Huang, A.S. Whittaker, R.P. Kennedy and R.L. Mayes, 8/20/09 (PB2010-102699).

MCEER-09-0009 "Quantification of Disaster Resilience of Health Care Facilities," by G.P. Cimellaro, C. Fumo, A.M Reinhorn and M. Bruneau, 9/14/09 (PB2010-105384).

MCEER-09-0010 "Performance-Based Assessment and Design of Squat Reinforced Concrete Shear Walls," by C.K. Gulec and A.S. Whittaker, 9/15/09 (PB2010-102700).

MCEER-09-0011 "Proceedings of the Fourth US-Taiwan Bridge Engineering Workshop," edited by W.P. Yen, J.J. Shen, T.M. Lee and R.B. Zheng, 10/27/09 (PB2010-500009).

MCEER-09-0012 "Proceedings of the Special International Workshop on Seismic Connection Details for Segmental Bridge Construction," edited by W. Phillip Yen and George C. Lee, 12/21/09 (PB2012-102402).

MCEER-10-0001 "Direct Displacement Procedure for Performance-Based Seismic Design of Multistory Woodframe Structures," by W. Pang and D. Rosowsky, 4/26/10 (PB2012-102403).

MCEER-10-0002 "Simplified Direct Displacement Design of Six-Story NEESWood Capstone Building and Pre-Test Seismic Performance Assessment," by W. Pang, D. Rosowsky, J. van de Lindt and S. Pei, 5/28/10 (PB2012-102404).

MCEER-10-0003 "Integration of Seismic Protection Systems in Performance-Based Seismic Design of Woodframed Structures," by J.K. Shinde and M.D. Symans, 6/18/10 (PB2012-102405).

MCEER-10-0004 "Modeling and Seismic Evaluation of Nonstructural Components: Testing Frame for Experimental Evaluation of Suspended Ceiling Systems," by A.M. Reinhorn, K.P. Ryu and G. Maddaloni, 6/30/10 (PB2012-102406).

MCEER-10-0005 "Analytical Development and Experimental Validation of a Structural-Fuse Bridge Pier Concept," by S. El-Bahey and M. Bruneau, 10/1/10 (PB2012-102407).

MCEER-10-0006 "A Framework for Defining and Measuring Resilience at the Community Scale: The PEOPLES Resilience Framework," by C.S. Renschler, A.E. Frazier, L.A. Arendt, G.P. Cimellaro, A.M. Reinhorn and M. Bruneau, 10/8/10 (PB2012-102408).

MCEER-10-0007 "Impact of Horizontal Boundary Elements Design on Seismic Behavior of Steel Plate Shear Walls," by R. Purba and M. Bruneau, 11/14/10 (PB2012-102409).

MCEER-10-0008 "Seismic Testing of a Full-Scale Mid-Rise Building: The NEESWood Capstone Test," by S. Pei, J.W. van de Lindt, S.E. Pryor, H. Shimizu, H. Isoda and D.R. Rammer, 12/1/10 (PB2012-102410).

MCEER-10-0009 "Modeling the Effects of Detonations of High Explosives to Inform Blast-Resistant Design," by P. Sherkar, A.S. Whittaker and A.J. Aref, 12/1/10 (PB2012-102411).

MCEER-10-0010 "L'Aquila Earthquake of April 6, 2009 in Italy: Rebuilding a Resilient City to Withstand Multiple Hazards," by G.P. Cimellaro, I.P. Christovasilis, A.M. Reinhorn, A. De Stefano and T. Kirova, 12/29/10.

MCEER-11-0001 "Numerical and Experimental Investigation of the Seismic Response of Light-Frame Wood Structures," by I.P. Christovasilis and A. Filiatrault, 8/8/11 (PB2012-102412).

MCEER-11-0002 "Seismic Design and Analysis of a Precast Segmental Concrete Bridge Model," by M. Anagnostopoulou, A. Filiatrault and A. Aref, 9/15/11.

MCEER-11-0003 'Proceedings of the Workshop on Improving Earthquake Response of Substation Equipment," Edited by A.M. Reinhorn, 9/19/11 (PB2012-102413).

MCEER-11-0004 "LRFD-Based Analysis and Design Procedures for Bridge Bearings and Seismic Isolators," by M.C. Constantinou, I. Kalpakidis, A. Filiatrault and R.A. Ecker Lay, 9/26/11.

MCEER-11-0005 "Experimental Seismic Evaluation, Model Parameterization, and Effects of Cold-Formed Steel-Framed Gypsum Partition Walls on the Seismic Performance of an Essential Facility," by R. Davies, R. Retamales, G. Mosqueda and A. Filiatrault, 10/12/11.

MCEER-11-0006 "Modeling and Seismic Performance Evaluation of High Voltage Transformers and Bushings," by A.M. Reinhorn, K. Oikonomou, H. Roh, A. Schiff and L. Kempner, Jr., 10/3/11.

MCEER-11-0007 "Extreme Load Combinations: A Survey of State Bridge Engineers," by G.C. Lee, Z. Liang, J.J. Shen and J.S. O'Connor, 10/14/11.

MCEER-12-0001 "Simplified Analysis Procedures in Support of Performance Based Seismic Design," by Y.N. Huang and A.S. Whittaker.

MCEER-12-0002 "Seismic Protection of Electrical Transformer Bushing Systems by Stiffening Techniques," by M. Koliou, A. Filiatrault, A.M. Reinhorn and N. Oliveto, 6/1/12.

MCEER-12-0003 "Post-Earthquake Bridge Inspection Guidelines," by J.S. O'Connor and S. Alampalli, 6/8/12.

MCEER-12-0004 "Integrated Design Methodology for Isolated Floor Systems in Single-Degree-of-Freedom Structural Fuse Systems," by S. Cui, M. Bruneau and M.C. Constantinou, 6/13/12.

MCEER-12-0005 "Characterizing the Rotational Components of Earthquake Ground Motion," by D. Basu, A.S. Whittaker and M.C. Constantinou, 6/15/12.

MCEER-12-0006 "Bayesian Fragility for Nonstructural Systems," by C.H. Lee and M.D. Grigoriu, 9/12/12.

MCEER-12-0007 "A Numerical Model for Capturing the In-Plane Seismic Response of Interior Metal Stud Partition Walls," by R.L. Wood and T.C. Hutchinson, 9/12/12.

MCEER-12-0008 "Assessment of Floor Accelerations in Yielding Buildings," by J.D. Wieser, G. Pekcan, A.E. Zaghi, A.M. Itani and E. Maragakis, 10/5/12.

MCEER-13-0001 "Experimental Seismic Study of Pressurized Fire Sprinkler Piping Systems," by Y. Tian, A. Filiatrault and G. Mosqueda, 4/8/13.

MCEER-13-0002 "Enhancing Resource Coordination for Multi-Modal Evacuation Planning," by D.B. Hess, B.W. Conley and C.M. Farrell, 2/8/13.

MCEER-13-0003 "Seismic Response of Base Isolated Buildings Considering Pounding to Moat Walls," by A. Masroor and G. Mosqueda, 2/26/13.

MCEER-13-0004 "Seismic Response Control of Structures Using a Novel Adaptive Passive Negative Stiffness Device," by D.T.R. Pasala, A.A. Sarlis, S. Nagarajaiah, A.M. Reinhorn, M.C. Constantinou and D.P. Taylor, 6/10/13.

MCEER-13-0005 "Negative Stiffness Device for Seismic Protection of Structures," by A.A. Sarlis, D.T.R. Pasala, M.C. Constantinou, A.M. Reinhorn, S. Nagarajaiah and D.P. Taylor, 6/12/13.

MCEER-13-0006 "Emilia Earthquake of May 20, 2012 in Northern Italy: Rebuilding a Resilient Community to Withstand Multiple Hazards," by G.P. Cimellaro, M. Chiriatti, A.M. Reinhorn and L. Tirca, June 30, 2013.

MCEER-13-0007 "Precast Concrete Segmental Components and Systems for Accelerated Bridge Construction in Seismic Regions," by A.J. Aref, G.C. Lee, Y.C. Ou and P. Sideris, with contributions from K.C. Chang, S. Chen, A. Filiatrault and Y. Zhou, June 13, 2013.

MCEER-13-0008 "A Study of U.S. Bridge Failures (1980-2012)," by G.C. Lee, S.B. Mohan, C. Huang and B.N. Fard, June 15, 2013.

MCEER-13-0009 "Development of a Database Framework for Modeling Damaged Bridges," by G.C. Lee, J.C. Qi and C. Huang, June 16, 2013.

MCEER-13-0010 "Model of Triple Friction Pendulum Bearing for General Geometric and Frictional Parameters and for Uplift Conditions," by A.A. Sarlis and M.C. Constantinou, July 1, 2013.

MCEER-13-0011 "Shake Table Testing of Triple Friction Pendulum Isolators under Extreme Conditions," by A.A. Sarlis, M.C. Constantinou and A.M. Reinhorn, July 2, 2013.

MCEER-13-0012 "Theoretical Framework for the Development of MH-LRFD," by G.C. Lee (coordinating author), H.A Capers, Jr., C. Huang, J.M. Kulicki, Z. Liang, T. Murphy, J.J.D. Shen, M. Shinozuka and P.W.H. Yen, July 31, 2013.

MCEER-13-0013 "Seismic Protection of Highway Bridges with Negative Stiffness Devices," by N.K.A. Attary, M.D. Symans, S. Nagarajaiah, A.M. Reinhorn, M.C. Constantinou, A.A. Sarlis, D.T.R. Pasala, and D.P. Taylor, September 3, 2014.

MCEER-14-0001 "Simplified Seismic Collapse Capacity-Based Evaluation and Design of Frame Buildings with and without Supplemental Damping Systems," by M. Hamidia, A. Filiatrault, and A. Aref, May 19, 2014.

MCEER-14-0002 "Comprehensive Analytical Seismic Fragility of Fire Sprinkler Piping Systems," by Siavash Soroushian, Emmanuel "Manos" Maragakis, Arash E. Zaghi, Alicia Echevarria, Yuan Tian and Andre Filiatrault, August 26, 2014.

MCEER-14-0003 "Hybrid Simulation of the Seismic Response of a Steel Moment Frame Building Structure through Collapse," by M. Del Carpio Ramos, G. Mosqueda and D.G. Lignos, October 30, 2014.

MCEER-14-0004 "Blast and Seismic Resistant Concrete-Filled Double Skin Tubes and Modified Steel Jacketed Bridge Columns," by P.P. Fouche and M. Bruneau, June 30, 2015.

MCEER-14-0005 "Seismic Performance of Steel Plate Shear Walls Considering Various Design Approaches," by R. Purba and M. Bruneau, October 31, 2014.

MCEER-14-0006 "Air-Blast Effects on Civil Structures," by Jinwon Shin, Andrew S. Whittaker, Amjad J. Aref and David Cormie, October 30, 2014.

MCEER-14-0007 "Seismic Performance Evaluation of Precast Girders with Field-Cast Ultra High Performance Concrete (UHPC) Connections," by G.C. Lee, C. Huang, J. Song, and J. S. O'Connor, July 31, 2014.

MCEER-14-0008 "Post-Earthquake Fire Resistance of Ductile Concrete-Filled Double-Skin Tube Columns," by Reza Imani, Gilberto Mosqueda and Michel Bruneau, December 1, 2014.

MCEER-14-0009 "Cyclic Inelastic Behavior of Concrete Filled Sandwich Panel Walls Subjected to In-Plane Flexure," by Y. Alzeni and M. Bruneau, December 19, 2014.

MCEER-14-0010 "Analytical and Experimental Investigation of Self-Centering Steel Plate Shear Walls," by D.M. Dowden and M. Bruneau, December 19, 2014.

MCEER-15-0001 "Seismic Analysis of Multi-story Unreinforced Masonry Buildings with Flexible Diaphragms," by J. Aleman, G. Mosqueda and A.S. Whittaker, June 12, 2015.

MCEER-15-0002 "Site Response, Soil-Structure Interaction and Structure-Soil-Structure Interaction for Performance Assessment of Buildings and Nuclear Structures," by C. Bolisetti and A.S. Whittaker, June 15, 2015.

MCEER-15-0003 "Stress Wave Attenuation in Solids for Mitigating Impulsive Loadings," by R. Rafiee-Dehkharghani, A.J. Aref and G. Dargush, August 15, 2015.

MCEER-15-0004 "Computational, Analytical, and Experimental Modeling of Masonry Structures," by K.M. Dolatshahi and A.J. Aref, November 16, 2015.

MCEER-15-0005 "Property Modification Factors for Seismic Isolators: Design Guidance for Buildings," by W.J. McVitty and M.C. Constantinou, June 30, 2015.

MCEER-15-0006 "Seismic Isolation of Nuclear Power Plants using Sliding Bearings," by Manish Kumar, Andrew S. Whittaker and Michael C. Constantinou, December 27, 2015.

MCEER-15-0007 "Quintuple Friction Pendulum Isolator Behavior, Modeling and Validation," by Donghun Lee and Michael C. Constantinou, December 28, 2015.

MCEER-15-0008 "Seismic Isolation of Nuclear Power Plants using Elastomeric Bearings," by Manish Kumar, Andrew S. Whittaker and Michael C. Constantinou, December 29, 2015.

MCEER-16-0001 "Experimental, Numerical and Analytical Studies on the Seismic Response of Steel-Plate Concrete (SC) Composite Shear Walls," by Siamak Epackachi and Andrew S. Whittaker, June 15, 2016.

MCEER-16-0002 "Seismic Demand in Columns of Steel Frames," by Lisa Shrestha and Michel Bruneau, June 17, 2016.

MCEER-16-0003 "Development and Evaluation of Procedures for Analysis and Design of Buildings with Fluidic Self-Centering Systems" by Shoma Kitayama and Michael C. Constantinou, July 21, 2016.

MCEER-16-0004 "Real Time Control of Shake Tables for Nonlinear Hysteretic Systems," by Ki Pung Ryu and Andrei M. Reinhorn, October 22, 2016.

MCEER-16-0006 "Seismic Isolation of High Voltage Electrical Power Transformers," by Kostis Oikonomou, Michael C. Constantinou, Andrei M. Reinhorn and Leon Kemper, Jr., November 2, 2016.

MCEER-16-0007 "Open Space Damping System Theory and Experimental Validation," by Erkan Polat and Michael C. Constantinou, December 13, 2016.

MCEER-16-0008 "Seismic Response of Low Aspect Ratio Reinforced Concrete Walls for Buildings and Safety-Related Nuclear Applications," by Bismarck N. Luna and Andrew S. Whittaker.

MCEER-16-0009 "Buckling Restrained Braces Applications for Superstructure and Substructure Protection in Bridges," by Xiaone Wei and Michel Bruneau, December 28, 2016.

MCEER-16-0010 "Procedures and Results of Assessment of Seismic Performance of Seismically Isolated Electrical Transformers with Due Consideration for Vertical Isolation and Vertical Ground Motion Effects," by Shoma Kitayama, Michael C. Constantinou and Donghun Lee, December 31, 2016.

MCEER-17-0001 "Diagonal Tension Field Inclination Angle in Steel Plate Shear Walls," by Yushan Fu, Fangbo Wang and Michel Bruneau, February 10, 2017.

MCEER-17-0002 "Behavior of Steel Plate Shear Walls Subjected to Long Duration Earthquakes," by Ramla Qureshi and Michel Bruneau, September 1, 2017.

MCEER-17-0003 "Response of Steel-plate Concrete (SC) Wall Piers to Combined In-plane and Out-of-plane Seismic Loadings," by Brian Terranova, Andrew S. Whittaker, Siamak Epackachi and Nebojsa Orbovic, July 17, 2017.

MCEER-17-0004 "Design of Reinforced Concrete Panels for Wind-borne Missile Impact," by Brian Terranova, Andrew S. Whittaker and Len Schwer, July 18, 2017.

MCEER-17-0005 "A Simple Strategy for Dynamic Substructuring and its Application to Soil-Foundation-Structure Interaction," by Aikaterini Stefanaki and Metttupalayam V. Sivaselvan, December 15, 2017.

MCEER-17-0006 "Dynamics of Cable Structures: Modeling and Applications," by Nicholas D. Oliveto and Mettupalayam V. Sivaselvan, December 1, 2017.

MCEER-17-0007 "Development and Validation of a Combined Horizontal-Vertical Seismic Isolation System for High-Voltage-Power Transformers," by Donghun Lee and Michael C. Constantinou, November 3, 2017.

MCEER-18-0001 "Reduction of Seismic Acceleration Parameters for Temporary Bridge Design," by Conor Stucki and Michel Bruneau, March 22, 2018.

MCEER-18-0002 "Seismic Response of Low Aspect Ratio Reinforced Concrete Walls," by Bismarck N. Luna, Jonathan P. Rivera, Siamak Epackachi and Andrew S. Whittaker, April 21, 2018.

MCEER-18-0003 "Seismic Damage Assessment of Low Aspect Ratio Reinforced Concrete Shear Walls," by Jonathan P. Rivera, Bismarck N. Luna and Andrew S. Whittaker, April 16, 2018.

MCEER-18-0004 "Seismic Performance Assessment of Seismically Isolated Buildings Designed by the Procedures of ASCE/SEI 7," by Shoma Kitayama and Michael C. Constantinou, April 14, 2018.

MCEER
EARTHQUAKE ENGINEERING TO EXTREME EVENTS
University at Buffalo, The State University of New York
133A Ketter Hall ▪ Buffalo, New York 14260-4300
Phone: (716) 645-3391 ▪ Fax: (716) 645-3399
Email: *mceer@buffalo.edu* ▪ Web: *http://mceer.buffalo.edu*
University at Buffalo *The State University of New York*

ISSN 1520-295X